Modifying the Fc Asn297 Glycan of Human IgG2 Subclass for Improved Antibody Therapeutics and Design of Site-Specific Antibody Drug Conjugates

By

Khalid Kadhem Abed Al-Kinani

M.S., Pharmaceutics, The University of Baghdad, 2010

B. Pharm., The University of Baghdad, 2004

Submitted to the graduate degree program in Pharmaceutical Chemistry and the Graduate Faculty of the University of Kansas in partial fulfillment of the requirements for the degree of Doctor of Philosophy.

_____

Chairperson Thomas Tolbert, Ph.D.

_____

C. Russel Middaugh, Ph.D.

_____

Teruna Siahaan, Ph.D.

_____

Michael Wang, Ph.D.

_____

Jarron Saint Onge, Ph.D.

Date Defended: July 7, 2017

The Dissertation Committee for Khalid Kadhem Abed Al-Kinani

certifies that this is the approved version of the following dissertation:

Modifying the Fc Asn297 Glycan of Human IgG2 Subclass for Improved Antibody Therapeutics and Design of Site-Specific Antibody Drug Conjugates

_____

Chairperson Thomas Tolbert, Ph.D.

Date Approved: July 7, 2017

Abstract

Immunoglobulin G (IgG) is a complex glycoprotein that is largely being used in the development of antibody-based therapeutics to treat a variety of diseases such as cancers, autoimmune diseases, and infectious diseases. A major challenge in developing such therapeutics originates from the heterogeneity of the Asn297 glycan of IgG. This sugar part (Asn297 glycan) of IgG has been shown to play an important role in the antibody properties such as antibody stability, effector functions, solubility, pharmacokinetics, and immunogenicity. To study the effect of Asn297 glycan composition on the properties of the human IgG2 (a preferred IgG subclass for developing antibody-based therapeutics when the antibody effector functions are not required), we developed an approach to produces homogeneous IgG2 Fc glycoforms. Studying these homogeneous IgG2 Fc glycoforms suggested that enriching the core fucose within IgG2 Asn297 glycan could add more advantages to developing IgG2-based therapeutics by providing more reduction in any possible undesirable effector functions of these therapeutics. The *in vitro* enzymatic synthesis developed here also enabled studies of different glycosylation sites accessibility to glycosyltransferase and expanded our understanding of the glycosylation heterogeneity. The Asn297 glycan also offers a great opportunity in developing antibody drug conjugates (ADCs), a therapeutic modality where a toxic payload is conjugated to IgG. The early ADC development relied on conjugating the payload non-specifically through either the lysine or cysteine residues of IgG using conventional chemistries. Producing ADCs in this way, results in heterogeneous products. ADC heterogeneity usually translates into poor pharmacokinetics, stability, and efficacy. In this work, we developed a chemoenzymatic synthesis platform to functionalize the Asn297 glycan in a novel way and use it as a specific site for conjugation. The work involved using and optimizing click chemistry reactions for conjugating different linkers

on IgG2 Fc. This approach enabled us to produce conjugates with excellent homogeneity. Subsequent studies of these conjugates showed the utility of the approach followed here in making of site-specific conjugates with good properties and the possibility of following this approach in designing and testing site-specific ADCs during the process of developing next generation ADCs.

In the name of God, the Most Gracious, the Most Merciful

Dedicated to:

My

Mother (Lateefa)

Father (Kadhem)

Wife (Alyaa)

and

Sons (Jaafar, Baqir, and Ahmed)

Acknowledgements

This dissertation could not have been finished without the help and advice of many professors, graduate students, colleagues, and family members.

First and foremost I would like to thank my advisor, Dr. Thomas Tolbert for his unlimited guidance and support during the various stages of my PhD journey. I really appreciate his open door policy, the time he dedicated to discuss my research projects and teach me the essential biotechnology skills, the constructive feedback, and the valuable suggestions. Also, I truly admire his knowledge and passion for science.

I also wish to extend my gratitude to the other members of my dissertation committee for their advice and valuable suggestions regarding this dissertation work: C. Russel Middaugh, Teruna Siahaan, Michael Wang, and Jarron Saint Onge. I would like to especially thank Dr. Middaugh for providing me with unlimited access to instruments in his laboratory to do some studies that were essential for this dissertation work. Also special thanks to Dr. Siahaan and Dr. Wang for the valuable scientific discussions and the support especially in the last year of my PhD program.

To all current and former members of the Tolbert's lab: Derek White, Ishan Shah, Solomon Okbazghi, Dr. Shaofeng Duan, Dr. Zahra Khedri, and Kevin Hutchison, it has been an honor to have you as colleagues. I truly appreciate your help in the lab, your scientific opinions, and your friendship. Special thanks go to Derek White for his help and guidance during my first year in Tolbert's lab. Kevin Hutchison, Ishan Shah, and Derek White have been constant friends for me and I would like to thank them again for being such great friends besides being nice and helpful lab mates.

The collaborative environment within the Department of Pharmaceutical Chemistry has provided me with a great opportunity to expand my research skills. I would like to thank our collaborators from the Macromolecule and Vaccine Stabilization Center (MVSC) especially Dr. C. Russel Middaugh and Dr. David Volkin for providing us with the required resources and equipment to do the biophysical studies reported in this dissertation work. Also, I would like to thank Apurva More, Yangjie Wei, Harshit Khasa, and Vishal Toprani for helping me in conducting the biophysical studies and processing the data. Their role was really instrumental in this regard.

Special thanks also go to the faculty and the administrative staff of the Department of Pharmaceutical Chemistry. The faculty, I would like to thank them for teaching us an awesome and unique coursework which helped significantly in broadening my knowledge and skills in the field of pharmaceutical sciences. The administrative staff, I would like to thank them for their great efforts in responding to my needs and requests in a timely manner and for the friendly environment they have created in the department.

I am also grateful for the financial support from a scholarship funded by Higher Committee for Education Development in Iraq (HCEDIraq) and from grants from the National Institutes of Health.

To my mother, Lateefa, and my father, Kadhem, I can never thank you enough. You have played a special role in this process and I thank you for your prayers and support. I am also very grateful to my sisters Manal and Rana and my brothers Jawaad, Dhiaa, and Safaa for their constant support, encouragements, and praying for me to succeed in my PhD journey and my life in general. I am also thankful to my father-in-law, Dr. Faris, and my mother-in-law, Nihad, for

their continuous love, support, and for visiting us several times while we were here in the United States and helped during my wife's pregnancy and after she gave birth to my son, Baqir.

Last but not least, words cannot express my gratitude and appreciation to my angel, my wife Alyaa. I would not have been able to persevere through the academic and personal challenges of the last few years if it were not for the love and support of the most understanding and patient woman in the world and that is you. Thank you for our lovely children Jaafar, Baqir, and Ahmed. There is no better motivation to finish than to be able to spend time with you and our children as they grow up. I love you so much!

Table of contents

Chapter 1

Introduction

Therapeutic monoclonal antibodies: An overview

Therapeutic monoclonal antibodies (mAb) represent one the fastest growing classes of pharmaceutical products with more than 60 approved by the United States FDA as of May, 2016. This rapid growth of therapeutic mAb as well as mAb-derived products will result in worldwide sales of about $94 billion by 2017 (compared to $75 billion in 2013 which represented nearly half of the total sales of all biopharmaceutical products).[1,2] Therapeutic mAb have been utilized in treating a wide variety of diseases and clinical conditions including infectious diseases, cancers, allergies, inflammatory diseases, and cardiovascular diseases.[3] Therapeutic mAb have the advantage of binding their targets in a specific manner which can result in fewer side effects than conventional pharmaceutical products. The high specificity of mAb toward certain antigens also enabled the use of these biotechnology products as vehicles to deliver other compounds (usually toxins) to cells expressing these antigens, such as in making of antibody drug conjugates (ADCs).[4,5] Also, the long biological half-life of mAb is a unique feature of this class of biopharmaceutical products and enables a high efficiency and reduced dose frequency of mAb making them more convenient in treating chronic diseases.[3,6]

Monoclonal antibodies were first generated successfully by Kohler and Milstein in 1975 when they used hybridoma technology to produce "antibody of predefined specificity".[7,8] Soon after this success, which led to Nobel Prize, mAb became widely used in clinical laboratories as indispensable biological tools in the diagnosis of many pathological conditions. At the same time, interest was growing in making therapeutic mAb to treat certain diseases, especially cancer. Early trials to make therapeutic mAb were not successful because most of these mAb produced by hybridoma technology were of murine origin.[3,9–11] Administration of murine mAb to humans was associated with the development of human anti-mouse antibodies (HAMA). This allergic

response (HAMA) results in reducing the effectiveness of the mAb and can range from mild allergic reactions, such as rash, to more severe reactions resulting in renal failure. In 1985, the first therapeutic mAb, Orthoclone OKT3 (muromonab-CD3), was approved by the FDA for the prevention of allograft rejection in renal transplantation. Orthoclone OKT3, a mouse IgG2a produced by hybridoma technology, was continued to be used until 2010 when it was voluntarily withdrawn from the market following subsequent advances in transplant medicines.[12]

Started by mid-1980 and taking advantage of the improvement in the fields of molecular biology and protein engineering, several strategies have been introduced to improve the characteristics of therapeutic mAb produced initially by hybridoma technology from murine plasma cells.[3,13,14] Most of these strategies were based on the rationale of reducing the extent of mouse amino acid sequence within the antibody (antibody humanization) in order to minimize any potential immunogenicity associated with injecting these antibodies into the human body. In one strategy, part of the variable domains amino acid sequence of a mouse-derived antibody is converted into the corresponding amino acid sequence of a human antibody. This strategy is used to produce a mAb containing as much human antibody amino acid sequence as possible such as in the production of chimeric (about 65% human) and humanized (about 95% human) antibodies. In other strategies, the produced mAb contains 100% human-derived amino acid sequence (human antibody) and this can be achieved through the use of certain technologies such as phage-display and transgenic-mouse technologies. These advanced technologies as well as the development in mAb production and purification resulted in more successful production and commercialization of mAb and the emergence of the therapeutic mAb class as a rapidly growing and promising class in the treatment of a variety of diseases.

Structure of human IgG and Asn297 glycan heterogeneity

Immunoglobulin G (IgG) antibody is a soluble glycoprotein secreted by B cells and plasma cells and represents a major component of the humoral immunity. IgG is the most abundant immunoglobulin isotype in the human serum and comprises about 75% of the total serum immunoglobulins.[15] All of the currently marketed therapeutic monoclonal antibodies are of IgG isotype. IgG is a Y- shaped multifunctional glycoprotein that is made up of four polypeptide chains, two identical heavy chains and two identical light chains, to form three structurally independent protein moieties (two Fab regions and one Fc region) connected through a flexible hinge region (Figure 1).[15–17] The heavy chain consists of one variable domain (V_H) followed by a constant domain (C_H1), a hinge region amino acid sequence, and two more constant domains (C_H2 and C_H3); while the light chain consists of one variable (V_L) domain and one constant (C_L) domain. The antigen-binding fragments (Fab) define the antibody-specificity against certain antigens by adapting a specific amino acid sequence within their complementary determining regions (CDR). The fragment crystallizable (Fc) of the antibody is responsible of mediating the antibody effector functions and antibody recycling through specific set of Fc-receptors and Fc-binding proteins.[18,19]

IgG isotype contains a well conserved N-glycan at Asn297 (Eu numbering) in the C_H2 domain of the Fc region which is critical for the structure and function of the antibody. In addition to the Asn297 glycan, about 20% of the human IgG pool contains N-linked glycans in the Fab region.[20,21] Also, certain IgG3 and IgG2 allotypes contain an extra N-linked glycan at Asn392 in the C_H3 domain of the Fc region. The structure of Asn297 glycan is variable but in general it can be divided in to three major types: high mannose, hybrid and complex N-linked

glycans (Figure 2).[22,23] All of these types share the same pentasaccharide core structure however they vary in the number and type of sugar units at their non-reducing termini.

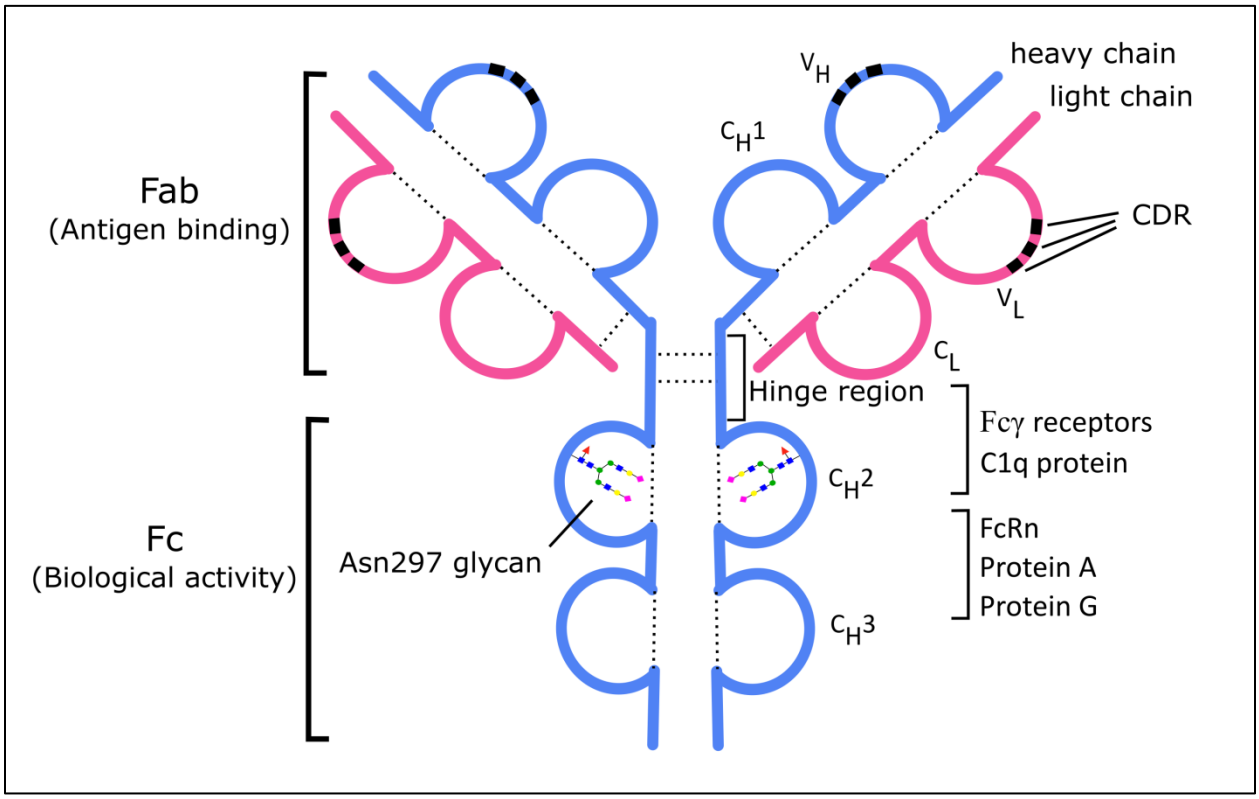

Figure 1. Diagrammatic representation of immunoglobulin G (IgG) molecule.

In high mannose N-glycans, the non-reducing termini are composed of only mannose sugar residues. In hybrid type N-glycans, some of the non-reducing termini are composed of mannose while other termini are composed of GlcNAc, galactose, or sialic acid. In complex type N-glycans, none of non-reducing termini are composed of mannose.[24] Asn297 glycan is mostly of bi-antennary complex type which may or may not contain bisecting GlcNAc and or core fucose.[22,23]

Being an N-liked glycan, the Asn297 glycan biosynthesis follows the same biosynthetic pathway of mammalian N-glycosylation (Figure 3).[24,25] This biosynthetic pathway is composed

of many steps that can occur in different compartments of the cell. Protein N-glycosylation begins by *en bloc* transfer of the glycan precursor $Glc_3Man_9GlcNAc_2$ from dolichol-p-p-$Glc_3Man_9GlcNAc_2$ to Asn residue of the N-glycosylation sequon (NXT/S) of the nascent polypeptide chain.

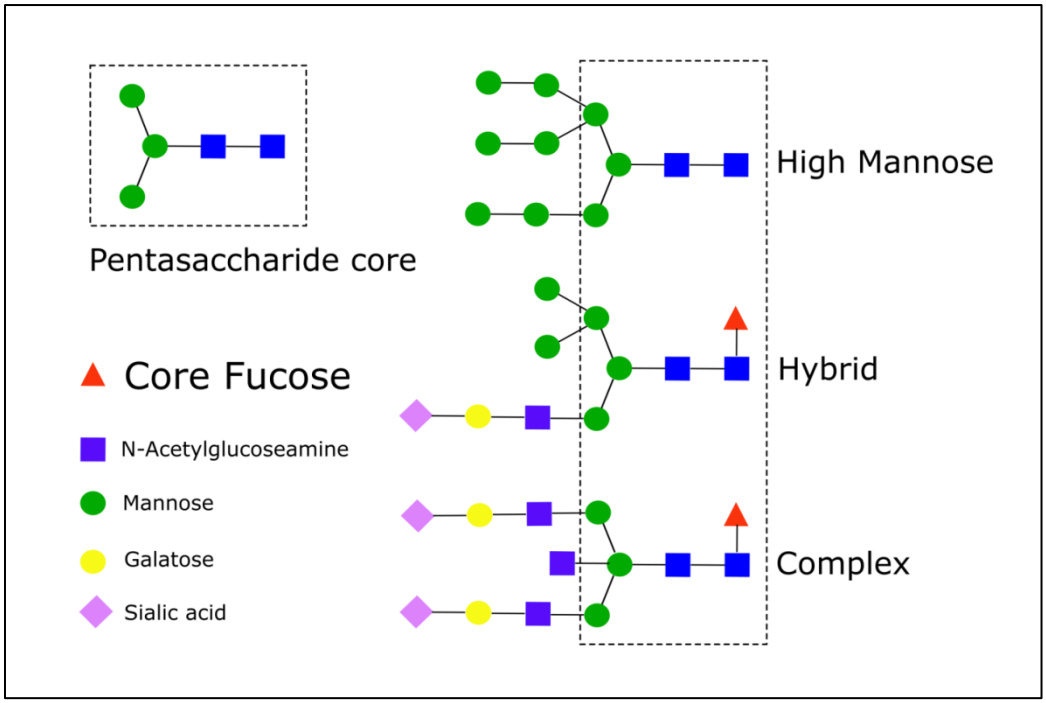

Figure 2. Major types and structure of N-linked glycans.

The transfer takes place inside the lumen of the endoplasmic reticulum and catalyzed by the enzyme oligosaccharyltransferase (OST). The three glucose units of $Glc_3Man_9GlcNAc_2$ were then cleaved off by α-glucosidases to form a high mannose glycan $Man_9GlcNAc_2$ (Man_9) and the protein is properly folded at this stage. The Man9 glycoprotein is then translocated to the Golgi apparatus for more processing of the oligosaccharide. The Golgi apparatus contains different glycosidases and glycosyltransferases localized at different compartments within its lumen. In the Cis-Golgi, mannosidases hydrolyses the α1,2-linked mannoses of the Man9 glycan to

produce a $Man_5GlcNAc_2$ (Man5) glycan. In the medial-Golgi, N-acetylglucosaminyltransferase-I (GnT-I) transfers GlcNAc from the activated nucleotide sugar UDP-GlcNAc to the Man5 glycan to form the hybrid glycan $GlcNAcMan_5GlcNAc_2$. UDP-GlcNAc and other activated nucleotide sugars are pumped into the Golgi lumen via the assistance of Golgi-bound nucleotide sugar transporter proteins. The hybrid glycan then becomes a substrate for mannosidase II which hydrolyzes two more mannose residues to prepare the glycan for N-acetylglucosaminyltransferase-II (GnT-II) reaction and form the complex glycan $GlcNAc_2Man_3GlcNAc_2$.

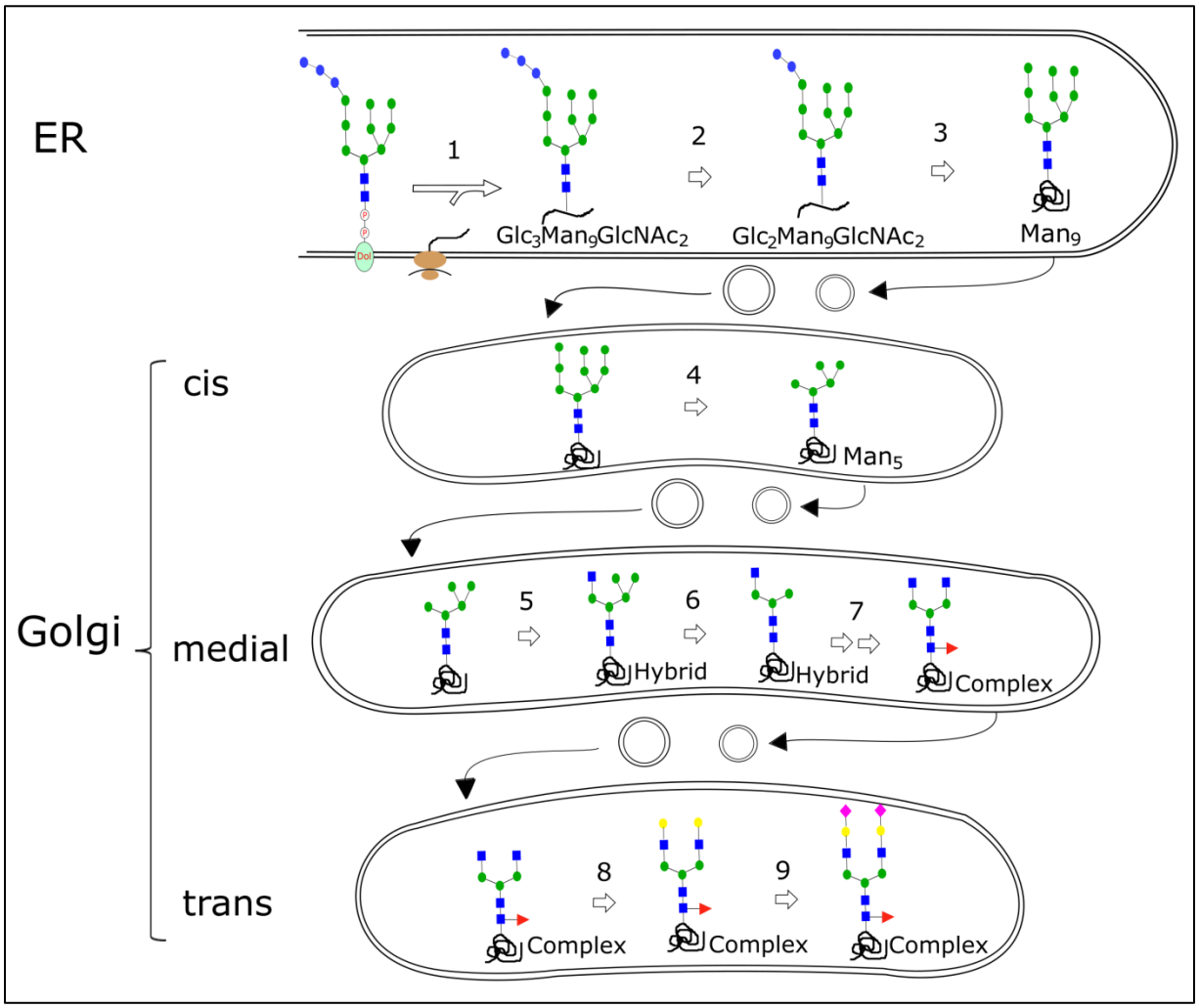

Figure 3. Schematic overview of the mammalian N-glycosylation pathway taking place in the endoplasmic reticulum (ER) and the Golgi apparatus. 1) Oligosaccharyltransferase (OST). 2, 3) α-glucosidases. 4) α1,2-mannosidases. 5) N-acetylglucosaminyltransferase-I (GnT-I) plus UDP-GlcNAc. 6) Mannosidase II. 7) N-acetylglucosaminyltransferase-II (GnT-II) plus UDP-GlcNAc and α1,6-fucosyltransferase (FUT8) plus GDP-fucose. 8) Galactosyltransferases plus UDP-galactose. 9) Sialyltransferases plus CMP-sialic acid.

Monoclonal antibodies modes of action

There are several modes by which IgG antibody and hence therapeutic mAb can exert their therapeutic effects especially in treatment of cancers (Figure 4).[26–28] Some of these modes of action rely on the binding of the Fc part of the antibody engaged in the immune complex (antibody-antigen complex) with the complement system C1q protein and Fcγ receptors. Interestingly, antibody binding to this protein and these receptors is highly affected by the glycosylation profile of the Asn297 glycan.[16,29,30] Other modes rely on just binding of the antibody through its Fab region to either a receptor or a ligand and hence block the receptor-ligand interaction and prevent subsequent biological effect. Also, antibodies can be used as carriers to deliver cytotoxic payloads to certain cells to obtain certain pharmacological effects, such as in antibody drug conjugates (ADCs) which are used mainly to treat cancers.[4] Combination of modes of action can also happen after binding of the antibody to its target and below is a description of each mode:

Antibody effector functions

Many antibody effector functions are mediated through Fcγ receptors. Human Fcγ receptors represent an important class of closely related receptors that can bind human IgG isotype through the Fc region.[18,31] These receptors are widely distributed on the surface of different immune cells and clustering of these receptors on the surface of the immune cell can either activate the cell such as in the case of clustering of FcγRI, FcγRIIa, FcγRIIc, and FcγRIIIa or inhibit the cell such as in the case of clustering of FcγRIIb. The activating Fcγ receptors contain an immunoreceptor tyrosine-based activation motif (ITAM) in their intracellular domains

or their adaptor protein, while the inhibitory receptor (FcγRIIb) contains an immunoreceptor tyrosine-based inhibitory motif (ITIM).[32,33]

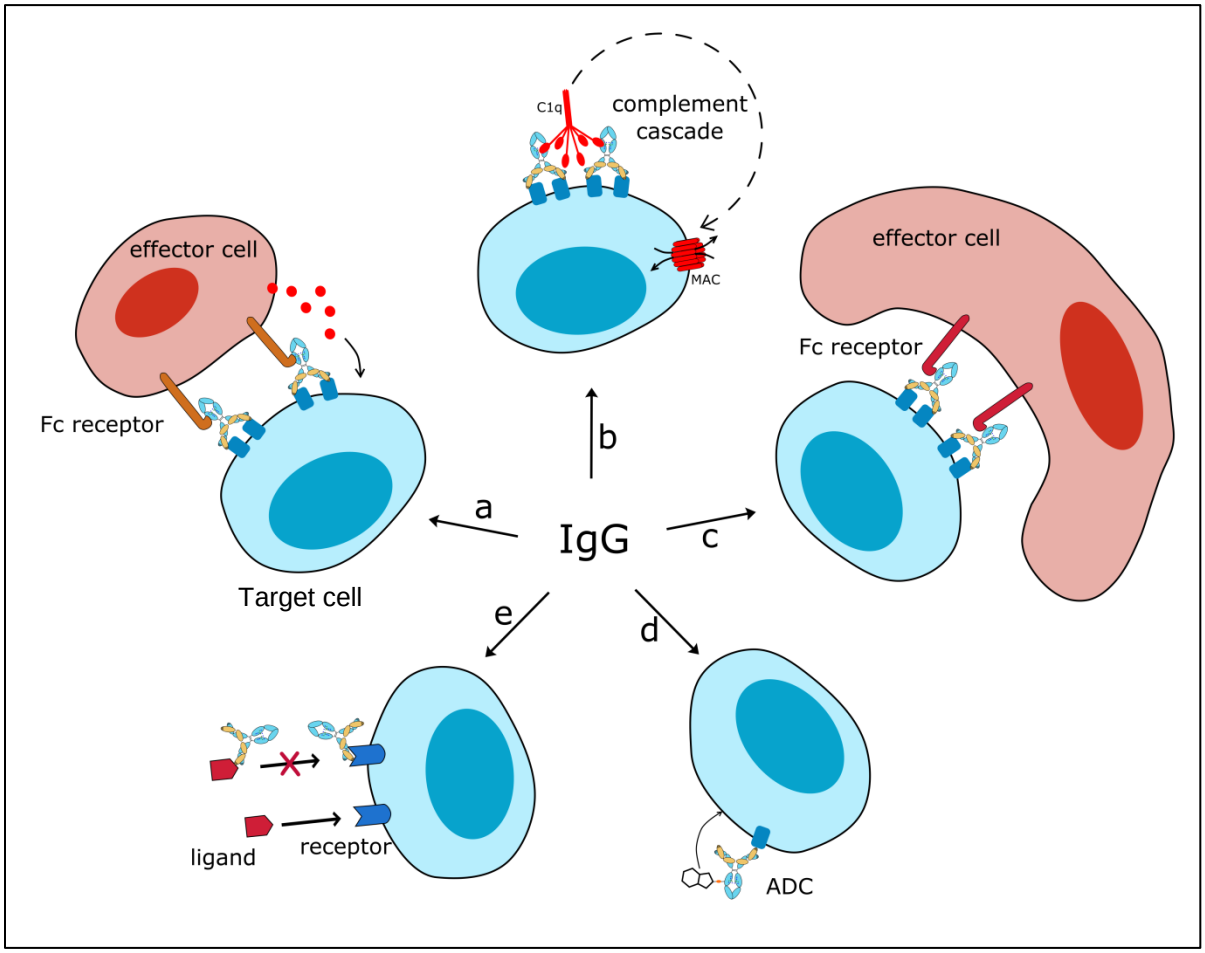

Figure 4. Therapeutic monoclonal antibodies possible modes of action. a) Activation of antibody dependent cellular cytotoxicity (ADCC). b) Activation of complement dependent cytotoxicity (CDC). c) Activation of antibody-dependent cell-mediated phagocytosis (ADCP). d) Antibody drug conjugates (ADC) mediated cytotoxicity. e) Blocking receptor-ligand interactions and inhibiting signal transduction and subsequent biological processes.

Among this class of receptors, FcγRIIIa has gained a particular attention in the design monoclonal antibodies with enhanced cytotoxic effect. FcγRIIIa is expressed on the surface of monocytes, dendritic cells, macrophages, and natural killer (NK) cells. FcγRIIIa is the sole receptor expressed on the surface of natural killer (NK) cells; however recent studies showed that about 20% of the population expresses FcγRIIc as well.[34] Clustering of FcγRIIIa on the surface of NK cells induces a powerful cytotoxic effect called antibody-dependent cellular cytotoxicity (ADCC).[16,27] During ADCC, the NK cell releases cytokines that mediate the lysis of the target cells that are brought to its proximity through the binding with IgG. There have been many antibody engineering approaches to increase the binding of the antibody to FcγRIIIa and hence the induction of more powerful ADCC. Some approaches involved changing of the antibody amino acid sequence while others involved glycoengineering of the Asn297 glycan, as it will be discussed later in this chapter.[35–39] Also, FcγRIIIa has a polymorphism at position 158 which results in two receptor variants, FcγRIIIa-V158 and FcγRIIIa-F158 that are different in their binding affinity to IgG subclasses. The valine variant of the receptor has a stronger binding affinity to IgG than the phenylalanine variant. This functional polymorphism has also been shown to affect the therapeutic efficacy of therapeutic mAb (such as rituximab) in different patients where patients who were homozygous for the valine variant of the receptor showed a higher therapeutic response.[40,41] The other receptor that plays an important role in antibody effector functions is FcγRIIa. This receptor is present on the surface of many phagocytic cells and can mediate a phagocytic effect called antibody-dependent cell-mediated phagocytosis (ADCP) through which the antibody-bound antigen is engulfed and destroyed by the phagocytic cell.[35,42,43] This receptor also exhibits two variants, FcγRIIa-H131 and FcγIIa-R131, which have different affinities to human IgG2 subclass, as discussed in next section.

Antibody can also activate the complement system through the classical pathway of activation of this system and results in mediating complement dependent cytotoxicity (CDC).[19,28,36] The complement system is part of the innate immune system which complements the ability of the antibodies and phagocytic cells to clear pathogens from the human body. In this mode of action, the antibody engaged in the immune complex binds the soluble component of the complement system, C1q protein. This binding induces conformational changes within the protein which lead to a cascade of proteolytic reactions and activation of other complement components such as the C4a that acts as an anaphylotoxin and activate the inflammatory cells. Also, activation of the complement system will eventually result in the formation of the complement membrane attack complex (MAC) which can insert itself in the membrane of the target cell and form a porous channel and induces cell lysis and death. Although the complement system plays an important role in protecting the body from foreign pathogens, its activation can also result in observed side effects of antibody therapeutics.[44,45] In addition, the role of CDC in the clinical effectiveness of some anticancer mAb, like rituximab, is not well confirmed, and it has been shown that there is no clear correlation between the therapeutic response of this mAb (rituximab) and its ability to induce CDC.[46]

Antibody blocking activities

Antibodies can also intercept a receptor-ligand interaction and block any undesirable biological effects that can result from this interaction.[26,27] The antibody can be designed to bind the receptor on the surface of the cell and block the ligand binding site. Also, the antibody can be designed to bind a receptor at different site than the ligand binding site; however upon binding, the antibody will induce conformational changes in the receptor to prevent its interaction with the ligand. The antibody can also be designed to prevent the receptor dimerization by binding to

the dimerization domain of the receptor such as in case of antibody designed to block ligand binding to epidermal growth factor (EGF) receptor.[11,47] Alternatively, the antibody can be designed to bind the ligand (instead of the receptor) and sterically prevent it from binding to its receptor and thus block the signal. Intercepting a receptor-ligand interaction can be well explained in the context of designing checkpoint blockade antibodies.[48] The checkpoint blockade antibodies, also called immune checkpoint inhibitors, are a class of mAb designed to treat cancer utilizing a novel mechanism of action by targeting activation of the immune effector cells. These mAb are designed to block certain receptors on the surface of T-cells, such as programmed cell-death protein (PD-1) and cytotoxic T-lymphocytes antigen 4 (CTLA-4). Binding of the natural ligands to these receptors causes inactivation of the T-cells, an immune regulatory mechanism that prevents the destruction of self-antigen and developing of autoimmune diseases. However, the cancer cells can use this mechanism to evade the immune system by overexpressing these ligands and thus shutting down the T-cells. Therefore, an immune checkpoint inhibitor mAb can reverse this inhibitory action and restore the activity of T-cells. Some antibodies were designed to bind PD-1 receptor such as pembrolizumab for the treatment of melanoma.[49] Other antibodies were designed to block CTLA-4 receptor such as ipilimumab, which is also used for the treatment of melanoma. Immune checkpoint inhibitor mAb were also designed to bind to PD-1 ligand (PD-L1), which can be overexpressed on the surface of the tumor cell, such as the antibody atezolizumab which is now in clinical trials for the treatment of several solid tumors.[48,50]

Antibody drug conjugates

Antibodies can be also used as carriers in the design of antibody drug conjugates (ADCs).[5,27] In ADC, the main mode of killing is attributed to the toxic payload attached to the

mAb component of the ADC. In general, ADC combines the cytotoxic effect of the toxic payload with the specificity of the mAb to target certain tumor cells. Also, the mAb part of the ADC reduces the clearance of the conjugate through the interaction of the Fc region with the neonatal Fc receptor (FcRn), which is an essential receptor playing a critical role in re-shuttling the antibody back to the extracellular fluids and prevent its lysosomal degradation inside the cell.[51] When designing ADC, the mAb component is designed to target antigen with certain criteria.[52,53] Target antigen should have high levels of expression on the surface of the tumor cell and should also undergo rapid and efficient internalization upon binding with the ADC to deliver sufficient amount of the toxic payload to the inside of the tumor cell. The payload should be a highly toxic drug that can result in death of the tumor cell upon delivery by ADC. There are several toxic drugs that can be used in making ADCs such as monomethyl auristatin E (MMAE), which inhibit the polymerization of tubulin; maytansines, which inhibits the assembly of microtubules; calicheamicin which cleaves the DNA strands; and pyrrolobenzodiazepines, which are DNA minor groove cross-linkers.[53] All of these drugs can inhibit the tumor cell proliferation and result in programmed cell death. Most of these drugs are hydrophobic in nature and this hydrophobicity could help the drug in escaping the lysosomal degradation upon internalization of the ADC and allow it (the drug) to diffuse out to the site of action.[54] ADCs should be designed carefully to prevent any deterioration in the mAb selectivity, internalization efficiency, pharmacokinetics, and physicochemical properties upon conjugation of the payload.[55,56] The right conjugation site and right drug to antibody ratio (DAR) coupled with the right conjugation chemistry and linker technology should minimize any negative effect on the ADC properties and deliver sufficient payload to cause efficient tumor cell killing with minimum side effects.[54,57,58]

Human IgG subclasses and the design of therapeutic monoclonal antibodies

Human IgG isotype is a major immunoglobulin isotype present in the serum and constitutes about 10-20% of the total serum protein. This immunoglobulin isotype comprises four subclasses, IgG1, IgG2, IgG3, and IgG4.[15,16,59] These IgG subclasses have different amino acid sequence within the constant region of their heavy chains. Although, these subclasses share about 90% amino acid sequence homology, the minor difference in their structure gives each subclass unique features that can be significantly different from the other (Table I). Most of the amino acid sequence difference lies in the hinge region and the upper C_H2 domain of the antibody, although there are minor differences in other regions. The difference in the properties of IgG subclass has been taken into consideration in designing therapeutic mAb to obtain better outcomes.[59,60]

IgG1 is the most abundant subclass and counts for about 67% of the total serum IgG pool.[15,59] This subclass plays an important role in the humoral immunity since it is the major IgG subclass and usually produced in response to soluble protein and membrane protein antigens. Most of therapeutic mAb, especially antitumor mAb, are of IgG1 subclass because this subclass is a strong activator of the ADCC and CDC. The biological half-life of IgG1 (as well as IgG2 and IgG4) is approximately 21 days and such long half-life is advantageous when designing mAb intended to treat chronic diseases such as cancer and autoimmune diseases.[6]

The second most abundant IgG in human serum is IgG2 which constitutes about 22% of the total serum IgG pool. Human body usually develops IgG2 antibody response when the immune system recognizes antigens of carbohydrate composition especially bacterial polysaccharide antigens.[15,16] IgG2 has four disulfide bonds in the hinge region while IgG1 has

only two. Recently, IgG2 disulfide bonds have been shown to undergo rearrangement.[61–64] As a result of this disulfide bonds rearrangement, IgG can exist in three different isoforms. It is believed that this flexibility in the hinge disulfide bonds could also give IgG2 the ability to exist in dimers with a possible increase in the antibody avidity against pathogens.[65] As shown in Table I, IgG2 binds weakly to most of Fcγ receptors except FcγRIIa. FcγRIIa undergoes a polymorphism at amino acid number 131 to result in two receptor variants, FcγRIIa-H131 and FcγRIIa-R131.

Table I. Properties of the four human IgG subclasses[15,59,60,66]

	IgG1	**IgG2**	**IgG3**	**IgG4**
Serum %	67	22	7	4
Serum concentration (mg/ml)	8	2.5	0.8	0.4
Size (kDa)	146	146	170	146
No. of hinge disulfide bonds	2	4	11	2
Half-life (days)	21	21	7	21
No. of allotypes	4	2	13	1
C1q binding	++	+	+++	-
FcγRI binding	+++	-	++++	++
FcγRIIa-H131	+++	++	+++++	++
FcγRIIa-R131	+++	+	+++++	++
FcγRIIIa-V158	+++	+	+++++	++
FcγRIIIa-F158	++	-	+++++	-
FcγRIIb	+	-	++	+

Interestingly, human IgG2 subclass has different affinities to these two receptor variants where it has a higher affinity for the FcγRIIa-H131 variant than the FcγRIIa-R131.[66–68] This receptor polymorphism has also been shown to be associated with some infectious and autoimmune

diseases such as systemic lupus erythematosus (higher incidence in R131 variant expressing individuals), ulcerative colitis (higher incidence in H131 variant expressing individuals), and malaria (higher incidence in H131 variant expressing individuals).[69–71] The susceptibility to these diseases could suggest a possible role for IgG2 subclass in the pathogenesis of these diseases. IgG2 is also known to have a weak binding affinity to C1q protein and thus a low ability to fix the complement system and induce CDC. The low effector functions of IgG2 subclass has been utilized in designing therapeutic mAb where only an antibody blocking effect is required for the mAb mechanism of action. However, the low affinity of IgG2 subclass to the inhibitory FcγRIIb may counteract its low affinity to the activating Fcγ receptors when both receptors are expressed on the same immune effector cell. Nonetheless, there are several IgG2-based mAb that are currently in the market such as denosumab and panitumumab which are used for treating osteoporosis and colorectal cancer, respectively.[72–74]

IgG3 subclass of human IgG isotype constitutes about 7% of the total serum IgG pool and characterized by a very long hinge region which contains eleven disulfide bonds (Table I).[15] In general IgG3 immune response is mediated during viral infections and it is usually accompanied by IgG1 response even though IgG3 appears first in the course of the infection.[15,16,59] IgG3 is characterized by having a shorter biological half-life (about 7 days) compared to the other IgG subclasses (IgG1, IgG2, and IgG4) which have relatively long biological half-lives (about 21 days).[75] Also, IgG3 has the largest number of allotypes among the other IgG subclasses.[16,59,76] Most of IgG3 variants have N-glycosylation site in the Fc region at Asn392 in addition to the well conserved N-glycosylation at Asn297. IgG3 subclass has a strong ability to activate the complement system and it also has a strong ADCC activity which can be useful in designing therapeutic mAb with enhanced cytotoxicity for cancer treatment. However,

this subclass has not been utilized yet to make therapeutic mAb probably because of its relatively short biological half-life and its long hinge region which makes it more prone to proteolysis.[59]

IgG4 is the least abundant IgG subclass in human serum and constitutes only about 4% of the total serum IgG pool.[15,77] The immune system produces IgG4, in addition to IgG1 and IgE, in response to allergens, especially after a repeated or a long term exposure. Also, IgG4 represent the dominant immune response to therapeutic proteins such as factor VIII and factor IX.[16] Like, IgG1, IgG4 has only two disulfide bonds in the hinge region. However, IgG4 undergoes a phenomenon called Fab arm exchange where the antibody can dissociate into two half-molecules under certain redox conditions.[77,78] Then, half-molecules from IgG4 having different specificities can recombine to result in the formation of a bispecific IgG4 molecule. The susceptibility of IgG4 to this phenomenon has been shown to be due to the presence of serine at position 228 in the hinge region instead of proline in the other subclasses. This mutation makes the hinge more flexible and allows easier disulfide bonds rearrangement within the hinge region. The presence of arginine at position 409 in IgG4, instead of lysine in IgG1, weakens the C_H3-C_H3 hydrophobic interaction and also allows the molecule to undergo Fab arm exchange. IgG4 is the weakest activator of the complement system and also it has weak affinities to Fcγ receptors (Table I). Hence, IgG4 has low Fc-mediated effector functions. Likewise IgG2, IgG4 has been utilized in making therapeutic mAb when the effector functions are not part of the mAb mode of action.[59,79] However, in one trial IgG4-based anti-CD28 monoclonal antibody (TGN1412) caused a serious adverse effect where six patients developed cytokines storm during clinical trials in 2006.[80] It has been believed that the susceptibility of IgG4 to Fab arm exchange was behind the development of this adverse effect. Recent IgG4-based mAb were engineered to have S228P mutation to eliminate the possibility of any Fab arm exchange and such therapeutic mAb have been marketed

successfully for treatment of a variety of diseases such as pembrolizumab, an immune checkpoint inhibitor used for treatment of melanoma and non-small cell lung cancer (NSCLC).[81,82]

Importance of Asn297 glycan for therapeutic monoclonal antibodies

Asn297 plays an important role in stabilizing the antibody peptide backbone by making a series of unique interactions with the amino acids in the C_H2 domain of the antibody. The hydrophilic nature of this glycan also helps in masking the hydrophobic amino acid residues in this domain and maintaining proper native IgG conformation.[30,83,84] Removal of the Asn297 glycan reduces the thermal stability of IgG1 and increases the aggregation propensity in many occasions.[85–87] It has also been shown that Asn297 glycan increases the solubility of IgG1 where deletion of the Asn297 glycosylation site by site-directed mutagenesis reduces the solubility of the non-glycosylated IgG1 Fc compared to the natural IgG1 Fc that is glycosylated at Asn297.[85] However, the solubility of the antibody may not always increase by having extra glycans and a reverse effect (i.e. reduced solubility) may also occur. The latter scenario can be seen in cryoimmunoglobulins where the decreased solubility of these immunoglobulins was shown to be associated with the antibody having extra N-glycans at certain sites in the Fab region.[88]

The antibody effector functions are highly dependent on the Asn297 glycan and removal of this glycan results in a dramatic reduction of in these effector functions such as reduction in antibody dependent cellular cytotoxicity (ADCC), antibody dependent cellular phagocytosis (ADCP), and complement dependent cytotoxicity (CDC).[30,89] The reason behind this reduction is that Asn297 is required to maintain a specific protein conformation in the C_H2 domain. The upper C_H2 domain and the lower hinge of the antibody are the regions where the antibody binds

to the receptors and proteins that mediate these effector functions. The composition of the Asn297 glycan also plays an important part in fine-tuning these effector functions. It has been shown that the absence of core fucose increases the binding to FcγRIIIa with subsequent increase in IgG1-mediated ADCC by 50-100 folds.[90–94] The reason for this reduced affinity has been shown to be due to core-linked fucose interrupting glycan-glycan interactions that are present between non-fucosylated IgG1 and the N-linked glycans of Asn162 on FcγRIIIa. This finding has sparked a tremendous interest in modifying the Asn297 glycan of IgG1 for designing better therapeutic mAb.[92] The presence of bisecting GlcNAc within the structure of Asn297 glycan has also been shown to increase ADCC, however this effect is most probably related to the absence of core fucose since bisecting GlcNAc hinders the addition of core fucose by α1,6-fucosyltransferase (FUT8).[91] The effect of galactose on the antibody effector functions is still not completely understood. The presence of terminal galactose in the structure of Asn297 glycan increases the antibody binding to C1q protein and activation of the complement system through the classical pathway to result in higher CDC.[95] Galactose has also been shown to be implicated with some autoimmune diseases where the level of Asn297 glycan galactosylation is reduced in these diseases such as rheumatoid arthritis (RA). Interestingly, women who have RA show an increase in the level of galactosylation when they become pregnant and go through a period of remission of RA symptoms.[96] Terminal sialic acid has been shown to make the antibody have anti-inflammatory effect. However, the anti-inflammatory effect of the sialylated IgG is not fully understood.[89,95,97] Many studies have been carried out with an attempt to correlate this effect with the antibody binding to Fcγ receptors as well as some other receptors such as Dendritic Cell-Specific Intercellular adhesion molecule-3-Grabbing Non-integrin (DC-SIGN). However, the

outcomes of these studies were conflicting and therefore more studies are needed to understand the role of sialic acid on IgG properties.[97–99]

The composition of the Asn297 glycan plays an important role in the antibody pharmacokinetics.[23] In general, IgG has a long biological half-life of about 21 days and this long half-life of this glycoprotein is attributed to the FcRn-recycling mechanism of IgG.[51] In this recycling mechanism the FcRn receptor binds tightly to the antibody at the C_H2-C_H3 domains interface at low pH that is characteristic of the lysosome environment and prevents the release of the antibody for lysosomal degradation. At the same time the receptor shuttles the antibody to the surface of the cell and releases it at the neutral extracellular environment where the affinity of binding is low. Added to that, the big size of the IgG (about 150 kDa) reduces the glomerular filtration and clearance of the antibody by the kidneys.[6] Although the Asn297 glycan does not affect the binding of IgG to FcRn and hence does not play a role in the FcRn-recycling mechanism, the type of the Asn297 glycan has been shown to affect the pharmacokinetics of IgG through other mechanisms. The high mannose glycoforms are cleared more rapidly from the blood due to increased binding to mannose receptors and uptake by cells that express these receptors.[100] Sialylated glycoforms have decreased clearance and longer biological half-lives due to their lower affinity to the asialoglycoprotein receptors present on the surface of the hepatocytes.[23,101,102]

Recently, two therapeutic mAb were developed through glycoengineering of the An297 glycan of IgG1 and these mAb are mogamulizumab[103] and obinutuzumab[104] which were approved in 2012 and 2013, respectively. The first mAb was expressed in a FUT8 knockout strain of Chinese hamster ovary (CHO) cells to block the addition of core fucose by FUT8 to the Asn297 glycan of IgG1 and hence increase the binding to FγRIIIa and subsequent effector

functions such as ADCC. The second mAb, obinutuzumab, was expressed in a cell line overexpressing the bisecting GlcNAc to again prevent the addition of core fucose to the Asn297 glycan by FUT8. In addition to these two technologies, many other approaches have been developed to reduce the amount of core fucose on the Asn297 glycan of IgG such as feeding the host cells with the fucose analogue, 2-Deoxy-2-fluoro-L-fucose, to inhibit FUT8.[105] Other approaches relied on the expression of the antibody in FUT8 null expression hosts such as the yeast *Pichia pastoris*.[106] Finally, glycoengineering represent an elegant approach to produce better therapeutic antibodies and the more understanding of the role of each glycoform on the antibody stability, function, immunogenicity, and pharmacokinetics, the faster the development of next generation therapeutic mAb.

Conclusions

Glycosylation of therapeutic mAb represent a unique posttranslational modification that has a high degree of heterogeneity as glycosylation is not a template-driven process.[24,25] The heterogeneity of this glycan is represented by the formation of different glycan types (high mannose, hybrid, and complex), presence or absence of core fucose, galactose, sialic acid, and bisecting GlcNAc, as well as glycosylation site occupancy.[22,23] The resulting heterogeneity of Asn297 glycan of human IgG isotype, especially IgG1 subclass, has been shown to have a significant effect on the antibody properties including stability[30,107], solubility[85], effector functions[30,108,109], pharmacokinetics[23], and immunogenicity[101]. Therefore, monitoring the composition of this glycan is critical to ensure that mAb has a consistent glycosylation profile among the different production batches. At the same time, glycoengineering the mAb to have enriched Asn297 glycan of certain composition provides a big chance to produce therapeutic mAb with better outcomes.[103,110]

Chapter 2 aims: To develop a platform for the synthesis of homogeneous and well-defined IgG2 Fc glycoforms on a relatively large laboratory-scale using a combination of glycosylation-deficient host, purification methods, and *in vitro* enzymatic synthesis. The produced IgG2 Fc glycoforms were to be studied for the effect of the structure of Asn297 glycan, especially the effect of core fucose, on IgG2 properties to ultimately create better IgG2-based therapeutic modalities.

Chapter 3 aims: To modify the Asn297 glycan of IgG2 beyond the natural sugar composition and introduce a modified sugar with a bioorthogonal handle to allow a unique site-specific conjugation through Asn297 glycan. The functionalized IgG2 Fc having a site-specific biorthogonal handle was to be conjugated with three alkyne-PEG linkers having different physicochemical properties and studies of the resulting conjugates, head to head, for the effect of these linkers on IgG2 Fc properties.

Chapter 4 aim: This final chapter summarizes the statement of the problem, the conclusions drawn based on the current work, as well as future directions.

References

(1) Ecker, D. M., Jones, S. D., and Levine, H. L. (2015) The therapeutic monoclonal antibody market. *MAbs*.

(2) Cai, H. H. (2016) Therapeutic Monoclonal Antibodies Approved by FDA in 2015. *MOJ Immunol. 3*, 2015–2016.

(3) Lansita, J. A., and Mounho-Zamora, B. (2015) The development of therapeutic monoclonal antibodies: overview of the nonclinical safety assessment. *Curr. Pain Headache Rep. 19*, 2.

(4) Peters, C., and Brown, S. (2015) Antibody-drug conjugates as novel anti-cancer chemotherapeutics. *Biosci. Rep. 35*, e00225.

(5) Chudasama, V., Maruani, A., and Caddick, S. (2016) Recent advances in the construction of antibody-drug conjugates. *Nat. Chem. 8*, 114–9.

(6) Wang, W., Wang, E. Q., and Balthasar, J. P. (2008) Monoclonal Antibody Pharmacokinetics and Pharmacodynamics. *Clin. Pharmacol. Ther. 84*, 548–558.

(7) KÖHLER, G., and MILSTEIN, C. (1975) Continuous cultures of fused cells secreting antibody of predefined specificity. *Nature 256*, 495–497.

(8) Nissim, A., and Chernajovsky, Y. (2008) Historical development of monoclonal antibody therapeutics. *Handb. Exp. Pharmacol. 181*, 3–18.

(9) Liu, J. K. H. (2014) The history of monoclonal antibody development - Progress, remaining challenges and future innovations. *Ann. Med. Surg. 3*, 113–116.

(10) Jefferis, R. (2009) Glycosylation as a strategy to improve antibody-based therapeutics. *Nat. Rev. Drug Discov. 8*, 226–34.

(11) Yang, X. D., Jia, X. C., Corvalan, J. R. F., Wang, P., and Davis, C. G. (2001) Development of ABX-EGF, a fully human anti-EGF receptor monoclonal antibody, for cancer therapy. *Crit. Rev. Oncol. Hematol. 38*, 17–23.

(12) Reichert, J. M. (2012) Marketed therapeutic antibodies compendium. *MAbs 4*, 413–415.

(13) Nelson, A. L., Dhimolea, E., and Reichert, J. M. (2010) Development trends for human monoclonal antibody therapeutics. *Nat. Rev. Drug Discov. 9*, 767–774.

(14) Gombotz, W. R., and Shire, S. J. (2010) Current Trends in Monoclonal Antibody Development and Manufacturing (Shire, S. J., Gombotz, W., Bechtold-Peters, K., and Andya, J., Eds.) First. Springer.

(15) Schroeder, H. W. J., and Cavacini, L. (2010) Structure and Function of Immunoglobulins. *J. Allergy Clin. Immunol. 125*, S41–S52.

(16) Vidarsson, G., Dekkers, G., and Rispens, T. (2014) IgG subclasses and allotypes: From structure to effector functions. *Front. Immunol. 5*, 1–17.

(17) Jr, J. C. a, York, N., and Science, G. (2001) The structure of a typical antibody molecule. *Immunobiology* 1–10.

(18) Cohen-Solal, J. (2004) Fc γ receptors. *Immunol. Lett. 92*, 199–205.

(19) Jefferis, R. (2009) Recombinant antibody therapeutics: the impact of glycosylation on mechanisms of action. *Trends Pharmacol. Sci. 30*, 356–362.

(20) Bondt, A., Rombouts, Y., Selman, M. H. J., Hensbergen, P. J., Reiding, K. R., Hazes, J. M. W., Dolhain, R. J. E. M., and Wuhrer, M. (2014) Immunoglobulin G (IgG) Fab Glycosylation Analysis Using a New Mass Spectrometric High-throughput Profiling Method Reveals Pregnancy-associated Changes. *Mol. Cell. Proteomics 13*, 3029–3039.

(21) del Val, I. J., Jedrzejewski, P. M., Exley, K., Sou, S. N., Kyriakopoulos, S., Polizzi, K. M., and Kontoravdi, C. (2012) Application of Quality by Design Paradigm to the Manufacture of Protein Therapeutics. *Glycosylation* 353–396.

(22) Baković, M. P., Selman, M. H. J., Hoffmann, M., Rudan, I., Campbell, H., Deelder, A. M., Lauc, G., and Wuhrer, M. (2013) High-throughput IgG Fc N-glycosylation profiling by mass spectrometry of glycopeptides. *J. Proteome Res. 12*, 821–831.

(23) Chen, X., Liu, D., Flynn, G. C., Liu, Y. D., and Flynn, G. C. (2009) The effect of Fc glycan forms on human IgG2 antibody clearance in humans. *Glycobiology 19*, 240–249.

(24) Stanley, P., Schachter, H., and Taniguchi, N. (2009) Chapter 8. N-Glycans, Essentials of Glycobiology, 2nd Edition. *Essentials Glycobiol.*

(25) Kornfeld, R., and Kornfeld, S. (1985) Assembly of Asparagine-Linked Oligosaccharides. *Annu. Rev. Biochem. 54*, 631–664.

(26) Weiner, G. J. (2015) Building better monoclonal antibody-based therapeutics. *Nat. Rev. Cancer 15*, 361–370.

(27) Glassman, P. M., and Balthasar, J. P. (2014) Mechanistic considerations for the use of monoclonal antibodies for cancer therapy. *Cancer Biol. Med. 11*, 20–33.

(28) Carter, P. (2001) Improving the efficacy of antibody-based cancer therapies. *Nat. Rev. Cancer 1*, 118–129.

(29) Abès, R., and Teillaud, J. L. (2010) Impact of glycosylation on effector functions of therapeutic IgG. *Pharmaceuticals 3*, 146–157.

(30) Mimura, Y., Church, S., Ghirlando, R., Ashton, P. R., Dong, S., Goodall, M., Lund, J., and Jefferis, R. (2000) The influence of glycosylation on the thermal stability and effector function expression of human IgG1-Fc: properties of a series of truncated glycoforms. *Mol Immunol 37*, 697–706.

(31) Nimmerjahn, F., and Ravetch, J. V. (2008) Fcgamma receptors as regulators of immune responses. *Nat. Rev. Immunol. 8*, 34–47.

(32) Bournazos, S., Wang, T. T., and Ravetch, J. V. (2016) The Role and Function of Fcγ Receptors on Myeloid Cells. *Microbiol. Spectr. 4*.

(33) Maenaka, K., Van der Merwe, P. A., Stuart, D. I., Jones, E. Y., and Sondermann, P. (2001) The Human Low Affinity Fcγ Receptors IIa, IIb, and III Bind IgG with Fast Kinetics and Distinct Thermodynamic Properties. *J. Biol. Chem. 276*, 44898–44904.

(34) van der Heijden, J., Breunis, W. B., Geissler, J., de Boer, M., van den Berg, T. K., and Kuijpers, T. W. (2012) Phenotypic Variation in IgG Receptors by Nonclassical FCGR2C Alleles. *J. Immunol. 188*, 1318–1324.

(35) Derer, S., Glorius, P., Schlaeth, M., Lohse, S., Klausz, K., Muchhal, U., Desjarlais, J. R., Valerius, T., and Peipp, M. (2014) Increasing Fc γ RIIa affinity of an Fc γ RIII-optimized anti-EGFR antibody restores neutrophil-mediated cytotoxicity 1–13.

(36) Moore, G. L., Chen, H., Karki, S., and Lazar, G. a. (2010) Engineered Fc variant antibodies with enhanced\nability to recruit complement and mediate\neffector functions. *MAbs 2*, 181–189.

(37) Mimoto, F., Igawa, T., Kuramochi, T., Katada, H., Kadono, S., Kamikawa, T., Shida-Kawazoe, M., and Hattori, K. (2013) Novel asymmetrically engineered antibody Fc variant with superior FcγR binding affinity and specificity compared with afucosylated Fc variant. *MAbs 5*, 229–236.

(38) Lazar, G. A., Dang, W., Karki, S., Vafa, O., Peng, J. S., Hyun, L., Chan, C., Chung, H. S., Eivazi, A., Yoder, S. C., Vielmetter, J., Carmichael, D. F., Hayes, R. J., and Dahiyat, B. I. (2006) Engineered antibody Fc variants with enhanced effector function. *Proc. Natl. Acad. Sci. 103*, 4005–4010.

(39) Kaneko, E., and Niwa, R. (2011) Optimizing therapeutic antibody function: Progress with fc domain engineering. *BioDrugs 25*, 1–11.

(40) Weng, W. K., and Levy, R. (2003) Two immunoglobulin G fragment C receptor polymorphisms independently predict response to rituximab in patients with follicular lymphoma. *J. Clin. Oncol. 21*, 3940–3947.

(41) Treon, S. P., Hansen, M., Branagan, A. R., Verselis, S., Emmanouilides, C., Kimby, E., Frankel, S. R., Touroutoglou, N., Turnbull, B., Anderson, K. C., Maloney, D. G., and Fox, E. A. (2005) Polymorphisms in FcgammaRIIIA (CD16) receptor expression are associated with clinical response to rituximab in Waldenström's macroglobulinemia. *J. Clin. Oncol.*

(42) Ramsland, P. a, Farrugia, W., Bradford, T. M., Sardjono, C. T., Esparon, S., Trist, H. M., Powell, M. S., Tan, P. S., Cendron, A. C., Wines, B. D., Scott, A. M., and Hogarth, P. M. (2011) Structural Basis for Fc{gamma}RIIa Recognition of Human IgG and Formation of Inflammatory Signaling Complexes. *J. Immunol. 187*, 3208–3217.

(43) Powell, M. S., Barton, P. A., Emmanouilidis, D., Wines, B. D., Neumann, G. M., Peitersz, G. A., Maxwell, K. F., Garrett, T. P., and Hogarth, P. M. (1999) Biochemical analysis and crystallisation of Fc gamma RIIa, the low affinity receptor for IgG. *Immunol. Lett. 68*, 17–23.

(44) van der Kolk, L. E., Grillo-Lopez, A. J., Baars, J. W., Hack, C. E., and van Oers, M. H. J. (2001) Complement activation plays a key role in the side-effects of rituximab treatment. *Br. J. Haematol. 115*, 807–811.

(45) Tawara, T., Hasegawa, K., Sugiura, Y., Harada, K., Miura, T., Hayashi, S., Tahara, T., Ishikawa, M., Yoshida, H., Kubo, K., Ishida, I., and Kataoka, S. (2008) Complement activation plays a key role in antibody-induced infusion toxicity in monkeys and rats. *J. Immunol. 180*, 2294–8.

(46) Weng, W. K., and Levy, R. (2001) Expression of complement inhibitors CD46, CD55, and CD59 on tumor cells does not predict clinical outcome after rituximab treatment in follicular non-Hodgkin lymphoma. *Blood 98*, 1352–1357.

(47) Bradbury, A. R. M., Sidhu, S., Dübel, S., and McCafferty, J. (2011) Beyond natural antibodies: the power of in vitro display technologies. *Nat. Biotechnol. 29*, 245–254.

(48) Ma, W., Gilligan, B. M., Yuan, J., and Li, T. (2016) Current status and perspectives in translational biomarker research for PD-1/PD-L1 immune checkpoint blockade therapy. *J. Hematol. Oncol. 9*, 47.

(49) Villadolid, J., and Amin, A. (2015) Immune checkpoint inhibitors in clinical practice: update on management of immune-related toxicities. *Transl. lung cancer Res. 4*, 560–575.

(50) Alexander, W. (2016) The Checkpoint Immunotherapy Revolution: What Started as a Trickle Has Become a Flood, Despite Some Daunting Adverse Effects; New Drugs, Indications, and Combinations Continue to Emerge. *P T 41*, 185–91.

(51) Roopenian, D. C., and Akilesh, S. (2007) FcRn: the neonatal Fc receptor comes of age. *Nat. Rev. Immunol. 7*, 715–725.

(52) Peters, C., and Brown, S. (2015) Antibody-drug conjugates as novel anti-cancer chemotherapeutics. *Biosci. Rep. 35*, e00225–e00225.

(53) Diamantis, N., and Banerji, U. (2016) Antibody-drug conjugates—an emerging class of cancer treatment. *Br. J. Cancer 114*, 362–367.

(54) Zhou, Q., Stefano, J. E., Manning, C., Kyazike, J., Chen, B., Gianolio, D. A., Park, A., Busch, M., Bird, J., Zheng, X., Simonds-Mannes, H., Kim, J., Gregory, R. C., Miller, R. J., Brondyk, W. H., Dhal, P. K., and Pan, C. Q. (2014) Site-specific antibody-drug conjugation through glycoengineering. *Bioconjug. Chem. 25*, 510–520.

(55) Junutula, J. R. J. R., Raab, H., Clark, S., Bhakta, S., Leipold, D. D. D., Weir, S., Chen, Y., Simpson, M., Tsai, S. P. S. P., Dennis, M. S. M. S., Lu, Y., Meng, Y. G., Ng, C., Yang, J., Lee, C. C., Duenas, E., Gorrell, J., Katta, V., Kim, A., McDorman, K., Flagella, K., Venook, R., Ross, S., Spencer, S. D., Lee Wong, W., Lowman, H. B., Vandlen, R., Sliwkowski, M. X., Scheller, R. H., Polakis, P., Mallet, W., and others. (2008) Site-specific conjugation of a cytotoxic drug to an antibody improves the therapeutic index. *Nat. Biotechnol. 26*, 925–32.

(56) Junutula, J. R., Bhakta, S., Raab, H., Ervin, K. E., Eigenbrot, C., Vandlen, R., Scheller, R. H., and Lowman, H. B. (2008) Rapid identification of reactive cysteine residues for site-specific labeling of antibody-Fabs. *J. Immunol. Methods 332*, 41–52.

(57) Schumacher, D., Hackenberger, C. P. R., Leonhardt, H., and Helma, J. (2016) Current Status: Site-Specific Antibody Drug Conjugates. *J. Clin. Immunol. 36*, 100–107.

(58) Panowski, S., Bhakta, S., Raab, H., Polakis, P., and Junutula, J. R. (2014) Site-specific antibody drug conjugates for cancer therapy. *MAbs 6*, 34–45.

(59) Irani, V., Guy, A. J., Andrew, D., Beeson, J. G., Ramsland, P. A., and Richards, J. S. (2015) Molecular properties of human IgG subclasses and their implications for designing therapeutic monoclonal antibodies against infectious diseases. *Mol. Immunol. 67*, 171–182.

(60) Salfeld, J. G. (2007) Isotype selection in antibody engineering. *Nat. Biotechnol. 25*, 1369–1372.

(61) Wypych, J., Li, M., Guo, A., Zhang, Z., Martinez, T., Allen, M. J., Fodor, S., Kelner, D. N., Flynn, G. C., Liu, Y. D., Bondarenko, P. V., Ricci, M. S., Dillon, T. M., and Balland, A. (2008) Human IgG2 antibodies display disulfide-mediated structural isoforms. *J. Biol. Chem. 283*, 16194–16205.

(62) Allen, M. J., Guo, A., Martinez, T., Han, M., Flynn, G. C., Wypych, J., Liu, Y. D., Shen, W. D., Dillon, T. M., Vezina, C., and Balland, A. (2009) Interchain disulfide bonding in human IgG2 antibodies probed by site-directed mutagenesis. *Biochemistry 48*, 3755–3766.

(63) Dillon, T. M., Ricci, M. S., Vezina, C., Flynn, G. C., Liu, Y. D., Rehder, D. S., Plant, M., Henkle, B., Li, Y., Deechongkit, S., Varnum, B., Wypych, J., Balland, A., and Bondarenko, P. V. (2008) Structural

and Functional Characterization of Disulfide Isoforms of the Human IgG2 Subclass. *J. Biol. Chem. 283*, 16206–16215.

(64) Liu, Y. D., Wang, T., Chou, R., Chen, L., Kannan, G., Stevenson, R., Goetze, A. M., Jiang, X. G., Huang, G., Dillon, T. M., and Flynn, G. C. (2013) IgG2 disulfide isoform conversion kinetics. *Mol. Immunol. 54*, 217–226.

(65) Yang, J., Goetze, A. M., and Flynn, G. C. (2014) Assessment of naturally occurring covalent and total dimer levels in human IgG1 and IgG2. *Mol. Immunol. 58*, 108–115.

(66) Bruhns, P., Iannascoli, B., England, P., Mancardi, D. A., Fernandez, N., Jorieux, S., and Daëron, M. (2009) Specificity and affinity of human Fcγ receptors and their polymorphic variants for human IgG subclasses. *Blood 113*, 3716–3725.

(67) Parren, P. W., Warmerdam, P. A., Boeije, L. C., Arts, J., Westerdaal, N. A., Vlug, A., Capel, P. J., Aarden, L. A., and van de Winkel, J. G. (1992) On the interaction of IgG subclasses with the low affinity Fc gamma RIIa (CD32) on human monocytes, neutrophils, and platelets. Analysis of a functional polymorphism to human IgG2. *J. Clin. Invest. 90*, 1537–46.

(68) Warmerdam, P. A., van de Winkel, J. G., Vlug, A., Westerdaal, N. A., and Capel, P. J. (1991) A single amino acid in the second Ig-like domain of the human Fc gamma receptor II is critical for human IgG2 binding. *J. Immunol. 147*, 1338–43.

(69) Asano, K., Matsushita, T., Umeno, J., Hosono, N., Takahashi, A., Kawaguchi, T., Matsumoto, T., Matsui, T., Kakuta, Y., Kinouchi, Y., Shimosegawa, T., Hosokawa, M., Arimura, Y., Shinomura, Y., Kiyohara, Y., Tsunoda, T., Kamatani, N., Iida, M., Nakamura, Y., and Kubo, M. (2009) A genome-wide association study identifies three new susceptibility loci for ulcerative colitis in the Japanese population. *Nat. Genet. 41*, 1325–1329.

(70) Li, X., Gibson, A. W., and Kimberly, R. P. (2014) Human FcR polymorphism and disease. *Curr. Top. Microbiol. Immunol.*

(71) Cooke, G. S., Aucan, C., Walley, A. J., Segal, S., Greenwood, B. M., Kwiatkowski, D. P., and Hill, A. V. S. (2003) Association of Fcγ receptor IIa (CD32) polymorphism with severe malaria in West Africa. *Am. J. Trop. Med. Hyg. 69*, 565–568.

(72) Suresh, E., and Abrahamsen, B. (2015) Denosumab: A novel antiresorptive drug for osteoporosis. *Cleve. Clin. J. Med. 82*, 105–114.

(73) Mahipal, A., Kothari, N., and Gupta, S. (2014) Epidermal growth factor receptor inhibitors: coming of age. *Cancer Control 21*, 74–9.

(74) Vafa, O., Gilliland, G. L., Brezski, R. J., Strake, B., Wilkinson, T., Lacy, E. R., Scallon, B., Teplyakov, A., Malia, T. J., and Strohl, W. R. (2014) An engineered Fc variant of an IgG eliminates all immune effector functions via structural perturbations. *Methods 65*, 114–126.

(75) Stapleton, N. M., Terje Andersen, J., Stemerding, A. M., Bjarnarson, S. P., Verheul, R. C., Gerritsen, J., Zhao, Y., Kleijer, M., Sandlie, I., de Haas, M., Jonsdottir, I., Ellen van der Schoot, C., Vidarsson, G., Andersen, J. T., Stemerding, A. M., Bjarnarson, S. P., Verheul, R. C., Gerritsen, J., Zhao, Y., Kleijer, M., Sandlie, I., de Haas, M., Jonsdottir, I., van der Schoot, C. E., and Vidarsson, G. (2011) Competition for FcRn-mediated transport gives rise to short half-life of human IgG3 and offers therapeutic potential. *Nat. Commun. 2*, 599.

(76) Abhinandan, K. R., and Martin, A. C. R. (2008) Analysis and improvements to Kabat and structurally correct numbering of antibody variable domains. *Mol. Immunol. 45*, 3832–3839.

(77) Nirula, A., Glaser, S. M., Kalled, S. L., and Taylor, F. R. (2011) What is IgG4? A review of the biology of a unique immunoglobulin subtype. *Curr. Opin. Rheumatol. 23*, 119–124.

(78) van der Neut Kolfschoten, M., Schuurman, J., Losen, M., Bleeker, W. K., Martinez-Martinez, P., Vermeulen, E., den Bleker, T. H., Wiegman, L., Vink, T., Aarden, L. A., De Baets, M. H., van de Winkel, J. G. J., Aalberse, R. C., and Parren, P. W. H. I. (2007) Anti-Inflammatory Activity of Human IgG4 Antibodies by Dynamic Fab Arm Exchange. *Science (80-.). 317*, 1554–1557.

(79) Reddy, M. P., Kinney, C. a, Chaikin, M. a, Payne, A., Fishman-Lobell, J., Tsui, P., Dal Monte, P. R., Doyle, M. L., Brigham-Burke, M. R., Anderson, D., Reff, M., Newman, R., Hanna, N., Sweet, R. W., and Truneh, A. (2000) Elimination of Fc receptor-dependent effector functions of a modified IgG4 monoclonal antibody to human CD4. *J. Immunol. 164*, 1925–1933.

(80) Suntharalingam, G., Perry, M. R., Ward, S., Brett, S. J., Castello-Cortes, A., Brunner, M. D., and Panoskaltsis, N. (2006) Cytokine storm in a phase 1 trial of the anti-CD28 monoclonal anti- body TGN1412. *N Engl J Med 355*, 1018–1028.

(81) Scapin, G., Yang, X., Prosise, W. W., McCoy, M., Reichert, P., Johnston, J. M., Kashi, R. S., and Strickland, C. (2015) Structure of full-length human anti-PD1 therapeutic IgG4 antibody pembrolizumab. *Nat. Struct. Mol. Biol. 22*, 953–958.

(82) Dang, T. O., Ogunniyi, A., Barbee, M. S., and Drilon, A. (2015) Pembrolizumab for the treatment of PD-L1 positive advanced or metastatic non-small cell lung cancer. *Expert Rev. Anticancer Ther. 7140*, 1–8.

(83) Liu, H., Bulseco, G. G., and Sun, J. (2006) Effect of posttranslational modifications on the thermal stability of a recombinant monoclonal antibody. *Immunol. Lett. 106*, 144–153.

(84) Krapp, S., Mimura, Y., Jefferis, R., Huber, R., and Sondermann, P. (2003) Structural analysis of human IgG-Fc glycoforms reveals a correlation between glycosylation and structural integrity. *J. Mol. Biol. 325*, 979–989.

(85) More, A. S., Toprani, V. M., Okbazghi, S. Z., Kim, J. H., Joshi, S. B., Middaugh, C. R., Tolbert, T. J., and Volkin, D. B. (2016) Correlating the Impact of Well-Defined Oligosaccharide Structures on Physical Stability Profiles of IgG1-Fc Glycoforms. *J. Pharm. Sci. 105*, 588–601.

(86) Alsenaidy, M. A., Okbazghi, S. Z., Kim, J. H., Joshi, S. B., Russell Middaugh, C., Tolbert, T. J., and Volkin, D. B. (2014) Physical stability comparisons of IgG1-Fc variants: Effects of N-glycosylation site occupancy and Asp/gln residues at site asn 297. *J. Pharm. Sci. 103*, 1613–1627.

(87) Latypov, R. F., Hogan, S., Lau, H., Gadgil, H., and Liu, D. (2012) Elucidation of acid-induced unfolding and aggregation of human immunoglobulin IgG1 and IgG2 Fc. *J. Biol. Chem. 287*, 1381–1396.

(88) Middaugh, C. R., and Litman, G. W. (1987) Atypical glycosylation of an IgG monoclonal cryoimmunoglobulin. *J. Biol. Chem. 262*, 3671–3673.

(89) Quast, I., Peschke, B., and Lünemann, J. D. (2017) Regulation of antibody effector functions through IgG Fc N-glycosylation. *Cell. Mol. Life Sci. 74*, 837–847.

(90) Shields, R. L., Lai, J., Keck, R., O'Connell, L. Y., Hong, K., Meng, Y. G., Weikert, S. H. A., and Presta, L. G. (2002) Lack of Fucose on Human IgG1 N-Linked Oligosaccharide Improves Binding to

Human Fcgamma RIII and Antibody-dependent Cellular Toxicity. *J. Biol. Chem. 277*, 26733–26740.

(91) Shinkawa, T., Nakamura, K., Yamane, N., Shoji-Hosaka, E., Kanda, Y., Sakurada, M., Uchida, K., Anazawa, H., Satoh, M., Yamasaki, M., Hanai, N., and Shitara, K. (2003) The absence of fucose but not the presence of galactose or bisecting N-acetylglucosamine of human IgG1 complex-type oligosaccharides shows the critical role of enhancing antibody-dependent cellular cytotoxicity. *J Biol Chem 278*, 3466–3473.

(92) Yamane-Ohnuki, N., and Satoh, M. (2009) Production of therapeutic antibodies with controlled fucosylation. *MAbs 1*, 230–6.

(93) Ferrara, C., Grau, S., Jager, C., Sondermann, P., Brunker, P., Waldhauer, I., Hennig, M., Ruf, A., Rufer, A. C., Stihle, M., Umana, P., and Benz, J. (2011) Unique carbohydrate-carbohydrate interactions are required for high affinity binding between Fc RIII and antibodies lacking core fucose. *Proc. Natl. Acad. Sci. 108*, 12669–12674.

(94) Mizushima, T., Yagi, H., Takemoto, E., Shibata-Koyama, M., Isoda, Y., Iida, S., Masuda, K., Satoh, M., and Kato, K. (2011) Structural basis for improved efficacy of therapeutic antibodies on defucosylation of their Fc glycans. *Genes to Cells 16*, 1071–1080.

(95) Raju, T. S. (2008) Terminal sugars of Fc glycans influence antibody effector functions of IgGs. *Curr. Opin. Immunol. 20*, 471–478.

(96) van de Geijn, F. E., Wuhrer, M., Selman, M. H., Willemsen, S. P., de Man, Y. A., Deelder, A. M., Hazes, J. M., and Dolhain, R. J. (2009) Immunoglobulin G galactosylation and sialylation are associated with pregnancy-induced improvement of rheumatoid arthritis and the postpartum flare: results from a large prospective cohort study. *Arthritis Res. Ther. 11*, R193.

(97) Kaneko, Y., Nimmerjahn, F., and Ravetch, J. V. (2006) Anti-Inflammatory Activity of Immunoglobulin G Resulting from Fc Sialylation. *Science (80-.). 313*, 670–673.

(98) Anthony, R. M., Wermeling, F., Karlsson, M. C. I., and Ravetch, J. V. (2008) Identification of a receptor required for the anti-inflammatory activity of IVIG. *Proc. Natl. Acad. Sci. 105*, 19571–19578.

(99) Quast, I., Keller, C. W., Maurer, M. A., Giddens, J. P., Tackenberg, B., Wang, L. X., Münz, C., Nimmerjahn, F., Dalakas, M. C., and Lünemann, J. D. (2015) Sialylation of IgG Fc domain impairs complement-dependent cytotoxicity. *J. Clin. Invest. 125*, 4160–4170.

(100) Goetze, A. M., Liu, Y. D., Zhang, Z., Shah, B., Lee, E., Bondarenko, P. V., and Flynn, G. C. (2011) High-mannose glycans on the Fc region of therapeutic IgG antibodies increase serum clearance in humans. *Glycobiology 21*, 949–959.

(101) Reusch, D., and Tejada, M. L. (2015) Fc glycans of therapeutic antibodies as critical quality attributes. *Glycobiology*.

(102) Gorovits, B., and Krinos-Fiorotti, C. (2013) Proposed mechanism of off-target toxicity for antibody-drug conjugates driven by mannose receptor uptake. *Cancer Immunol. Immunother. 62*, 217–223.

(103) Beck, A., and Reichert, J. M. (2012) Marketing approval of mogamulizumab A triumph for glyco-engineering. *MAbs 4*, 419–425.

(104) Gagez, A.-L., and Cartron, G. (2014) Obinutuzumab: a new class of anti-CD20 monoclonal antibody. *Curr. Opin. Oncol. 26*, 484–491.

(105) Okeley, N. M., Alley, S. C., Anderson, M. E., Boursalian, T. E., Burke, P. J., Emmerton, K. M., Jeffrey, S. C., Klussman, K., Law, C.-L., Sussman, D., Toki, B. E., Westendorf, L., Zeng, W., Zhang, X., Benjamin, D. R., and Senter, P. D. (2013) Development of orally active inhibitors of protein and cellular fucosylation. *Proc. Natl. Acad. Sci. U. S. A. 110*, 5404–9.

(106) Bobrowicz, P., Davidson, R. C., Li, H., Potgieter, T. I., Nett, J. H., Hamilton, S. R., Stadheim, T. a., Miele, R. G., Bobrowicz, B., Mitchell, T., Rausch, S., Renfer, E., and Wildt, S. (2004) Engineering of an artificial glycosylation pathway blocked in core oligosaccharide assembly in the yeast Pichia pastoris: Production of complex humanized glycoproteins with terminal galactose. *Glycobiology 14*, 757–766.

(107) Zheng, K., Bantog, C., and Bayer, R. (2011) The impact of glycosylation on monoclonal antibody conformation and stability. *MAbs 3*, 568–576.

(108) Huang, W., Giddens, J., Fan, S. Q., Toonstra, C., and Wang, L. X. (2012) Chemoenzymatic glycoengineering of intact IgG antibodies for gain of functions. *J. Am. Chem. Soc. 134*, 12308–12318.

(109) Quast, I., and Lunemann, J. D. (2014) Fc glycan-modulated immunoglobulin G effector functions. *J. Clin. Immunol. 34*.

(110) Sha, S., Agarabi, C., Brorson, K., Lee, D.-Y., and Yoon, S. (2016) N-Glycosylation Design and Control of Therapeutic Monoclonal Antibodies. *Trends Biotechnol. 34*, 835–846.

Chapter 2

Production of IgG2 Fc with core-linked fucose and studies of its effects on stability, receptor binding and FUT8 glycosylation site kinetics

Introduction

The immunoglobulin G (IgG) class of antibody is the prevalent immunoglobulin (Ig) isotype in blood and is responsible for a wide range of systemic immune responses. In humans, the IgG isotype is made up of four subclasses, IgG1, IgG2, IgG3, and IgG4, which are numbered to reflect decreasing amounts in serum, such that IgG1 is present in the highest concentration and IgG4 the least.[1,2] The four human IgG subclasses are highly homologous, but differences in the heavy chain sequences of their constant and hinge regions result in a range of effector functions that can adapt antibody-dependent immune responses to different pathogens. Human IgG2 is the second most abundant IgG in serum and has been found to have distinct properties from the more studied IgG1 subclass. In general, IgG2 has the weakest interaction of the subclasses with Fcγ receptors that direct cellular immune responses, and it has the second weakest ability to activate complement for complement-dependent cytotoxicity. Even though IgG2 is thought to have weak effector functions, IgG2 antibodies are associated with immune responses to bacterial polysaccharide antigens, and deficiencies of the IgG2 subclass have been associated with susceptibility to bacterial infections.[3–6] Like IgG1, IgG2 is glycosylated on Asn297 (Eu numbering) [1,7,8] in the Fc region C_H2 domain and this N-linked glycosylation is important for antibody stability and essential to most immune responses directed by IgG2 antigen binding.[9,10] Because of IgG2's properties, it is an attractive subclass for the development of monoclonal antibody therapeutics where blocking of targets by binding but weaker effector functions are desired. There are currently only two human IgG2-based monoclonal antibodies (mAb) in use clinically, panitumumab and denosumab.[11–13]

Core-linked fucosylation of N-linked glycans in the IgG class of antibodies has been shown to act as a modulator of IgG effector functions.[14] Fucosylation has been linked to weaker

interactions of the IgG class of antibodies with Fcγ receptor IIIa (FcγRIIIa), which is a receptor involved in directing antibody dependent cellular cytotoxicity (ADCC) of many immune cells and the only Fcγ receptor found on most human natural killer cells (NK cells).[15] The effects of core-linked fucosylation on interactions with FcγRIIIa have been best studied in the IgG1 subclass, where the presence of fucose has been shown to reduce IgG1 affinity for FcγRIIIa by up to 50-fold[14,16–19] and thereby decrease ADCC activity of FcγRIIIa expressing immune cells. The reason for this reduced affinity has been shown to be due to core-linked fucose interrupting glycan-glycan interactions that are present between non-fucosylated IgG1 and the N-linked glycans of Asn162 on FcγRIIIa.[18,19] Since the absence of core-linked fucosylation on IgG1 significantly increases ADCC, there has been much effort to develop methods to produce non-fucosylated antibodies with increased ADCC activity for use as therapeutics where strong effector functions are desired.[20] The addition of core-linked fucose to N-glycans is mediated by a single enzyme, α-1,6-fucosyltransfurase 8 (FUT8) in mammals.[21,22] The production of antibodies in cell lines with FUT8 deleted will result in non-fucosylated antibodies with increased ability to direct ADCC, and such cell lines have been utilized to produce therapeutic mAb.[23]

Since the use of the IgG2 subclass as a therapeutic currently focuses largely on IgG2's reduced ability to direct effector functions, we were interested in studying the effect of the presence of core-fucosylation on IgG2 rather than its absence. These studies were hampered to some extent by the necessity of producing fully fucosylated IgG2 Fc and by the presence of glycoprotein microheterogeneity in glycoproteins produced in common cell lines.[24–28] Glycoprotein microheterogeneity, such as incomplete core fucosylation, presents a substantial barrier to the study of the function of protein glycosylation. Assays of glycoform mixtures in glycoprotein studies can result in unclear results due to the fact that each component of the

mixture can respond differently. This problem can be exacerbated when the presence of a contaminating glycoform, such as a non-fucosylated IgG, gives a stronger signal in an assay such as receptor binding than the fucosylated glycoform under study.[14,16,18,19] For this reason, it is desirable to conduct experiments on samples as close to homogeneous as can be practically achieved. Thus to study the effects of core fucosylation on IgG2 Fc we developed methods to produce homogeneously core-fucosylated IgG2 Fc on relatively large laboratory-scale as part of a larger project to produce a wide range of homogeneously glycosylated glycoproteins to facilitate glycobiology studies.

N-linked glycoprotein biosynthesis can result in the formation of a large number of possible high mannose, hybrid and complex glycoforms due to branching pathways, competing reactions and incomplete processing. Nonetheless, many glycoproteins contain only a specific subset of the possible N-glycan structures after processing.[29] For instance, IgG glycosylation at Asn297 is largely of the complex, biantennary type with varying amounts of core-fucose, galactose, and sialic acid depending on expression host and culture conditions.[30–32] In addition, glycoproteins with multiple glycosylation sites often have distinct types of glycosylation at their different sites, indicating these differences are not due to simple compartmentalization of glycosidases and glycosyltransferases in the Golgi apparatus. An example of this is glycosylation of two sites on IgD, where it has been reported that the Asn445 glycosylation site is about 40% fucosylated while the Asn496 site is not fucosylated.[33] Such specific glycan repertoires could be due to local protein structure or dynamics, accessory protein interactions, or a variety of other factors.

The strategy that was utilized to produce IgG2 Fc with and without core-linked fucosylation for comparative studies was to utilize glycosylation-deficient yeast which lack the

ability to add core-linked fucose to produce high mannose IgG2 Fc, and then use *in vitro* enzymatic synthesis to convert the initial high mannose glycoform into homogeneous high mannose, hybrid and core-linked fucosylated hybrid (Fuc(+) hybrid) IgG2 Fc. This allowed the production of hybrid and Fuc(+)-hybrid glycoforms that differ only in the presence or absence of core-linked fucose for comparative studies. During this process, we developed methods to produce the FUT8 enzyme in *E. coli* and utilized it to produce fucosylated glycoproteins. This enabled studies of the effects of core-fucosylation on IgG2 Fc stability and receptor binding by a comparison of the behavior of the homogeneous hybrid and Fuc(+) hybrid glycoforms. In addition, during the course of developing *in vitro* enzymatic methods to produce core-linked fucosylated IgG2 Fc, we noticed differences in the rates that FUT8 accepted free glycans versus protein-bound glycans. Due to the relatively large-scale production of the homogeneous IgG2 Fc glycoforms described here we were able to further investigate these results with kinetic studies. The glycosylation site preferences of FUT8 for two different IgG2 Fc glycosylation site variants were studied and compared to the kinetics of fucose transfer to the free glycan. These studies show that FUT8 has significant substrate specificity for different glycosylation sites on the same protein and these preferences appear to be caused by differences in glycosylation site accessibility.

Results

Production and characterization of IgG2 Fc glycosylation site variants

The consensus sequence for human IgG2 heavy chain contains a single conserved N-linked glycosylation site at Asn297 in the C_H2 domain (Eu numbering).[1,7,8] The human IgG2 heavy chain cDNA used as a template for the subcloning of IgG2 Fc in this work, MGC-71314

obtained from the mammalian gene collection[34], contains an unusual polymorphism which results in an additional N-linked glycosylation site at Asn392 in the C_H3 domain. Because of this, site-directed mutagenesis was utilized to convert the Asn392 residue from the cDNA template to a Lys392 residue to match the human IgG2 Fc consensus sequence.[1] In addition, to better study the effect of different types of glycosylation sites on FUT8 kinetics, a second mutation was produced in which the Asn297 glycosylation site was removed by mutating it to a glutamine (Q297). The result of the subcloning and mutagenesis described here is three glycosylation variants of IgG2 Fc, one which matches the human IgG2 Fc consensus sequence with a single glycosylation site at Asn297 (N297, K392), one with a single glycosylation site at N392 (Q297, N392), and one derived from the original cDNA with two N-linked glycosylation sites (N297, N392), as illustrated in Figure 1. Hereafter the IgG2 Fc glycosylation variant which matches the consensus sequence (N297, K392) will be referred to as IgG2 Fc, and the other two glycosylation variants will be referred to as IgG2 Fc-(Q297, N392) and IgG2 Fc-(N297, N392) to distinguish them from the IgG2 Fc consensus sequence.

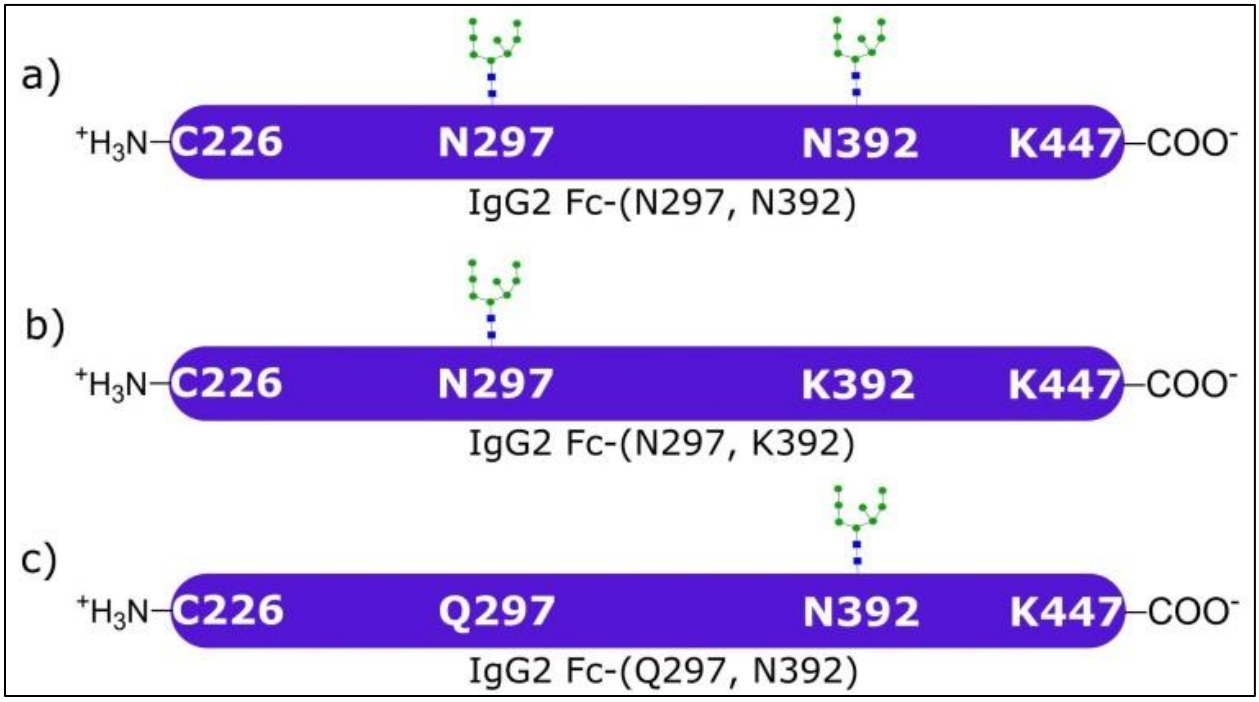

Figure 1. IgG2 Fc glycosylation site variants utilized in this study: a) IgG2 Fc-(N297, N392); a naturally occurring but uncommon IgG2 glycosylation variant having an additional glycosylation site at residue 392 in addition to the well conserved Asn297 glycosylation site, b) IgG2 Fc-(N297, K392); the widely accepted IgG2 Fc consensus sequence having a single conserved N-glycosylation site at residue 297 in the C_H2 domain and a lysine (K) residue at position 392, c) IgG2 Fc-(Q297, N392); an IgG2 Fc mutant designed to have an N-glycosylation site at residue 392 in the C_H3 domain but without the conserved N-glycosylation site at residue 297, for subsequent use in the enzyme kinetic studies of this chapter.

IgG2 Fc was expressed in an OCH1 deleted strain of SMD1168 *Pichia pastoris* produced previously in our laboratory.[35] In this study, three 7-L BioFlo 415 fermentations were conducted to produce approximately 1 g of IgG2 Fc (Table I). The majority of this IgG2 Fc was diglycosylated. However, a minor fraction of hemiglycosylated Fc (one chain of the Fc dimer is glycosylated while the other chain is non-glycosylated) was present contaminating the diglycosylated Fc due to incomplete N-glycosylation site occupancy (Appendix: Figure A1 lane 2 and Figure A2 panel A).[36,37] The diglycosylated IgG2 Fc was separated from the hemiglycosylated Fc using hydrophobic interaction chromatography (HIC). After HIC, 395 mg of the purified diglycosylated IgG2 Fc was produced consisting of glycoforms containing mainly high mannose glycans with a small fraction of mannose phosphorylated glycans [38] present as shown in Figure A2 (panel B) of the appendix. We were able, however, to remove the mannose phosphorylated fractions by using weak cation exchange (WCX) chromatography to produce 185 mg of purely high mannose IgG2 Fc containing mainly $Man_8GlcNAc_2$ and $Man_9GlcNAc_2$ high mannose glycoforms (Appendix: Figure A2, panel E). Presumably mannose phosphorylation adds additional negative charges to the glycoprotein (IgG2 Fc) and results in the reduction of the overall positive charge of the protein. Therefore, the phosphorylated fractions elute earlier from the WCX column than the non-phosphorylated fractions, which are more positively charged. Moreover, removal of the phosphorylation heterogeneity in this way allows subsequent complete digestion of the initial high mannose glycoforms to a homogeneous Man5 glycoform which can then be used as a starting material in the synthesis of hybrid and Fuc(+) hybrid glycoforms.

Production of soluble mammalian α1,6-fucosyltransferase (FUT8) in E. coli

FUT8, as a mammalian enzyme having four disulfide bonds, presents a potential problem for expression in the generally reducing environment of the bacterial cytoplasm. Due to the

number of disulfide bonds in FUT8, we decided to use an *E. coli* strain capable of forming disulfide bonds in the cytoplasm during protein expression. Recently, an *E. coli* protein expression strain named SHuffle has been engineered.[39] This strain has diminished cytoplasmic reductive pathways and contains a cytoplasmic DsbC (an oxido-reductase chaperon) to facilitate the formation of correctly-folded, disulfide-bonded heterologous proteins with a high yield in the bacterial cytoplasm. An IPTG inducible plasmid construct was produced here to express the soluble domain of FUT8 in this bacterial strain. Transforming this strain directly with the FUT8 expression construct resulted in an undetectable level of FUT8 expression (Appendix: Figure A3 lane 6). However, transforming the FUT8-tranformed SHuffle T7 Express with the supplemental tRNA plasmid pRARE2 enabled expression of the recombinant FUT8 enzyme (Appendix: Figure A3 lane 9). The specific activity of FUT8 after purification was measured and found to be 0.12 μmole/min/mg. The total FUT8 activity obtained from one liter bacterial expression was 0.21 U (μmol/min).

In vitro enzymatic synthesis of IgG2 Fc glycoforms

Starting with high mannose IgG2 Fc obtained from yeast expression as a starting material, homogeneous Man5, hybrid, and Fuc(+) hybrid glycoforms were synthesized as outlined in Figure 2.

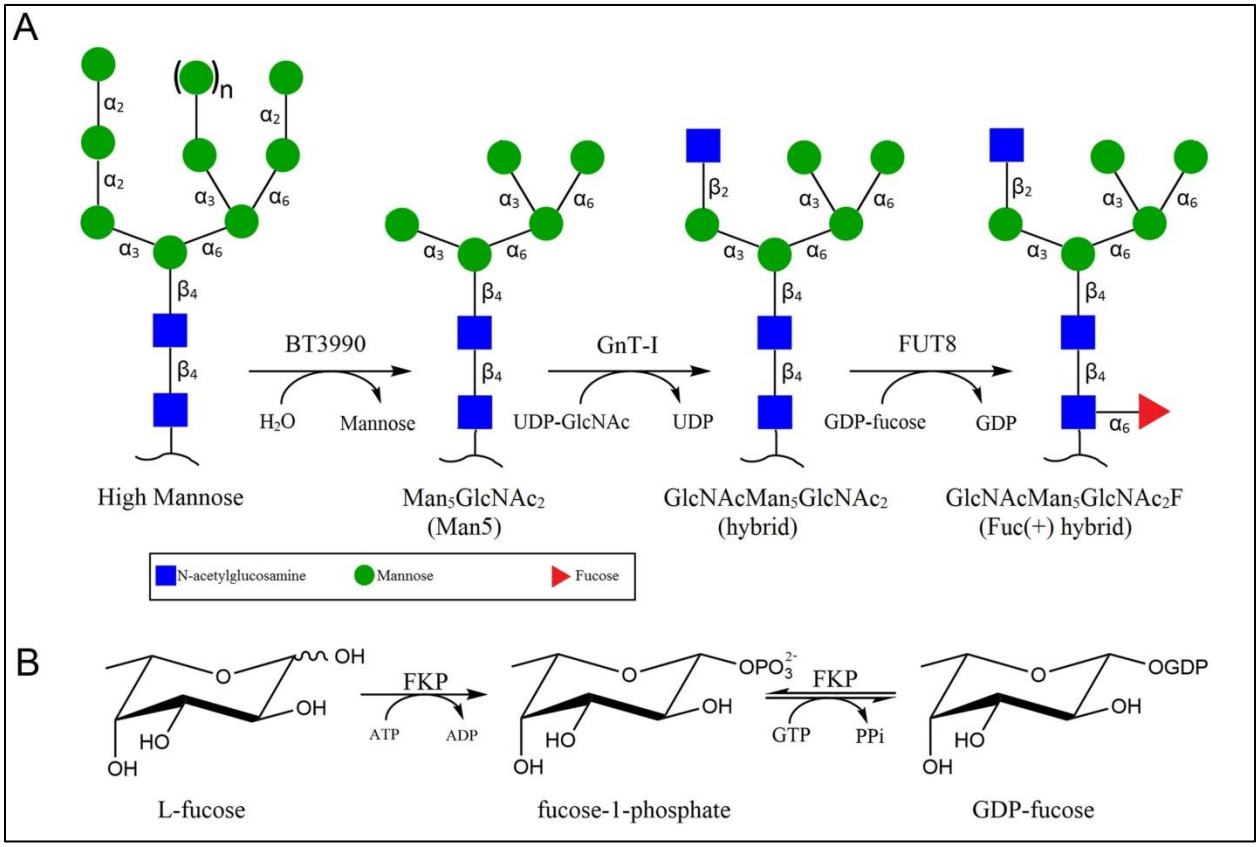

Figure 2. Enzymatic synthesis of homogeneous IgG2 Fc glycoforms and GDP-fucose. **A)** *In vitro* enzymatic synthesis of Man5, hybrid and Fuc(+) hybrid IgG2 Fc glycoforms using high mannose IgG2 Fc as a starting material. BT3990: bacterial α1,2- mannosidase; GnT-I: N-Acetylglucosaminyltransferase I; FUT8: mammalian α1,6-fucosyltransferase. **B)** Reaction catalyzed by L-fucokinase/guanosine 5'-diphosphate-L-fucose pyrophosphorylase (FKP) for the synthesis of guanosine 5′-diphospho-β-L-fucose (GDP-L-fucose) from L-fucose.

The quantities and the yield of the different IgG2 Fc glycoforms produced in this study are summarized in Table I. First, 185 mg of high mannose IgG2 Fc (Figure 3A, also see Appendix Figure A4 lane 1) was digested with bacterial α1,2-mannosidase BT3990 (Zhu et al. 2010; Cuskin et al. 2015; Okbazghi et al. 2016). Isolation of the product using protein G affinity chromatography resulted in 162 mg of Man5 IgG2 Fc which corresponds to 89% yield (Figure 3B, also see Appendix Figure A4 lane 2). Next, treatment of 140 mg of Man5 IgG2 Fc with GnT-I (produced in house as described previously[42]) in the presence of UDP-GlcNAc resulted in formation of the hybrid glycoform. After protein G affinity chromatography, 130 mg of hybrid IgG2 Fc was obtained in 92% isolated yield (Figure 3C, also see Appendix Figure A4 lane 3). Finally, the Fuc(+) hybrid IgG2 Fc was produced from the hybrid IgG2 Fc glycoform using a FUT8-catalyzed reaction. The FUT8 reaction requires the presence of β1,2- linked GlcNAc on the α1,3-mannose arm of the acceptor substrate N-glycan[43], which is provided in the hybrid glycoform. It also requires GDP-L-fucose as a donor substrate, which was made available by *in situ* formation of GDP-fucose from fucose, ATP, and GTP catalyzed by the enzyme FKP (Figure 2B).[44] FUT8 reaction progress was followed by intact protein mass spectrometry which showed that a full conversion of hybrid glycoform into the Fuc(+) hybrid glycoform over the course of two days (Figure 3D and 3E-H, also see Appendix Figure A4 lane 4). In this study, we converted 20 mg of the hybrid IgG2 Fc glycoform into Fuc(+) hybrid glycoform.

Table I. IgG2 Fc glycoforms yields summary

Step	**Amount Fc used (mg)**	**Amount Fc obtained (mg)**	**Yield (%)**
Fermentation	NA[a]	1000	NA[a]
HIC purification	730	395	54
WCX purification	395	205	52
BT3990 reaction (synthesis of Man5 Fc)	185	162	89
GnT-I reaction (synthesis of hybrid Fc)	140	130	92
FUT8 reaction (synthesis of Fuc(+) hybrid)	20	19	94

[a]Not applicable

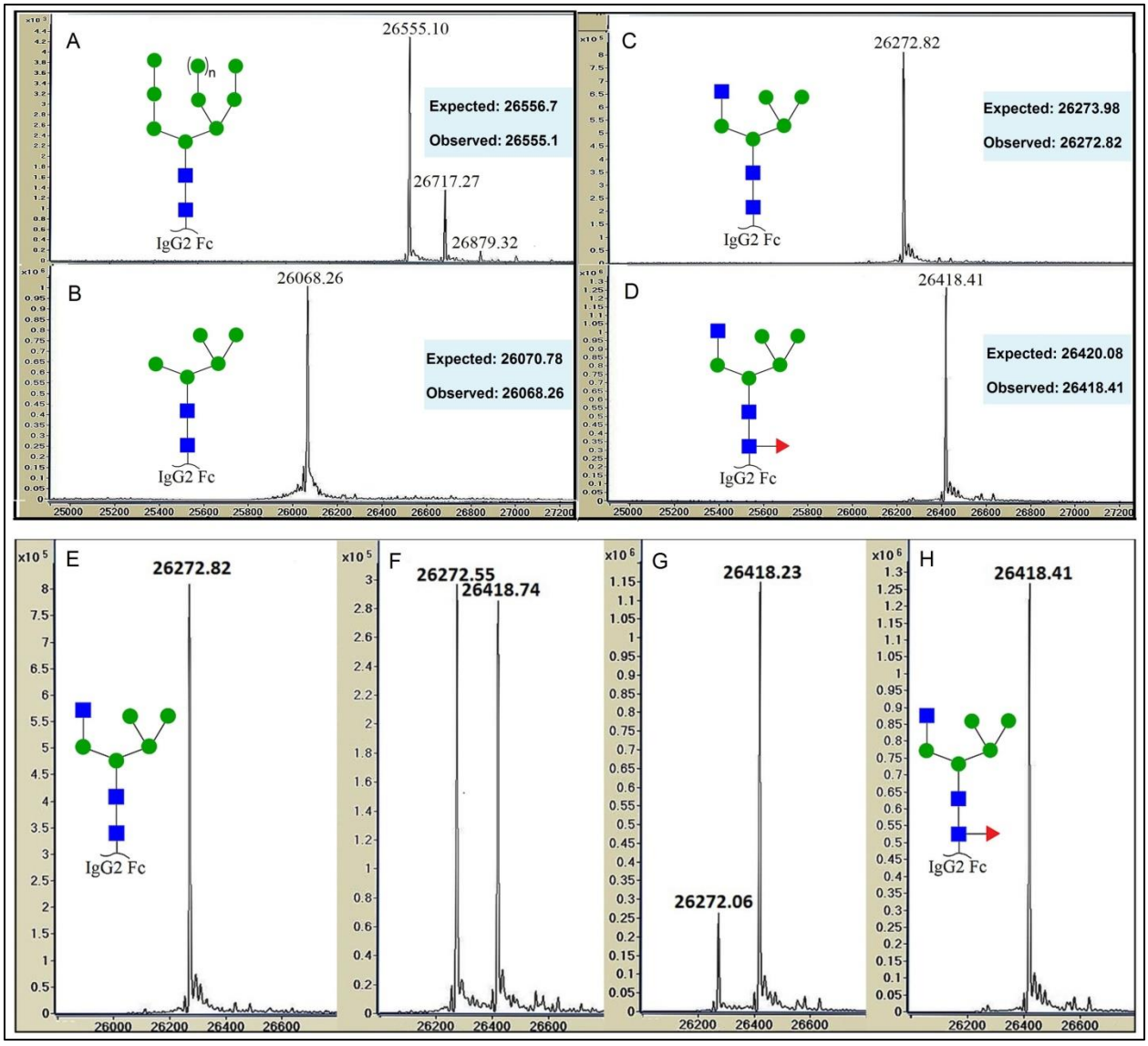

Figure 3. Intact protein mass spectra under reducing conditions for IgG2 Fc glycoforms, and time course for *in vitro* enzymatic synthesis of Fuc(+) hybrid IgG2 Fc. **A)** Heterogeneous high mannose IgG2 Fc glycoform obtained directly from *Pichia pastoris* after purification by Protein G, HIC and WCX chromatography, **B)** Man5 IgG2 Fc, **C)** hybrid IgG2 Fc, **D)** Fuc(+) hybrid IgG2 Fc. **E-H:** Time course for the enzymatic synthesis of the Fuc(+) hybrid IgG2 Fc glycoform as monitored by Q-TOF LC/MS at different time points: **E)** 0 h, **F)** 12 h, **G)** 22 h, **H)** 48 h.

Binding studies using biolayer interferometry (BLI)

Biolayer interferometry (BLI) was used to measure the kinetics and strength of IgG2 Fc/ FcγRs interaction. For robust immobilization of the receptors, site-specific biotinylation of FcγRIIIa-V158, FcγRIIa-H131, and FcγRIIa-R131 at their C-termini was performed using sortase-mediated ligation.[45] This biotinylation enabled site-specific immobilization of these receptors on streptavidin biosensors (Appendix: Figure A5).

Although IgG2 is known to have the weakest binding for FcγRIIIa-V158 among all human IgG subclasses [46], our IgG2 Fc binding studies (Figure 4 and Table II) showed that hybrid IgG2 Fc binds detectibly, although weakly to FcγRIIIa-V158 (K_D = 188 μM). Addition of core fucose to IgG2 Fc clearly reduced the binding to this receptor since the binding of Fuc(+) hybrid IgG2 Fc at 70 μM gave a weaker signal compared to the binding of hybrid IgG2 Fc at the same concentration. The concentration of Fuc(+) hybrid IgG2 Fc was raised to a higher level in an attempt to obtain stronger binding signals to calculate the binding constants. Unfortunately, the higher protein concentration resulted in massive distortion of the binding sensorgram (Appendix: Figure A6). Therefore, to get rough numbers for the binding of Fuc(+) IgG2 Fc to FcγRIIIa-V158, we calculated these numbers based on a single concentration (70 μM) repeated in triplicate as shown in Figure A7 of the appendix. The K_D calculated in this way was 2420 μM which is about 13-fold higher than the K_D of binding the hybrid glycoform to FcγRIIIa-V158. On the other hand, the binding of the hybrid IgG2 Fc and Fuc(+) hybrid IgG2 Fc to FcγRIIa-H131 variant was similar (K_D= 2.1 μM). Finally, the effect of core fucosylation was also tested on the binding of IgG2 to FcγRIIa-R131 variant. The results showed similar binding constants for the hybrid (K_D= 18.6 μM) and Fuc(+) hybrid (K_D= 17.4μM) IgG2 Fcs to FcγRIIa-R131, and a

general reduction (~ 8-fold) in IgG2 Fc binding affinity to this receptor variant of FcγRIIa compared to the H131 variant.

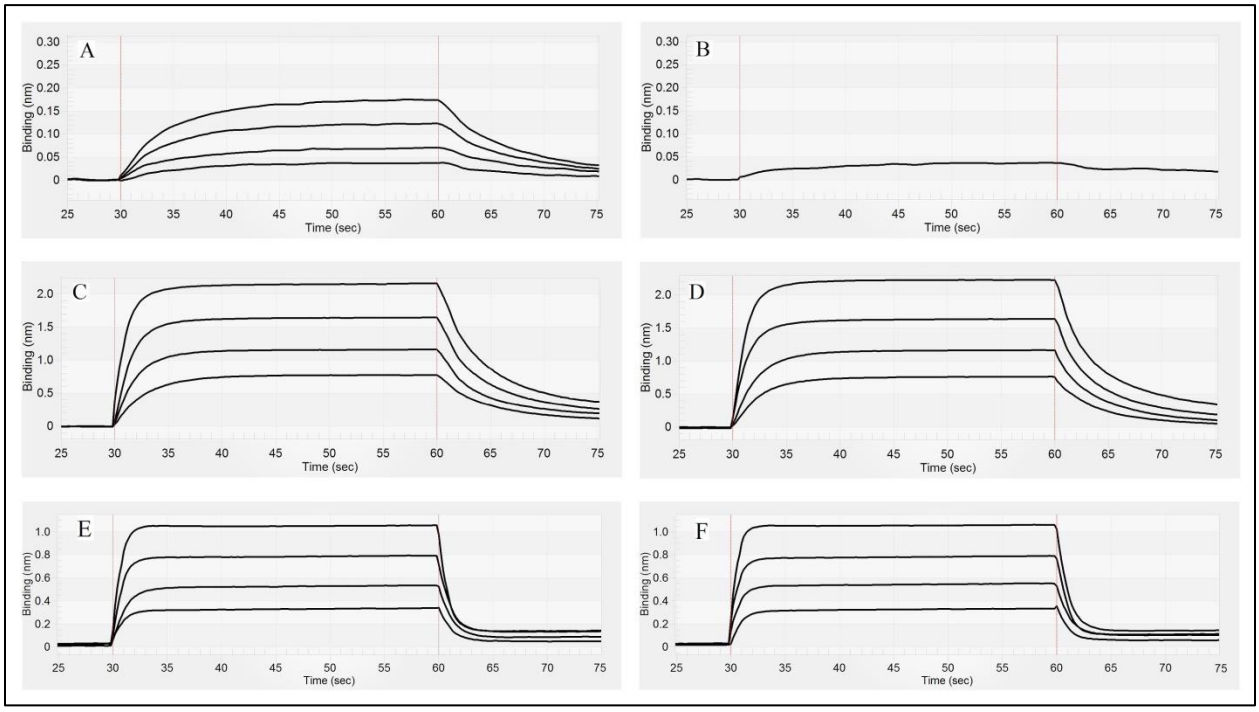

Figure 4. Biolayer interferometry (BLI) analyses showing the sensorgrams for IgG2 Fc glycoforms binding to Fcγ receptors. **A)** binding of hybrid IgG2 Fc to immobilized FcγRIIIa-V158, **B)** binding of Fuc(+) hybrid IgG2 Fc to immobilized FcγRIIIa-V158, **C)** binding of hybrid IgG2 Fc to immobilized FcγRIIa-H131, **D)** binding of Fuc(+) hybrid IgG2 Fc to immobilized FcγRIIa-H131, **E)** binding of hybrid IgG2 Fc to immobilized FcγRIIa-R131, **F)** binding of Fuc(+) hybrid IgG2 Fc to immobilized FcγRIIa-R131. Binding curves in **A)** correspond to hybrid IgG2 Fc concentrations of 70, 52.5, 35, and 17.5 µM from top to bottom. The binding curve in **B)** corresponds to a Fuc(+) hybrid IgG2 Fc concentration of 70 µM. Binding curves in **C)** and **D)** correspond to IgG2 Fc concentrations of 7.6, 3.8, 1.9, 0.9 µM from top to bottom. Binding curves in **E)** and **F)** correspond to IgG2 Fc concentrations of 9, 4.5, 2.2, 1.1 µM from top to bottom.

Table II. Kinetic rate constants and dissociation constants for binding of IgG2 Fc glycoforms to Fcγ receptors

Interaction Type	**$k_a \times 10^2$ (1/Ms)**	**$k_d \times 10^{-1}$ (1/s)**	**K_D (μM), kinetic**
hybrid/FcγRIIIa-V158	8.01 ± 2.51	1.41 ± 0.05	188 ± 62
Fuc(+)hybrid/FcγRIIIa-V158[a]	3.55 ± 2.94	8.58 ± 1.32	2420 ± 2030
hybrid/FcγRIIa-**H**131	817 ± 42	1.70 ± 0.14	2.08 ± 0.17
Fuc(+) hybrid/FcγRIIa-**H**131	821 ± 113	1.71 ± 0.13	2.12 ± 0.36
hybrid/FcγRIIa-**R**131	174 ± 30	3.25 ± 0.3	18.6 ± 3.6
Fuc(+) hybrid/FcγRIIa-**R**131	189 ± 37	3.29 ± 0.06	17.4 ± 3.4

[a]Calculated from a single concentration (70 μM) as shown in Figure A7 of the appendix

Biophysical characterization and studies of IgG2 Fc glycoforms

The stability and the structure of the C_H2 domain of IgG isotype has been shown to be affected by the Asn297 glycan attached to this domain making it an important determinant of the overall Fc and antibody stability.[9,47] The following biophysical techniques were used to probe the effect of core fucose on the stability of IgG2 Fc: size exclusion chromatography (SEC), circular dichroism (CD), differential scanning fluorimetry (DSF), and differential scanning calorimetry (DSC).

Size exclusion chromatography (SEC) was used to measure any possible difference in the hydrodynamic radius between the fucosylated and non-fucosylated IgG2 Fc glycoforms as well as to check for the presence of any high molecular weight (HMW) species. The SEC chromatograms (Figure 5A) showed no sign of HMW species for both glycoforms. Also, there was no significant difference between the retention times of the hybrid (12.81 ± 0.02 min) and the Fuc(+) hybrid (12.80 ± 0.01 min) IgG2 Fc glycoforms suggesting no dramatic change in the Fc hydrodynamic radius due to core fucosylation.

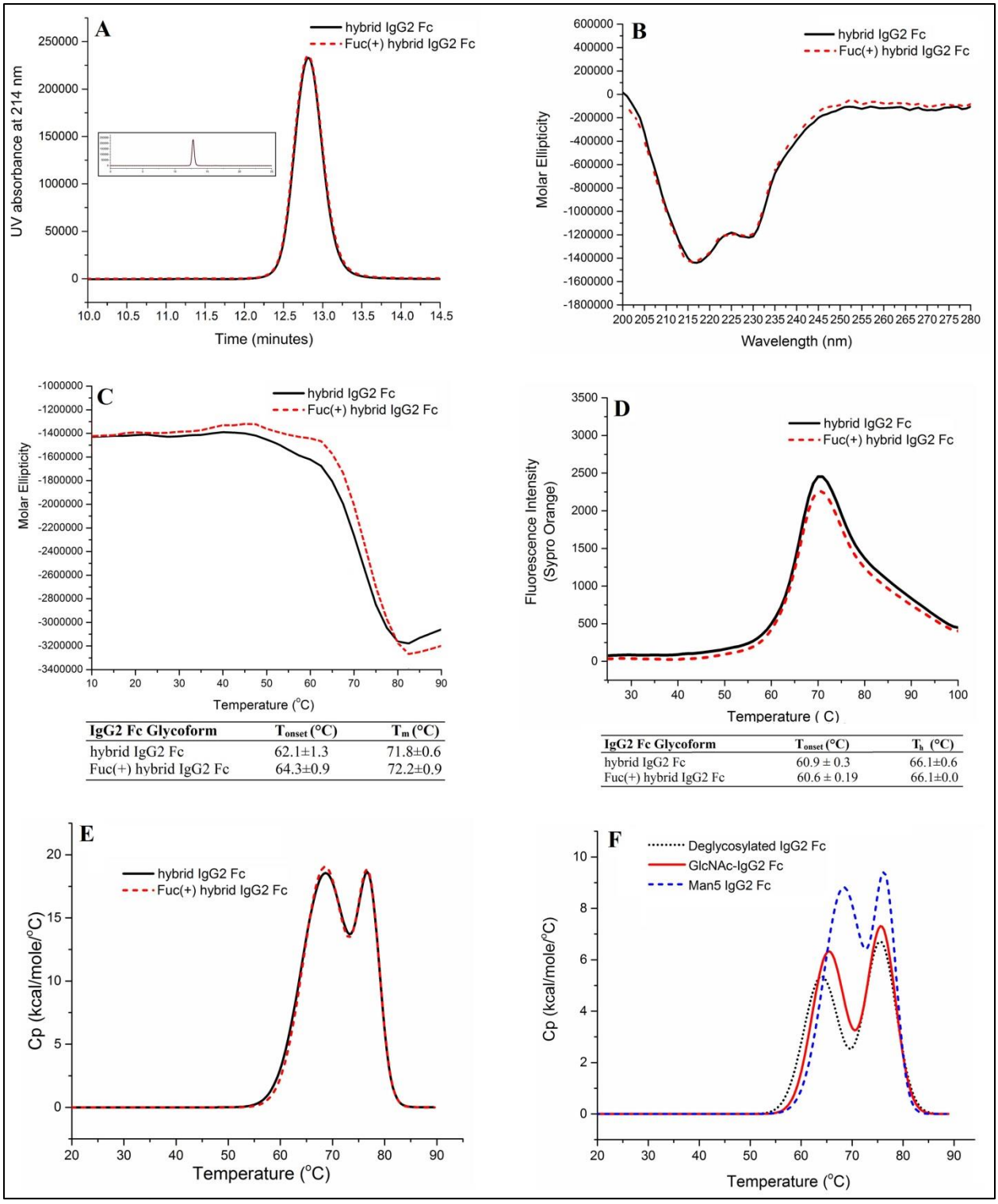

IgG2 Fc Glycoform	T_{onset} (°C)	T_m (°C)
hybrid IgG2 Fc	62.1±1.3	71.8±0.6
Fuc(+) hybrid IgG2 Fc	64.3±0.9	72.2±0.9

IgG2 Fc Glycoform	T_{onset} (°C)	T_h (°C)
hybrid IgG2 Fc	60.9 ± 0.3	66.1±0.6
Fuc(+) hybrid IgG2 Fc	60.6 ± 0.19	66.1±0.0

Figure 5. Biophysical analyses of IgG2 Fc glycoforms. **A)** Size exclusion chromatography (SEC) chromatograms of the hybrid and Fuc(+) hybrid IgG2 Fc glycoforms analyzed under native conditions (no heat or reduction). The mobile phase was 0.05M NaH2PO4 buffer pH6.1

containing 0.4 M NaClO4. The mobile phase flow rate was 0.25 ml/min. Retention times were 12.807 ± 0.018 min and 12.804 ± 0.009 min for the hybrid and Fuc(+) hybrid IgG2 Fc glycoforms, respectively. Also, the chromatograms indicate that both of these glycoforms are monomeric with no sign of high-molecular weight (HMW) species. **B)** Circular dichroism (CD) characterization of hybrid and Fuc(+) hybrid IgG2 Fc glycoforms. Both IgG2 Fc glycoforms exhibit similar CD spectra recorded in the far UV range (200–280 nm) at 10 °C in PBS (50 mM sodium phosphate, 150 mM NaCl, pH 7.4). **C)** CD-melt results recorded at 218 nm for hybrid and Fuc(+) hybrid IgG2 Fcs in PBS using a 10-90 °C temperature range. The results show a high similarity in the CD-melt profiles of both glycoforms and also no significant differences in their thermal unfolding temperatures (T_{onset} and T_m, onset and midpoint of transition, respectively). Each sample was run in triplicate and buffer subtracted during data analysis. **D)** Differential scanning fluorimetry analyses using SYPRO Orange fluorescent dye for probing of the conformational differences between hybrid and Fuc(+) hybrid IgG2 Fcs. The Dye was diluted to 1X concertation and the samples buffer was PBS. The results show a typical mAb DSF profile for both glycoforms and similar transition temperatures (T_{onset} and $T_{h,}$ onset and midpoint of transition respectively). Each sample was run in triplicate and buffer subtracted. **E)** and **F)** Differential scanning calorimetry thermograms of different IgG2Fc glycoforms. **E)** Deconvoluted thermograms of hybrid and Fuc(+) hybrid IgG2 Fcs. **F)** Deconvoluted thermograms of deglycosylated, EndoH-digested (GlcNAc-IgG2 Fc), and Man5 IgG2 Fcs. In each thermogram, the first transition represents the unfolding of the C_H2 domain of the Fc while the second transition represents the unfolding of the C_H3 domain. Each sample was run in triplicate and buffer subtracted.

The secondary structure of the hybrid and the Fuc(+) hybrid IgG2 Fc were examined by circular dichroism (CD). Both of these glycoforms showed the typical CD-spectrum of immunoglobulin G (Figure 5B) in which the beta sheet constitute the majority of its secondary structure giving rise to an ellipticity minimum around 218 nm.[48] The spectra are also shown to be almost superimposable with no significant difference between them. A CD-melt was also conducted to detect changes in the protein secondary structure.[48,49] In this analysis, the unfolding of the protein structure was followed up by recording the change in the protein ellipticity at 218 nm as a function of temperature (Figure 5C). Data analysis showed no significant differences in T_{onset} (the starting temperature of the transition) and T_m (the midpoint of the transition) between the hybrid (T_{onset}= 62.1 ± 1.3 °C, Tm= 71.8 ± 0.6 °C) and the Fuc(+) hybrid (T_{onset} = 64.3 ± 0.9 °C, Tm = 72.2 ± 0.9 °C) IgG2 Fc glycoforms.

Fluorescence thermal shift analysis also known as differential scanning fluorimetry (DSF)[50] was also used in this study to probe the effect of core fucosylation on IgG2 Fc conformational stability. In this experiment, SYPRO Orange was used as an extrinsic fluorophore. The DSF profiles of hybrid and Fuc(+) hybrid IgG2 Fc are shown in Figure 5D. Both glycoforms show a DSF profile which strongly resembles a typical DSF profile of a full length antibody.[51] A typical antibody DSF profile shows a sharp sigmoid-like increase followed by a decrease in the fluorophore florescence intensity as the temperature increases. The initial increase in SYPRO Orange fluorescence intensity is due to the exposure of this dye to the apolar environment of the protein as it unfolds, while the later decrease in the intensity is at least partially due to florescence quenching by the intrinsic effect of temperature.[50] T_h of each glycoform, which is the midpoint of the first fluorescence transition in the corresponding DSF profile, was determined using the first derivative curve. T_h primarily reflects the transition of the

C_H2 domain of mAb, since it is the least thermally stable domain.[50] Data analysis showed no significant differences in T_{onset} (the starting temperature of the transition) and T_h (the temperature of hydrophobic exposure) between the hybrid (T_{onset}= 60.9 ± 0.3 °C, T_h= 66.1 ± 0.6 °C) and the Fuc(+) hybrid (T_{onset} = 60.6 ± 0.19 °C, T_h = 66.1 ± 0.0 °C) IgG2 Fc glycoforms.

The DSC thermograms of the different IgG2 Fc glycoforms are presented in Figure 5 (panels E and F) while the melting temperatures are shown in Table III. In general, IgG2 Fc showed two endothermal transitions similar to the DSC thermogram of IgG1 Fc.[9] This and previous results[47] indicate that the first transition that occurs at a lower temperature (Tm1) represents the unfolding of the C_H2 domain while the second transition which occurs at a higher temperature (Tm2) represents the unfolding of the C_H3 domain of IgG2 Fc. In the first set of glycoforms (Figure 5E), we wished to test any possible effect of core fucose on the thermal stability of the C_H2 domain using this biophysical technique. To this end, we used the homogeneous non-fucosylated and the Fuc(+) IgG2 Fc glycoforms generated in this study. Tm1 was statistically identical for the hybrid and Fuc(+) hybrid IgG2 Fc glycoforms (68.4±0.1 °C and 68.5±0.1 °C, respectively). The Tm2 transitions for hybrid and Fuc(+) hybrid IgG2 Fc glycoforms were also identical (76.5±0.1 °C each). In the second set of glycoforms (Man5 IgG2 Fc, GlcNAc-IgG2 Fc, and deglycosylated IgG2 Fc), produced as described in the appendix, Tm1 showed a progressive decrease in its value as the size of the Asn297 glycan becomes smaller while Tm2 did not change dramatically (Figure 5F). Interestingly, Tm1 of the Man5, hybrid, and Fuc(+) hybrid IgG2 Fc glycoforms were nearly the same (68.3±0.1, 68.4±0.1 and 68.5±0.1, respectively). This experiment also shows that Tm1 of Asn297 glycosylated forms of IgG2 Fc (ranging from 68.3 to 68.5 °C) is higher than Tm1 of the deglycosylated IgG2 Fc (64.1 °C) by

more than 4 °C. This difference reflects the importance of the glycosylation of Asn297 for the stabilization of the IgG2 Fc C_H2 domain, as has been shown in previous studies.[9,47]

Table III. Melting temperatures of C_H2 domain (Tm1) and C_H3 domain (Tm2) of different IgG2 Fc glycoforms obtained by DSC

	GlcNAcMan5F	GlcNAcMan5	Man5	GlcNAc-Fc	Deglycosylated-Fc
Tm1[a] (°C)	68.5±0.1	68.4±0.1	68.3±0.1	65.5±0.0	64.1±0.0
Tm2[a] (°C)	76.5±0.1	76.5±0.1	76.3±0.2	75.7±0.0	75.6±0.0

[a]Melting temperatures were obtained by fitting the corresponding thermogram shown in Figure 5 to a non-2- state model with two transitions

Mammalian α1,6-fucosyltransferase (FUT8) kinetics studies

To get a better understanding of the amounts of bacterially produced FUT8 that would be necessary for large scale production of the Fuc(+) hybrid glycoform, kinetic studies of the FUT8 enzyme were conducted using free and protein-bound hybrid glycan. During the course of these experiments, it was recognized that there was a significant difference between the rates of fucose transfer for free vs. protein-bound glycan. This was explored in more detail in an additional set of experiments by studying the rates of FUT8 action at two different protein glycosylation positions, the IgG2 Fc Asn297 and Asn392 glycosylation sites (Figure 1).

FUT8 activity was measured using a continuous coupled spectrophotometric assay which requires no substrate labeling.[52] Initial kinetic studies of the amount and purity of the bacterially produced FUT8 were conducted with free hybrid glycan. It was found that 0.21 units (μmol/min) of FUT8 with a specific activity of 0.12 μmole/min/mg were obtained from 1 L of bacterial culture. The K_M of the bacterially produced mouse FUT8 for the hybrid glycan acceptor substrate was determined to be 17.0 μM, while the K_M of this enzyme for the GDP-fucose donor substrate was 18.2 μM (Figure 6 and Table IV).

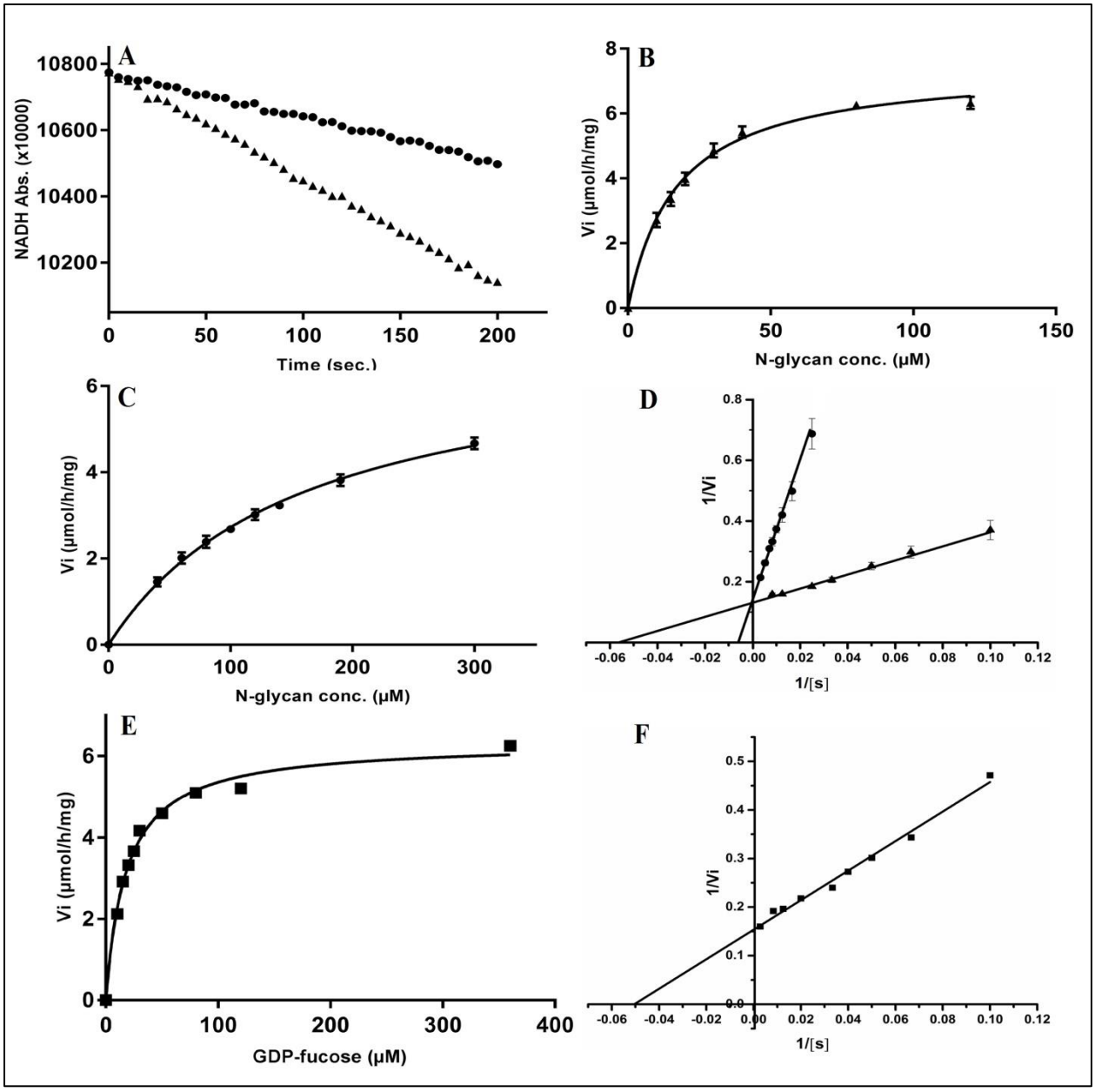

Figure 6. FUT8 kinetics analyses. **A)** FUT8 reaction progress using 80 µM of free (▲) and Asn297-bound N-glycans (●). The initial velocities for each substrate were calculated based on the drop in NADH concentration during the linear phase of the reaction using the pyruvate kinase/lactate dehydrogenase continuous coupled assay. **B** and **C)** Michaelis-Menten plots of FUT8 using free N-glycan (B) or Asn297-bound N-glycan (C) as an acceptor substrate for the calculation of apparent K_M and V_{max}. Each curve was constructed using initial velocities of varied acceptor substrate concentrations. For the free glycan (▲); 10, 15, 20, 30, 40, 80, and 120 µM

were used while for the Asn297-bound N-glycan (●); 40, 60, 80, 100, 120, 140,190, and 300 μM were used. Data points are shown as the average of triplicate values. **D)** Lineweaver-Burk plot constructed using data from plots B and C, showing the difference in FUT8 kinetics between the free and the Asn297-bound N-glycan. **E** and **F)** Michaelis-Menten (E) and Lineweaver-Burk (F) plots of FUT8 using varied concentrations (10, 15, 20, 25, 30, 50, 80, 120, 360 μM) of the donor substrate (GDP-fucose) but fixed concentration (80 μM) of the free N-glycan as an acceptor substrate.

Table IV. Kinetic parameters for mouse α1,6-fucosyltransferase FUT8

Parameter	**Value[a] (standard error)**
$K_{M\ \text{(free glycan)}}$ (μM)	17.0 (1.0)
$V_{max\ \text{(free glycan)}}$ (μmol/min/mg)	0.12 (0.002)
$K_{M\ \text{(Asn297-bound glycan)}}$ (μM)	167.8 (10.0)
$V_{max\ \text{(Asn297-bound glycan)}}$ (μmol/min/mg)	0.12 (0.003)
$K_{M\ \text{(GDP-fucose)}}$ (μM)	18.2

[a]Values were calculated using GraphPad Prism 7 software utilizing the data shown in Figure 6

The simplicity of the pyruvate kinase/lactate dehydrogenase coupled FUT8 assay gave us the opportunity to compare the acceptor substrate kinetics of a free hybrid glycan with a protein-bound hybrid glycan. This was accomplished by conducting the FUT8 activity assay in the presence of varying concentrations of the Asn297 hybrid glycoform of IgG2 Fc (Figures 6). It was apparent immediately from initial rate studies that the free hybrid glycan is converted to the Fuc(+) hybrid glycan at a much higher rate than the IgG2 Fc Asn297 hybrid glycan under same conditions. Determination of kinetic parameters for the IgG2 Fc Asn297 hybrid glycan resulted in an interesting result. The K_M of mouse FUT8 for the protein bound acceptor substrate was 167.8 μM, which is approximately 10-fold higher than that of the free hybrid glycan (Table IV).

In addition, the V_{max} of the free hybrid glycan and the protein-bound Asn297 hybrid glycan were essentially identical, 0.12 ± 0.002 μmol/min/mg and 0.12 ± 0.003 μmol/min/mg, respectively. This can also be seen in the Lineweaver-Burk plot in Figure 6D.

The kinetics of the FUT8 reaction at a second protein glycosylation site was studied to determine if FUT8 differs in its ability to transfer fucose at different protein glycosylation sites. This was accomplished by producing a glycosylation site variant of IgG2 Fc with the Asn297 site mutated to glutamine, and the consensus Lys392 residue converted to an asparagine to create a new N-linked glycosylation site as described in the appendix. This IgG2 Fc-(Q297, N392) variant has a single N-linked glycosylation site at Asn392 (Figure 1). Though the N392 glycosylation site is not part of the IgG2 Fc consensus sequence, it is a naturally occurring polymorphism which is present in the initial human IgG2 heavy chain cDNA obtained from the mammalian gene collection[34] and used for subcloning in this study. In addition, the human IgG3 subclass heavy chain does have an asparagine at residue 392. Our laboratory and others [27] have shown that this site is glycosylated to some extent in human IgG3, and that the N-linked glycoforms present at this site are distinct from those found at the Asn297 glycosylation site (unpublished results). To study FUT8 reaction kinetics with the IgG2 Fc-(Q297, N392) glycosylation site variant, it was first necessary to synthesize the hybrid glycoform of IgG2 Fc-(Q297, N392). This was accomplished using the same strategy that was utilized to produce the Asn297 hybrid glycoform of IgG2 Fc described previously, only using high mannose IgG2 Fc-(Q297, N392) as a starting material. During the course of the synthesis of hybrid IgG2 Fc-(Q297, N392) glycoform, it became apparent that the Asn392 glycosylation site is not as good of a substrate when compared to the Asn297 site for glycosidase and glycosyltransferase enzymes. This can be seen in Figure 7A, which shows the transfer of GlcNAc by GnT-I to the Man5

glycoforms of the Asn297 and Asn392 glycosylation sites on IgG2 Fc. The Man5 IgG2 Fc-(Q297, N392) substrate is converted to the hybrid glycoform at a much slower rate than the Asn297 site of Man5 IgG2 Fc. Calculations based on mass spectra peak intensities and initial rate calculations showed that the GnT-I catalyzed reaction using Asn392 glycan as a substrate is slower than the enzyme reaction using Asn297 glycan as a substrate by a factor of 4. Once the hybrid glycoform of IgG2 Fc-(Q297, N392) was produced, it was incubated with FUT8 and GDP-fucose to determine the rate of fucose transfer to the Asn392 glycosylation site. No fucose transfer was detected for the Asn392 glycosylation site even though the Asn297 site was fully fucosylated in approximately 60 h under the same reaction conditions (Figure 7B). Based on these results, we have concluded that the Asn392 glycosylation site is not accepted as a substrate by FUT8.

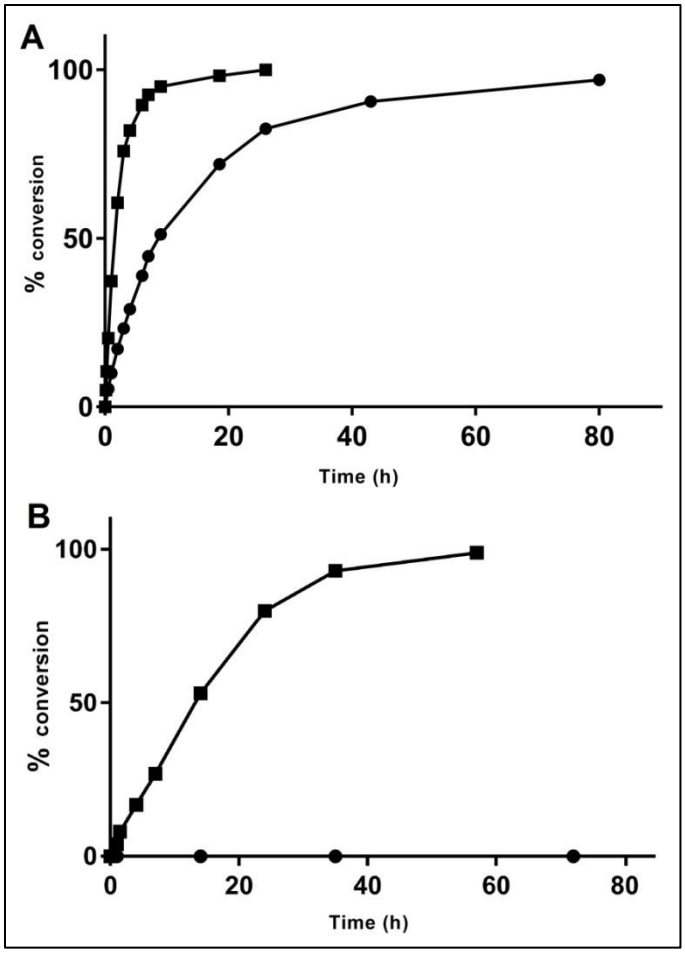

Figure 7. Effect of glycosylation site on glycosyltransferases reactions. **A)** GnT-I catalyzed reaction progress for the synthesis of the hybrid glycoform from Man5 glycoforms. The reaction was carried out in 20 mM HEPES pH 7.5 buffer containing 150 mM NaCl, GnT-I (25 µg/ml), UDP-GlcNAc (2 mM), $MnCl_2$ (20 mM) and 20 µM of Man5 glycoform of either the wild type IgG2 Fc which contains only the Asn297 glycosylation site (■) or IgG2 Fc-(Q297, N392) which contains only the N392 glycosylation site (●). The reaction was followed up by Q-TOF LC/MS analysis of intact protein and the peak intensities were used to calculate the percentage of conversion of the Man5 glycoform into the hybrid glycoform. **B)** FUT8 catalyzed reaction progress for the addition of core fucose. The reaction was carried out in 50 mM Tris HCl pH 7.5 buffer containing FUT8 (0.35 µU/ml), GDP-fucose (150 µM), and 20 µM of the hybrid glycoform of either the wild type IgG2 Fc (■) or IgG2 Fc-(Q297, N392) (●). The reaction was followed by Q-TOF LC/MS analysis of intact protein and the peak intensities were used to calculate the percentage of conversion of the hybrid glycoform into the fucosylated hybrid.

Discussion

Synthesis of homogeneous glycoproteins can facilitate studies of protein glycosylation by providing access to material to conduct experiments that is not available from natural sources. Natural glycoprotein microheterogeneity presents a significant obstacle to the analysis of glycoprotein receptor interactions, stability, and kinetic studies. As part of a larger project to produce homogeneous glycoproteins for glycobiology studies, human IgG2 Fc was produced as homogeneous Man5, hybrid, and Fuc(+) hybrid glycoforms in this work in a relatively large laboratory-scale using a combination of glycosylation-deficient host, purification, and enzymatic synthesis as shown in Table I. These glycoforms were then used to study the effects of changes in glycosylation on IgG2 Fc stability, receptor binding, and the kinetics of glycosyltransferase reactions on IgG2 Fc glycosylation variants. IgG2 Fc was first produced in bulk in a BioFlo 415 fermentor using an OCH1 deleted strain of SMD1168 *Pichia pastoris*.[53,54] Approximately 1 g of high mannose IgG2 Fc was isolated from growth media using protein G chromatography. The protein G purified IgG2 Fc was then purified further using HIC and WCX chromatography. Though this results in a large loss of material, the purified high mannose IgG2 Fc obtained after chromatography is diglycosylated and consisting mainly of $Man_8GlcNAc_2$ and $Man_9GlcNAc_2$ glycoforms that can be completely digested by α-1,2-mannosidases. Once the diglycosylated high mannose IgG2 Fc was produced, enzymatic conversion to homogeneous Man5 and hybrid glycoforms was conducted successfully as described in the methods section of this chapter.

For the production of the Fuc(+) glycoform and kinetic studies of fucose transfer to IgG2 Fc, a novel method was developed to produce mouse FUT8 by cloning and expressing it in the cytoplasm of *E. coli* in a soluble and active form. Previously, FUT8 has been obtained from many sources including rat liver, porcine liver and cultured human skin fibroblasts.[43,55,56] In

addition, recombinant expression of human FUT8 has been carried out in insect cells, and this recombinant FUT8 has been utilized for characterization of the FUT8 reaction mechanism, substrate specificity, and determination of FUT8 crystal structure.[22,57] Though FUT8 can be obtained from all of the previously mentioned sources, we decided to explore the possibility of producing FUT8 in *E. coli* to take advantage of the ease and speed of bacterial protein expression. Using a modified *E. coli* strain, 1.8 mg of FUT8 with a total activity of 0.21 units (μmol/min) was produced from a one-liter shake flask expression. This amount of enzyme activity was sufficient to produce all of the fucosylated proteins and to do all the required characterization and the kinetic experiments described in this study. Initial kinetic studies of the bacterially produced mouse FUT8 enzyme demonstrated that it had similar properties to the insect cell produced human FUT8 described by Ihara et al.[22] The acceptor substrate K_M of the bacterially produced mouse FUT8 from this study is 17.0 μM, which is close to the 12.9 μM acceptor substrate K_M determined for insect cell-produced human FUT8 reported by Ihara et al.[22] At the same time, the donor substrate K_M of mouse FUT8 is 18.2 μM, which is nearly identical to the 19.3 μM donor substrate K_M Ihara et al. reported for human FUT8 [22], despite the difference in FUT8 assay formats used in these studies.

Several studies have demonstrated that the N-linked glycan at Asn297 stabilizes the C_H2 domain of antibody IgG Fc regions. Removal or truncation of this glycan affects conformational stability, aggregation rates and biological activity.[9,45,58–61] Given that little is known about hybrid glycoforms in IgG2, we conducted a series of biophysical experiments to determine if core-linked fucosylation affects its conformational stability. Previously, Sondermann et al. [62] demonstrated that the addition of sialic acid (a terminal glycan heterogeneity) to the Asn297 glycan of IgG1 Fc induces structural alterations in the C_H2 domain in addition to a reduction in

the thermal stability of this domain as measured by circular dichroism. However, in this study overall results from biophysical experiments to probe the effect of core fucosylation on the structure of IgG2 Fc confirm the similarity in the Fc structure upon core fucosylation and suggest that core fucose does not make a significant contact with the protein backbone. These results are also consistent with previous results, where stable isotope-assisted NMR analyses confirmed the similarity of the overall structures of fucosylated and non-fucosylated IgG1 Fc fragments in solution. [63]

Of the human IgG subclasses, IgG2 has the weakest interaction with most Fcγ receptors, with the only exception being FcγRIIa where IgG2 has moderate affinity.[46] Because of this, IgG2 is a weak initiator of cellular immune responses except for those linked to cells expressing FcγRIIa. These relatively low effector functions of IgG2 have been utilized by the pharmaceutical industry to make mAb when the effector functions are not required for the antibody mechanism of action. Even so, IgG2 has measurable affinity to other Fc receptors and may contribute to cellular immune responses initiated by those other Fc receptors by acting alone or with other IgG subclasses. Binding of IgG subclass to these receptors is highly affected by the microheterogeneity of the Asn297 glycan, especially the level of core fucosylation.[14] To explore the effect of core fucosylation on the binding of IgG2 to Fcγ receptors, we conducted kinetic binding studies of the interactions of two Fc receptors (FcγRIIa and FcγRIIIa) with non-fucosylated and core-linked fucosylated IgG2. Since IgG2 has generally weak affinity for FcγRIIIa, we chose to study the high affinity variant of this receptor, i.e. FcγRIIIa-V158. Meanwhile, in FcγRIIa binding studies, we chose both the high affinity (FcγRIIa-H1131) as well as the low affinity (FcγRIIa-R131) variants of this receptor. Biolayer interferometry studies of these interactions resulted in the finding that core-linked fucosylation has no effect on FcγRIIa

binding while at the same time it appears to reduce binding to FcγRIIIa-V158 by about 13-fold. Thus, the reduction in binding to FcγRIIIa-V158 upon complete core fucosylation of IgG2 Fc could add more advantages to this IgG subclass and improve its benign nature when designing mAb intended to have low effector functions for certain disease conditions.

The reduction in the binding of fucosylated IgG2 Fc to FcγRIIIa-V158 in this study is shown to be due to a reduction in the rate of the formation of the Fc/Fcγ receptor complex as well as an increase in the rate of dissociation of this complex. Previously, it was shown that the presence of core fucose on the Asn297 glycan of IgG1 interrupt glycan-glycan interactions that are present between non-fucosylated Asn297 glycan of IgG1 and Asn162 glycan of FcγRIIIa-V158.[18,19] Therefore, a similar interaction might also be happening between IgG2 Fc and FcγRIIIa-V158 glycans and could explain the results reported in this study. Noticeably, our binding studies showed that the k_a of binding of IgG2 Fc to FcγRIIa-H131 is about 100-fold bigger than that for binding to FcγRIIIa-V158 while the k_d values from these interactions were about the same. This means that the higher affinity of IgG2 subclass for FcγRIIa-H131 relative to FcγRIIIa-V158 is mainly due to an increase in the rate of the formation of the Fc/Fcγ receptor complex rather than the stability of this complex. Even though these receptors have a high degree of homology, the difference in some of the amino acid sequence, and hence different receptor conformation and different number of N-linked glycans, may result in different modes of interaction and may account for these differences in binding kinetics. Our binding studies with FcγRIIa-R131 variant also showed that the reduction in IgG2 Fc binding affinity to this receptor variant compared to FcγRIIa-H131 variant (~ 8-fold reduction) is due to a combination of reduction in the rate of formation of the complex and reduced stability of the complex. Interestingly, core fucosylation did not affect the binding of IgG2 to FcγRIIa-R131 even though

core fucose has been shown to reduce the binding of IgG1 to this receptor variant as reported in previous studies.[14] This result also suggests that IgG2 has a different mode of interaction with FcγRIIa-R131 than IgG1.

The amount of hybrid IgG2 Fc produced in these studies and the use of a pyruvate kinase/lactate dehydrogenase coupled assay to monitor FUT8 activity enabled studies of FUT8 fucose transfer kinetics with both free and protein-bound hybrid glycans. Initial kinetic studies comparing the rates of fucose transfer to free and IgG2 Fc Asn297-bound hybrid glycans indicated that transfer of fucose was much more rapid to the free hybrid glycan. This was further investigated by more detailed kinetic studies to determine the FUT8 K_M and V_{max} parameters for both free and protein-bound hybrid glycan acceptor substrates. Interestingly, the free hybrid glycan had a K_M of 17 μM and the IgG2 Fc Asn297-bound hybrid glycan had a K_M of 168 μM, indicating that the free glycan is the preferred acceptor substrate for FUT8. Unlike the K_M values, the V_{max} values determined for the free and IgG2 Fc Asn297-bound hybrid glycans were essentially identical at 0.12 μmol/min/mg. A standard interpretation of the K_M*'s* from this experiment indicates that the apparent affinity of the FUT8 active site for free hybrid glycan is approximately 10-fold higher than its affinity for the IgG2 Fc Asn297-bound hybrid glycan. In addition, the fact that the V_{max} values determined for each substrate were identical indicates that the catalytic rate constants and by implication the transition states for these two substrates are very similar, regardless of differences in active site affinity for initial substrates. Recent crystal structures of IgG1 Fc glycoforms showing both open and closed conformations around the Asn297 glycan in the interface between C_H2 domains, and NMR studies of IgG1 Fc by the Barb laboratory which demonstrate that the first GlcNAc residue of the Asn297 glycan experiences multiple chemical environments, both suggest another intriguing possibility.[64–66] An alternate

explanation for these kinetic results would be that the IgG2 Fc Asn297-hybrid glycan is dynamic and can exist in two or more conformations where at least one conformation would be fully accessible to the FUT8 active site and another conformation or conformations would be completely inaccessible. This sort of a model would be consistent with the kinetic results if 10% of the IgG2 Fc Asn297-hybrid glycans were in a fully accessible conformation and 90% were completely inaccessible, and the glycans were able to exchange between these different states. Regardless of whether FUT8 simply has lower affinity for protein-bound hybrid glycans or the IgG2 Fc Asn297-hybrid glycan is dynamically moving between accessible and inaccessible states, the slower rates observed for fucose transfer to the IgG2 Fc Asn297-does appear to agree with what is known of the FUT8 mechanism.[22,57,67] FUT8 requires significant access to N-linked glycans to catalyze fucose transfer because for substrate recognition it must bind to non-reducing end sugar residues and then transfer fucose to the reducing end GlcNAc residue attached to Asn297. To further investigate the steric requirements for FUT8 transfer of fucose to hybrid glycans, we decided to investigate a second IgG2 Fc glycosylation site.

Recent studies in our laboratory (unpublished results) and others [27] have shown that the IgG3 Asn392 glycosylation site is occupied and has distinctly different types of N-glycans attached to it when compared to the Asn297 glycosylation site. While the glycans of the IgG3 N297 site are mainly complex biantennary glycans containing core-linked fucose, the glycans found on IgG3 Asn392 contain no core-linked fucose at all and also contain a large amount of bisecting GlcNAc. Since the presence of bisecting GlcNAc blocks the enzymatic activity of FUT8[68], one question about the differences between the types of glycosylation found on the IgG3 Asn297 and Asn392 sites is whether the addition of bisecting GlcNAc is blocking the Asn392 site as a FUT8 substrate. The stark difference between the types of glycosylation found

on the Asn297 and Asn392 IgG3 sites indicated that we might expect to observe similar differences between the homologous Asn297 and Asn392 glycosylation sites on IgG2 Fc since IgG2 Fc is highly homologous to IgG3 Fc. A mutant was produced to eliminate the Asn297 glycosylation site but retain the Asn392 glycosylation site of IgG2 Fc (IgG2 Fc-(Q297, N392)) so that both sites could be studied independently. Studies of the rates of glycosyltransfer for formation of the hybrid glycoform with GnT-I and for formation of the Fuc(+)-hybrid glycoform using FUT8 were conducted on both sites. The IgG2 Fc Asn392 glycosylation site appears to be significantly less accessible to glycosyltransferases than the Asn297 site. GnT-I transferred GlcNAc to the Asn297 site approximately 4 times faster than to the Asn392 glycosylation site, and FUT8 did not transfer fucose to the Asn392 site at all while the Asn297 site was completely fucosylated. This is in some ways surprising since the Asn297 glycans appear in crystal structures to be sterically hindered by their location between the two C_H2 domains of the Fc dimer, while the N392 side chain appears to be directed towards solvent in models. These results indicate that the protein structure around the Asn392 site makes it less accessible for transfer of GlcNAc to the non-reducing end of the Man5 glycoform and completely inaccessible for transfer of fucose by FUT8. Also, if the IgG2 Fc results are indicative of what can be expected for IgG3, then the lack of fucose found on the human IgG3 Asn392 site is due to FUT8 not being able to accept the Asn392 site as a substrate rather than the presence of bisecting GlcNAc blocking FUT8 activity.

In conclusion, we were successful in performing an *in vitro* enzymatic synthesis for the addition of core fucose to the Asn297 of IgG2 Fc. Complete core fucosylation of IgG2 Fc using this synthesis resulted in a large reduction (~ 13-fold) in binding of this IgG subclass to FcγRIIIa, a point should be taken into account in the design of IgG2-based mAb with reduced or

no effector functions. As part of this *in vitro* enzymatic synthesis, methods were developed to express mouse FUT8 in *E. coli* for rapid production of FUT8 for enzymatic synthesis and kinetics studies. Biophysical studies comparing the stability of hybrid and Fuc(+)-hybrid IgG2 Fc glycoforms were carried out, and it was found that the two glycoforms had nearly identical stability. The acceptor substrate specificity of FUT8 for a free hybrid glycan and two different IgG2 Fc hybrid glycosylation sites was determined. FUT8 accepted the free hybrid glycan with a 10-fold lower K_M than the IgG2 Fc Asn297-hybrid glycoform, but with equal V_{max} indicating similar transition states for the free and protein-bound glycans. The IgG2 Fc Asn392-hybrid glycoform was not accepted by FUT8 as a substrate, indicating that this site is probably sterically hindered by the surrounding protein structure. Based on these kinetic results, the protein structure around hybrid glycans affect fucose transfer catalyzed by FUT8 by altering K_M but not V_{max}, and this observed substrate specificity could explain differences in the types of N-linked glycans found attached to different glycosylation sites on the same protein.

Materials and methods

Materials

Restriction endonucleases, endoglycosidase H, and SHuffle T7 Express *E. coli* were purchased from New England Biolabs (Ipswich, MA). Amicon Ultra-15 Centrifugal Filter Units were purchased from EMD Millipore (Billerica, MA). SYPRO Orange dye, and Top10F' *E. coli* cells were obtained from Invitrogen Inc. (Carlsbad, CA). The bacterial α1,2-mannosidase, BT3990[40,41], was produced in house. The biotinylated FcγRIIIa-V158 variant was produced in house by the procedure described by Okbazghi et al.[45] The plasmid pRARE2 was isolated from Rosetta2 competent cells (EMD Millipore). Antibodies for western and immune blotting were

purchased from ThemoScientific (Grand Island, NY). UDP-GlcNAc, Inorganic pyrophosphatase from baker's yeast (*S. cerevisiae*), NADH, Pyruvate Kinase/Lactic Dehydrogenase enzymes from rabbit muscle, ATP, GTP, and L-fucose were obtained from Sigma-Aldrich (St. Louis, MO).

Production and characterization of IgG2 Fc

A description of the cloning and site-directed mutagenesis used to produce yeast expression strains for the IgG2 Fc glycosylation site variants shown in Figure 1 is provided in the appendix. IgG2 Fc variants were expressed in an OCH1 deleted strain of *Pichia pastoris*, using a BioFlo 415 fermenter (Eppendorf) on a 7-liter scale. The expression and purification of IgG2 Fc are described in more details in the appendix. Briefly, three 7-L fermentations were conducted to produce about 1g of the IgG2 Fc. A second purification step using hydrophobic interaction chromatography (HIC) was also carried out to separate hemiglycosylated Fc from the diglycosylated Fc.[37,60] Weak cation exchange chromatography was also utilized to purify IgG2 Fc further and get rid of the phosphorylated glycoforms.

Production of soluble mammalian α1,6-fucosyltransferase (FUT8) in E. coli

An expression plasmid (pFUT8) for the production of the catalytic domain of mouse FUT8 fused to a hexa histidine-tag was produced as described in the appendix. The pFUT8 plasmid was then transformed into SHuffle T7 Express *E. coli*. The expression and purification of FUT8 are described in the appendix. After purification, the enzyme solution was dialyzed against 50 mM Tris HCl, pH 7.5 buffer and concentrated by Amicon ultra-15 centrifugal filter unit. Finally, the enzyme concentration was measured using Pierce BCA protein assay kit (ThermoScientific) and stored in 50% glycerol at -20 °C.

In vitro enzymatic synthesis of IgG2 Fc glycoforms

The enzymatic synthesis scheme shown in Figure 2 was followed to make homogeneous IgG2 Fc glycoforms as described in the following sections:

Man5-IgG2 Fc

High mannose IgG2 Fc produced by yeast expression and subsequent purification was converted into a homogeneous $Man_5GlcNAc_2$ (Man5) IgG2 Fc glycoform using a bacterial α1,2-mannosidase (BT3990).[40,41,45] Prior to BT3990 digestion, 185 mg of high mannose IgG2 Fc (Figure 3A) was dialyzed against the reaction buffer (20 mM MES buffer pH 6.6 containing 150 mM NaCl and 5 mM $CaCl_2$). Then, the reaction mixture (92.5 ml) containing IgG2 Fc (2 mg/ml) and BT3990 (100 µg/ml) was incubated at room temperature and the conversion was monitored by intact protein Q-TOF LC/MS and required two days for completion. Finally, the Man5 glycoform was purified from the reaction mixture using the general protein G affinity chromatography procedure described in the appendix.

Hybrid-IgG2 Fc

Man5 IgG2 Fc was converted into $GlcNAcMan_5GlcNAc_2$ (hybrid) IgG2 Fc using in-house produced N-acetylglucosaminyltransferase I (GnT-I).[42] Before the reaction, Man5 IgG2 Fc was dialyzed against 20 mM HEPES pH 7.5 buffer containing 150 mM NaCl. The reaction mixture (15.5 ml) containing 139.5 mg Man5 IgG2 Fc (9 mg/ml), GnT-I (117 µg/ml), UDP-GlcNAc (2 mM), and $MnCl_2$ (20 mM) was incubated at 28 °C. The reaction was monitored using intact protein Q-TOF LC/MS until completion (11 hours). The hybrid Fc was purified from the reaction mixture using the general protein G affinity chromatography procedure described in the appendix.

Core-linked fucosylated IgG2 Fc (Fuc(+) hybrid-IgG2 Fc)

FUT8 produced as described above was utilized to convert the hybrid IgG2 Fc glycoform into the $GlcNAcMan_5GlcNAc_2F$ (Fuc(+) hybrid) IgG2 Fc glycoform. The donor substrate, GDP-L-fucose, required for FUT8 reaction was produced *in situ* from L-fucose, ATP, and GTP using the bifunctional enzyme L-fucokinase/guanosine 5'-diphosphate-L-fucose pyrophosphorylase (FKP) (Figure 2B). FKP was cloned and expressed as described previously by Wang et al.[44] with minor modification as shown in the appendix. The FKP reaction was carried out in 50 mM Tris HCl pH 7.5 buffer containing ATP (5 mM), GTP (5 mM), L-fucose (5 mM), $MgCl_2$ (5 mM), and FKP (120 µg/ml) at room temperature. After 12 hours, the FKP reaction mixture was added to an equal volume (8 ml) of a solution containing 20 mg of hybrid IgG2 Fc (2.5 mg/ml Fc in 20 mM Tris HCl buffer pH 7.5) and the conversion to Fuc(+) hybrid was initiated by adding 37.3 µU of FUT8 and monitored by intact protein mass spectrometry. By the end of the reaction, the Fuc(+) hybrid Fc was purified from the reaction mixture using the general protein G affinity chromatography procedure described in appendix.

Binding studies using biolayer interferometry (BLI)

The interactions of the non-fucosylated and fucosylated IgG2 Fc glycoforms with Fcγ receptors FcγRIIa-H131, FcγRIIa-R131, and FcγRIIIa-V158 were studied using a BLItz® instrument (Pall ForteBio LLC). The soluble form of human FcγRIIIa-V158 receptor used in these binding studies was previously cloned and produced in our laboratory.[35,45] The cloning, expression, and purification of the soluble form of human FcγRIIa-H131 and FcγRIIa-R131 receptors are described in the appendix. In these binding experiments, streptavidin biosensors (Pall ForteBio LLC) were chosen for the immobilization of the receptors while the studied IgG2 Fc glycoform was kept in solution. Four different concentrations of each IgG2 Fc glycoform

were used in each binding experiment and each binding experiment was repeated three times. The association rate constant and the dissociation rate constant (k_a and k_d, respectively) as well as the equilibrium dissociation constant (K_D) at 25 °C were calculated by fitting the binding sensorgrams from these different concentrations using the global fit function of BLItz Pro software. More details on the binding experiments are provided in the appendix.

Biophysical studies

Size exclusion chromatography (SEC)

Size exclusion chromatography (SEC) analyses were conducted using a TSKgel Super SW3000 (4.6 mm ID x 30 cm, Tosoh Bioscience, King of Prussia, PA) column and Prominence HPLC system (Shimadzu, Kyoto, Japan). A 6-µl sample volume of 4.5 µM (about 0.24 mg/ml) of either hybrid or Fuc(+) hybrid IgG2 Fc glycoform in PBS (50 mM sodium phosphate, 150 mM NaCl, pH 7.4) was injected into the column. The mobile phase used was 0.05 M NaH_2PO_4 buffer pH 6.1 containing 0.4 M $NaClO_4$. The flow rate was 0.25 ml/min and the UV detector was set at 214 nm.

Circular dichroism (CD) spectroscopy

The far UV-CD spectra (from 280-200 nm) of the hybrid and the Fuc(+) hybrid IgG2 Fc in PBS were recorded at 10 °C using a Chirascan instrument (Applied Photophysics, Surrey, United Kingdom) equipped with a six position temperature-controlled sample holder. Samples were prepared by loading 200 µl of 3.8 µM (about 0.2 mg/ml) of each IgG2 Fc glycoform in PBS (50 mM sodium phosphate, 150 mM NaCl, pH 7.4) into 0.1 cm path length quartz cuvettes. The scanning speed was 2 nm/sec at 1.0 nm resolution. Each sample was run in triplicate and buffer subtracted before data analysis. The CD-melt experiments were performed by following

the molar ellipticity at 218 nm of each sample as a function of temperature. The temperature was raised from 10-90 °C at 2.5 °C intervals using a heating rate of 15 °C/h with the samples allowed to equilibrate for 5 min at each temperature. The CD-melt profile for each glycoform was obtained by plotting the molar ellipticity at 218 nm as a function of temperature.[49]

Differential scanning fluorimetry (DSF)

DSF was performed using a MX3005P qPCR system (Agilent Technologies). The samples were prepared by adding sufficient SYPRO Orange dye to protein solutions (3.8 µM IgG2 Fc in PBS) to create a 1X- final SYPRO Orange concentration. 150 µl of each sample was loaded into a 96-well plate. The samples solution was excited at 492 nm, and the emission intensity at 610 nm was followed with a concomitant raise in the temperature from 25-100 °C at 1°C/min ramping speed. Each sample was also run in triplicate and buffer subtracted. Data analysis was performed using Origin software and DSF profiles were constructed by plotting SYPRO Orange fluorescence intensity as a function of temperature.[50,60,61]

Differential scanning calorimetry (DSC)

DSC experiments were performed with a MicroCal VP-AutoDSC instrument (MicroCal, LLC, Northampton, MA). Data was collected from 15 to 90 °C at a scanning rate of 60 °C/h for Fc solutions of 1 mg/ml concentration in 20 mM sodium phosphate buffer pH 6.00. The sample volume was 400 µl and each sample was run in triplicate. Data analysis was performed using the DSC data analysis software supplied by Microcal (Origin 7). In this analysis, the protein sample thermogram was subtracted from the buffer thermogram, baseline fitted, and normalized by concentration to obtain the final thermogram. The resulting thermograms were then fit to a non-2- state model with two transitions to calculate the melting temperatures of the first (Tm1) and

second (Tm2) transitions which correspond to the heat capacity peak maximum of the first and second endotherms in the thermograms, respectively.[61]

FUT8 (α1,6-fucosyltransferase) kinetics studies

FUT8 activity assay

A continuous coupled spectrophotometric assay similar to one described previously for α1,3-fucosyltransferase[52] was used to determine FUT8 catalytic activity. In this assay, the FUT8 reaction progress was followed by measuring UDP production (produced when FUT8 transfers fucose from GDP-L-fucose to the acceptor substrate, Figure 2A) with a pyruvate kinase/ lactate dehydrogenase (PK/LDH) coupled system to monitor NADH disappearance at 340 nm. This assay was performed in 50 mM HEPES buffer pH 7.5 containing GDP-fucose (350 µM, prepared as described in the appendix), potassium chloride (50 mM), phosphoenolpyruvate (0.75 mM), NADH (0.15 mM), free hybrid ($GlcNAcMan_5GlcNAc_2$) glycan (80 µM, prepared as descried in the appendix), 3 U pyruvate kinase (PK), and 4.2 U lactate dehydrogenase (LDH). The final volume was 150 µl and the reaction was started by the addition of FUT8 (4.5 µg) after letting the other components equilibrate for 5 min inside the cuvette at 37 °C. The decrease in NADH absorbance at 340 nm with time was followed using Evolution 260 Bio UV-visible spectrophotometer (ThermoScientific). The assay was done in triplicate and each time a blank (no GDP-fucose) was subtracted.

Determination of FUT8 kinetic parameters (K_M and V_{max})

For determination of FUT8 kinetic parameters (apparent K_M and V_{max}), the same assay conditions described above were used but with varied substrate concentrations. To determine FUT8 K_M and V_{max} of Asn297-bound N-glycan, the concentration of this glycan was varied from

40-300 µM. To determine FUT8 K_M and V_{max} of the free glycan (Asn297 released N-glycan), the concentration of this glycan was varied from 10-120 µM. In both cases, the concentration of the donor substrate (GDP-fucose) was fixed at 360 µM. Glycan concentration calculation was based on initial IgG2 Fc concentration, as determined by absorbance at 280 nm, in which the glycan concentration is twofold the Fc concentration (two glycans per Fc dimer). To determine FUT8 K_M and V_{max} with respect to GDP-fucose, the concentration of this nucleotide sugar was varied from 10-360 µM while the concentration of the acceptor substrate (free glycan used in this case) was kept at 80 µM. In all cases, equal amounts of FUT8 (0.52 µU in a reaction volume of 150 µl) were used to measure the kinetic parameters. Data analysis was performed using GraphPad Prism 7 software. The initial velocities at various concentrations were measured for each substrate and the data were fitted to the Michaelis-Menten kinetics model:

$$v_i = \frac{V_{max}[S]}{K_M + [S]}$$

Statistical analysis

Statistical analysis was done using unpaired *t* test to compare the different parameters. All statistical analyses were performed using GraphPad software. A p-value of less than 0.05 was used as the criterion for statistical significance.

References

(1) Vidarsson, G., Dekkers, G., and Rispens, T. (2014) IgG subclasses and allotypes: From structure to effector functions. *Front. Immunol. 5*, 1–17.

(2) Irani, V., Guy, A. J., Andrew, D., Beeson, J. G., Ramsland, P. A., and Richards, J. S. (2015) Molecular properties of human IgG subclasses and their implications for designing therapeutic monoclonal antibodies against infectious diseases. *Mol. Immunol. 67*, 171–182.

(3) Barrett, D. J., and Ayoub, E. M. (1986) IgG2 subclass restriction of antibody to pneumococcal polysaccharides. *Clin. Exp. Immunol. 63*, 127–34.

(4) Jefferis, R., and Kumararatne, D. S. (1990) Selective IgG subclass deficiency: quantification and clinical relevance. *Clin. Exp. Immunol. 81*, 357–67.

(5) Mikolajczyk, M. G., Concepcion, N. F., Wang, T., Frazier, D., Golding, B., Frasch, C. E., and Scott, D. E. (2004) Characterization of antibodies to capsular polysaccharide antigens of Haemophilus influenzae type b and Streptococcus pneumoniae in human immune globulin intravenous preparations. *Clin. Diagn. Lab. Immunol. 11*, 1158–64.

(6) Parker, A. R., Lock, E., Iftikhar, A., Barber, R., Stubbs, P. D., Harding, S., and Wallis, G. L. F. (2017) Purification and characterisation of anti-pneumococcal capsular polysaccharide IgG immunoglobulins. *Clin. Biochem. 50*, 80–83.

(7) Edelman, G. M., Cunningham, B. A., Gall, W. E., Gottlieb, P. D., Rutishauser, U., and Waxdal, M. J. (1969) The covalent structure of an entire gammaG immunoglobulin molecule. *Proc. Natl. Acad. Sci. U. S. A. 63*, 78–85.

(8) Abhinandan, K. R., and Martin, A. C. R. (2008) Analysis and improvements to Kabat and structurally correct numbering of antibody variable domains. *Mol. Immunol. 45*, 3832–3839.

(9) Mimura, Y., Church, S., Ghirlando, R., Ashton, P. R., Dong, S., Goodall, M., Lund, J., and Jefferis, R. (2000) The influence of glycosylation on the thermal stability and effector function expression of human IgG1-Fc: properties of a series of truncated glycoforms. *Mol Immunol 37*, 697–706.

(10) Abès, R., and Teillaud, J. L. (2010) Impact of glycosylation on effector functions of therapeutic IgG. *Pharmaceuticals 3*, 146–157.

(11) Kaneko, E., and Niwa, R. (2011) Optimizing therapeutic antibody function: Progress with fc domain engineering. *BioDrugs 25*, 1–11.

(12) Glassman, P. M., and Balthasar, J. P. (2014) Mechanistic considerations for the use of monoclonal antibodies for cancer therapy. *Cancer Biol. Med. 11*, 20–33.

(13) Vafa, O., Gilliland, G. L., Brezski, R. J., Strake, B., Wilkinson, T., Lacy, E. R., Scallon, B., Teplyakov, A., Malia, T. J., and Strohl, W. R. (2014) An engineered Fc variant of an IgG eliminates all immune effector functions via structural perturbations. *Methods 65*, 114–126.

(14) Shields, R. L., Lai, J., Keck, R., O'Connell, L. Y., Hong, K., Meng, Y. G., Weikert, S. H.

A., and Presta, L. G. (2002) Lack of Fucose on Human IgG1 N-Linked Oligosaccharide Improves Binding to Human Fcgamma RIII and Antibody-dependent Cellular Toxicity. *J. Biol. Chem. 277*, 26733–26740.

(15) Nimmerjahn, F., and Ravetch, J. V. (2008) Fcgamma receptors as regulators of immune responses. *Nat. Rev. Immunol. 8*, 34–47.

(16) Shinkawa, T., Nakamura, K., Yamane, N., Shoji-Hosaka, E., Kanda, Y., Sakurada, M., Uchida, K., Anazawa, H., Satoh, M., Yamasaki, M., Hanai, N., and Shitara, K. (2003) The absence of fucose but not the presence of galactose or bisecting N-acetylglucosamine of human IgG1 complex-type oligosaccharides shows the critical role of enhancing antibody-dependent cellular cytotoxicity. *J Biol Chem 278*, 3466–3473.

(17) Yamane-Ohnuki, N., Kinoshita, S., Inoue-Urakubo, M., Kusunoki, M., Iida, S., Nakano, R., Wakitani, M., Niwa, R., Sakurada, M., Uchida, K., Shitara, K., and Satoh, M. (2004) Establishment of FUT8 knockout Chinese hamster ovary cells: An ideal host cell line for producing completely defucosylated antibodies with enhanced antibody-dependent cellular cytotoxicity. *Biotechnol. Bioeng. 87*, 614–622.

(18) Ferrara, C., Grau, S., Jager, C., Sondermann, P., Brunker, P., Waldhauer, I., Hennig, M., Ruf, A., Rufer, A. C., Stihle, M., Umana, P., and Benz, J. (2011) Unique carbohydrate-carbohydrate interactions are required for high affinity binding between Fc RIII and antibodies lacking core fucose. *Proc. Natl. Acad. Sci. 108*, 12669–12674.

(19) Mizushima, T., Yagi, H., Takemoto, E., Shibata-Koyama, M., Isoda, Y., Iida, S., Masuda, K., Satoh, M., and Kato, K. (2011) Structural basis for improved efficacy of therapeutic antibodies on defucosylation of their Fc glycans. *Genes to Cells 16*, 1071–1080.

(20) Yamane-Ohnuki, N., and Satoh, M. (2009) Production of therapeutic antibodies with controlled fucosylation. *MAbs 1*, 230–6.

(21) Uozumi, N., Yanagidani, S., Miyoshi, E., Ihara, Y., Sakuma, T., Gao, C., Teshima, T., Fujii, S., Shiba, T., and Taniguchi, N. (1996) Purification and cDNA Cloning of Porcine Brain GDP-L-Fuc:N-Acetyl-β-D-Glucosaminide α1→6Fucosyltransferase. *Biochemistry 271*, 27810 –27817.

(22) Ihara, H., Ikeda, Y., and Taniguchi, N. (2006) Reaction mechanism and substrate specificity for nucleotide sugar of mammalian α1,6-fucosyltransferase - A large-scale preparation and characterization of recombinant human FUT8. *Glycobiology 16*, 333–342.

(23) Beck, A., and Reichert, J. M. (2012) Marketing approval of mogamulizumab A triumph for glyco-engineering. *MAbs 4*, 419–425.

(24) Miurae, R. (1990) Structural Heterogeneity of Sugar Chains in Immunoglobulin bovine. *J. Biol. Chem. 265*, 6009–6018.

(25) Rudd, P. M., and Dwek, R. a. (1997) Glycosylation: heterogeneity and the 3D structure of proteins. *Crit. Rev. Biochem. Mol. Biol. 32*, 1–100.

(26) Jabs, W., Resemann, A., Evers, W., Evans, C., Main, L., Baessmann, C., Suckau, D., Wagner-Rousset, E., Ayoub, D., and Beck, B. (2012) Fast and Extensive Mass Spectrometry

Characterization of Therapeutic mAbs: The Panitumumab Case Study. *CASSS Mass Spec 2012 Poster*, P–125.

(27) Stavenhagen, K., Plomp, R., and Wuhrer, M. (2015) Site-specific protein N- and O-glycosylation analysis by a C18-porous graphitized carbon-liquid chromatography-electrospray ionization mass spectrometry approach using pronase treated glycopeptides. *Anal. Chem. Just accep*.

(28) Upton, R., Bell, L., Guy, C., Caldwell, P., Estdale, S., Barran, P. E., and Firth, D. (2016) Orthogonal Assessment of Biotherapeutic Glycosylation: A Case Study Correlating N-Glycan Core Afucosylation of Herceptin with Mechanism of Action. *Anal. Chem. 88*, 10259–10265.

(29) Thaysen-Andersen, M., and Packer, N. H. (2012) Site-specific glycoproteomics confirms that protein structure dictates formation of N-glycan type, core fucosylation and branching. *Glycobiology 22*, 1440–1452.

(30) Fujii, S., Nishiura, T., Nishikawa, A., Miura, R., and Taniguchi, N. (1990) Structural heterogeneity of sugar chains in immunoglobulin G: Conformation of immunoglobulin G molecule and substrate specificities of glycosyltransferases. *J. Biol. Chem. 265*, 6009–6018.

(31) Ritamo, I., Cloutier, M., Valmu, L., Néron, S., and Räbinä, J. (2014) Comparison of the glycosylation of in vitro generated polyclonal human IgG and therapeutic immunoglobulins. *Mol. Immunol. 57*, 255–262.

(32) Reusch, D., and Tejada, M. L. (2015) Fc glycans of therapeutic antibodies as critical quality attributes. *Glycobiology*.

(33) Melliss, S. J., and Baenzigere, U. (1983) Structures of the Oligosaccharides Present at the Three Asparagine- linked Glycosylation Sites of Human IgD *. *J. Biol. Chem. 258*, 11546–11556.

(34) Temple, G. F. (2009) The completion of the Mammalian Gene Collection (MGC). *Genome Res. 19*, 2324–2333.

(35) Xiao, J., Chen, R., Pawlicki, M. A., and Tolbert, T. J. (2009) Targeting a homogeneously glycosylated antibody Fc to bind cancer cells using a synthetic receptor ligand. *J. Am. Chem. Soc. 131*, 13616–13618.

(36) Wang, S., Ionescu, R., Peekhaus, N., Leung, J. Y., Ha, S., and Vlasak, J. (2010) Separation of post-translational modifications in monoclonal antibodies by exploiting subtle conformational changes under mildly acidic conditions. *J. Chromatogr. A 1217*, 6496–6502.

(37) Ha, S., Ou, Y., Vlasak, J., Li, Y., Wang, S., Vo, K., Du, Y., Mach, A., Fang, Y., and Zhang, N. (2011) Isolation and characterization of IgG1 with asymmetrical Fc glycosylation. *Glycobiology 21*, 1087–1096.

(38) Miura, M., Hirose, M., Miwa, T., Kuwae, S., and Ohi, H. (2004) Cloning and characterization in Pichia pastoris of PNO1 gene required for phosphomannosylation of N-linked oligosaccharides. *Gene 324*, 129–137.

(39) Lobstein, J., Emrich, C. A., Jeans, C., Faulkner, M., Riggs, P., and Berkmen, M. (2012) SHuffle, a novel Escherichia coli protein expression strain capable of correctly folding disulfide bonded proteins in its cytoplasm. *Microb. Cell Fact. 11*, 56.

(40) Zhu, Y., Suits, M. D. L., Thompson, A. J., Chavan, S., Dinev, Z., Dumon, C., Smith, N., Moremen, K. W., Xiang, Y., Siriwardena, A., Williams, S. J., Gilbert, H. J., and Davies, G. J. (2010) Mechanistic insights into a Ca2+-dependent family of alpha-mannosidases in a human gut symbiont. *Nat. Chem. Biol. 6*, 125–32.

(41) Cuskin, F., Lowe, E. C., Temple, M. J., Zhu, Y., Cameron, E. A., Pudlo, N. A., Porter, N. T., Urs, K., Thompson, A. J., Cartmell, A., Rogowski, A., Hamilton, B. S., Chen, R., Tolbert, T. J., Piens, K., Bracke, D., Vervecken, W., Hakki, Z., Speciale, G., Munoz-Munoz, J. L., Day, A., Pena, M. J., McLean, R., Suits, M. D., Boraston, A. B., Atherly, T., Ziemer, C. J., Williams, S. J., Davies, G. J., Abbott, D. W., Martens, E. C., and Gilbert, H. J. (2015) Human gut Bacteroidetes can utilize yeast mannan through a selfish mechanism. *Nature 517*, 165–169.

(42) Chen, R., Pawlicki, M. A., Hamilton, B. S., and Tolbert, T. J. (2008) Enzyme-Catalyzed Synthesis of a Hybrid N-Linked Oligosaccharide using N-Acetylglucosaminyltransferase I. *Adv. Synth. Catal. 350*, 1689–1695.

(43) Longmore, G. D., and Schachter, H. (1982) Product-identification and substrate-specificity studies of the GDP-L-fucose:2-acetamido-2-deoxy-beta-D-glucoside (FUC goes to Asn-linked GlcNAc) 6-alpha-L-fucosyltransferase in a Golgi-rich fraction from porcine liver. *Carbohydr. Res. 100*, 365–392.

(44) Wang, W., Hu, T., Frantom, P. A., Zheng, T., Gerwe, B., Del Amo, D. S., Garret, S., Seidel, R. D., and Wu, P. (2009) Chemoenzymatic synthesis of GDP-L-fucose and the Lewis X glycan derivatives. *Proc. Natl. Acad. Sci. U. S. A. 106*, 16096–101.

(45) Okbazghi, S. Z., More, A. S., White, D. R., Duan, S., Shah, I. S., Joshi, S. B., Middaugh, C. R., Volkin, D. B., and Tolbert, T. J. (2016) Production, Characterization, and Biological Evaluation of Well-Defined IgG1 Fc Glycoforms as a Model System for Biosimilarity Analysis. *J. Pharm. Sci. 105*, 559–574.

(46) Bruhns, P., Iannascoli, B., England, P., Mancardi, D. A., Fernandez, N., Jorieux, S., and Daëron, M. (2009) Specificity and affinity of human Fcγ receptors and their polymorphic variants for human IgG subclasses. *Blood 113*, 3716–3725.

(47) Latypov, R. F., Hogan, S., Lau, H., Gadgil, H., and Liu, D. (2012) Elucidation of acid-induced unfolding and aggregation of human immunoglobulin IgG1 and IgG2 Fc. *J. Biol. Chem. 287*, 1381–1396.

(48) Vermeer, A. W. P., and Norde, W. (2000) The Thermal Stability of Immunoglobulin: Unfolding and Aggregation of a Multi-Domain Protein. *Biophys. J. 78*, 394–404.

(49) Cheng, W., Joshi, S. B., He, F., Brems, D. N., He, B., Kerwin, B. A., Volkin, D. B., and Middaugh, C. R. (2012) Comparison of high-throughput biophysical methods to identify stabilizing excipients for a model IgG2 monoclonal antibody: Conformational stability and kinetic aggregation measurements. *J. Pharm. Sci. 101*, 1701–1720.

(50) He, F., Hogan, S., Latypov, R. F., Narhi, L. O., and Razinkov, V. I. (2010) High throughput thermostability screening of monoclonal antibody formulations. *J. Pharm. Sci. 99*, 1707–1720.

(51) Alsenaidy, M. A., Kim, J. H., Majumdar, R., Weis, D. D., Joshi, S. B., Tolbert, T. J., Middaugh, C. R., and Volkin, D. B. (2013) High-throughput biophysical analysis and data visualization of conformational stability of an igg1 monoclonal antibody after deglycosylation. *J. Pharm. Sci. 102*, 3942–3956.

(52) Gosselin, S., Alhussaini, M., Streiff, M. B., Takabayashi, K., and Palcic, M. M. (1994) A continuous spectrophotometric assay for glycosyltransferases. *Anal. Biochem.*

(53) Nakanishi-Shindo, Y., Nakayama, K. I., Tanaka, A., Toda, Y., and Jigami, Y. (1993) Structure of the N-linked oligosaccharides that show the complete loss of α-1,6-polymannose outer chain from och1, och1 mnn1, and och1 mnn1 alg3 mutants of Saccharomyces cerevisiae. *J. Biol. Chem. 268*, 26338–26345.

(54) Nett, J. H., and Gerngross, T. U. (2003) Cloning and disruption of the PpURA5 gene and construction of a set of integration vectors for the stable genetic modification of Pichia pastoris. *Yeast 20*, 1279–1290.

(55) Wilson JR, Williams D, S. H. (1976) The control of glycoprotein synthesis: N-acetylglucosamine linkage to a mannose residue as a signal for the attachment of L-fucose to the asparagine-linked N-acetylglucosamine residue of glycopeptide from alpha1-acid glycoprotein. *Biochem. Biophys. Res. Commun. 72*, 909–916.

(56) Voynow, J. A., Kaiser, R. S., Scanlin, T. F., and Catherine, M. (1991) Purification and Characterization of GDP-L-fucose-N-acetyl β-D-glucosaminide α1-6 Fucosyltransferase from Cultured Human Skin Fibroblasts. *J. Biol. Chem. 266*, 21572–21577.

(57) Ihara, H., Ikeda, Y., Toma, S., Wang, X., Suzuki, T., Gu, J., Miyoshi, E., Tsukihara, T., Honke, K., Matsumoto, A., Nakagawa, A., and Taniguchi, N. (2007) Crystal structure of mammalian α1,6-fucosyltransferase, FUT8. *Glycobiology 17*, 455–466.

(58) Mimura, Y., Sondermann, P., Ghirlando, R., Lund, J., Young, S. P., Goodall, M., and Jefferis, R. (2001) Role of Oligosaccharide Residues of IgG1-Fc in Fc γ RIIb Binding. *J. Biol. Chem. 276*, 45539–45547.

(59) Hari, S. B., Lau, H., Razinkov, V. I., Chen, S., and Latypov, R. F. (2010) Acid-induced aggregation of human monoclonal IgG1 and IgG2: Molecular mechanism and the effect of solution composition. *Biochemistry 49*, 9328–9338.

(60) Alsenaidy, M. A., Okbazghi, S. Z., Kim, J. H., Joshi, S. B., Russell Middaugh, C., Tolbert, T. J., and Volkin, D. B. (2014) Physical stability comparisons of IgG1-Fc variants: Effects of N-glycosylation site occupancy and Asp/gln residues at site asn 297. *J. Pharm. Sci. 103*, 1613–1627.

(61) More, A. S., Toprani, V. M., Okbazghi, S. Z., Kim, J. H., Joshi, S. B., Middaugh, C. R., Tolbert, T. J., and Volkin, D. B. (2016) Correlating the Impact of Well-Defined Oligosaccharide Structures on Physical Stability Profiles of IgG1-Fc Glycoforms. *J. Pharm. Sci. 105*, 588–601.

(62) Sondermann, P., Pincetic, A., Maamary, J., Lammens, K., and Ravetch, J. V. (2013) General mechanism for modulating immunoglobulin effector function. *Proc. Natl. Acad. Sci. U. S. A. 110*, 9868–72.

(63) Matsumiya, S., Yamaguchi, Y., Saito, J., Nagano, M., Sasakawa, H., Otaki, S., Satoh, M., Shitara, K., and Kato, K. (2007) Structural comparison of fucosylated and nonfucosylated Fc fragments of human immunoglobulin G1. *J Mol Biol 368*, 767–779.

(64) Chen, C.-L., Hsu, J.-C., Lin, C.-W., Wang, C.-H., Tsai, M.-H., Wu, C.-Y., Wong, C.-H., and Ma, C. (2017) Crystal structure of a homogeneous IgG-Fc glycoform with the N-glycan designed to maximize the antibody dependent cellular cytotoxicity. *ACS Chem. Biol.* acschembio.7b00140.

(65) Subedi, G. P., and Barb, A. W. (2015) The Structural Role of Antibody N-Glycosylation in Receptor Interactions. *Structure 23*, 1–11.

(66) Bowden, T. A., Baruah, K., Coles, C. H., Harvey, D. J., Yu, X., Song, B. D., Stuart, D. I., Aricescu, A. R., Scanlan, C. N., Jones, E. Y., and Crispin, M. (2012) Chemical and structural analysis of an antibody folding intermediate trapped during glycan biosynthesis. *J. Am. Chem. Soc. 134*, 17554–17563.

(67) Nishima, W., Miyashita, N., Yamaguchi, Y., Sugita, Y., and Re, S. (2012) Effect of bisecting GlcNAc and core fucosylation on conformational properties of biantennary complex-type N-glycans in solution. *J. Phys. Chem. B 116*, 8504–8512.

(68) Ferrara, C., Brünker, P., Suter, T., Moser, S., Püntener, U., and Umaña, P. (2006) Modulation of therapeutic antibody effector functions by glycosylation engineering: influence of Golgi enzyme localization domain and co-expression of heterologous beta1, 4-N-acetylglucosaminyltransferase III and Golgi alpha-mannosidase II. *Biotechnol. Bioeng. 93*, 851–861.

Chapter 3

FUT8-catalyzed functionalization of Asn297 glycan of IgG2 Fc for the design of site-specific antibody drug conjugates

Introduction

Antibody drug conjugates (ADCs) represent a rapidly growing class of pharmaceutical products and hold a considerable promise for the treatment of many diseases, especially cancer.[1] Antibody drug conjugates are hybrid molecules combining the tumor-targeting specificity and long circulating half-life of the monoclonal antibody (mAb) with the enhanced antitumor activity of toxic payload attached to them. The recent approval of Seattle Genetics's brentuximab vedotin (in 2011) and Immunogen's trastuzumab emtansine (in 2013) has sparked a tremendous interest in the development of new ADCs and currently there are more than 60 ADCs at different stages of clinical trials.[2]

The first generation ADCs relied on the conventional conjugation chemistries through the epsilon-amino group of lysine and the thiol group of reduced disulfide bond cysteine. However, these early conjugation methods result in heterogeneous ADCs that are mixtures of molecules different in the number and sites of attachment of the drug on the mAb part of the ADC. For example, there are about 40 lysine residues per mAb and a stochastic drug conjugation using this amino acid in a mAb would generate more than million different species.[3] This heterogeneity of the ADC prepared by conventional methods adds more complication to the development and regulatory approval of ADCs since the mAb part of these products may already have a certain level of heterogeneity to start with due to posttranslational modifications, such as the variation in the Asn297 glycosylation profile.[4] Therefore, such products require more control of the production processes and extensive characterization to ensure an acceptable consistency across different production batches.

The site of conjugation has also been shown to be critical for ADC stability and pharmacokinetics and a better control of the conjugation site could improve the overall ADC tolerability and widen the therapeutic index.[5,6] With the need for a well-defined product and with

the advances in the fields of protein engineering and conjugation chemistry, the focus of the pharmaceutical industry and many other research groups has changed to produce ADCs through site-specific conjugation[2,7–11] One of the leading technologies to make site-specific ADC is the so called THIOMAB technology.[5] In this technology, an antibody was engineered to have extra cysteine residues at specific sites to be used in conjugating the payload through thiol reactive linkers instead of using the reduced disulfide bonds cysteines of the antibody for conjugation. This technology yielded nearly homogeneous conjugates with good safety profiles. The emergence of the THIOMAB technology has paved the way for many other approaches designed to make site-specific ADC with better control of the location of the cytotoxic drug, drug to antibody ratio (DAR), and homogeneity as critical parameters in determining the efficacy and safety profile of the resultant ADC. Some of these approaches relied on genetic engineering of the expression host to introduce an unnatural amino acid (UAA) containing a bioorthogonal handle at certain sites within the amino acid sequence of the mAb to enable site-specific conjugation.[12,13] Other approaches utilized certain enzymes such as formylglycine generating enzyme (FGE)[14] and sortase A (Srt A)[15] that can recognize a specific amino acid sequence within the antibody peptide backbone to introduce a handle that enables site-specific attachment of payload using suitable conjugation chemistries.

An interesting site for making site-specific ADC is the well-conserved Asn297 glycan located in the C_H2 domain of the antibody (IgG).[11] Conjugation through this glycan could minimize any potential reduction in the ADC affinity for the target ligand since it is relatively distant from the Fab region of the antibody. Also, located away from the FcRn binding site, the Asn297 glycan does not affect binding of the antibody to this receptor, which is an essential receptor in mediating the recycling of IgG and gives it a long biological half-life.[16–18] Several

approaches have been developed to functionalize this glycan for site-specific conjugation. Some of these approaches relied on the use of chemical means to functionalize certain sugar units within this glycan such as periodate oxidation of the core fucose to introduce an aldehyde group for conjugation with hydrazide derivatives.[19] Metabolic engineering was also used to introduce unnatural sugar units to the Asn297 glycan such as the 6-thiofucose, where this unnatural thio-sugar could be used for conjugation using thiol-maleimide chemistry to produce ADCs.[20] *In vitro* chemoenzymatic synthesis using glycosyltransferases to place unnatural sugar units containing a suitable handle on this glycan was also utilized.[11] For example, an engineered galactosyltransferase (Y289L) was used to add GalNAc analogues, such as GalNAz or 2-keto-Gal, to the Asn297 glycan for subsequent conjugation using bioorthogonal chemistry.[21–24] Conjugation through the Asn297 glycan can be a promising and a straightforward strategy to equip antibodies with a suitable payload without the need for antibody engineering.

In this work we developed an efficient method for bioorthogonal functionalization of the Asn297 glycan using *in vitro* mammalian α1,6-fucosyltransferase (FUT8)-catalyzed chemoenzymatic synthesis to place the unnatural sugar 6-azido-L-fucose on this glycan. This method was utilized in making homogeneous conjugates using different types of linkers having different physicochemical properties combined with different bioorthogonal click chemistry. These conjugates were characterized in terms of their structural stability, solubility, and binding properties.

Results

In vitro chemoenzymatic functionalization of Asn297 glycan for bioorthogonal click reactions

The core linked fucose (α1,6-fucose) position of the Asn297 glycan of IgG was targeted in this study as a site for adding a modified sugar (6-azido-L-fucose) to provide a bioorthogonal handle for site-specific conjugation to make ADCs. Due to the need for milligram quantities of a highly homogeneous afucosylated IgG2 Fc to perform this study, we used the yeast *Pichia pastoris* to express this Fc coupled with *in vitro* enzymatic synthesis as described in chapter 2. The addition of 6-azido-L-fucose was carried out via *in vitro* FUT8-catalyzed reaction shown in Figure 1A. FUT8 is a mammalian enzyme that catalyzes core fucosylation of N-glycans.[25,26] Initially, we tried to perform the addition of the modified sugar to the Asn297 glycan by following a one-pot strategy similar to the one-pot strategy that we followed in chapter 2 for the addition of the natural sugar fucose to the Asn297 glycan. During the one-pot strategy, the formation of the nucleotide sugar (GDP-azidofucose), required for FUT8 reaction, from the simple sugar (6-azido-L-fucose) is catalyzed *in situ* by FKP. FKP is a bifunctional enzyme where it catalyzes the formation of GDP-azidofucose from 6-azido-L-fucose in two steps as shown in Figure 1B.[27,28] In the first step, it converts 6-azido-L-fucose into 6-azido-L-fucose-1-phosphate through its kinase activity while in the second step it converts 6-azido-L-fucose-1-phosphate into GDP-azidofucose through its guanylyltransferase activity.

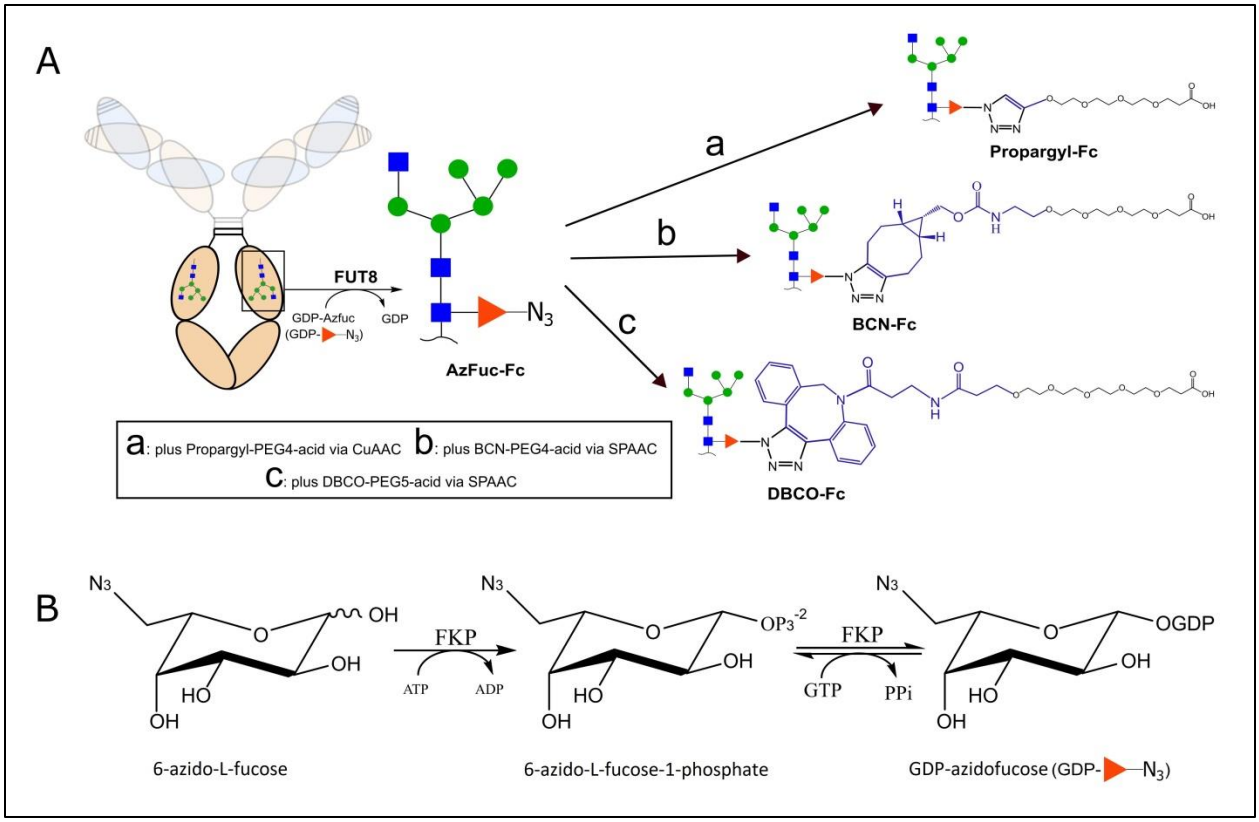

Figure 1. Site-specific functionalization and conjugation through Asn297 glycan of IgG2 Fc. **A)** FUT8-catalyzed functionalization of IgG2 Fc followed by conjugation of different linkers using biorthogonal click reactions. **B)** Reaction catalyzed by FKP for the synthesis of guanosine 5′-diphospho-β-L-6-azido-fucose (GDP-azidofucose) from 6-azido-L-fucose. FUT8: mammalian α1,6-fucosyltransferase. FKP: L-fucokinase/guanosine 5'-diphosphate-L-fucose pyrophosphorylase.

Although the one-pot strategy eventually results in complete functionalization of the IgG2 Fc (Appendix: Figure B1), the conversion was slow and required nine days compared to only two days conversion when the natural sugar fucose is used instead of the modified sugar 6-azido-L-fucose (Figure 2A). The one-pot strategy involved three enzyme catalytic steps: two steps are catalyzed by FKP to form the nucleotide sugar and one step is catalyzed by FUT8 to

add the sugar to the glycan (Figure 1). The rate of the first step of the FKP reaction was tested by using a continuous coupled spectrophotometric assay similar to the one described previously.[29]

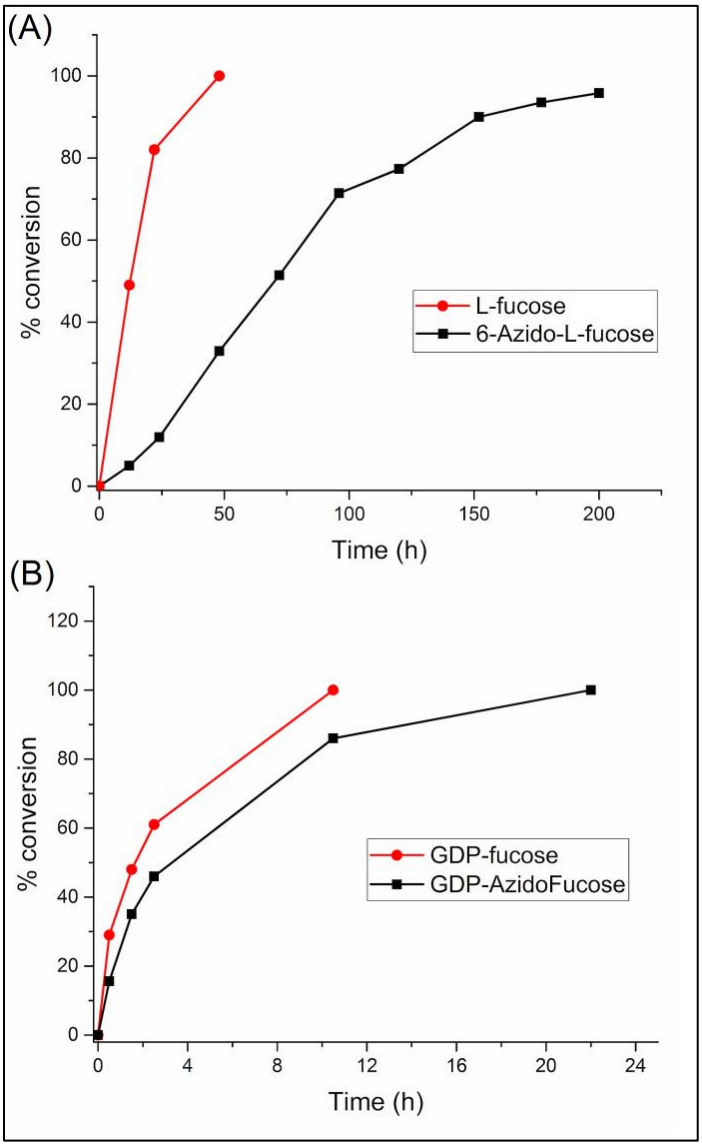

Figure 2. Effect of sugar type and reaction conditions on FUT8 reaction rate and progress. **A)** One-pot (three steps) reaction utilizing *in situ* formed GDP-fucose (●) or GDP-azidofucose (■). **B)** One-step reaction utilizing purified GDP-fucose (●) or GDP-azidofucose (■). Reactions progress was followed by Q-TOF LC/MS analysis of intact protein and the peak intensities were used to calculate the percentage of conversion of the afucosylated IgG2 Fc glycoform into the corresponding IgG2 Fc variant (fucosylated Fc or AzFuc-Fc).

During this assay, the rate of the FKP kinase step was measured for 6-azido-L-fucose and compared directly to that of the natural sugar, fucose. As expected and in agreement with the literature[28], the rate of this step was about 8 times slower when using the modified sugar 6-azido-L-fucose (Appendix: Figure B2). On the other hand, the second step of FKP is a reversible step and although we did not measure it directly, it also appeared to be slower when the modified sugar 6-azido-L-fucose is used instead of fucose during the chemoenzymatic synthesis of the corresponding nucleotide sugar (see appendix B for the chemoenzymatic synthesis of GDP-azidofucose and also appendix A for the synthesis GDP-fucose).

To speed up the functionalization of IgG2 Fc with 6-azido-L-fucose for bioorthogonal click reactions, the nucleotide sugar form of this sugar (i.e. GDP-azidofucose) was synthesized and purified as described in the appendix. Then, the purified nucleotide sugar was used directly in the functionalization reaction where only one step (the FUT8 step) is required to make the product. Before scaling up the production of the functionalized Fc (AzFuc-Fc), a small scale FUT8 reaction using the purified GDP-azidofucose was carried out and compared directly with a FUT8 reaction utilizing the natural nucleotide sugar GDP-fucose. This experiment was done to optimize the FUT8 functionalization reaction conditions and also as a measure of the promiscuity of FUT8 and its efficiency in transferring the modified sugar relative to the natural sugar. The reaction kinetics from these small scale reactions showed that FUT8 is quite promiscuous and transferred the modified sugar to the Asn297 glycan at only half the rate of the natural substrate under the same reaction conditions (Figure 2B). Afterward, a large scale reaction was carried out using the same reaction conditions to produce enough of the AzFuc-Fc to act as a substrate for site-specific conjugation studies using the bioorthogonal azide-alkyne cycloaddition (AAC) reactions. During this large scale reaction, 36 mg of the AzFuc-IgG2 Fc

was produced from 40 mg afucosylated Fc (90% yield). The purity and integrity of this functionalized Fc was confirmed by SDS-PAGE, while the homogeneity and the mass of the product were confirmed using intact protein LC-MS (Figure 3A). The calculated mass of AzFuc-IgG2 Fc is 26461.1 Da and the observed mass is 26459.6 Da.

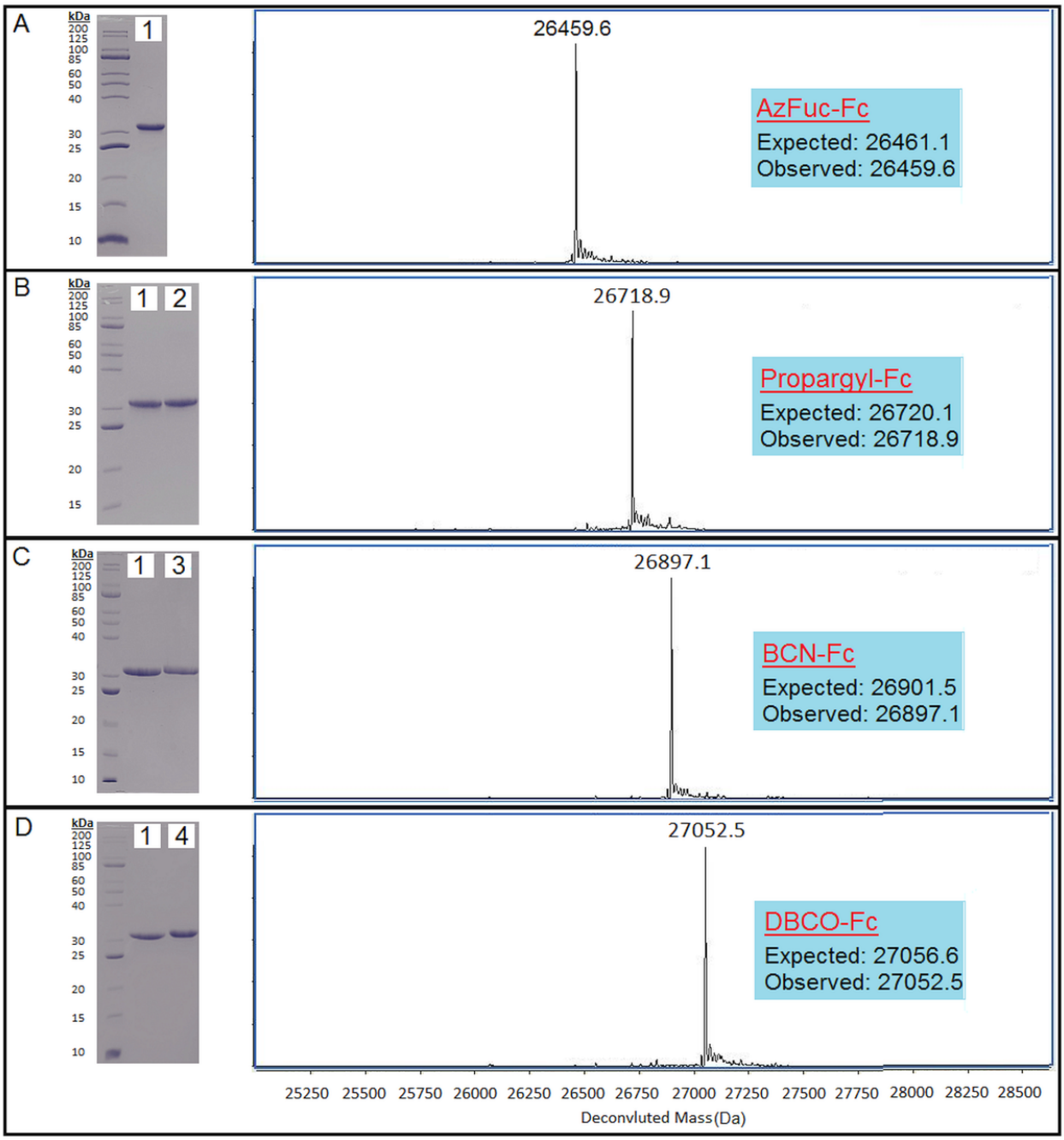

Figure 3. Initial characterization of IgG2 Fc variants using SDS-PAGE and Q-TOF LC/MS analyses under reducing conditions. SDS-PAGE lanes are as following: (1) 6-azido-L-fucose functionalized IgG2 Fc (AzFuc-Fc); (2) Propargyl-PEG4-acid-IgG2 Fc conjugate (Propargyl-Fc); (3) BCN-PEG4-acid-IgG2 Fc conjugate (BCN-Fc); (4) DBCO-PEG5-acid-IgG2 Fc conjugate (DBCO-Fc).

Preparation of site-specific IgG2 Fc conjugates using azide-alkyne cycloaddition

The AzFuc-IgG2 Fc was then utilized in AAC conjugation reactions using polyethylene glycol (PEG) linkers functionalized with different alkynes (Figure 1A).

One way we performed the conjugation was through the use of copper(I)-catalyzed azide-alkyne cycloaddition (CuAAC). In CuAAC, copper(I) acts a catalyst to promote the reaction between the azide and the linear alkyne to form a stable triazole linkage. The most common way to provide the reaction with copper(I) is by generating this metal *in situ* by reducing a copper(II) compound, such as $CuSO_4$, by sodium ascorbate. Our first trials to perform the CuAAC using AzFuc-Fc and the alkyne propargyl-PEG4-acid did not go smoothly, as the protein started to aggregate and precipitate out of the solution shortly after starting the reaction. However, by including Tris(3-hydroxypropyltriazolylmethyl)amine (THPTA)[30,31] in the reaction, no more aggregates were seen and the reaction proceeded smoothly towards the product as checked by intact protein mass spectrometry. However, as the reaction proceeds further towards the product, the protein started to undergo oxidation as evidenced by intact protein mass spectrometry (Appendix: Figure B3). In order to address the oxidation problem, we added an excess of free amino acids to the reaction mixture, such as methionine and arginine, to potentially intercept any reactive oxygen species. Reactive oxygen species generated by the copper(II) sulfate/ascorbate system are well known oxidizers of protein susceptible amino acids.[32] However, the addition of these free amino acids did not appear to reduce the oxidation problem as shown from intact protein mass spectra (Appendix: Figure B4 and B5). Another way we tried to address the oxidation issue is through the use of copper(I) directly in the form of Cu(I)Br instead of the copper(II) sulfate/ascorbate system. Unfortunately, this trial did not appear to solve the problem (Appendix: Figure B6).

To solve the oxidation problem and produce the IgG2 Fc-propargyl conjugate (Propargyl-Fc) necessary for subsequent studies described in this chapter, we tried to accelerate the CuAAC so that the conjugation reaction is completed in less than one hour. During the first hour of the reaction, and based on our preliminary reactions for optimizing the CuAAC, the IgG2 Fc did not exhibit a detectable level of oxidation as evidenced by the intact protein mass spectra. Therefore, a larger excess (about 2.5-fold) of the alkyne (propargyl-PEG4-acid) was used in the reaction mixture to drive the reaction to completion before any significant level of oxidation started to show up in the intact protein mass spectrum. By doing that, we were able to accelerate the reaction and make it completed in less than 40 minutes as shown in the Figure B7of the appendix. However, to remove the copper and prevent the formation of reactive oxygen species, the reaction mixture was immediately diluted with 15 volume of 1 mM EDTA in 50 mM HEPES buffer at pH 7.5. The reaction mixture was then concentrated back to initial volume using Amicon Ultra-15 centrifugal filter units. This process was repeated twice followed by dialysis of the reaction mixture in a suitable buffer for subsequent studies. The protein mass spectrum of the Propargyl-Fc conjugate prepared following this procedure showed no sign of oxidation (Figure 3B), while the control Propargyl-Fc conjugate showed an extensive level of oxidation (Appendix: Figure B7D).

The other way to conjugate certain compounds through the 6-azido-L-fucose attached to the Asn297 glycan of IgG2 Fc in a specific manner is through the use of copper-free azide-alkyne cycloaddition, which is widely known as strain promoted azide-alkyne cycloaddition (SPAAC).[33] In one SPAAC reaction, we chose to use bicyclononyne (BCN) linker represented by BCN-PEG4-Acid (Figure 1A). This reaction was carried out by mixing the AzFuc-Fc with excess BCN linker in aqueous solution at room temperature. The strain within the cyclic alkyne

(BCN) is the driving force for the reaction to proceed forward towards the formation of the conjugate without the need for copper(I). The reaction progress was followed using intact protein LC-MS. Under the reaction conditions described in the materials and methods section (380 μM BCN linker) of this chapter, the reaction required two days for full conjugation of the BCN linker to Asn297 glycan of IgG2 Fc (Figure 3C). To confirm the conjugation site specificity, the resultant IgG2 Fc-BCN conjugate (BCN-Fc) was subjected to PNGase F digestion followed by intact protein mass spectrometry analysis. The mass spectrum showed a single peak corresponding to the mass of the deglycosylated IgG2 Fc (Appendix: Figure B8).

In another SPAAC reaction, we chose to use dibenzocyclooctyne (DBCO) linker represented by DBCO-PEG5-acid. Again, the reaction was carried out by simply mixing of AzFuc-Fc with excess DBCO linker (25 μM) in aqueous media using 50 mM HEPES buffer at pH 7.5. The reaction was quite efficient and full conjugation was achieved in 22 hours (Figure 3D). Interestingly, the SPAAC reaction kinetics using DBCO linker was much faster than that when using the BCN linker despite the fact that the concentration of BCN linker was more than 15 times higher than the concentration of the DBCO linker in these reactions. The site of conjugation in DBCO-Fc conjugate was also confirmed by PNGase F digestion and intact protein mass spectrometry analyses (Appendix: Figure B8).

Characterization and studies of the conjugates

Dynamic light scattering

The hydrodynamic sizes of all IgG2 Fc variants (functionalized Fc, Fc-conjugates, and deglycosylated Fc) in 20 mM phosphate buffer (pH 6.0) were measured using dynamic light scattering. The intensity-derived size distribution plots of all Fc variants also show the absence

of large aggregates (Appendix: Figure B9) and low polydispersity (< 15%) values suggesting a monodisperse size distribution. As shown in Figure 4, hydrodynamic diameters of Fc variants were found to be between 6.9 and 7.5 nm. The size of the AzFuc-Fc (6.99 ± 0.05 nm) and the deglycosylated Fc (6.93 ± 0.03 nm) were found to be similar (p=0.13) showing that the removal of glycans had no significant influence on protein hydrodynamic sizes. This is presumably because the Asn297 glycans are buried between the C_H2 domains as they appear in most IgG Fc crystal structures.[34–36] However, the sizes of the DBCO-, Propargyl-, and BCN-conjugates were 7.47, 7.44, and 7.21 nm, respectively, reflecting a slight increase in the size of the Fc upon conjugating the corresponding linker to the Asn297 glycan.

Comparison of thermal stability

The secondary structure stability of the prepared Fc variants in response to increasing temperature (10 to 90 ºC) in 20 mM phosphate buffer (pH 6.0) was evaluated using Far-UV CD spectroscopy. As shown in Figure B10 of the appendix, CD spectra of all Fc variants showed minima around 216 nm indicating as expected primarily beta-sheet structure in the samples at 10 ºC. A strong negative shoulder is also seen at 230 nm due to tryptophan. The mean residue molar ellipticity at 218 nm was plotted as a function of temperature to monitor the loss of secondary structure during thermal stress. As shown in Figure 5A, the CD signal of protein samples became more negative above 60 °C indicating a loss of protein secondary structure. The order of T_m values is as following: AzFuc-Fc, DBCO-Fc, Propargyl-Fc > BCN-Fc > deglycosylated Fc (Figure 5E and Table B1 of the appendix). No significant difference in T_m values among AzFuc-Fc, DBCO-Fc, and Propargyl-Fc was observed. In contrast, the deglycosylated Fc showed a transition at least 6 °C lower indicating a major loss of stability.

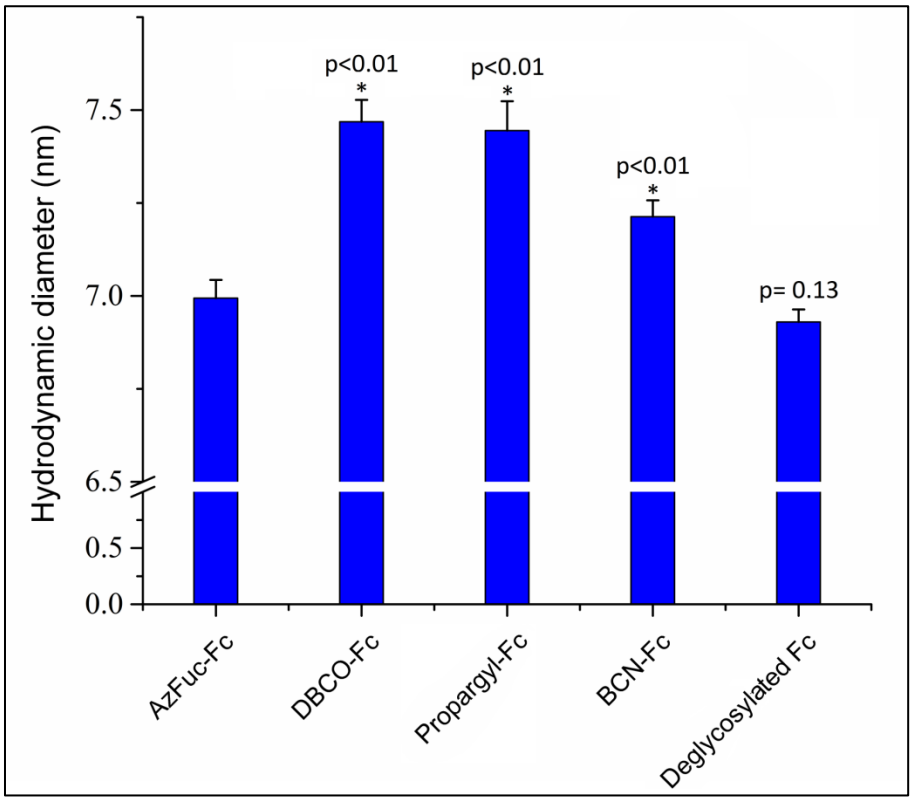

Figure 4. Hydrodynamic diameter of various IgG2 Fc variants prepared in this work as determined by dynamic light scattering (DLS). Measurements were conducted at 25 °C with each Fc variant prepared in 20 mM phosphate buffer (pH 6.0) at 1 mg/ml concentration. Error bar indicates standard deviation (N =3).

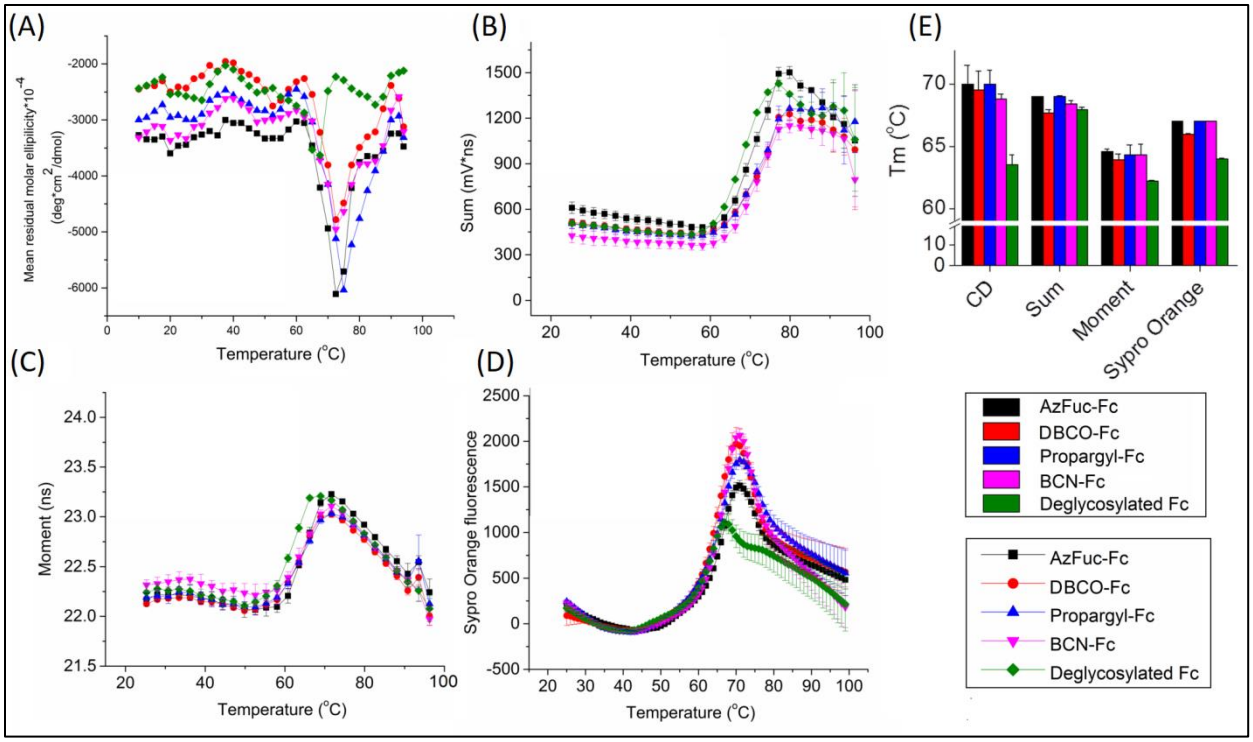

Figure 5. Thermal unfolding profiles of IgG2 Fc variants in 20 mM phosphate buffer (pH=6.0) measured by: **A)** Far-UV circular dichroism; **B)** Intrinsic fluorescence sum; **C)** Intrinsic fluorescence moment; **D)** Extrinsic fluorescence (Sypro Orange). **E)** Corresponding Tm values obtained from these biophysical techniques. Error bars indicate standard deviation (N=3).

The protein tertiary structure was studied using time-resolved intrinsic tryptophan fluorescence. The fluorescence intensity and lifetime of tryptophan is sensitive to the polarity of its surrounding environment. A total of 8 tryptophan residues reside at various locations in an Fc molecule and monitoring tryptophan fluorescence is therefore a sensitive measurement of alterations in protein tertiary structures. Sum and moment reflect the fluorescence intensity and "intensity-averaged" lifetime, respectively and were plotted as a function of temperature (Figure 5B and C). Sum plot suggests that AzFuc-Fc and Propargyl-Fc have the highest T_m values, followed by DBCO-Fc and BCN-Fc. Moment analysis indicates no significant difference

between the T_m values of AzFuc-Fc, DBCO-Fc, Propargyl-Fc and BCN-Fc, while deglycosylated Fc has the lowest T_m value as seen in CD measurements (Figure 5E and Table B1 of the appendix).

Sypro Orange dye, as an extrinsic fluorescence probe, is weakly fluorescent in water and becomes highly fluorescent when it binds to hydrophobic regions of proteins during protein unfolding. The intensity of Sypro Orange at 610 nm reflects the overall exposure of hydrophobic regions of protein and is therefore used to monitor protein tertiary structural alterations.[37] AzFuc-Fc, Propargyl-Fc, and BCN-Fc showed the highest thermal stability with no significant differences among their T_m values. In contrast, the T_m of DBCO-Fc is lower by 1 ºC indicating a slight destabilization effect of DBCO-linker on protein tertiary structure (Figure 5D, E and Table B1 of the appendix). The deglycosylated Fc again had the lowest thermal stability.

The overall conformational stability of Fc variants was studied using differential scanning calorimetry (DSC). DSC thermograms show two distinct thermal transitions for all Fc samples (Figure 6). The first and second thermal transitions originate from the unfolding of C_H2 and C_H3 domains, respectively. AzFuc-Fc, Propargyl-Fc, and BCN-Fc showed no difference in their T_m1 values (Appendix: Table B1). Compared to AzFuc-Fc, DBCO-Fc is less stable by 0.6 °C with respect to T_m1. AzFuc-Fc, DBCO-Fc, Propargyl-Fc, and BCN-Fc shared similar T_m2 values suggesting that the conjugation did not significantly affect the thermal stability of the C_H3 domain. The deglycosylated Fc sample showed a significantly lower T_m1 value.

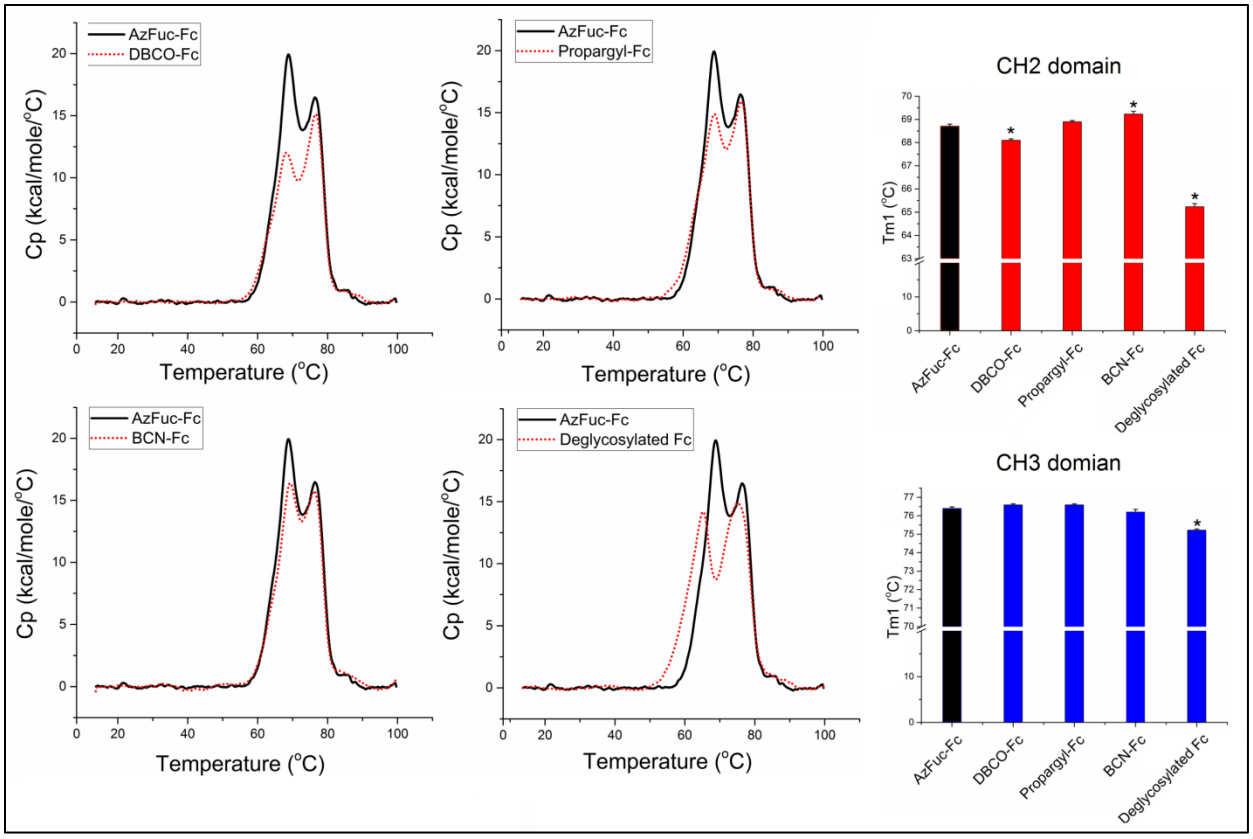

Figure 6. Thermograms and domains (C_H2 and C_H3) melting temperatures of IgG2 Fc variants in comparison with 6-azido-L-fucose-functionalized IgG2 Fc (AzFuc-Fc) as measured by differential scanning calorimetry. Error bars indicate the standard deviation of 3 replicates and statistical significance (*) compared to the AzFuc-Fc with a p value < 0.01 is indicated. Samples were at 0.5 mg/mL in 20 mM phosphate buffer (pH=6.0).

Effect of conjugation chemistry on the conjugate solubility

The apparent solubility (thermodynamic activity) of the prepared conjugates was assessed using a PEG-precipitation assay described previously[38–40] and compared to that of the functionalized IgG2 Fc with no conjugation as shown in Figure 7. In this assay, polyethylene glycol (PEG) was used to decrease the solubility of the protein present at low concentration in a quantifiable manner where protein precipitation can occur mainly through a PEG-excluded

volume mechanism. Plotting the results from this assay resulted in a sigmoidal curve. Although these PEG-curves can provide a qualitative way for comparing solubility, the solubility of closely related proteins or the same protein under different formulation conditions can be compared in a quantifiable manner using the $\%PEG_{midpt}$ and the apparent solubility (thermodynamic activity). The $\%PEG_{midpt}$ is the weight %PEG required to reduce the protein concentration to 50% of its initial value while the apparent solubility (thermodynamic activity) is calculated by curve fitting and extrapolation to zero PEG concentration.

The assay showed a mild increase ($p<0.05$) in the $\%PEG_{midpt}$ of the propargyl-conjugate compared to the AzFuc Fc; conversely there was a mild decrease ($p<0.05$) in the $\%PEG_{midpt}$ due to the conjugating of the DBCO and BCN linkers to the AzFuc Fc. As expected, a larger decrease in $\%PEG_{midpt}$ was observed for the deglycosylated IgG2 Fc when compared to the glycosylated Fc.[39] Results from apparent solubility (thermodynamic activity) calculations showed the same trend of relative solubility predicted based on $\%PEG_{midpt}$. However there was no difference ($p<0.05$) in the apparent solubility (thermodynamic activity) of the BCN conjugate when compared to the functionalized Fc. Overall results from PEG-precipitation assay predict a decrease in the solubility of DBCO-Fc, BCN-Fc, and deglycosylated Fc and an increase in the solubility of the Propargyl-Fc when compared to the AzFuc-Fc.

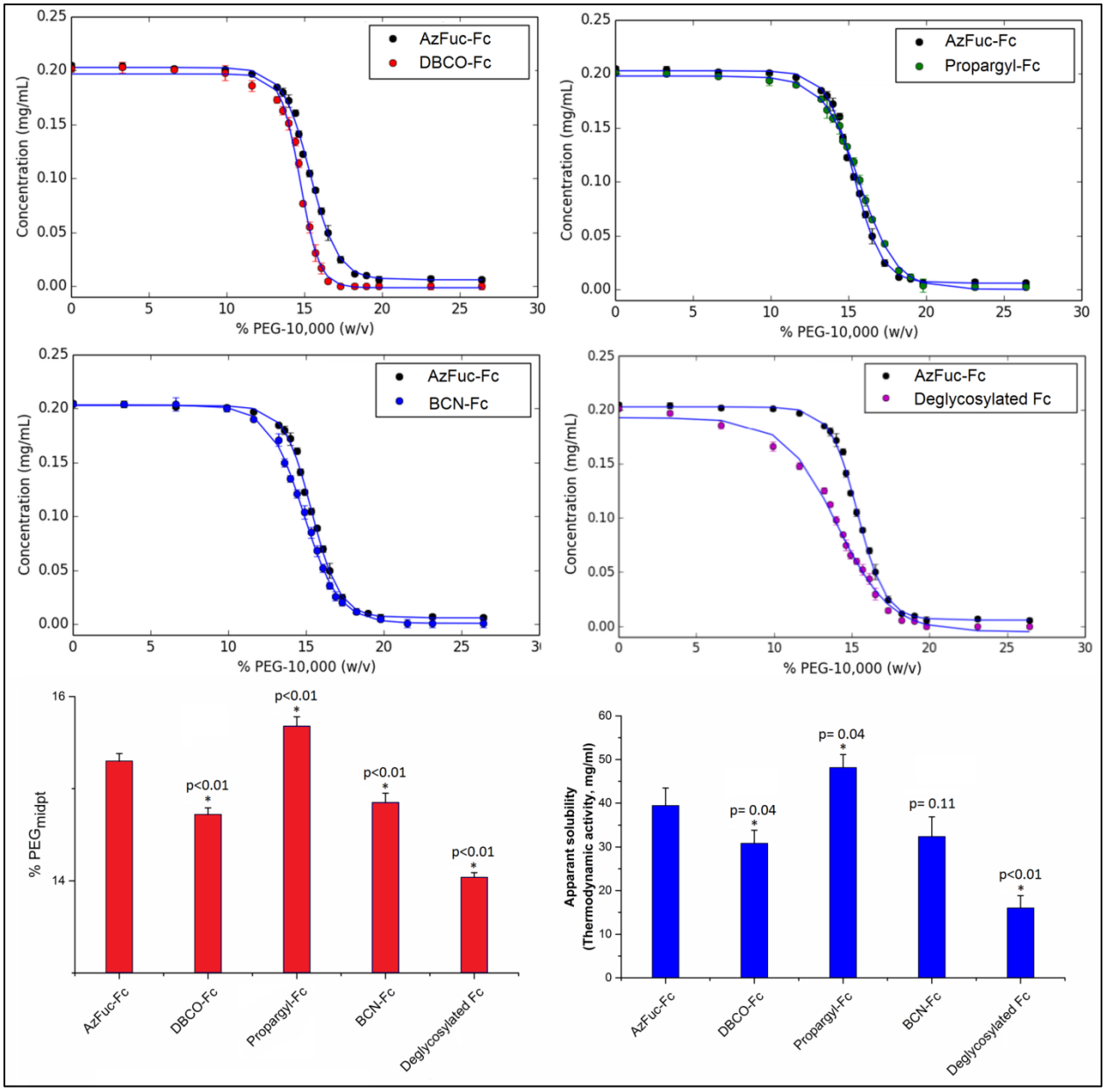

Figure 7. (**A**, **B**, **C**, and **D**) Comparison of the PEG_{curves} (protein vs. PEG concentration) of different IgG2 Fc variants (DBCO-Fc, Propargyl-Fc, BCN-Fc, and deglycosylated Fc) to AzFuc-Fc. **E)** Comparison of PEG_{midpt} values (w/v) of IgG2 Fc variants to AzFuc-Fc. **F)** Comparison of apparent solubility (thermodynamic activity) of each of IgG2 Fc variants to AzFuc-Fc. Error bars indicate the standard deviation of 3 replicates and statistical significance (*) compared to the AzFuc-Fc with a p value < 0.05 is indicated. Sample were at 20 mM phosphate buffer (pH=6.0).

Comparison of binding to Fc gamma receptors

The binding kinetics and affinity of the conjugates to Fcγ receptors were assessed using biolayer interferometry (BLI) and compared to the binding kinetics and affinity of the functionalized Fc (AzFuc-Fc). The purpose behind conducting these binding studies was to check for any possible Fc conformational changes or steric interference due to conjugating these linkers, on the binding to these receptors. Previous studies have shown that the human IgG2 subclass of antibodies binds weakly to most of Fcγ receptors however it shows a considerable binding to FcγRIIa.[41] The binding of IgG2 to FcγRIIa is also affected by the naturally occurring polymorphism within this receptor where it has a stronger binding affinity for the H131 variant (FcγRIIa-H131) of the receptor than the R131 variant (FcγRIIa-R131).[41–43] Both FcγRIIa receptor variants were used in our binding studies in addition to the high affinity FcγRIIIa variant (FcγRIIIa-V158). Binding of IgG to FcγRIIIa is also known to be reduced by the presence of α1,6- fucose (core fucose) on the Asn297 glycan of IgG.[44–46]

Representative binding sensorgrams for binding of the AzFuc-Fc and the conjugates are shown in Figure 8. Also the calculated binding constants are shown in Table I. Based on these binding results, the affinity constant (K_D) of the azidofucose containing IgG2 Fc lies in the micro-molar range affinity (2.23 μM) consistent with previously reported K_Ds for binding of IgG2 Fc to FcγRIIa-H131 and suggesting no significant change in the affinity of IgG2 Fc upon functionalization (chapter 2). Interestingly, the binding of DBCO-Fc to FcγRIIa-H131 (K_D= 6.13 μM) was reduced by 1.4-fold ($p<0.05$) compared to binding of the AzFuc-Fc to the same receptor variant. However, there was no statistical difference ($p<0.05$) in the affinities of the BCN-Fc and Propargyl-Fc to this receptor compared to the functionalized Fc. On the other hand, binding of IgG2 Fc (the functionalized Fc or the conjugates) demonstrated a lower binding

affinity to the FcγRIIa-R131 variant where the K_D of the AzFuc-Fc was 14.1 μM (6-fold bigger compared to binding to FcγRIIa-H131 variant). All the conjugates showed similar ($p<0.05$) K_Ds to FcγRIIa-R131. Finally, the functionalized Fc and the conjugates showed a very weak binding signal to FcγRIIIa-V158 at their highest concentration tested in these binding studies.

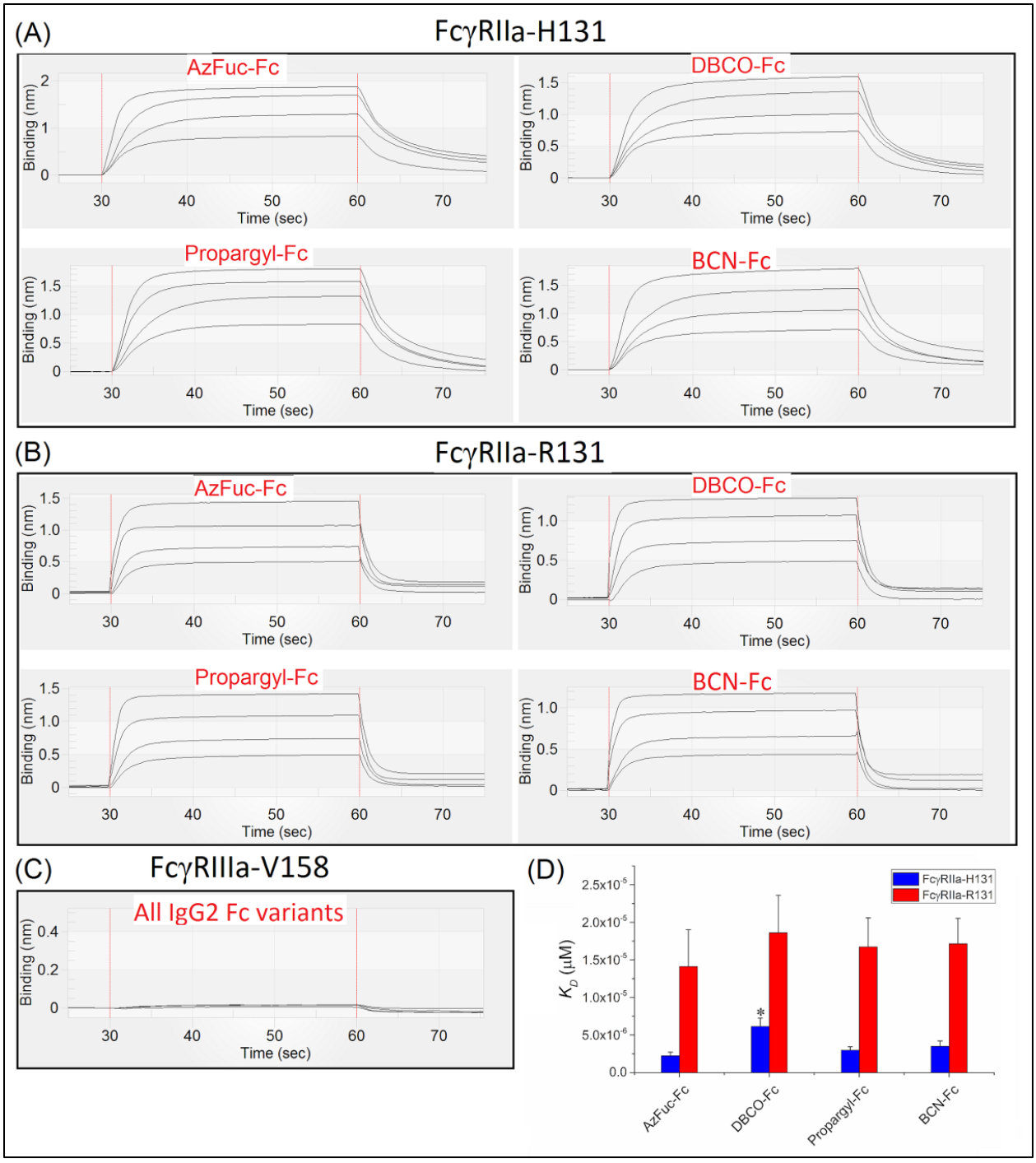

Figure 8. Biolayer interferometry (BLI) analyses of IgG2 Fc variants binding to Fcγ receptors. (**A**), (**B**), and (**C**) represents binding to immobilized FcγRIIa-H131, FcγRIIa-R131, and FcγRIIIa-V158, respectively. Binding curves in (**A**) correspond to IgG2 Fc variants concentrations of 4, 2, 1, and 0.5 μM from top to bottom. Binding curves in (**B**) corresponds to IgG2 Fc variants concentrations of 10, 5, 2.5, and 1.25 μM from top to bottom. Binding curves in

(**C**) corresponds to IgG2 Fc variants concentration of 70 µM. (**D**) comparison of affinity constants (K_Ds) of IgG2-Fc variants to FcγRIIa-H131 and FcγRIIa-R131. Error bars indicate the standard deviation of 3 replicates and statistical significance (*) compared to the AzFuc-Fc with a p value < 0.05 is indicated**.**

Table I. Kinetic rate and affinity constants for binding of IgG2 Fc variants to Fcγ receptors

	FcγRIIa-131H			**FcγRIIa-131R**		
Fc-variant	$k_a \times 10^2$ (1/Ms)	$k_d \times 10^{-1}$ (1/s)	K_D (µM), kinetic	$k_a \times 10^2$ (1/Ms)	$k_d \times 10^{-1}$ (1/s)	K_D (µM), kinetic
AzFuc-Fc	833 ± 171	1.86 ± 0.10	**2.23 ± 0.47**	320 ± 98.6	4.52 ± 0.70	**14.1 ± 4.8**
DBCO-Fc	380 ± 60.5	2.33 ± 0.19	**6.13 ± 1.10**	203 ± 26.5	3.78 ± 0.88	**18.6 ± 4.9**
Propargyl-Fc	726 ± 94.7	2.16 ± 0.15	**2.98 ± 0.44**	205 ± 44.1	3.43 ± 0.28	**16.7 ± 3.8**
BCN-Fc	662 ± 123	2.31 ± 0.19	**3.49 ± 0.71**	171 ± 32.8	3.72 ± 0.47	**17.1 ± 3.4**

Discussion

During the past few years there has been a growing interest in designing site-specific ADCs.[2,7–11,47] Many methods have been reported to achieve this goal and each method has its own advantages and disadvantages. Some of these methods utilized the Asn297 glycan of the antibody as a site for biorthogonal functionalization and specific conjugation.[11] One way of functionalization of this glycan is through the introduction of a modified sugar unit with a suitable handle within the structure of this glycan using enzymes. Another way of introducing a handle within this glycan is through the use of chemical reagents to chemically modify certain sugar units within this glycan. Introducing a handle through the single fucose residue attached to

this glycan by an α1,6- linkage would result in an antibody with two handles and a possibility of DAR of 2, a widely targeted DAR in many recent studies.[20,48–50] To the best of our knowledge, only two trials focused on utilizing core fucose for site-specific conjugation. In one trial, Okeley et al. (2013)[20] introduced several modified fucose units, especially 6-thifucose, on this glycan by feeding the mammalian cells producing the antibody with the acetylated form of the modified fucose units. Even though the trial was somewhat successful, unfortunately the incorporation efficiency of the thiofucose was only about 60% where the rest of the Asn297 glycan was either modified with the natural fucose or left afucosylated. In the second trial, Zuberbühler et al. (2012) developed a method to selectively oxidize the *cis* diol of core fucose of Asn297 glycan using sodium metaperiodate to introduce an aldehyde handle within this glycan for subsequent reaction with hydrazide linkers and form hydrazone linkages.[19] Their functionalization method however relied on the use of harsh reaction conditions; oxidizing agents and low pH (pH 4.0). The oxidation was difficult to control and some of the fucose cis *diols* were over-oxidized to carboxylic acids making them unavailable to react with the hydrazide linkers. The other problem of subjecting the antibody to oxidation is the possibility of oxidizing some amino acids within the antibody. Some of these amino acids are critical for FcRn binding and the antibody pharmacokinetics and their oxidation results in reducing the antibody and ADC biological half-life, such as Met-252 and Met-428.[18,51]

Our approach of functionalizing the Asn297 glycan for site-specific ADCs was through the core fucose residue. Efficient and complete introduction of a modified fucose was achieved in this work through the use of α1,6-fucosyltransferase (FUT8), a mammalian glycosyltransferase responsible for adding the natural sugar fucose to the first GlcNAc of the pentasaccharide core structure of N-linked glycans.[26] FUT8 was recently expressed and

characterized in our laboratory using a novel way in *E. coli*. The enzyme was also used successfully in generating of fully fucosylated IgG2 Fc as shown in chapter 2. We sought to introduce a modified fucose with a suitable handle to fully functionalize the Asn297 glycan of IgG2 Fc for site-specific conjugation. An elegant fucose handle would be the bioorthogonal azide or alkyne handles to allow a click chemistry conjugation, such as 6-azido-L-fucose and 6-alkynyl-L-Fucose. However, based on previous studies, it has been shown that the 6-Alkynyl-L-fucose analogue has low incorporation efficiency and could also behave as an inhibitor of FUT8.[20,52] In addition to this limitation, the 6-Alkynyl-L-fucose would provide a lower flexibility and allow only the copper catalyzed version of the biorthogonal azide-alkyne cycloaddition reaction (i.e. CuAAC), while the 6-azido-L-fucose would allow both versions of AAC, i.e. the Strain prompted azide-alkyne cycloaddition (SPAAC) as well as CuAAC. Our initial trials included the use of one-pot reaction containing FUT8 and FKP to transfer the modified fucose (6-azido-L-fucose) from the GPD-azidofucose, formed *in situ* from FKP reaction, to the Asn297 glycan of IgG2 Fc by the action of FUT8 in a similar way of making fully fucosylated IgG2 Fc described in chapter 2. Although using this one-pot strategy resulted in efficient incorporation of the 6-azido-L-fucose in the Asn297 glycan, the process was much slower (more than 9 days) compared to the incorporation of the natural sugar fucose under the same reaction conditions (2 days), making it less convenient for generating site-specific ADCs. Subsequent investigations to determine the step(s) that are responsible for this slowness in the one-pot reaction led us to make and purify GDP-azidofucose and use it directly in FUT8 reaction. The result was efficient functionalization of the Fc in less than 24 hours. Using purified GDP-azidofucose does not only skip the slowness in making this activated nucleotide sugar *in situ* by FKP, which catalyzes a reversible reaction, but also excludes the presence of ATP, ADP,

and inorganic pyrophosphate that can be formed during FKP reaction and act as inhibitors for FUT8.[26]

Stability of the linkage between the antibody and the payload represent a critical factor in the safety and efficacy of ADCs. The AAC has been widely used in recent studies as an alternative to conventional conjugation chemistry in making site-specific ADCs. Although in most of these studies[13,23,53] the authors preferred to use the SPAAC version of AAC over the use of CuAAC, an optimized CuAAC process, as the one we carried out in this work, can add another dimension and give more flexibility in using click chemistry conjugation reactions to make site-specific ADCs. The AAC is a highly specific conjugation reaction which can be carried out efficiently in neutral aqueous solutions containing the protein of interest.[11,30,54] This reaction results in the formation of a stable triazole linkage between the alkyne and the azide. Premature release of the payload has been shown to occur in the plasma when using thiol-maleimide chemistry in constructing ADC, due to retro-Michael reaction.[48] Thiol-maleimide chemistry has been utilized in making the commercial products Kadcyla and Adcetris as well as utilized in many experimental ADCs such as the one developed by Okeley et al. (2013).[20] Also, premature release of the payload from ADC made through a liable hydrazone linkage, as the one developed by Zuberbühler and described above, is likely to happen in the human plasma.[19,55] The premature release of potent toxic payloads in the plasma can result in serious off-target toxicity and narrowing of therapeutic index of the corresponding ADC.[48,56] Therefore, new chemistries such as AAC have been used recently in making next generation ADCs to solve these stability problems along with other shortcomings associated with first generation ADCs. The strategy we followed here which shows a full functionalization of the antibody Fc with an azido-modified sugar followed by full conjugation using AAC type click chemistry, can well serve the goal.

Similar to mAb therapeutics, the structural stability of the antibody part of an ADC is critical for the stability of these therapeutic products and prevention of aggregation which results in loss of activity and potential immunogenicity reactions when introduced into biological systems.[57,58] Introducing a linker and a toxin on the mAb is expected to alter the structure of the mAb part of the ADC and can reduce the stability of the product compared to the naked mAb; however this effect is also expected to be highly dependent on the site of conjugation.[59,60] In a study of trastuzumab-DM1 (commercially became Kadcyla), Wakanker et al. (2010) showed that the conjugation of DM1 to trastuzumab resulted in reducing the thermal stability of the intermediate (mAb-linker) and the product (mAb-linker-toxin) by about 2 and 4.4 °C, respectively as measured by differential scanning calorimetry.[61] This reduction in the thermal stability was also accompanied by an increase in the aggregation propensity of these modified forms of trastuzumab. Accordingly, we sought to test the impact of using different linkers having different physicochemical properties on the overall conjugate secondary and tertiary structure thermal stabilities using a variety of biophysical techniques.[62] The alkyne parts of the used linkers are among the most commonly used alkynes in AAC reactions both the CuAAC and SPAAC. The biophysical techniques used to probe the effect of conjugation are widely used in our laboratories in probing the physical stability of proteins. Some techniques were able to detect differences among the tested IgG2 Fc variants while other techniques showed similarity in results. These techniques usually complement each other to find differences and similarities in proteins physical stability and some of them can be run in high throughput format to enable rapid screening of drug candidates. Among the noticeable differences was a reduction in thermal stability of the DBCO-Fc by 1 °C as detected by extrinsic fluorescence, and 0.6 °C as detected by differential scanning calorimetry. This reduction in the thermal stability of the DBCO-

conjugate can be attributed to a mild structural perturbation of IgG2 Fc due the bulkiness and hydrophobicity of this cyclic alkyne compared to BCN and the linear alkynes. However, this reduction in the thermal stability is obviously less than a larger reduction in the thermal stability of the Fc upon the removal of the Asn297 glycan (i.e. deglycosylated Fc), which was used as a benchmark to assess the thermal stability of these conjugates. These structural stability studies could also suggest the ability of the Asn297 glycan as a conjugation site to accommodate compounds having different physicochemical properties without impacting the antibody stability significantly.

The physicochemical properties of an ADC are crucial in determining the safety, efficacy, and stability of this category of biologics.[58,63] The site of conjugation and the DAR are important factors in determining an ADC's physicochemical properties. For example, it has been shown that an ADC with a DAR of 4 is more effective and has a broader therapeutic index than a similar ADC with a DAR of 8, although the latter has more payload and theoretically should be more potent.[23,64] The rationale behind this discrepancy resides in the fact that most of the ADC payloads and linkers are hydrophobic in nature. Hydrophobicity has been thought to be a property which allows these payloads escaping the lysosomal degradation and helps diffusion out to the site of action.[65,66] However, the higher hydrophobicity of the ADCs having higher DAR can also lead to poor pharmacokinetics and higher uptake of the ADCs by non-target cells such as hepatocytes.[64] Another possibility for poor pharmacokinetics of ADC with high DAR, especially ADCs prepared using random payload conjugation through the natural amino acid lysine, is the interruption of the antibody-FcRn recycling mechanism, which represent a unique process in elongating the half-life of the antibody-based therapeutics.[16–18] Conjugation through the Asn297 glycan or even through a site that is close to this glycan has been shown to mitigate

the hydrophobicity of payloads and increase ADC stability.[39,64,66–68] This is probably due to the hydrophilic nature of this sugar chain which has been shown to affect the solubility of antibodies significantly. Also, a higher solubility of an antibody therapeutic is usually desirable, especially when formulating a drug product for subcutaneous injection where the injection volume is relatively small and a highly concentrated protein needs to be formulated.[69] In this work we demonstrated the effect of different linkers on the hydrophobicity of the prepared conjugate compared to the functionalized Fc using the PEG-precipitation assay, a high throughput assay which compares the apparent solubility (thermodynamic activity) of closely related proteins.[38–40] Although cyclic alkyne (DBCO and BCN) linkers resulted in some reduction in the Fc apparent solubility, interestingly the linear alkyne linker (propargyl) resulted in an increase in the Fc apparent solubility. Therefore, the type of the alkyne may also be considered when screening for ADC with better solubility profiles and linear alkynes may be a better choice and may minimize any further reduction in the solubility of the ADC upon conjugating a hydrophobic payload. On the other hand, the dramatic reduction in the deglycosylated IgG2 Fc solubility (thermodynamic activity) compared to the glycosylated Fc shown in this study and previous studies should be taken into consideration in studies where the removal or truncation of Asn297 glycan had to be done to enable site-specific conjugation.[23,50]

In an ADC, the main cytotoxic effect comes from the payload, while in a naked anticancer mAb the toxicity depends largely on the antibody effector functions such as ADCC.[70,71] Therefore, many strategies have been adopted to enhance effector functions especially through glycoengineering of the Asn297 glycan by eliminating the core fucose.[72] In an ADC, recruiting effector cells may not always be desirable since the uptake of the immune complex by effector cells could result in premature release of the cytotoxic payload inside these

normal effector cells and hence narrowing the therapeutic index of the ADC.[1,70] Recently, IgG subclasses with lower effector functions mediated through Fcγ receptors, such as human IgG2 and IgG4, have been utilized in constructing ADCs to minimize this off-target toxicity.[2] We chose the IgG2 Fc sequence in this study since it has the weakest binding to Fcγ receptors except for FcγRIIa. We wanted to test the effect of functionalizing IgG2 Fc and making these conjugates on the binding to these receptors. It is well known that binding to these receptors is highly affected by the Asn297 glycan. Removal of this glycan in general abrogates Fcγ receptor binding.[73,74] Our results showed that the addition of 6-azido-L-fucose to the Asn297 glycan of IgG2 Fc reduced the binding to FcγRIIIa-V131 just like the natural sugar, fucose (chapter 2). Likewise, the conjugates showed no detectable binding to this receptor and hence lower probability of ADCC. On, the other hand the DBCO-conjugate showed a reduced affinity (K_D=6.13 μM) to FcγRIIa-H131 compared to the naked Fc (K_D=2.23 μM) which was mainly due to reduced association rate of the conjugate to this receptor variant. Again, the DBCO-linker has the biggest alkyne used in this study and has one extra PEG residue and the mild structural perturbation of the DBCO-conjugate shown in this study by the DSC and extrinsic fluorescence and/or a possible steric hindrance of the Fc/receptor interaction may explain this reduced affinity. Any possible further reduction in binding to Fcγ receptors after adding the required payload, and hence lower effector function, could also be advantageous.[70] From this perspective, and from the perspective of faster conjugation kinetics of DBCO-linker compared to BCN-linker, the DBCO-linker might be a better choice in making site-specific ADCs through this strategy.

In conclusion, we developed a method for site-specific conjugation through the Asn297 glycan of IgG for a potential use in the development of next generation ADCs. In this method, we utilized FUT8 for full functionalization of IgG2 Fc Asn297 glycan with 6-azido-L-fucose, a

modified fucose with a biorthogonal handle suitable for click chemistry conjugation. To demonstrate the suitability of this handle for conjugation, we used different linkers functionalized with different alkynes for site-specific conjugation through this handle. All of these linkers showed excellent conjugation efficiency and resulted in the formation of homogeneous conjugates under mild reaction conditions. The conjugates were also tested for any possible impact of the linkers added at this site on the structural stability, solubility and binding properties of the naked IgG2 Fc. These properties were tested in a systematic way using complementary biophysical analytical techniques, solubility assessment assay, and BLI-based binding studies. Therefore a combination of our synthetic platform, which can be used to produce highly homogeneous conjugates, with the experimental set up described here could represent a powerful approach to screen for the impact of linkers or linker-drug on ADC properties during different stages of drug development. Results from this study suggests the use of linear alkyne-based linkers coupled with optimized CuAAC to avoid a larger solubility reduction and destabilization issues that might be associated with using cyclic alkynes-based linkers. However, if the destabilization effect due to DBCO-based linkers and solubility are considered to be acceptable then linkers of this type might be preferred over others due to the fast conjugation kinetics and possibility of reduced effector functions mediated through Fcγ receptors. If SPAAC is intended to be used without even mild reduction in ADC stability, solubility, and binding properties then BCN-based linkers might be a better choice over DBCO-linkers.

Materials and methods

Materials

GDP-fucose produced in house as shown in chapter 2. Amicon Ultra-15 Centrifugal Filter Units with a molecular weight cutoff of 10 Da were purchased from EMD Millipore (Billerica, MA). Protein G resin was produced as described previously.[74,75] CuSO4 was obtained from Alpha Aesar (Tewksbury, MA). UDP-GlcNAc, Inorganic pyrophosphatase from baker's yeast (S. cerevisiae), NADH, Pyruvate Kinase/Lactic Dehydrogenase enzymes from rabbit muscle, ATP, GTP, L-fucose, and sodium ascorbate, were obtained from Sigma-Aldrich (St. Louis, MO). 6-azido-L-fucose was purchased form Apollo Scientific (Denton, Manchester). DBCO-PEG5-Acid, endo-BCN-PEG4-Acid, and Propargyl-PEG4-Acid were purchased from Broadpharm (San Diego, CA). Deglycosylated IgG2 Fc was prepared as described in chapter 2 by treating glycosylated IgG2 Fc with PNGase F.

Production of afucosylated IgG2 Fc

A homogeneous afucosylated glycoform of IgG2 Fc as a substrate for FUT8 catalyzed reaction (Figure 1 A) was produced in our laboratory as described in chapter 2. Briefly, the DNA sequence corresponding to the amino acid sequence of human IgG2 Fc (C_{226}PPC…..SPGK_{447}, Eu numbering) was subcloned into pPICZαA (EasySelect™ *Pichia* Expression Kit, Invitrogen) plasmid for expression in the methylotrophic yeast *Pichia pastoris*. The IgG2 Fc is then purified from the growth media via protein G affinity chromatography followed by hydrophobic interaction chromatography and weak cation exchange for further purification and homogenization. Then the high mannose IgG2 Fc glycoform obtained from yeast expression was subjected to an *in vitro* enzymatic synthesis to finally obtain the afucosylated hybrid IgG2 Fc glycoform.

Functionalization of IgG2 Fc Asn297 glycan

On-pot reaction

A one-pot reaction using FKP and FUT8 (Figure 1) was followed for site-specific addition of the modified sugar 6-azido-L-fucose to the Asn297 glycan of IgG2 Fc as following. First, the FKP reaction was carried out in 50 mM Tris HCl pH 7.5 buffer containing ATP (5 mM), GTP (5 mM), 6-azido-L-fucose (5 mM), $MgCl_2$ (5 mM), and FKP (120 µg/ml) at room temperature to generate the activated sugar GDP-azidofucose. After 12 hours, the FKP reaction mixture was added to an equal volume (250 µl) of the hybrid IgG2 Fc (2.5 mg/ml Fc in 20 mM Tris HCl buffer pH 7.5) solution. The transfer of 6-zido-L-fucose from GDP-azidofucose generated *in situ* to the IgG2 Fc Asn297 glycan was then initiated by adding 1.2 µU (10 µg) of FUT8 produced in *E. coli* as described in chapter 2.The reaction was incubated at 30 °C and monitored for progress using Q-TOF LC/MS. This one-pot reaction eventually went to completion; however it required nine days to convert all the afucosylated Fc into AzidoFucose-modified Fc (AzFuc-Fc) as shown in Figure B1 of the appendix.

Reaction utilizing purified GDP-azidofucose

GDP-azidofucose was synthesized chemoenzymatically and purified from the reaction mixture as described in details in appendix B. Then the purified nucleotide sugar was used in FUT8-catalyzed reaction for the functionalization of the Asn297 glycan of IgG2 Fc as following. Before the reaction, afucosylated IgG2 Fc was dialyzed against 20 mM HEPES buffer pH 7.5. The reaction mixture (20 ml) containing afucosylated IgG2 Fc (2 mg/ml), GDP-azidofucose (1 mM), and 130 µU of FUT8 was incubated at 30 °C. The reaction was monitored by Q-TOF LC/MS until completion (1 day). By the end of the chemoenzymatic conversion, the reaction

mixture was diluted with 20 mM MES buffer pH 6.2 (equilibration buffer) to a final IgG2 Fc concentration of 0.1 mg/ml. Then, the diluted Fc solution is loaded into a protein G column (10-ml bed volume protein G column), pre-equilibrated with equilibration buffer, using a loading flow rate of 6 ml/min. The flow-through is also loaded into the column to ensure full recovery of the Fc from the reaction mixture. The column is then washed with 5 CV of the equilibration buffer followed by 5 CV of the equilibration buffer containing 500 mM NaCl. A final wash step using 5 CV of the equilibration buffer is also conducted to get rid of the high salt concentration. Eluting IgG2 Fc was done by using 100 mM glycine buffer, pH 2.7 and the protein solution is immediately neutralized using 1M Tris HCl buffer, pH 9.0. The expected mass of the functionalized IgG2 Fc is 26461.1 Da and the observed mass was 26459.6 Da (Figure 3A). In this process, 36 mg of the AzFuc-IgG2 Fc was produced which corresponds to a yield of 90%.

Preparation of site-specific IgG2 Fc conjugates using azide-alkyne cycloaddition

Production of the Propargyl conjugate

The propargyl-PEG4-acid was conjugated to AzFuc-IgG2 Fc using CuAAC to produce Propargyl-Fc conjugate (Figure 1A). Before the reaction, the afucosylated IgG2 Fc was dialyzed in 50 mM HEPES buffer pH 7.5. Also, a 20 mM propargyl-PEG4-Acid stock solution was prepared by dissolving the required amount of propargyl-PEG5-acid in deionized water. The solutions of CuSO4 (20 mM), THPTA (50 mM), and sodium ascorbate (100 mM) were prepared freshly before the reaction by dissolving the required amount of these reagents in deionized water. Then, the CuAAC reaction was carried out as following. The afucosylated IgG2 Fc was mixed with propargyl-PEG4-acid in a separate vial prior to the reaction to achieve a final reaction concentration of 7.6 µM and 205 µM of the AzFuc-Fc and propargyl-PEG4-acid,

respectively. On the other hand, the freshly prepared $CuSO_4$ was mixed with THPTA in a separate vial to achieve a final reaction concentration of 0.2 mM and 1 mM of $CuSO_4$ and THPTA, respectively. Then both solutions were mixed together and the reaction was started by adding the freshly prepared sodium ascorbate to a final reaction concentration of 5 mM. The reaction was incubated at room temperature for 40 minutes then immediately followed by adding 15 volumes of EDTA solution (1 mM in 50 mM HEPES pH 7.5 buffers) to 1 volume of the reaction mixture. Then, the mixture was concentrated back to initial volume using Amicon Ultra-15 Centrifugal Filter Units. The dilution and concentration step of the reaction mixture was repeated one more time then followed by dialysis in the required buffer for subsequent studies. In this process, 6 mg of propargyl-conjugate was obtained from 6.5 mg AzFuc-Fc which corresponds to a yield of 91%. The conjugate purity and integrity was checked using SDS-PAGE gel. The expected mass of the propargyl-conjugate is 26720.1 Da and the observed mass was 26718.9 Da as shown Figure 3B.

Production of the BCN-conjugate

The BCN-PEG4-acid was conjugated to AzFuc-IgG2 Fc using SPAAC to produce BCN-Fc conjugate (Figure 1A). Before the reaction, the AzFuc-Fc was dialyzed in 50 mM HEPES buffer pH 7.5. Also, a 7.5 mM BCN-PEG4-acid stock solution was prepared by diluting the BCN-PEG4-acid solution in DMSO (75 mM) with distilled water (1:10 dilution). Then the reaction was carried out by mixing the AzFuc-Fc and BCN-PEG4-acid to final concentrations of 7.5 µM and 380 µM, respectively. The reaction was incubated at room temperature and checked for progress by intact protein mass spectrometry. After two days, the reaction mixture was diluted with 15 volumes of 50 mM HEPES buffer pH 7.5 to get rid of excess alkyne then concentrated back to the original reaction volume using Amicon Ultra-15 Centrifugal Filter Units

followed by dialysis in the required buffer. In this process, 6.2 mg of BCN-conjugate was obtained from 6.5 mg AzFuc-Fc which corresponds to a yield of 94%. The integrity and purity of the BCN-conjugate was checked by SDS-PAGE gel. The expected mass of the BCN-conjugate is 26901.5 Da and the observed mass was 26897.1 Da as shown in Figure 3C.

Production of the DBCO-conjugate

The DBCO-PEG5-acid was also conjugated to AzFuc-IgG2 Fc through the SPAAC reaction to produce DBCO-Fc conjugate as shown in Figure 1A. Again, before the reaction, the AzFuc-Fc was dialyzed in 50 mM HEPES buffer pH 7.5. Also, a 4.5 mM DBCO-PEG5-acid stock solution was prepared by diluting the DBCO-PEG5-acid solution in DMSO (4.5 mM) with distilled water (1:10 dilution). Then the reaction was carried out by mixing the AzFuc-Fc and BCN-PEG4-acid to final concentrations of 7.5 and 25 μM, respectively. The reaction was incubated at room temperature and checked for progress by intact protein mass spectrometry. After 22 hours, the reaction mixture was diluted with 15 volumes of 50 mM HEPES buffer (pH=7.5) to get rid of excess alkyne and concentrated back to the original reaction volume using Amicon Ultra-15 Centrifugal Filter Units followed by dialysis in the required buffer. In this process, 6.2 mg of BCN-conjugate was obtained from 6.5 mg AzFuc-Fc which corresponds to a yield of 93%. The integrity and purity of the DBCO-conjugate was checked by SDS-PAGE gel. The expected mass of the BCN-conjugate is 27056.6 Da and the observed mass was 27052.5 Da as shown in Figure 3D.

Dynamic light scattering

Dynamic light scattering (DLS) was performed using a DynaPro plate reader (Wyatt Technology, Santa Barbara, CA). Samples of IgG2 Fc variants were dialyzed overnight at 4 ºC

into 20 mM phosphate buffer (pH 6.0). The samples were analyzed at a concentration of 1 mg/ml. Samples were loaded into a 384 well flat clear bottom black plate (Corning Incorporated, Corning, NY) and each sample was measured five times with an acquisition time of 30 sec each time. The measurement was performed at 25 ºC by illuminating the samples with a semiconductor laser of 830 nm-wavelength, and the intensity of scattered light was measured at an angle of 158°. A viscosity value of 1.019 cP was used to calculate the hydrodynamic diameter. The data was processed using a regularization analysis and intensity averaged diameter values were reported.

Far-UV Circular dichroism

Far-UV circular dichroism (CD) was performed using a Chirascan-plus CD spectrometer (Applied Photophysics, Leatherhead, UK) equipped with a 6-position, peltier-controlled cell holder. IgG2 Fc variants were dialyzed overnight at 4 ºC into 20 mM phosphate buffer (pH 6.0). The samples were analyzed at a concentration of 0.2 mg/ml. The CD spectra of each IgG2 Fc variant were recorded from 190 to 260 nm in 1-nm increment using a 1-mm pathlength quartz cuvette. The temperature ramp was set from 10 to 90 ºC with an increment of 2.5 ºC per step and an equilibration time of 2 min at each temperature. The mean residue molar ellipticity at 218 nm was plotted as a function of temperature and T_m values were determined by a first-derivative method using Origin 2017 (OriginLab; Northampton, MA). The same method was used to calculate T_m values for the following studies unless noted otherwise.

Extrinsic fluorescence

An extrinsic fluorescence melting study was performed with an Mx3005P qPCR system (Agilent Technologies, Santa Clara, CA). IgG2 Fc variants samples were first dialyzed overnight

at 4 ºC into 20 mM phosphate buffer (pH 6.0). Sypro Orange dye stock (5000x) (Invitrogen, Carlsbad, CA) was added into protein solution (0.2 mg/ml) at a dilution factor of 1000. Protein samples were excited at 492 nm and emission was collected at 610 nm. Samples were heated from 25 to 99 ºC using a 1 ºC step size and an equilibration time of 2 min at each temperature. The emission intensity was plotted as a function of temperature and T_m values were determined.

Time-resolved intrinsic fluorescence

The time-resolved intrinsic fluorescence of each IgG2 Fc variant was measured using a fluorescence lifetime plate-reader (Fluorescence Innovations, Minneapolis, MN) equipped with a tunable pulse dye laser and a RIC20 temperature controlled 384-well plate holder (Torrey Pines Scientific, Carlsbad, CA). The excitation wavelength was set at 295 nm and two emission filters (310 nm longpass and 360/20 nm band-pass) were placed before a photomultiplier tube detector. Protein samples (0.2 mg/ml in 20 mM phosphate buffer pH 6.0) were loaded into a 384 well black bottom plate (Hard-Shell, Bio-Rad, USA) and silicon oil was loaded onto protein samples to avoid sample evaporation during thermal melt. The thermal melt was run from 25 to 90 °C at 2.5 °C intervals and samples were equilibrated for 2 min at each temperature. Fluorescence decay waveforms were recorded up to 100 ns. Two parameters (sum and moment) were determined from the raw waveform by the FII data analysis software (Fluorescence Innovations, Minneapolis, MN). The sum (in mV*ns) is the peak area under the waveform curve and represents the fluorescence intensity of the sample collected from the PMT detector. The moment (in ns) is the intensity-averaged time of the waveform plot and its mathematical definition was described previously.[76] Sum and moment were plotted as a function of temperature and corresponding T_m values were determined.

Differential scanning calorimetry

Differential scanning calorimetry (DSC) was performed using a MicroCal VP-Capillary calorimeter (Malvern, UK) equipped with an autosampler (MicroCal, LLC, Northampton, MA) and a sample tray holder. The temperature ramp was set from 10 to 100 ℃ at a scan rate of 60 ºC/hr. Protein samples (0.5 mg/ml in 20 mM phosphate buffer pH 6.0) were equilibrated for 15 min at 10 ºC before each run and a filtering period of 16 sec was used. Thermal transitions were deconvoluted and apparent transition temperatures were calculated using a non-two-state equilibrium model in Origin 7.0 (OriginLab; Northampton, MA).

PEG-precipitation assay

The protocol for the high throughput version of the PEG assay for assessing apparent solubility (thermodynamic activity) of the prepared IgG2 Fc variants was adopted from Toprani *et. al.* (2016).[38] Stock solutions of 20 mM phosphate buffer,pH 6.0 and 20 mM phosphate buffer containing 40% w/v PEG-10,000 at pH 6.0 were mixed to prepare various concentrations of PEG solutions ranging from 0 to 40% w/v PEG. A volume of 80 µL of the various PEG-10,000 solutions was added to wells of a 96-well polystyrene filter plate (Corning #3504, Corning Life Sciences, Corning, NY). All protein samples were dialyzed into 20 mM phosphate, pH 6.0 and then diluted to 1 mg/mL with the respective buffer. Twenty microliters (20 µL) of the protein stock solution (1 mg/mL) was then added to each well to a final protein concentration of 0.2 mg/mL. The plates were incubated overnight at room temperature and then centrifuged at 3,500 rpm (1,233 rcf) for 15 min and the filtrate was collected in a clear 96 well collection plate (Greiner Bio-One#655001, Greiner Bio-One North America Inc., Monroe, NC). Subsequently, 50 µL of filtrate was transferred into a 384 well UV Star microplate (Grenier#788101). The

filtrate was measured on a SpectraMax M5 UV-Visible plate reader (Molecular Devices, Suunyvale, CA) at 280 nm to determine the protein concentration.

Curve fitting algorithm for PEG_{midpt} and apparent solubility determinations:

The absorbance at 280 nm versus PEG-10,000 (% w/v) data were fit to a standard four-parameter, modified Hill-slope sigmoidal curve equation using Python (x,y) v.2.7.6.0, an open source scientific and engineering development software based on python language.

$$y = b + \left(\frac{t-b}{1+ e^{s(mid-x)}}\right) \qquad (1)$$

where t= top plateau, b= bottom plateau, mid= x-axis midpoint, and s=slope.

The $\%PEG_{midpt}$ values and apparent solubility value parameters were then calculated from the resulting curve fit as described in detail elsewhere.[40]

Fc gamma receptors binding assays

The binding affinity and kinetics of the functionalized IgG2 Fc and the prepared IgG2 Fc conjugates to Fcγ receptors were assessed using biolayer interferometry (BLI). The receptors used in these binding studies (FcγRIIa-131H, FcγRIIa-131R, and FcγRIIIa-158V) were expressed in our laboratory using the yeast *Pichia pastoris*. The purified receptors were then subjected to biotinylation at their C-termini using sortase mediated ligation (chapter 2). Samples were dialyzed in PBS (50 mM sodium phosphate, 150 mM NaCl, pH 7.4) to perform the binding assays. Casein was added to all samples and buffers at a concentration of 1 mg/ml to block any possible non-specific binding. In these binding assays, the biotinylated receptor is first immobilized on a streptavidin biosensor (Pall ForteBio LLC) to a response level of 1 nm. A new baseline was then established by using a blank PBS solution. The sample solution is placed in the sample holder to acquire the association phase of the binding sensorgram for 30 seconds. Immediately after that, the sample solution was replaced by a blank PBS solution to acquire the

dissociation phase for 20 seconds. In FcγRIIa-131H and FcγRIIa-131R binding assay, four different sample concentrations were used and the sensorgrams from these concentrations were used to fit the data and calculate the kinetic rate constants (ka and kd) and the equilibrium dissociation rate constant *(K_D).* During the FcγRIIa-131H binding assay, the sample concentrations were 0.5, 1, 2, and 4 μM while in FcγRIIa-131R binding assay, the sample concentrations were 1.25, 2.5, 5, and 10 μM. In case of the FcγRIIIa-158V binding assay, a high sample concentration (70 μM) was tested for any possible binding to this receptor. The binding assays were performed at 25 °C and the data were fit using BLItz Pro software.

Sodium dodecyl sulfate-polyacrylamide gel electrophoresis (SDS-PAGE)

SDS-PAGE was performed as previously described[77] using 12% gels. First, a protein sample of about 5 μg was mixed with the appropriate volume of a 3X reducing sample loading buffer (240 mM Tris HCl pH 6.8, 6% SDS, 30% glycerol, 2.3 M 2-Mercaptoethanol, and 0.04% bromophenol blue) and boiled for five minutes before loading into the SDS-PAGE wells. After loading, the gel was developed by a applying a voltage of 180 Volts for 55 minutes using Bio-Rad power supply (PowerPac™ Basic Power). The protein bands were then visualized by staining the gel with Coomassie blue R-250 (Bio-Rad) solution for about one hour followed by an overnight destaining using a mixture of 25% methanol, 5% acetic acid, and 70% Millipore water.

Intact protein mass spectrometry

Agilent 6520 Accurate-Mass Q-TOF LC/MS equipped with ESI source was used to do all the mass spectrometry analyses described in this chapter as described below. The protein sample at a concentration of approximately 0.3 mg/ml was first reduced with DTT (Invitrogen, Carlsbad,

CA) to a final concentration of 10 mM. Then, 30 µl of the reduced protein sample was injected into a reverse phase C4 column, 50 mm, 4.6 mm I.D. (Vydac 214 MS, 300 A° pore size, 5µm particle size) followed by a 5%-90% solvent B gradient elution development within 7 minutes at a flow rate of 0.5 mL/min. Solvent A was composed of 99.9% water, 0.08% formic acid, and 0.02% trifluoroacetic acid while solvent B was composed of 99.9% acetonitrile, 0.08% formic acid, and 0.02% trifluoroacetic acid. Data acquisition was performed using Agilent Mass Hunter Acquisition software (Version B.02.00) while data analysis was performed using Agilent Mass Hunter Qualitative Analysis software (Version B.03.01).

Statistical analysis

Statistical analysis was done using unpaired *t* test to compare the different parameters. All statistical analyses were performed using GraphPad software. A p-value of less than 0.05 was used as the criterion for statistical significance.

References

(1) Diamantis, N., and Banerji, U. (2016) Antibody-drug conjugates—an emerging class of cancer treatment. *Br. J. Cancer 114*, 362–367.

(2) Beck, A., Goetsch, L., Dumontet, C., and Corvaia, N. (2017) Strategies and challenges for the next generation of therapeutic antibodies. *Nat. Rev. Drug Discov. 16*, 315–337.

(3) Panowski, S., Bhakta, S., Raab, H., Polakis, P., and Junutula, J. R. (2014) Site-specific antibody drug conjugates for cancer therapy. *MAbs 6*, 34–45.

(4) Reusch, D., and Tejada, M. L. (2015) Fc glycans of therapeutic antibodies as critical quality attributes. *Glycobiology*.

(5) Junutula, J. R. J. R., Raab, H., Clark, S., Bhakta, S., Leipold, D. D. D., Weir, S., Chen, Y., Simpson, M., Tsai, S. P. S. P., Dennis, M. S. M. S., Lu, Y., Meng, Y. G., Ng, C., Yang, J., Lee, C. C., Duenas, E., Gorrell, J., Katta, V., Kim, A., McDorman, K., Flagella, K., Venook, R., Ross, S., Spencer, S. D., Lee Wong, W., Lowman, H. B., Vandlen, R., Sliwkowski, M. X., Scheller, R. H., Polakis, P., Mallet, W., and others. (2008) Site-specific conjugation of a cytotoxic drug to an antibody improves the therapeutic index. *Nat. Biotechnol. 26*, 925–32.

(6) Strop, P., Liu, S. H., Dorywalska, M., Delaria, K., Dushin, R. G., Tran, T. T., Ho, W. H., Farias, S., Casas, M. G., Abdiche, Y., Zhou, D., Chandrasekaran, R., Samain, C., Loo, C., Rossi, A., Rickert, M., Krimm, S., Wong, T., Chin, S. M., Yu, J., Dilley, J., Chaparro-Riggers, J., Filzen, G. F., O'Donnell, C. J., Wang, F., Myers, J. S., Pons, J., Shelton, D. L., and Rajpal, A. (2013) Location matters: Site of conjugation modulates stability and pharmacokinetics of antibody drug conjugates. *Chem. Biol. 20*, 161–167.

(7) Schumacher, D., Hackenberger, C. P. R., Leonhardt, H., and Helma, J. (2016) Current Status: Site-Specific Antibody Drug Conjugates. *J. Clin. Immunol. 36*, 100–107.

(8) Dennler, P., Fischer, E., and Schibli, R. (2015) Antibody Conjugates: From Heterogeneous Populations to Defined Reagents. *Antibodies 4*, 197–224.

(9) Chudasama, V., Maruani, A., and Caddick, S. (2016) Recent advances in the construction of antibody-drug conjugates. *Nat. Chem. 8*, 114–9.

(10) Kline, T., Steiner, A. R., Penta, K., Sato, A. K., Hallam, T. J., and Yin, G. (2015) Methods to Make Homogenous Antibody Drug Conjugates. *Pharm. Res. 32*, 3480–3493.

(11) Agarwal, P., and Bertozzi, C. R. (2015) Site-specific antibody-drug conjugates: The nexus of bioorthogonal chemistry, protein engineering, and drug development. *Bioconjug. Chem. 26*, 176–192.

(12) Vanbrunt, M. P., Shanebeck, K., Caldwell, Z., Johnson, J., Thompson, P., Martin, T., Dong, H., Li, G., Xu, H., D'Hooge, F., Masterson, L., Bariola, P., Tiberghien, A., Ezeadi, E., Williams, D. G., Hartley, J. A., Howard, P. W., Grabstein, K. H., Bowen, M. A., and Marelli, M. (2015) Genetically Encoded Azide Containing Amino Acid in Mammalian Cells Enables Site-Specific Antibody-Drug Conjugates Using Click Cycloaddition Chemistry. *Bioconjug. Chem. 26*, 2249–2260.

(13) Zimmerman, E. S., Heibeck, T. H., Gill, A., Li, X., Murray, C. J., Madlansacay, M. R., Tran, C., Uter, N. T., Yin, G., Rivers, P. J., Yam, A. Y., Wang, W. D., Steiner, A. R., Bajad, S. U., Penta, K., Yang, W., Hallam, T. J., Thanos, C. D., and Sato, A. K. (2014) Production of Site-Speci fi c Antibody − Drug Conjugates Using Optimized Non-Natural Amino Acids in a Cell-Free Expression System. *Bioconjug. Chem. 25*, 351–361.

(14) Rabuka, D., Rush, J. S., deHart, G. W., Wu, P., and Bertozzi, C. R. (2012) Site-specific chemical protein conjugation using genetically encoded aldehyde tags. *Nat. Protoc. 7*, 1052–1067.

(15) Warden-Rothman, R., Caturegli, I., Popik, V., and Tsourkas, A. (2013) Sortase-tag expressed protein ligation: Combining protein purification and site-specific bioconjugation into a single step. *Anal. Chem. 85*, 11090–11097.

(16) Martin, W. L., West, A. P., Gan, L., and Bjorkman, P. J. (2001) Crystal structure at 2.8 A of an FcRn/heterodimeric Fc complex: mechanism of pH-dependent binding. *Mol. Cell 7*, 867–877.

(17) Dall'Acqua, W. F., Kiener, P. A., and Wu, H. (2006) Properties of Human IgG1s engineered for enhanced binding to the neonatal Fc Receptor (FcRn). *J. Biol. Chem. 281*, 23514–23524.

(18) Wright, a, Sato, Y., Okada, T., Chang, K., Endo, T., and Morrison, S. (2000) In vivo trafficking and catabolism of IgG1 antibodies with Fc associated carbohydrates of differing structure. *Glycobiology 10*, 1347–1355.

(19) Zuberbuhler, K., Casi, G., Bernardes, G. J. L., and Neri, D. (2012) Fucose-specific conjugation of hydrazide derivatives to a vascular-targeting monoclonal antibody in IgG format. *Chem. Commun. 48*, 7100–7102.

(20) Okeley, N. M., Toki, B. E., Zhang, X., Jeffrey, S. C., Burke, P. J., Alley, S. C., and Senter, P. D. (2013) Metabolic engineering of monoclonal antibody carbohydrates for antibody-drug conjugation. *Bioconjug. Chem. 24*, 1650–5.

(21) Ramakrishnan, B., and Qasba, P. K. (2002) Structure-based design of β1,4-galactosyltransferase I (β4Gal-T1) with equally efficient N-acetylgalactosaminyltransferase activity: Point mutation broadens β4Gal-T1 donor specificity. *J. Biol. Chem. 277*, 20833–20839.

(22) Zhu, Z., Ramakrishnan, B., Li, J., Wang, Y., Feng, Y., Prabakaran, P., Colantonio, S., Dyba, M. a, Qasba, P. K., and Dimitrov, D. S. (2014) Site-specific antibody-drug conjugation through an engineered glycotransferase and a chemically reactive sugar. *MAbs 6*, 1–11.

(23) Van Geel, R., Wijdeven, M. A., Heesbeen, R., Verkade, J. M. M., Wasiel, A. A., Van Berkel, S. S., and Van Delft, F. L. (2015) Chemoenzymatic Conjugation of Toxic Payloads to the Globally Conserved N-Glycan of Native mAbs Provides Homogeneous and Highly Efficacious Antibody-Drug Conjugates. *Bioconjug. Chem. 26*, 2233–2242.

(24) Zeglis, B. M., Davis, C. B., Aggeler, R., Kang, H. C., Chen, A., Agnew, B. J., and Lewis, J. S. (2013) Enzyme-mediated methodology for the site-specific radiolabeling of antibodies based on catalyst-free click chemistry. *Bioconjug. Chem. 24*, 1057–1067.

(25) Uozumi, N., Yanagidani, S., Miyoshi, E., Ihara, Y., Sakuma, T., Gao, C., Teshima, T., Fujii, S., Shiba, T., and Taniguchi, N. (1996) Purification and cDNA Cloning of Porcine Brain GDP-L-Fuc:N-Acetyl-β-D-Glucosaminide α1→6Fucosyltransferase. *Biochemistry 271*, 27810 –27817.

(26) Ihara, H., Ikeda, Y., and Taniguchi, N. (2006) Reaction mechanism and substrate specificity for nucleotide sugar of mammalian α1,6-fucosyltransferase - A large-scale preparation and characterization of recombinant human FUT8. *Glycobiology 16*, 333–342.

(27) Coyne, M. J. (2005) Human Symbionts Use a Host-Like Pathway for Surface Fucosylation. *Science (80-.). 307*, 1778–1781.

(28) Wang, W., Hu, T., Frantom, P. A., Zheng, T., Gerwe, B., Del Amo, D. S., Garret, S., Seidel, R. D., and Wu, P. (2009) Chemoenzymatic synthesis of GDP-L-fucose and the Lewis X glycan derivatives. *Proc. Natl. Acad. Sci. U. S. A. 106*, 16096–101.

(29) Gosselin, S., Alhussaini, M., Streiff, M. B., Takabayashi, K., and Palcic, M. M. (1994) A continuous spectrophotometric assay for glycosyltransferases. *Anal. Biochem.*

(30) Hong, V., Presolski, S. I., Ma, C., and Finn, M. G. (2009) Analysis and optimization of copper-catalyzed azide-alkyne cycloaddition for bioconjugation. *Angew. Chemie - Int. Ed. 48*, 9879–9883.

(31) Presolski, S. L., Hong, V. P., and Finn, M. G. (2011) Copper-Catalyzed Azide–Alkyne Click Chemistry for Bioconjugation. *Curr. Protoc. Chem. Biol. 3*, 153–162.

(32) Schöneich, C., and Williams, T. D. (2002) Cu(II)-catalyzed oxidation of β-amyloid peptide targets His13 and His14 over His6: Detection of 2-oxo-histidine by HPLC-MS/MS. *Chem. Res. Toxicol. 15*, 717–722.

(33) Agard, N. J., Prescher, J. A., and Bertozzi, C. R. (2004) A strain-promoted [3 + 2] azide-alkyne cycloaddition for covalent modification of biomolecules in living systems. *J. Am. Chem. Soc. 126*, 15046–15047.

(34) Deisenhofer, J. (1981) Crystallographic refinement and atomic models of a human Fc fragment and its complex with fragment B of protein A from Staphylococcus aureus at 2.9- and 2.8-.ANG. resolution. *Biochemistry 20*, 2361–2370.

(35) Krapp, S., Mimura, Y., Jefferis, R., Huber, R., and Sondermann, P. (2003) Structural analysis of human IgG-Fc glycoforms reveals a correlation between glycosylation and structural integrity. *J. Mol. Biol. 325*, 979–989.

(36) Teplyakov, A., Zhao, Y., Malia, T. J., Obmolova, G., and Gilliland, G. L. (2013) IgG2 Fc structure and the dynamic features of the IgG CH2-CH3 interface. *Mol. Immunol. 56*, 131–139.

(37) He, F., Hogan, S., Latypov, R. F., Narhi, L. O., and Razinkov, V. I. (2010) High throughput thermostability screening of monoclonal antibody formulations. *J. Pharm. Sci. 99*, 1707–1720.

(38) Toprani, V. M., Joshi, S. B., Kueltzo, L. A., Schwartz, R. M., Middaugh, C. R., and Volkin, D. B. (2016) A Micro-Polyethylene Glycol Precipitation Assay as a Relative Solubility Screening Tool for Monoclonal Antibody Design and Formulation Development. *J. Pharm. Sci.*

105, 2319–2327.

(39) More, A. S., Toprani, V. M., Okbazghi, S. Z., Kim, J. H., Joshi, S. B., Middaugh, C. R., Tolbert, T. J., and Volkin, D. B. (2016) Correlating the Impact of Well-Defined Oligosaccharide Structures on Physical Stability Profiles of IgG1-Fc Glycoforms. *J. Pharm. Sci. 105*, 588–601.

(40) Gibson, T. J., Mccarty, K., Mcfadyen, I. J., Cash, E., Dalmonte, P., Hinds, K. D., Dinerman, A. A., Alvarez, J. C., and Volkin, D. B. (2011) Application of a high-throughput screening procedure with PEG-induced precipitation to compare relative protein solubility during formulation development with IgG1 monoclonal antibodies. *J. Pharm. Sci. 100*, 1009–1021.

(41) Bruhns, P., Iannascoli, B., England, P., Mancardi, D. A., Fernandez, N., Jorieux, S., and Daëron, M. (2009) Specificity and affinity of human Fcγ receptors and their polymorphic variants for human IgG subclasses. *Blood 113*, 3716–3725.

(42) Warmerdam, P. A., van de Winkel, J. G., Vlug, A., Westerdaal, N. A., and Capel, P. J. (1991) A single amino acid in the second Ig-like domain of the human Fc gamma receptor II is critical for human IgG2 binding. *J. Immunol. 147*, 1338–43.

(43) Parren, P. W., Warmerdam, P. A., Boeije, L. C., Arts, J., Westerdaal, N. A., Vlug, A., Capel, P. J., Aarden, L. A., and van de Winkel, J. G. (1992) On the interaction of IgG subclasses with the low affinity Fc gamma RIIa (CD32) on human monocytes, neutrophils, and platelets. Analysis of a functional polymorphism to human IgG2. *J. Clin. Invest. 90*, 1537–46.

(44) Shields, R. L., Lai, J., Keck, R., O'Connell, L. Y., Hong, K., Meng, Y. G., Weikert, S. H. A., and Presta, L. G. (2002) Lack of Fucose on Human IgG1 N-Linked Oligosaccharide Improves Binding to Human Fcgamma RIII and Antibody-dependent Cellular Toxicity. *J. Biol. Chem. 277*, 26733–26740.

(45) Ferrara, C., Stuart, F., Sondermann, P., Brunker, P., and Umana, P. (2006) The Carbohydrate at Fc RIIIa Asn-162: AN ELEMENT REQUIRED FOR HIGH AFFINITY BINDING TO NON-FUCOSYLATED IgG GLYCOFORMS. *J. Biol. Chem. 281*, 5032–5036.

(46) Mizushima, T., Yagi, H., Takemoto, E., Shibata-Koyama, M., Isoda, Y., Iida, S., Masuda, K., Satoh, M., and Kato, K. (2011) Structural basis for improved efficacy of therapeutic antibodies on defucosylation of their Fc glycans. *Genes to Cells 16*, 1071–1080.

(47) Junutula, J. R., and Gerber, H. P. (2016) Next-Generation Antibody-Drug Conjugates (ADCs) for Cancer Therapy. *ACS Med. Chem. Lett. 7*, 972–973.

(48) Shen, B.-Q., Xu, K., Liu, L., Raab, H., Bhakta, S., Kenrick, M., Parsons-Reponte, K. L., Tien, J., Yu, S.-F., Mai, E., Li, D., Tibbitts, J., Baudys, J., Saad, O. M., Scales, S. J., McDonald, P. J., Hass, P. E., Eigenbrot, C., Nguyen, T., Solis, W. a, Fuji, R. N., Flagella, K. M., Patel, D., Spencer, S. D., Khawli, L. a, Ebens, A., Wong, W. L., Vandlen, R., Kaur, S., Sliwkowski, M. X., Scheller, R. H., Polakis, P., and Junutula, J. R. (2012) Conjugation site modulates the in vivo stability and therapeutic activity of antibody-drug conjugates. *Nat. Biotechnol. 30*, 184–189.

(49) Zimmerman, E. S., Heibeck, T. H., Gill, A., Li, X., Murray, C. J., Madlansacay, M. R., Tran, C., Uter, N. T., Yin, G., Rivers, P. J., Yam, A. Y., Wang, W. D., Steiner, A. R., Bajad, S.

U., Penta, K., Yang, W., Hallam, T. J., Thanos, C. D., and Sato, A. K. (2014) Production of site-specific antibody-drug conjugates using optimized non-natural amino acids in a cell-free expression system. *Bioconjug. Chem. 25*, 351–361.

(50) Dennler, P., Chiotellis, A., Fischer, E., Bregeon, D., Belmant, C., Gauthier, L., Lhospice, F., Romagne, F., and Schibli, R. (2014) Transglutaminase-based chemo-enzymatic conjugation approach yields homogeneous antibody-drug conjugates. *Bioconjug. Chem. 25*, 569–578.

(51) Pan, H., Chen, K., Chu, L., Kinderman, F., Apostol, I., and Huang, G. (2009) Methionine oxidation in human IgG2 Fc decreases binding affinities to protein A and FcRn. *Protein Sci. 18*, 424–433.

(52) Okeley, N. M., Alley, S. C., Anderson, M. E., Boursalian, T. E., Burke, P. J., Emmerton, K. M., Jeffrey, S. C., Klussman, K., Law, C.-L., Sussman, D., Toki, B. E., Westendorf, L., Zeng, W., Zhang, X., Benjamin, D. R., and Senter, P. D. (2013) Development of orally active inhibitors of protein and cellular fucosylation. *Proc. Natl. Acad. Sci. U. S. A. 110*, 5404–9.

(53) Li, X., Fang, T., and Boons, G. J. (2014) Preparation of well-defined antibody-drug conjugates through glycan remodeling and strain-promoted azide-alkyne cycloadditions. *Angew. Chemie - Int. Ed. 53*, 7179–7182.

(54) Besanceney-Webler, C., Jiang, H., Zheng, T., Feng, L., Soriano Del Amo, D., Wang, W., Klivansky, L. M., Marlow, F. L., Liu, Y., and Wu, P. (2011) Increasing the efficacy of bioorthogonal click reactions for bioconjugation: A comparative study. *Angew. Chemie - Int. Ed. 50*, 8051–8056.

(55) Kalia, J., and Raines, R. T. (2008) Hydrolytic stability of hydrazones and oximes. *Angew. Chemie - Int. Ed. 47*, 7523–7526.

(56) Lhospice, F., Brégeon, D., Belmant, C., Dennler, P., Chiotellis, A., Fischer, E., Gauthier, L., Boëdec, A., Rispaud, H., Savard-Chambard, S., Represa, A., Schneider, N., Paturel, C., Sapet, M., Delcambre, C., Ingoure, S., Viaud, N., Bonnafous, C., Schibli, R., and Romagné, F. (2015) Site-Specific conjugation of monomethyl auristatin e to Anti-CD30 antibodies improves their pharmacokinetics and therapeutic index in rodent models. *Mol. Pharm. 12*, 1863–1871.

(57) Voynov, V., Chennamsetty, N., Kayser, V., Helk, B., Forrer, K., Zhang, H., Fritsch, C., Heine, H., and Trout, B. L. (2009) Dynamic fluctuations of protein-carbohydrate interactions promote protein aggregation. *PLoS One 4*.

(58) Ross, P. L., and Wolfe, J. L. (2016) Physical and Chemical Stability of Antibody Drug Conjugates: Current Status. *J. Pharm. Sci. 105*, 391–397.

(59) Acchione, M., Kwon, H., Jochheim, C. M., and Atkins, W. M. (2012) Impact of linker and conjugation chemistry on antigen binding, Fc receptor binding and thermal stability of model antibody-drug conjugates *4*, 362–372.

(60) Dimasi, N., Fleming, R., Zhong, H., Bezabeh, B., Kinneer, K., Christie, R. J., Fazenbaker, C., Wu, H., and Gao, C. (2017) Efficient preparation of site-specific antibody drug conjugates using cysteine-insertion. *Mol. Pharm.* acs.molpharmaceut.6b00995.

(61) Wakankar, A. A., Feeney, M. B., Rivera, J., Chen, Y., Kim, M., Sharma, V. K., and Wang, Y. J. (2010) Physicochemical stability of the antibody - Drug conjugate trastuzumab-DM1: Changes due to modification and conjugation processes. *Bioconjug. Chem. 21*, 1588–1595.

(62) Chaudhuri, R., Cheng, Y., Middaugh, C. R., and Volkin, D. B. (2014) High-Throughput Biophysical Analysis of Protein Therapeutics to Examine Interrelationships Between Aggregate Formation and Conformational Stability. *AAPS J. 16*, 48–64.

(63) Wu, S. J., Luo, J., O'Neil, K. T., Kang, J., Lacy, E. R., Canziani, G., Baker, A., Huang, M., Tang, Q. M., Raju, T. S., Jacobs, S. A., Teplyakov, A., Gilliland, G. L., and Feng, Y. (2010) Structure-based engineering of a monoclonal antibody for improved solubility. *Protein Eng. Des. Sel. 23*, 643–651.

(64) Lyon, R. P., Bovee, T. D., Doronina, S. O., Burke, P. J., Hunter, J. H., Neff-LaFord, H. D., Jonas, M., Anderson, M. E., Setter, J. R., and Senter, P. D. (2015) Reducing hydrophobicity of homogeneous antibody-drug conjugates improves pharmacokinetics and therapeutic index. *Nat. Biotechnol. 33*, 733–736.

(65) Stefano, J. E., Busch, M., Hou, L., Park, A., and Gianolio, D. A. (2013) Micro- and mid-scale maleimide-based conjugation of cytotoxic drugs to antibody hinge region thiols for tumor targeting. *Methods Mol. Biol.*

(66) Zhou, Q., Stefano, J. E., Manning, C., Kyazike, J., Chen, B., Gianolio, D. A., Park, A., Busch, M., Bird, J., Zheng, X., Simonds-Mannes, H., Kim, J., Gregory, R. C., Miller, R. J., Brondyk, W. H., Dhal, P. K., and Pan, C. Q. (2014) Site-specific antibody-drug conjugation through glycoengineering. *Bioconjug. Chem. 25*, 510–520.

(67) Okeley, N. M., Toki, B. E., Zhang, X., Je, S. C., Burke, P. J., Alley, S. C., and Senter, P. D. (2013) Metabolic Engineering of Monoclonal Antibody Carbohydrates for Antibody − Drug Conjugation. *Bioconjug. Chem.*

(68) Nathan Tumey, L., Leverett, C. A., Vetelino, B., Li, F., Rago, B., Han, X., Loganzo, F., Musto, S., Bai, G., Sukuru, S. C. K., Graziani, E. I., Puthenveetil, S., Casavant, J., Ratnayake, A., Marquette, K., Hudson, S., Doppalapudi, V. R., Stock, J., Tchistiakova, L., Bessire, A. J., Clark, T., Lucas, J., Hosselet, C., O'Donnell, C. J., and Subramanyam, C. (2016) Optimization of Tubulysin Antibody-Drug Conjugates: A Case Study in Addressing ADC Metabolism. *ACS Med. Chem. Lett. 7*, 977–982.

(69) Shire, S. J., Shahrokh, Z., and Liu, J. U. N. (2004) Challenges in the Development of High Protein Concentration Formulations. *J. Pharm. Sci. 93*, 1390–1402.

(70) McDonagh, C. F., Kim, K. M., Turcott, E., Brown, L. L., Westendorf, L., Feist, T., Sussman, D., Stone, I., Anderson, M., Miyamoto, J., Lyon, R., Alley, S. C., Gerber, H.-P., and Carter, P. J. (2008) Engineered anti-CD70 antibody-drug conjugate with increased therapeutic index. *Mol. Cancer Ther. 7*, 2913–2923.

(71) Vafa, O., Gilliland, G. L., Brezski, R. J., Strake, B., Wilkinson, T., Lacy, E. R., Scallon, B., Teplyakov, A., Malia, T. J., and Strohl, W. R. (2014) An engineered Fc variant of an IgG eliminates all immune effector functions via structural perturbations. *Methods 65*, 114–126.

(72) Beck, A., and Reichert, J. M. (2012) Marketing approval of mogamulizumab A triumph for glyco-engineering. *MAbs 4*, 419–425.

(73) Mimura, Y., Church, S., Ghirlando, R., Ashton, P. R., Dong, S., Goodall, M., Lund, J., and Jefferis, R. (2000) The influence of glycosylation on the thermal stability and effector function expression of human IgG1-Fc: properties of a series of truncated glycoforms. *Mol Immunol 37*, 697–706.

(74) Okbazghi, S. Z., More, A. S., White, D. R., Duan, S., Shah, I. S., Joshi, S. B., Middaugh, C. R., Volkin, D. B., and Tolbert, T. J. (2016) Production, Characterization, and Biological Evaluation of Well-Defined IgG1 Fc Glycoforms as a Model System for Biosimilarity Analysis. *J. Pharm. Sci. 105*, 559–574.

(75) Xiao, J., and Tolbert, T. J. (2009) Synthesis of polymerizable protein monomers for protein-acrylamide hydrogel formation. *Biomacromolecules 10*, 1939–1946.

(76) Petersen, K. J., Peterson, K. C., Muretta, J. M., Higgins, S. E., Gillispie, G. D., and Thomas, D. D. (2014) Fluorescence lifetime plate reader: Resolution and precision meet high-throughput. *Rev. Sci. Instrum. 85*.

(77) Laemmli, U. K. (1970) Cleavage of structural proteins during the assembly of the head of bacteriophage T4. *Nature 227*, 680–685.

Chapter 4

Summary, conclusion, and future directions

The highly-conserved N-glycan in the C_H2 domain of IgG isotype (Asn297 glycan) has been shown to have a significant effect on the antibody properties. The Asn297 glycan supports the underlying protein backbone and helps in maintaining the right conformation of IgG. This glycan plays a crucial role in the antibody effector functions[1–3], pharmacokinetics[4], stability[1,5,6], physicochemical properties such as solubility of the antibody[5], as well-as immunogenicity[7]. The challenge in producing an antibody with a homogeneous glycan (i.e. single glycoform) comes from the fact that the glycosylation process is not a template-driven cellular process.[8,9] Unlike the DNA transcription and RNA translation, the N-glycosylation is mediated by a series of glycosyltransferases and glycosidases present at different locations and abundancies in the endoplasmic reticulum and Golgi apparatus. Therefore, during the protein journey through these organelles, it will be decorated with different sugars depending on the availability of these enzymes, availability of donor sugar substrates, protein transit time, and cell type. The net result is a production of a protein having different glycoforms. It is interesting to see a marketed monoclonal antibody (mAb) product as supposed to contain a single active pharmaceutical ingredient while in reality it can be a mixture of tens to hundreds of glycoforms that have the same amino acid sequence but different glycan composition. Therefore, to study each glycoform carefully, we need a robust method that can generate homogeneous glycoforms in sufficient quantities.

Human IgG2 is a less-well characterized IgG subclass in terms of it Asn297 glycan. IgG2 subclass has been utilized in making therapeutic mAb such as denosumab and panitumumab. The relatively low effector functions of this IgG subclass made it a viable choice for designing therapeutic mAb when the effector function mode of action is not needed or when the effector functions, such as activation of the complement system, results in harmful effects. Several

research studies were carried out recently with the aim of introducing more reduction in the effector functions of IgG2 through changing the amino acid sequence of the protein. Most of these mutagenesis studies were carried out on amino acids that participate directly or indirectly in the binding of IgG2 to the Fcγ receptors and C1q protein, a binding that can initiate cell-mediated effector functions and activation of the complement system, respectively. IgG binds Fcγ receptors and C1q protein through the area of lower hinge region and upper C_H2 domain which is highly affected by Asn297 glycan. In most of these studies, the Asn297 glycosylation profile was not taken into account especially the level of core fucosylation.[10] In addition to that, there is always a potential immunogenicity associated with changing the amino acid sequence of a natural protein. Conversely, glycoengineering carries a lower immunogenicity potential and might be used alone or in combination with other approaches to pursue same goals.

In order to study the effect of composition of Asn297 glycan on the properties of IgG2 subclass, we developed an enzymatic synthesis approach to produce homogeneous and highly purified IgG2 Fc glycoforms. Before this synthesis, we cloned the Fc region of the human IgG2 subclass in a suitable vector for expression of this glycoprotein in the glycosylation-deficient yeast *Pichia pastoris* to produce relatively large laboratory-scale quantities of IgG2 Fc. The *Pichia pastoris* glycosylation machinery produced a well-characterized IgG2 Fc with a high mannose glycan which can be used as a starting material to produces other glycoforms. Large amount of IgG2 Fc was produced from multiple fermenter runs. Since, the yeast lack the Golgi apparatus, further glycan processing *in vivo* is stopped and therefore the secreted IgG2 Fc glycoform was of the high mannose type. The secreted high mannose IgG2 Fc was subjected to further purification processes using protein G affinity chromatography, hydrophobic interaction (HIC) chromatography, and weak cation exchange (WCX) chromatography to isolate the

glycoprotein from the growth media and produce diglycosylated IgG2 Fc. The purified diglycosylated IgG2 Fc of the high mannose type then became a convenient substrate to produce the other interesting IgG2 Fc glycoforms such as the hybrid and the fucosylated hybrid IgG2 Fc glycoforms using *in vitro* enzymatic synthesis. The developed *in vitro* enzymatic synthesis to produce different IgG2 Fc glycoforms described in details in **chapter 2,** provides a detailed description on how to produce well-characterized and homogeneous glycoforms not only for IgG2 Fc but also for all the other proteins that have N-glycosylation sites (NXS/T sequon) that are accessible for N-glycosylation. In this enzymatic synthesis we utilized a series of glycosidase and glycosyltransferases such as the bacterial α1,2-mannosidase (BT3990), N-acetylglucosaminlytransferase-I (GnT-I), and mammalian α1,6-fucosyltransferase (FUT8). In this synthesis we also utilized L-fucokinase/guanosine 5'-diphosphate-L-fucose pyrophosphorylase (FKP), an enzyme that enabled us to synthesize and purify the natural nucleotide sugar, GDP-fucose, that is necessary for FUT8 action and core fucosylation of the An297 glycan. With the aid of FKP, we also succeeded in synthesizing and purifying the non-natural sugar nucleotide, GDP-azidofucose, which enabled functionalization of the Asn297 glycan for bioorthogonal click reactions to make site-specific antibody drug conjugates as described in **chapter 3**. FUT8, as a key enzyme used in this *in vitro* enzymatic synthesis was produced in a novel way where, for the first time, we produced this mammalian enzyme in a modified strain of *E.coli* in sufficient quantities to do all the required experiments described in this work.

An important Asn297 glycan posttranslational modification is the core fucosylation. More than a decade ago, the core fucosylation was shown to reduce the binding of IgG1 to FcγRIIIa expressed on the surface of the natural killer cells.[11] This reduction in binding was well

correlated with the reduction in IgG1 antibody dependent cellular cytotoxicity (ADCC). This finding drew the attention of many pharmaceutical companies and research groups to glycoengineer mAb to have low level of core fucose and increase their efficacy through the ADCC mode of action. This finding eventually resulted in a successful marketing of afucosylated mAb with better efficacy such as mogamulizumab and obinutuzumab for treating different types of cancer. However, here we decided to do the reverse, i.e. increasing the level of core fucose within the Asn297 glycan of IgG2 subclass. Since, IgG2 has lower effector functions dictated by its lower binding affinities to Fcγ receptors and the complement protein C1q, our goal was to reduce the binding more, especially to FcγRIIIa, to make a more silent IgG2 Fc. Therefore, we utilized the developed enzymatic synthesis for scaling up the production of the homogeneous fully fucosylated IgG2 Fc and compare it head to head with the afucosylated IgG2 Fc. The study was also designed to test the effect of adding core fucose to Asn297 glycan on the conformation and stability of IgG2 Fc using biophysical characterization methods. The addition of core fucose resulted in a significant reduction (~ 13-fold) of IgG2 Fc binding to FcγRIIIa compared to the absence of core fucose. Although IgG2 has a weak affinity to this receptor to start with, the avidity that can result from clustering of multiple receptors on the surface of the immune effector cells upon engagement with the immune complex, can be high enough to induce a considerable magnitude of undesirable ADCC.[12] Therefore, more reduction in the monomeric binding through glycoengineering by introducing more core fucose to Asn297 glycan would result in more reduction in any undesirable ADCC. Interestingly, the presence or absence of core fucose did not change the binding of IgG2 to FcγRIIa-R131 variant. This result also suggests that IgG2 has a different mode of interaction to this receptor than IgG1 because binding of IgG1 to this receptor has been shown to be affected by core fucose in other studies. The

addition of core fucose to IgG2 Fc did not appear to perturb the conformational stability of the Fc probed using various biophysical characterization techniques and this means that producing highly fucosylated mAb can be acceptable from the stability perspective. Also, during the course of *in vitro* enzymatic synthesis, FUT8 kinetics studies of the transfer of core fucose to free glycan compared to Asn297-bound glycan showed about 10-fold differences in K_M but same V_{max}, indicating lower affinity of FUT8 for protein-bound glycan but similar transition states for both glycans. This result could also provide additional evidence on the dynamic nature of the Asn297 glycan relative to the surrounding protein backbone seen in other studies[13,14] and may also expand our understanding of the role of Asn297 glycan in fine-tuning the antibody conformation and effector functions. Our enzyme kinetics studies also showed that Asn297 is more accessible site for GnT-I and FUT8 than a second but unusual glycosylation site in the C_H3 domain of IgG2 Fc (i.e. Asn392 site). This difference in glycosylation site accessibility may also explain the glycosylation heterogeneity observed among different glycosylation sites on the same protein as reported in previous studies and can increase our understanding of glycoproteins biosynthesis.

Since, antibody drug conjugates (ADCs) mode of action relies on the cytotoxicity of the payload to eliminate the cancer cells and does not require activation of the effector functions; we were also interested in designing ADCs employing human IgG2 subclass as the mAb part of this type of products. It has been postulated that elimination of the cell-mediated effector functions could increase the ADC specificity and reduce any possible off-target toxicity by the uptake of these molecules by the immune effector cells.[15] Also, current ADC research focuses on reducing the heterogeneity of the marketed ADCs and developing new technologies to introduce the payload on specific sites on the mAb part of ADC instead of random conjugation through the

lysine or cysteine residues using conventional conjugation chemistry. This approach of conjugating the payload at specific sites with a defined drug to antibody (DAR) ratio has been shown to improve the ADC stability, pharmacokinetics, and eventually increase the safety and efficacy of the product.[16,17] Therefore, we sought to create a specific site of conjugation within the Asn297 glycan of the antibody to expand the number of the present technologies of producing site-specific ADCs. This specific site was created with the aid of FUT8 as described in **chapter 3**. First, our synthetic platform described in chapter 2 enabled us to produce sufficient quantity of the afucosylated hybrid IgG2 Fc glycoform that can work as a substrate for FUT8 since this enzyme requires the presence of unblocked N-acetylglucosamine (GlcNAc) on the non-reducing terminal of the glycan. In addition, we were able to produce and purify a modified fucose nucleotide sugar (GDP-azidofucose) that can be utilized by FUT8 to transfer the modified fucose (6-azido-L-fucose) to the Asn297 glycan of IgG2 Fc. We succeeded in optimizing FUT8 reaction conditions to produce fully functionalized IgG2 Fc with this azido-modified sugar for conjugation with alkyne functionalized compounds through the bioorthogonal azide-alkyne cycloaddition (AAC). As a proof of concept to test the accessibility of the created site for conjugation reactions, we used three compounds (linkers) functionalized with different types of alkyne. The alkynes used needed different reaction conditions to react with the 6-azido-L-fucose presents on the Asn297 glycan of IgG2 Fc. Also, the alkyne parts of these three compounds (linkers) have different physicochemical properties (different size and hydrophobicity) which could ultimately affect the final construct properties. The linkers used were one linear alkyne linker (Propargyl-PEG4-acid) and two cyclic alkyne likers (BCN-PEG4-acid, and DBCO-PEG5-acid). The Propargyl linker is the smallest and the least hydrophobic linker among these linkers while the DBCO-linker is the largest linker and the most hydrophobic one. The conjugation

reactions were carried out either through copper(I)-catalyzed azide-alkyne cycloaddition (CuAAC) or through strain promoted azide-alkyne cycloaddition (SPAAC) using different types of cyclic alkynes. After successful optimization of the conjugation reactions, we produced sufficient quantities of homogeneous conjugates to study the effect of the linker type on the structural stability, solubility, and binding of these conjugates to Fcγ receptors. As expected, these studies showed that the overall conjugate properties can be also affected by the payload (linker) properties. For example, the Propargyl-linker did not reduce the solubility (thermodynamic activity) of the conjugate while the cyclic linkers, especially the DBCO-linker, resulted in some reduction in the conjugate solubility (Thermodynamic activity) measured by PEG-precipitation assay. Another effect observed here was the reduction in the DBCO-Fc conjugate thermal stability as tested by differential scanning calorimetry and extrinsic fluorescence compared to the thermal stability of the naked Fc or the other conjugates. Binding to FcγRIIa was also reduced for the DBCO-Fc conjugate compared to the other conjugates presumably due to the larger size of the DBCO-linker which can produce more conformational changes in the C_H2 domain of the Fc. Interestingly, such reduction in binding to Fcγ receptors can be also advantageous when designing ADCs and could reduce any potential off-target toxicity. However, the reduction in the DBCO-conjugate stability can be considered marginal when comparted to the stability of IgG2 Fc upon the removal of the whole Asn297glycan (i.e. deglycosylated Fc). Therefore, conjugation through the core fucose site of Asn297 glycan without eliminating this glycan, which could help in mitigating any negative effect due to conjugating the usually hydrophobic payloads, would be an attractive approach for the production of site-specific ADCs with improved properties. Moreover, combining the site-specific functionalization of IgG2 Fc described in this study with the optimized conjugation

reaction conditions and the experimental setup followed, could provide a powerful approach to screen for different linkers/ linker-payloads at different stages of drug development to eventually develop ADC with better safety, stability, and efficacy profiles.

Lastly, the developed enzymatic synthesis described in this work can be extended further by producing the other type of glycoforms, especially the galactosylated and sialylated glycoforms. This can be done by utilizing other enzymes such as mannosidase II, galactosyltransferase, and sialyltransferases as well as the necessary nucleotide sugars for reactions catalyzed by these enzymes. These terminal sugars in the Asn297 glycan of IgG1 subclass have been shown to affect the antibody effector functions where sialic acid mediate anti-inflammatory effect, while the presence or absence of galactose can affect the antibody interaction with the complement system. On the other hand, the novel site-specific functionalization of IgG2 Fc at Asn297 glycan described here using FUT8 can be used to functionalize a suitable full-length IgG2 with certain specificity to tumor cells. The functionalization of IgG2 can be then followed by conjugating different types of toxic payloads connected to different linkers to produce site-specific ADCs that can be tested in cell-based assays and animal models.

References

(1) Mimura, Y., Church, S., Ghirlando, R., Ashton, P. R., Dong, S., Goodall, M., Lund, J., and Jefferis, R. (2000) The influence of glycosylation on the thermal stability and effector function expression of human IgG1-Fc: properties of a series of truncated glycoforms. *Mol Immunol 37*, 697–706.

(2) Huang, W., Giddens, J., Fan, S. Q., Toonstra, C., and Wang, L. X. (2012) Chemoenzymatic glycoengineering of intact IgG antibodies for gain of functions. *J. Am. Chem. Soc. 134*, 12308–12318.

(3) Quast, I., and Lunemann, J. D. (2014) Fc glycan-modulated immunoglobulin G effector functions. *J. Clin. Immunol. 34*.

(4) Chen, X., Liu, D., Flynn, G. C., Liu, Y. D., and Flynn, G. C. (2009) The effect of Fc glycan forms on human IgG2 antibody clearance in humans. *Glycobiology 19*, 240–249.

(5) More, A. S., Toprani, V. M., Okbazghi, S. Z., Kim, J. H., Joshi, S. B., Middaugh, C. R., Tolbert, T. J., and Volkin, D. B. (2016) Correlating the Impact of Well-Defined Oligosaccharide Structures on Physical Stability Profiles of IgG1-Fc Glycoforms. *J. Pharm. Sci. 105*, 588–601.

(6) Zheng, K., Bantog, C., and Bayer, R. (2011) The impact of glycosylation on monoclonal antibody conformation and stability. *MAbs 3*, 568–576.

(7) Reusch, D., and Tejada, M. L. (2015) Fc glycans of therapeutic antibodies as critical quality attributes. *Glycobiology*.

(8) Stanley, P., Schachter, H., and Taniguchi, N. (2009) Chapter 8. N-Glycans, Essentials of Glycobiology, 2nd Edition. *Essentials Glycobiol.*

(9) Kornfeld, R., and Kornfeld, S. (1985) Assembly of Asparagine-Linked Oligosaccharides. *Annu. Rev. Biochem. 54*, 631–664.

(10) Vafa, O., Gilliland, G. L., Brezski, R. J., Strake, B., Wilkinson, T., Lacy, E. R., Scallon, B., Teplyakov, A., Malia, T. J., and Strohl, W. R. (2014) An engineered Fc variant of an IgG eliminates all immune effector functions via structural perturbations. *Methods 65*, 114–126.

(11) Shields, R. L., Lai, J., Keck, R., O'Connell, L. Y., Hong, K., Meng, Y. G., Weikert, S. H. A., and Presta, L. G. (2002) Lack of Fucose on Human IgG1 N-Linked Oligosaccharide Improves Binding to Human Fcgamma RIII and Antibody-dependent Cellular Toxicity. *J. Biol. Chem. 277*, 26733–26740.

(12) Gong, Q., Hazen, M., Marshall, B., Crowell, S. R., Ou, Q., Wong, A. W., Phung, W., Vernes, J. M., Meng, Y. G., Tejada, M., Andersen, D., and Kelley, R. F. (2016) Increased in vivo effector function of human IgG4 isotype antibodies through afucosylation. *MAbs 8*, 1098–1106.

(13) Barb, A. W., and Prestegard, J. H. (2011) NMR analysis demonstrates immunoglobulin G N-glycans are accessible and dynamic. *Nat. Chem. Biol. 7*, 147–153.

(14) Barb, A. W., Meng, L., Gao, Z., Johnson, R. W., Moremen, K. W., and Prestegard, J. H. (2012) NMR characterization of immunoglobulin G Fc glycan motion on enzymatic sialylation. *Biochemistry 51*, 4618–4626.

(15) Beck, A., Goetsch, L., Dumontet, C., and Corvaia, N. (2017) Strategies and challenges for the next generation of therapeutic antibodies. *Nat. Rev. Drug Discov. 16*, 315–337.

(16) Junutula, J. R. J. R., Raab, H., Clark, S., Bhakta, S., Leipold, D. D. D., Weir, S., Chen, Y., Simpson, M., Tsai, S. P. S. P., Dennis, M. S. M. S., Lu, Y., Meng, Y. G., Ng, C., Yang, J., Lee, C. C., Duenas, E., Gorrell, J., Katta, V., Kim, A., McDorman, K., Flagella, K., Venook, R., Ross, S., Spencer, S. D., Lee Wong, W., Lowman, H. B., Vandlen, R., Sliwkowski, M. X., Scheller, R. H., Polakis, P., Mallet, W., and others. (2008) Site-specific conjugation of a cytotoxic drug to an antibody improves the therapeutic index. *Nat. Biotechnol. 26*, 925–32.

(17) Lhospice, F., Brégeon, D., Belmant, C., Dennler, P., Chiotellis, A., Fischer, E., Gauthier, L., Boëdec, A., Rispaud, H., Savard-Chambard, S., Represa, A., Schneider, N., Paturel, C., Sapet, M., Delcambre, C., Ingoure, S., Viaud, N., Bonnafous, C., Schibli, R., and Romagné, F. (2015) Site-Specific conjugation of monomethyl auristatin e to Anti-CD30 antibodies improves their pharmacokinetics and therapeutic index in rodent models. *Mol. Pharm. 12*, 1863–1871.

Appendix

Appendix

Two appendices are attached to this dissertation where appendix A provides supplementary information for **Chapter 2** while appendix B provides supplementary information for **Chapter 3**:

Appendix A

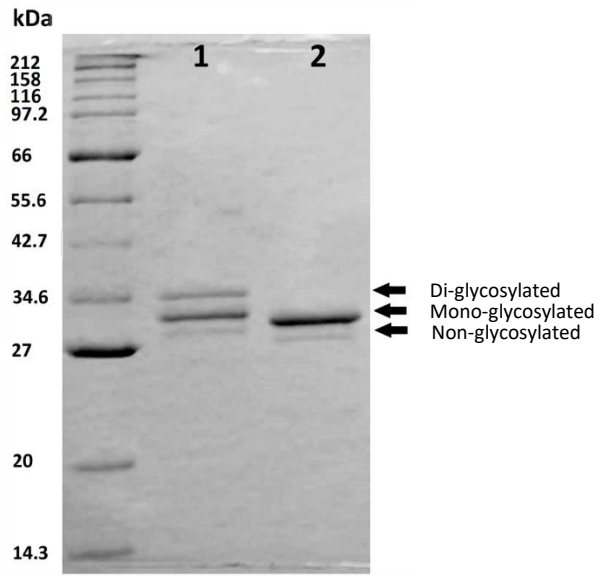

Figure A1. SDS-PAGE analysis under reducing conditions using 12% gels of IgG2 Fc variants expressed in *Pichia pastoris* and purified by protein G affinity chromatography. Lane 1 is IgG2 Fc-(N297, N392) which has a second N- glycosylation site at Asn392 and shows three bands (di-glycosylated, mono-glycosylated, and non-glycosylated Fc monomers from top to bottom) on the gel depending on the extent of site occupancy of these two glycosylation sites. Lane 2 is for IgG2 Fc-(N297, K392) which has only the consensus Asn297 N-glycosylation site and shows only two bands (no di-glycosylated Fc monomer) on the gel depending on whether this site is occupied with N-glycan or not.

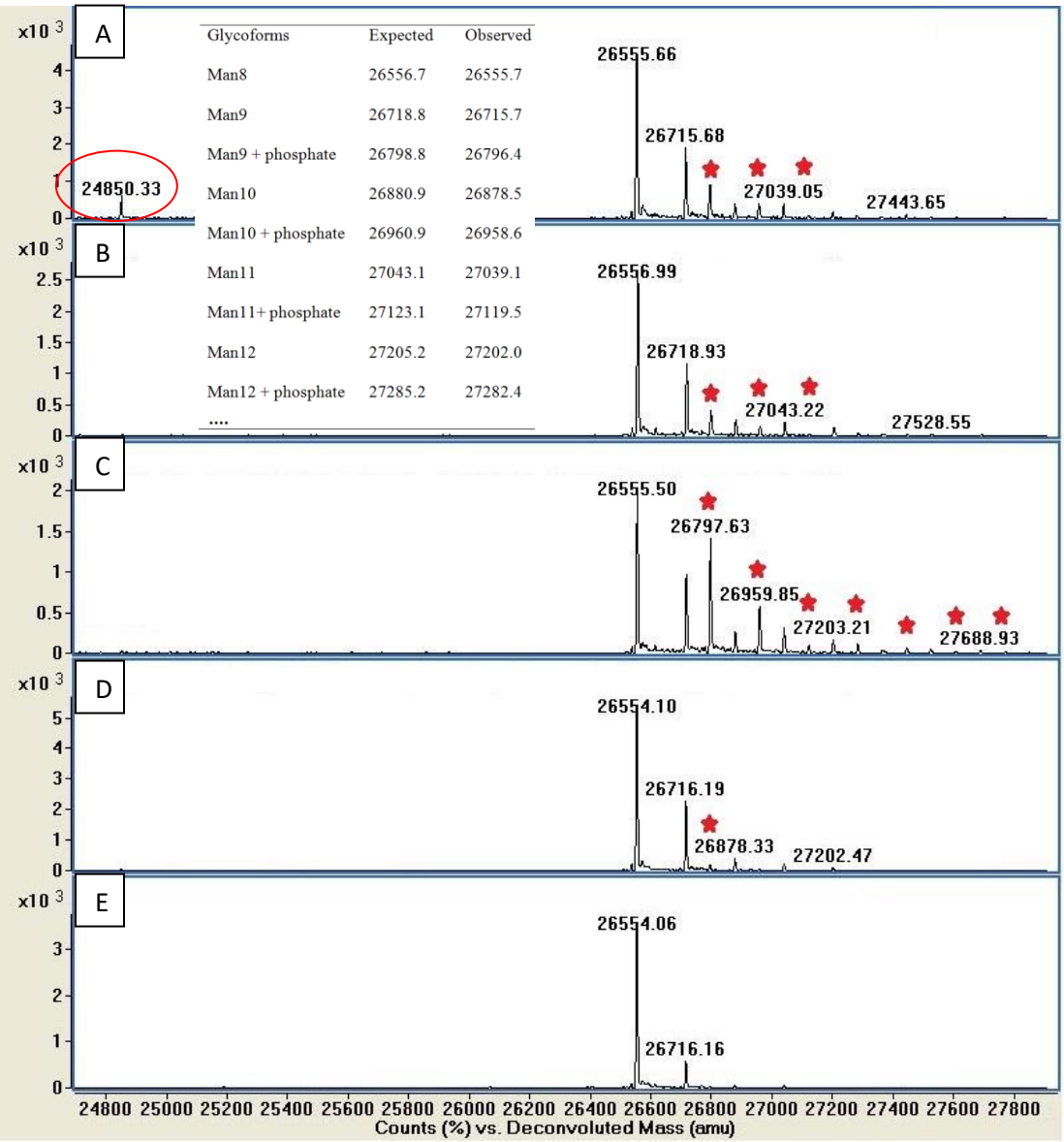

Figure A2. Removal of phosphorylated IgG2 Fc fractions from IgG2 Fc expressed in OCH1 deleted strain of *Pichia pastoris* using weak cation exchange (WCX). Intact protein mass spectra under reducing conditions of: A) IgG2 Fc purified only by protein G chromatography from the expression media. The encircled peak corresponds to the mass of non-glycosylated Fc monomer; B) IgG2 Fc obtained by further purification using HIC (removing hemiglycosylated Fc); C, D, and E) represent earlier, intermediate, and later fractions in the elution of IgG2 Fc from the WCX column. Starred peaks correspond to the IgG2 Fcs containing phosphorylated glycans.

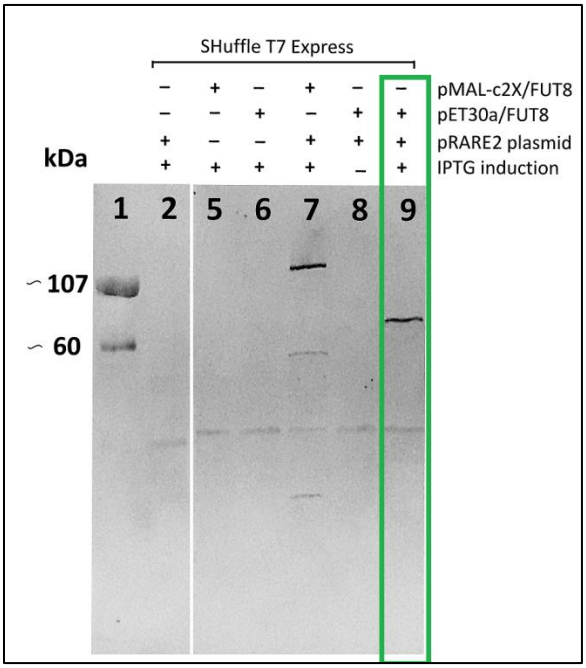

Figure A3. Western blot analysis showing different results of FUT8 expression in SHufflle T7 Express *E. coli* using different plasmid constructs. Mouse anti-histidine$_6$-tag antibody and goat anti-mouse alkaline phosphatase antibody were used as the primary and secondary antibodies, respectively. The histidine tagged proteins were visualized using 1-Step™ NBT/BCIP color development substrate. Lane 1 shows two histidine$_6$-tagged proteins with known molecular weight used as references. The rest of labels are shown above the lanes. The calculated molecular weights of FUT8-H_6 and MBP-FUT8-H_6 are 58 kDa and 100.5 kDa, respectively. Enzyme from lane 9 was used in all subsequent experiments that required FUT8 in this study.

Note: Maltose binding protein (MBP) fusion to FUT8 was tried at the beginning to make FUT8 in the SHuffle T7 Express *E. coli.* However, FUT8 within this fusion protein was inactive.

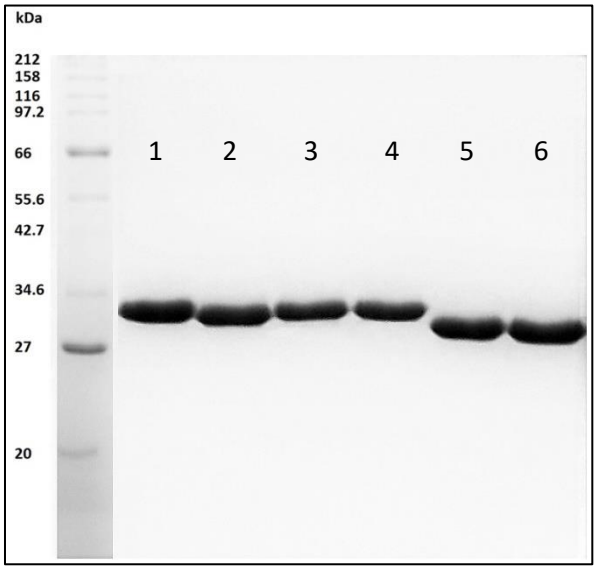

Figure A4. SDS-PAGE analysis under reducing conditions using 12% gels of different IgG2 Fc glycoforms. Lane 1 is high mannose glycoform. Lane 2 is Man5 glycoform. Lane 3 is GlcNAcMan5 (hybrid) glycoform. Lane 4 is GlcNAcMan5F (Fuc(+) hybrid) glycoform. Lane 5 is EndoH-digested glycoform. Lane 6 is PNGase F- digested Fc.

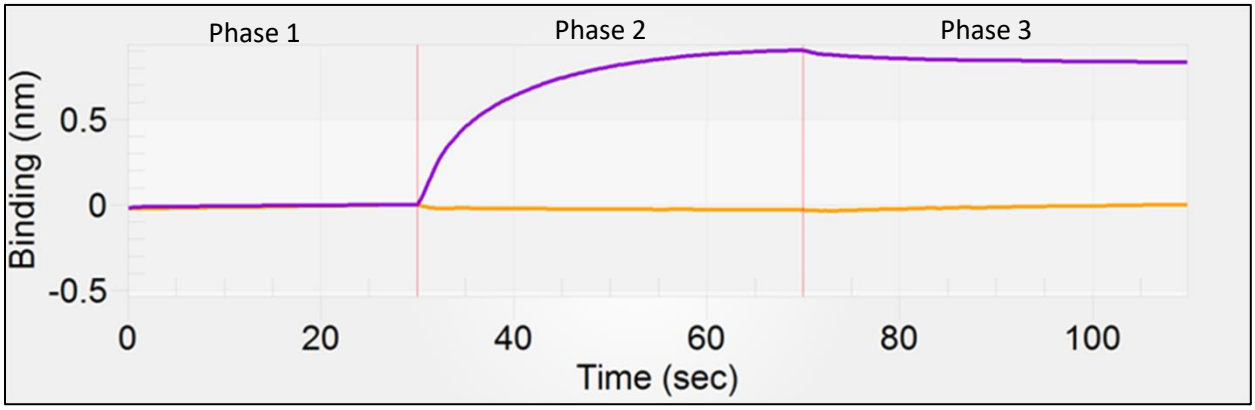

Figure A5. Using biolayer interferometry (BLI) to check for biotinylation of Fcγ receptors through sortase-mediated ligation. During phase 1, PBS checked against a pre-hydrated streptavidin biosensor. During phase 2, either the biotinylated Fcγ receptor (purple sensorgram) or non-biotinylated Fcγ receptor (orange sensorgram) were checked for their association ability to streptavidin biosensors. Phase 3 is switching back to PBS. The experiment indicated that sortase-mediated ligation reaction resulted in biotinylating the receptor for immobilization onto the surface of the biosensor. However, there was no detectable level of immobilization of the non-biotinylated receptor, which was used as s negative control to check for any possible non-specific immobilization.

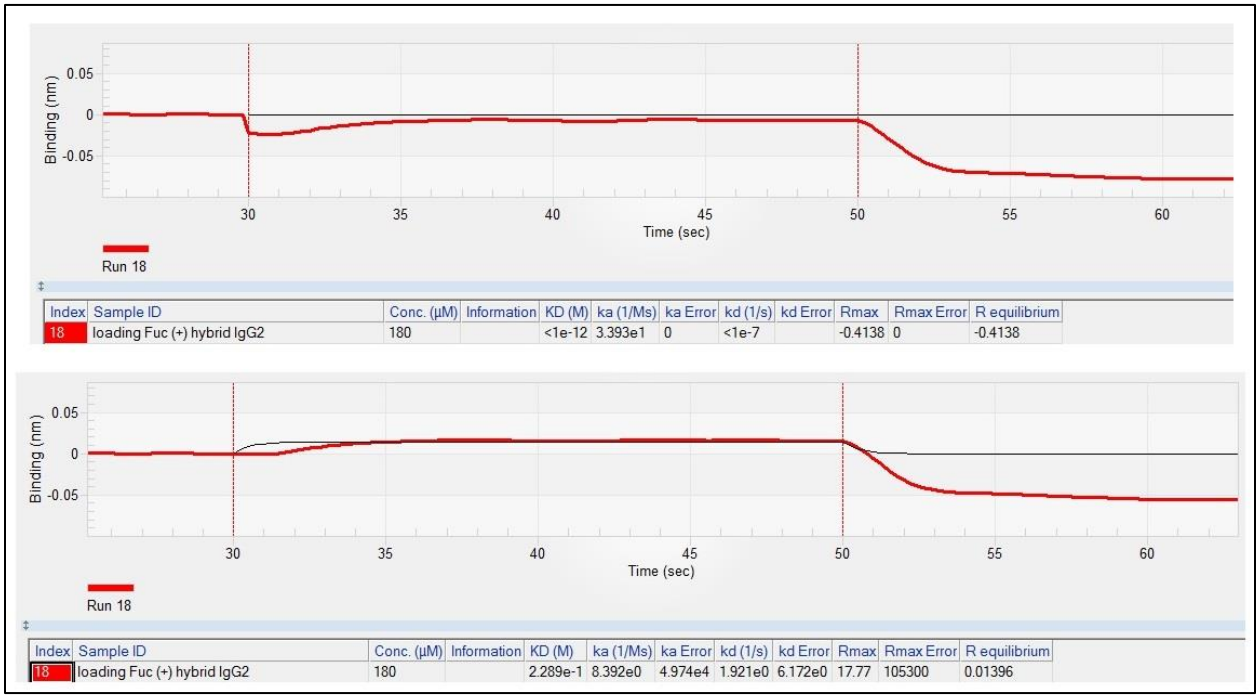

Figure A6. Distorted biolayer interferometry (BLI) binding sensorgram for binding of the concentrated Fuc(+) hybrid IgG2 Fc glycoform (180 µM) to FcγRIIIa-V158. Upper sensorgram is before baseline correction while the lower sensorgram is after based line correction.

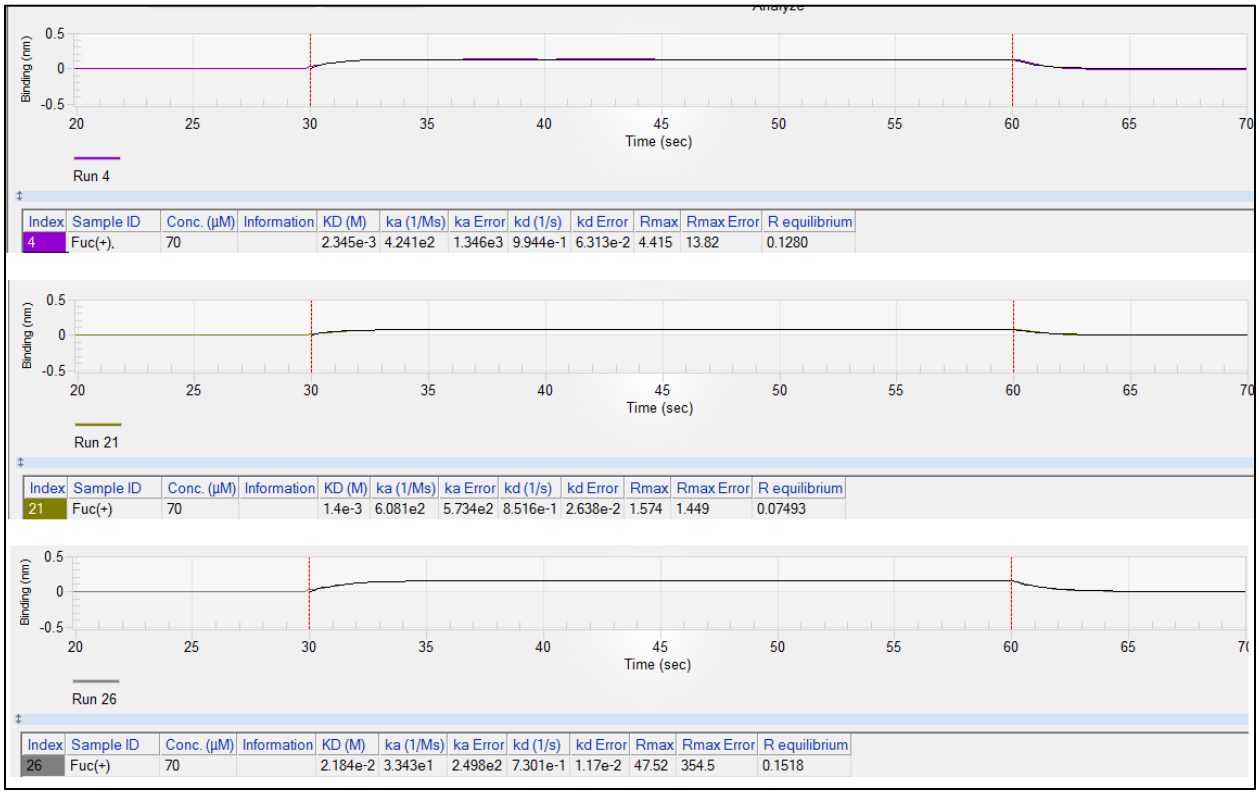

Fuc(+) hybrid/ FcγRIIIa interaction	**$k_a \times 10^2$ (1/Ms)**	**$k_d \times 10^{-1}$ (1/s)**	**K_D (µM), Kinetic[a]**
1st run	4.24	9.94	2.34×10^3
2nd run	6.10	8.52	1.40×10^3
3rd run	0.33	7.30	2.18×10^4
Average	3.55	8.58	**2.42×10^3**
Std. Dev.	2.94	1.32	2.03×10^3

[a]Calculated via error propagation calculator using the kinetic rate constants

Figure A7. BLI sensorgrams for the binding Fuc(+) IgG2 Fc glycoform to FcγRIIIa-V158 using 70 µM Fc concentration and subsequent calculation of the binding constants from this interaction. The binding at 70 µM was repeated three times as shown in the above sensorgrams to calculate the average k_a, k_d, and K_D.

Production of IgG2 Fc with truncated Asn297 glycans for stability (DSC) studies

Other IgG2 Fc glycosylation variants were also produced in this study using *in vitro* enzymatic truncation reactions and these glycoforms are the deglycosylated IgG2 Fc, and an IgG2 Fc that bears only the first GlcNAc in its Asn297 glycosylation site (GlcNAc-IgG2 Fc). The deglycosylated IgG2 Fc was produced by treating high mannose IgG2 Fc with PNGase F followed by protein G affinity purification, while the GlcNAc-IgG2 Fc was produced by treating high mannose IgG2 Fc with Endoglycosydase H followed by protein G affinity purification. A total of about 20 mg of each of these truncated IgG2 Fc glycoforms were produced and their intact masses were checked using Q-TOF LC/MS (Figure AA1, also see Figure A4 lanes 5 and 6).

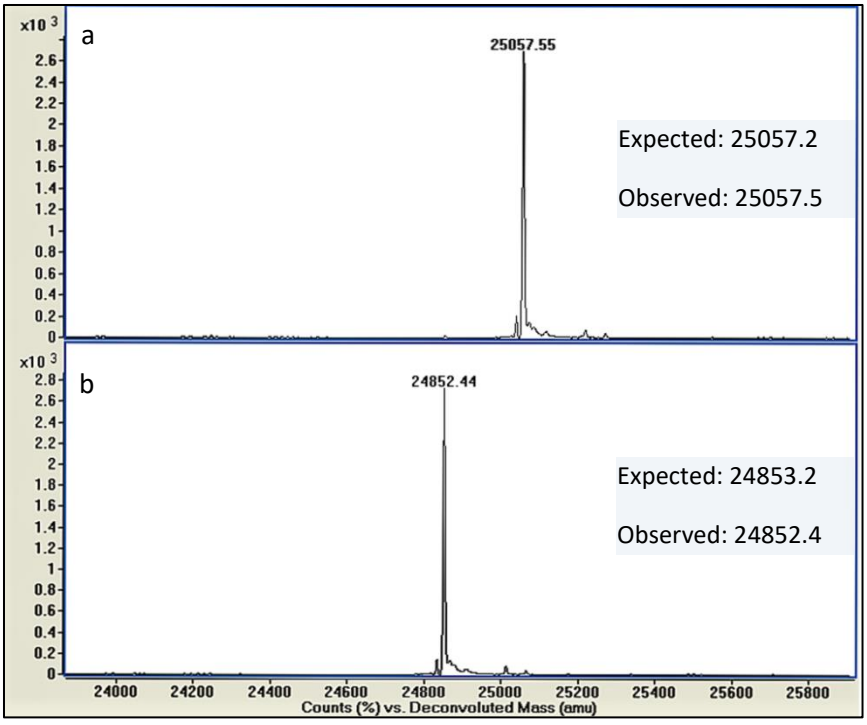

Figure AA1. Intact protein mass spectra under reducing conditions of: a) EndoH-digested IgG2 Fc; b) PNGase F-digested IgG2 Fc. Both of these forms of truncated Fcs were purified from the endoglycosidases by protein G affinity chromatography.

IgG2 Fc expression construct

A cDNA of a human IgG2 heavy chain constant region (plasmid MGC-71314) was obtained from the mammalian gene collection [1] and utilized as a template for PCR amplification of human IgG2 Fc encoding DNA (C226-K447) using 5'-ggcccgctcgagaaaagatgcccaccgtgcccagcacca-3' as a forward primer and 5'-gggcccgcggcggccgc tcatttacccggagacagggagag-3' as a reverse primer.[2–4] The resulting PCR product and the plasmid pPICZα A (EasySelect™ *Pichia* Expression Kit, Invitrogen) were then digested with XhoI and NotI restriction endonucleases. T4 DNA ligase was used to ligate the cut PCR product into the plasmid and the ligation product was transformed into electrocompetent Top10F' *E. coli*. Selection of positive colonies was done using LB plates containing zeocin, and plasmid DNA from positive colonies was submitted for DNA sequencing to confirm correct insertion of IgG2 Fc DNA. The resulting construct, named pIgG2 Fc-(N297, N392), was linearized by SacI endonuclease and transformed into an electrocompetent, OCH1-deleted strain of SMD1168 *Pichia pastoris* produced previously in our laboratory.[5] Positive yeast colonies for recombinant protein production were selected on YPD plates containing zeocin antibiotic.

Site-directed mutagenesis to produce IgG2 Fc glycosylation site variants

Different IgG2 Fc glycosylation site variants (Figure 1, Chapter 2) were produced in this study using the cDNA of human IgG2 heavy chain (plasmid MGC-71314) obtained from the mammalian gene collection.[1] The plasmid MGC-71314 codes for an unusual IgG2 Fc polymorphism, Asn392. This polymorphism results in an additional N-linked glycosylation site in the C_H3 domain of IgG2 Fc in addition to the conserved Asn297 glycosylation site located in the C_H2 domain.[2] This results in an IgG2 Fc with two glycosylation sites, one at Asn297 and the other at Asn392. While this is a naturally occurring polymorphism, it is not the accepted consensus sequence for IgG2 Fc.[2] Therefore, site-directed mutagenesis was conducted with primers 5'-gcagccggagaacaactacaagaccacacctcc-3' and 5'-ggaggtgtggtcttgtagttgttctccggctgc-3' using the pIgG2 Fc-(N297, N392) plasmid as template to convert the asparagine at position 392 to a lysine to match consensus sequence and produce plasmid pIgG2 Fc-(N297, K392), hereby referred to as pIgG2 Fc to reflect it being the consensus sequence. In addition, to study the effect of glycosylation sites on FUT8 enzyme kinetics, an additional glycosylation site variant was produced where the original pIgG2 Fc-(N297, N392) plasmid was mutated using primers 5'-cacacggaacgtgctttggaactgctcctcccg-3' and 5'-cgggaggagcagttccaaagcacgttccgtgtg-3' to produce an IgG2 Fc variant where the asparagine at position 297 has been mutated to a glutamine, resulting in the plasmid pIgG2 Fc-(Q297, N392). Both plasmids pIgG2 Fc and pIgG2 Fc-(Q297, N392) were transformed into the same glycosylation-deficient yeast strain as described above for pIgG2 Fc-(N297, N392).

Expression and purification of IgG2 Fc

IgG2 Fc was expressed in an OCH1 deleted strain of *Pichia pastoris*, using a BioFlo 415 fermenter (Eppendorf) on a 7 liter scale as described previously by Okbazghi et al.[6] During fermentation, glycerol is used first to build up the yeast biomass followed by methanol feeding to induce IgG2 Fc expression from the IgG2 Fc gene cloned downstream to the *AOX1* promoter. The expressed IgG2 Fc, which is secreted into the growth media, was purified by protein G affinity chromatography. In this purification, the media was centrifuged and filtered and then loaded into a protein G column (20-ml bed volume) equilibrated with 10 column volumes (CV) of 20 mM potassium phosphate buffer, pH 6.0. The column was then washed with 5 CV using column washing buffer (20 mM potassium phosphate buffer pH 6.0 containing 500 mM NaCl) and then with 5 CV using the same buffer but without NaCl. The protein was eluted with 100 mM glycine buffer, pH 2.7 and the protein solution was immediately neutralized using 1M Tris HCl buffer, pH 9.0. Using this procedure, about 50 mg of IgG2 Fc is obtained from 1-L fermentation media. Three 7-L fermentations were conducted to produce about 1g of the IgG2 Fc used in these studies. A second purification step using hydrophobic interaction chromatography (HIC) was also carried out to separate hemiglycosylated Fc from the diglycosylated Fc. Briefly, a phenyl sepharose™ high-performance resin (GE Healthcare) column (125 ml, packed in house) was equilibrated with 5 CV of buffer A (20 mM sodium phosphate buffer, pH 7.0 containing 1 M ammonium sulfate) using an ÄKTAmicro chromatographic system (GE Healthcare). Then, 50 mg of the protein G- purified IgG2 Fc pre-dialyzed in buffer A was loaded into the column followed by a 2 CV washing step using buffer A. A segmented gradient elution using buffer B (20 mM sodium phosphate, pH 7.0) was then applied to the column using three gradient segments as following: gradient segment 1 (0%-33% buffer B, 2.5 CV), gradient segment 2

(33%-55% buffer B, 3.5 CV), and gradient segment 3 (55%-100% buffer B, 2.0 CV). The elution fractions containing the diglycosylated IgG2 Fc (as checked by SDS-PAGE and intact protein mass spectrometry) were pooled together and concentrated by an Amicon ultra-15 centrifugal filter unit with a resulting yield of 27 mg diglycosylated Fc. Finally, weak cation exchange chromatography (WCX) was utilized to further purify IgG2 Fc. In this purification, 50 mg of diglycosylated IgG2 Fc was dialyzed in buffer C (20 mM sodium acetate buffer pH 5.8) before loading into a Macro-Prep CM ion exchange support (Bio-Rad laboratories) column (100 ml, packed in house). The column was then washed with 2 CV of buffer C. Then buffer D (20 mM sodium acetate buffer pH 5.8 containing 500 mM NaCl) was used to develop a linear gradient (0%-50% buffer D, 10 CV) for elution of IgG2 Fc. Several fractions were collected across the eluted Fc peak and checked by Q-TOF LC/MS for intact protein mass (Figure A2). Using this WCX, a yield of 26 mg of non-phosphorylated high mannose IgG2 Fc was obtained from the originally loaded 50 mg Fc.

Expression and purification of IgG2 Fc-(Q297, N392)

IgG2 Fc-(Q297, N392) was produced in spinner flasks in a manner similar to that described for IgG2 Fc. The protein expression was started by inoculating 2 ml of YPD media (1% yeast extract, 2% peptone, 5% glucose) containing 100 µg/mL zeocin antibiotic with the transformed yeast. After three days of incubation at 25 °C with shaking, the culture was transferred into 50-ml YPD media and incubation continued for three additional days. The 50-ml culture was then transferred into 1 L of buffered glycerol-complex media (BMGY) containing 0.004% histidine and 0.00004% biotin. The yeast growth was continued in 1-L spinner flasks for two days to build up the yeast biomass and consume the initially supplied glycerol. IgG2 Fc-(Q297, N392) expression was then induced by feeding the yeast with methanol. During the methanol feeding phase, the yeast was supplied with methanol to a final concentration of 0.5% by adding 25 ml of 20% methanol in water solution to each spinner flask every 12 h. Methanol feeding continued for 2.5 days and IgG2 Fc-(Q297, N392) was then harvested following the same procedure described above for harvesting of IgG2 Fc using protein G affinity chromatography. Using this procedure, 140 mg of high mannose IgG2 Fc-(Q297, N392) was obtained from the 7-L fermentation. Hydrophobic interaction chromatography was also used as described above to isolate the diglycosylated Fc from the hemiglycosylated Fc (Figure AA2). The expected masses for the Man8 and Man9 ($Man_8GlcNAc_2$ and $Man_9GlcNAc_2$) glycoforms of high mannose IgG2 Fc-(Q297, N392) are 26556.65 Da and 26718.79 Da, and the observed masses for these glycoforms as shown in Figure AA2 below are 26553.9 Da and 26715.85 Da.

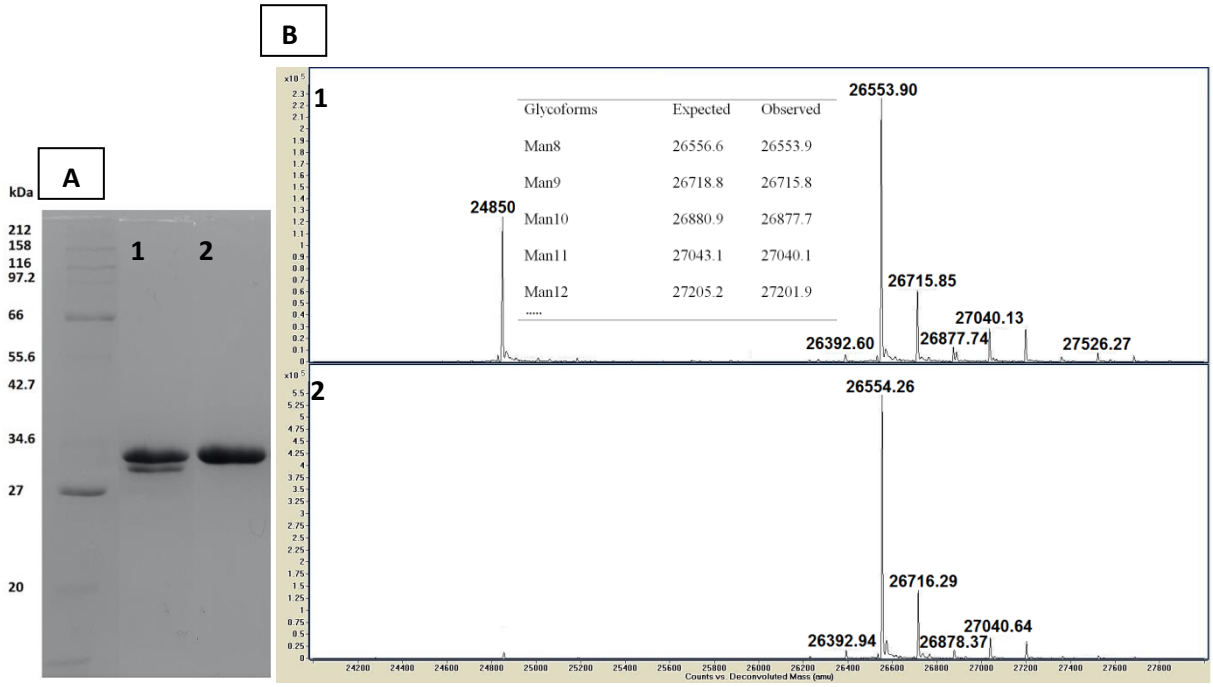

Figure AA2. Characterization of the produced IgG2 Fc-(Q297, N392) variant expressed in glycosylation deficient *Pichia pastoris* A) SDS-PAGE analysis under reducing conditions of IgG2 Fc-(Q297, N392). Lane 1 shows the recombinantly expressed Fc in *Pichia pastoris* after purification by protein G affinity chromatography. The upper band represents the mono-glycosylated Fc chain, while the lower band represents the non-glycosylated Fc chain due to incomplete glycosylation site occupancy usually encountered following the expression of the Fc in *Pichia pastoris*. Lane 2 shows IgG2 Fc-(Q297, N392) after removal of the hemiglycosylated Fc dimer using hydrophobic interaction chromatography (HIC) described in the methods section of the manuscript. The single band in lane 2 represents only the mono-glycosylated Fc chain that comes from reducing the diglycosylated Fc dimer. B) Intact protein mass spectra under reducing conditions (10 mM dithiothreitol) of the expressed Fc in *Pichia pastoris* after purification by only protein G affinity chromatography (spectrum 1) and after HIC purification (spectrum 2)

FUT8 expression construct

A construct was designed to express the soluble catalytic domain of mouse FUT8 (residues 68 to 575) with a C-terminal histidine$_6$-tag in *E. coli*. PCR was used to amplify the FUT8 DNA sequence from cDNA clone MGC-11418 obtained from the mammalian gene collection [1] using 5'-ggcccgcatatgcgaataccagaaggccccattgaccagggg-3' as a forward primer and 5'-ggcccggcggagctcttaatgatgatgatgatgatgtttttcagcttcaggatatgtggg-3' as a reverse primer. The PCR product as well as the pET30a vector (Novagen) were digested with NdeI and SacI restriction endonucleases. T4 DNA ligase was used to ligate the cut PCR product into the cut plasmid and the ligated product was transformed into electrocompetent Top10F' *E. coli* cells. Selection of positive colonies was done using kanamycin on LB plates and the correct FUT8 DNA sequence was confirmed by DNA sequencing.

FUT8 expression and purification

A 6-ml Luria Broth (LB) culture containing (50 μg/mL) kanamycin was inoculated with the pFUT8/pRARE2-SHuffle T7 Express strain and incubated in a shaker incubator at 30 °C for about 12 h. This starting culture was then transferred into 1-L of LB medium and incubated at 37 °C for few hours with shaking until the O.D. at 600 nm was 1.2. Then FUT8 expression was induced with IPTG (0.2 mM) and the culture was incubated with shaking for 16 hours at 16 °C. The culture was then centrifuged and the cell pellet was re-suspended in 30 ml of resuspension buffer (20 mM Tris pH = 7.8, 300 mM NaCl, 5% glycerol). The cells were disrupted with sonication followed by centrifugation at 23700 g for 30 min. The supernatant was then loaded into a 5 ml Ni-NTA agarose resin (QIAGEN) column pre-equilibrated with the resuspension buffer. The column was washed with 500 mL of washing buffer (20 mM Tris pH 7.8, 300 mM

NaCl, 5% glycerol, 20 mM imidazole) and the enzyme was eluted with 250 mM imidazole. The enzyme solution was then dialyzed against 50 mM Tris HCl, pH 7.5 buffer and concentrated by Amicon ultra-15 centrifugal filter unit.

General procedure utilizing protein G affinity chromatography for the purification of IgG2 Fc glycoforms

At the end of the chemoenzymatic conversion of IgG2 Fc into the desired IgG2 Fc glycoform, the reaction mixture is diluted with 20 mM MES buffer pH 6.2 (equilibration buffer) to a final IgG2 Fc concentration of 0.1 mg/ml. Then, the diluted Fc solution is loaded into a protein G column (about 20 mg total Fc is loaded into a 10-ml bed volume protein G column), pre-equilibrated with equilibration buffer, using a loading flow rate of 6 ml/min. The flow-through is also loaded into the column to ensure full recovery of the Fc from the reaction mixture. The column is then washed with 5 CV of the equilibration buffer followed by 5 CV of the equilibration buffer containing 500 mM NaCl. A final wash step using 5 CV of the equilibration buffer is also conducted to remove the high concentration of salt. Elution of IgG2 Fc is accomplished by using 100 mM glycine buffer, pH 2.7 and the protein solution is immediately neutralized using 1M Tris HCl buffer, pH 9.0.

Expression and purification of FKP

A 6-ml Luria Broth medium (LB) containing kanamycin (50 μg/mL) were inoculated with the FKP expressing Rosetta 2 frozen stock and incubated in a shaker incubator at 37˚C for about 12 h. These three starting cultures were then transferred into 2.8 L culture flask containing 1 liter of LB having 50 μg/ml kanamycin and incubated at 37 °C with shaking until $O.D._{600nm}$ reached about 1.5 (usually about 4-6 h).Protein expression was induced with 0.2 mM IPTG at room temperature for about 8 h. The culture was then centrifuged and the cell pellets were re-suspended in 30 ml of resuspension buffer (20 mM Tris pH=7.8, 300 mM NaCl, 5% glycerol) after discarding the supernatant. Then, the cells were subjected to a 5 min sonication time at 60% amplitude and spun down at 14,000 rpm. The supernatant was then loaded onto a 5 ml Ni-NTA agarose resin column pre-equilibrated with the resuspension buffer. The column was washed with 200 mL of resuspension buffer plus 10 mM imidazole. The H_6-tagged protein was eluted with the suspension buffer containing 250 mM imidazole. Eluted protein was then dialyzed against 25 mM HEPES (pH 7.5) buffer. The protein was checked with SDS-PAGE, its concentration was measured by UV absorbance at 280 nm using 150690 M^{-1} cm^{-1} extinction coefficient, and finally stored in 50% glycerol at -20 °C.

Production of FcγRIIa receptor variants

Expression plasmids for producing soluble human FcγRIIa with a C-terminal sortase/histidine$_6$-tag, were constructed by amplifying the cDNA encoding the receptor extracellular domain (residues 36 to 214) by PCR using plasmid MGC:23887 (FcγRIIa-H131) and MGC:30032 (FcγRIIa-R131) from the mammalian gene collection [1] as templates and 5'-ggcccgctcgagaaaagagctgctcccccaaaggctgtgctg-3' and 5'-ggcccggcgcgcggccgcttaatgatgatgatgatgtccacctccagtttctggcaatgaagagctgcccatgctgggcac-3' as PCR primers. Then the PCR products and pPICZα A plasmid were digested with XhoI and NotI restriction endonucleases. T4 DNA ligase was used to ligate the cut PCR product into the plasmid then the ligation products were transformed into electrocompetent Top10F' E. coli. Selection of positive colonies was done using LB plates containing 25 µg/ml zeocin. The correct DNA sequence for a positive colony was confirmed by DNA sequencing, and each construct was then linearized by SacI endonuclease and transformed into an electrocompetent, OCH1-deleted strain of SMD1168 *Pichia pastoris* produced previously in our laboratory.[5] Positive yeast colonies for recombinant protein production were selected on YPD plates containing 100 µg/ml zeocin. Expression of FcγRIIa-H131 or FcγRIIa-R131 was then carried out in a 1-L spinner flask following the procedure described above for the expression of IgG2 Fc-(Q297, N392). During this expression, glycerol was used to build up the yeast biomass while methanol feeding was used to induce protein expression. Then, the secreted protein, FcγRIIa-H131, was purified from the expression media using Ni-NTA affinity chromatography followed by HIC for further purification.[6] The receptor purity was checked using SDS-PAGE (Figure AA3 below). The purified receptors were then subjected to site-specific biotinylation using a sortase-mediated ligation reaction described previously for the biotinylation of FcγRIIIa-V158.[6] Briefly, the purified FcγRIIa, which carries a sortase tag at its C-terminus, was dialyzed in 50 mM Tris HCl

buffer, pH 7.5. The reaction mixture containing 18 μM FcγRIIa-H131, 1 mM GGG-linker-Biotin, 3 mM $CaCl_2$, and 5 mM sortase was incubated at room temperature. After 24 hours, the reaction was quenched by adding ethylenediaminetetraacetic acid (EDTA) to 15 mM final concentration followed by extensive dialysis in PBS buffer to remove the unreacted GGG-linker-Biotin.

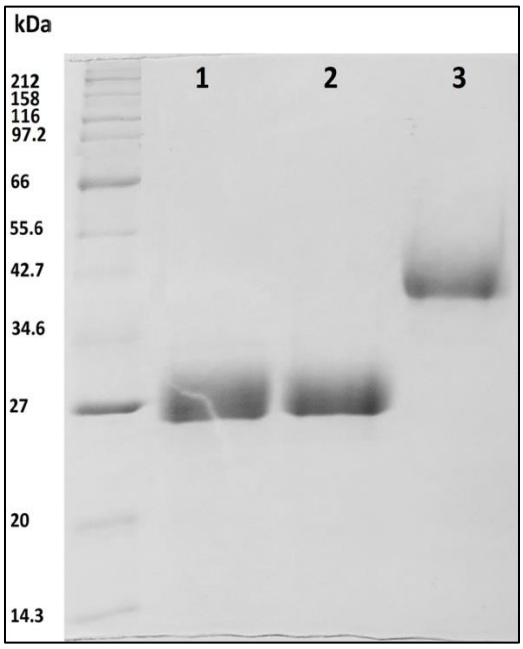

Figure AA3. SDS-PAGE analysis under reducing conditions using 12% gels of Fc gamma receptors (FcγRs) expressed in *Pichia pastoris* and purified by Ni-NTA affinity chromatography and hydrophobic interaction chromatography. Lanes 1 represents FcγRIIa-R131 (contains only two N-glycosylation sites), lanes 2 represents FcγRIIa-H131 (contains only two N-glycosylation sites), and lane 3 represents FcγRIIIa-V158 (contains five N-glycosylation sites)

Biolayer interferometry (BLI) binding experiment

Before starting the binding experiments, the receptors (FcγRIIa-H131, FcγRIIa-R131, or FcγRIIIa-V158) and the analytes (different IgG2 Fc glycoforms) were dialyzed in PBS (50 mM sodium phosphate, 150 mM NaCl, pH 7.4). In these binding experiments, streptavidin biosensors (Pall ForteBio LLC) were chosen for the immobilization of the receptors while the studied IgG2 Fc glycoform was kept in solution. First, the biosensor is hydrated in PBS buffer for 10 min and then followed by incubation in PBS buffer containing 1 mg/ml casein to block any non-specific interaction on the surface of the biosensor. The biotinylated receptor is then immobilized on the biosensor to 1 nm response level above the baseline using 0.2 μM receptor solution. A new baseline was established by placing PBS buffer containing 1 mg/ml casein in the sample holder and incubation for 30 s. The analyte (IgG2 Fc) is then placed in the sample holder to initiate the association phase (30 s). At the end of this association phase the analyte tube is replaced by a tube containing PBS to obtain the dissociation phase (30 s) as shown in Figure AA4 below. Four different concentrations of each IgG2 Fc glycoform were used in each binding experiment and each binding experiment was repeated three times. The association rate constant and the dissociation rate constant (k_a and k_d, respectively) as well as the equilibrium dissociation constant (K_D) at 25°C were then calculated by fitting the binding sensorgrams from these different concentrations using the global fit function of BLItz Pro software. In case of binding of the hybrid and the Fuc(+) hybrid IgG2 Fc glycoforms to FcγRIIIa-V158, the following Fc concentrations of each glycoform were used: 17.5, 35, 52.5, and 70 μM. In the case of binding of these different glycoforms to FcγRIIa-H131 the following Fc concentrations were used: 0.9, 1.9, 3.8, and 7.6 μM. In the case of binding of these different glycoforms to FcγRIIa-R131 the following Fc concentrations were used: 1.1, 2.2, 4.5, and 9 μM.

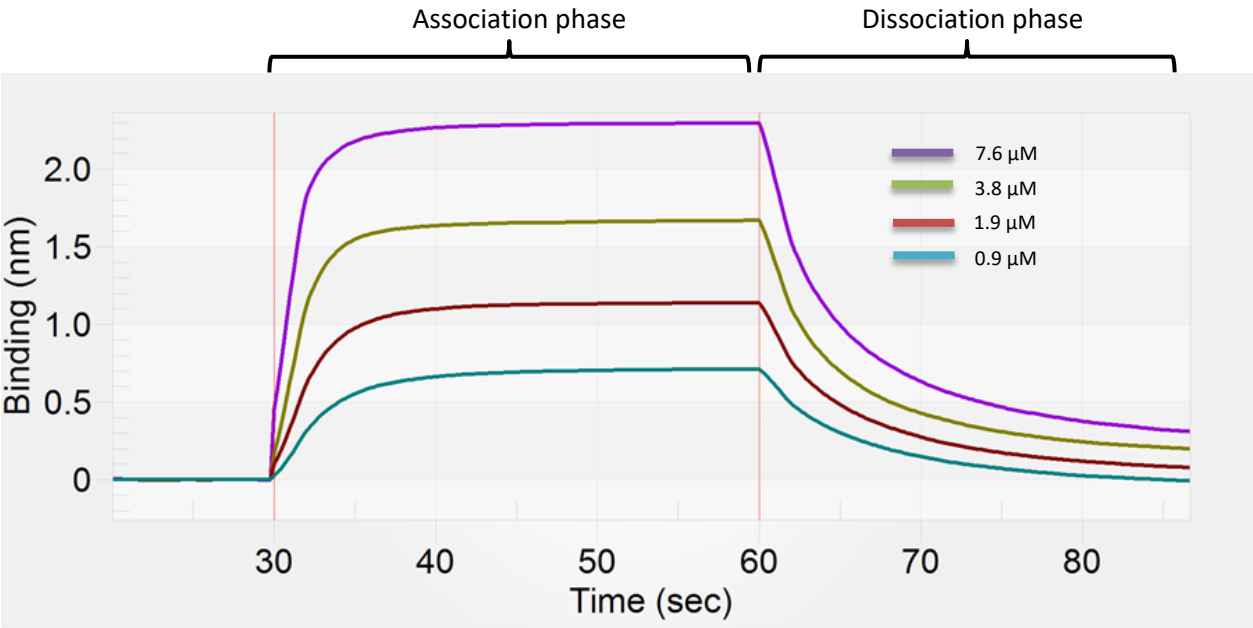

Figure AA4. Representative sensorgrams for the binding experiments of IgG2 Fc glycoforms interacting with Fc gamma receptors (FcγRs) using biolayer interferometry (BLI). In this particular binding experiment, hybrid IgG2 Fc glycoform, at four different concentrations, was allowed to bind to FcγRIIa-H131 immobilized on a streptavidin biosensor for the determination of kinetic rate constants (k_a and k_d) and the equilibrium dissociation constant (K_D) of the FcγRIIa/IgG2 Fc interaction.

Chemoenzymatic synthesis and purification of GDP-fucose for α1,6-fucosyltransferase (FUT8) activity assay and kinetic measurements

Pure GDP-fucose was prepared based on a protocol described in the literature [7] with some modifications and the synthesis was followed up using a previously described method of ion-pair reversed-phase HPLC.[8] 400 µl of FKP (about 1.5 mg) was added into 4-ml solution containing 100 mM HEPES buffer pH 7.5, 5 mM ATP, 2.5 mM GTP, 10 mM L-fucose, and 10 mM MgCl2. The reaction was incubated at 28 °C for about 3 hours, and then 15 µl (3 units) of yeast inorganic pyrophosphatase (Sigma-Aldrich) was added to the reaction mixture and incubated for 9 additional hours. The addition of yeast inorganic pyrophosphatase resulted in converting all of GTP into GDP-fucose (Figure AA5). Then 10 units of alkaline Phosphatase (CIP, from New England BioLabs) were added to simplify subsequent GDP-fucose purification and the reaction was incubated for 4 additional hours. The reaction was then boiled for 5 minutes and chilled immediately on ice followed by centrifugation. The supernatant was then concentrated in to 1-ml volume by the mean of rotary evaporator and loaded on a Bio-Gel P-2 (Bio-Rad) column using deionized water as a mobile phase. Several fractions were collected and tested for pure GDP-fucose content. The fractions containing pure GDP-fucose were pooled together and concentrated by the rotary evaporator. The purified GDP-fucose (Figure AA5) was aliquoted and stored at – 80 °C.

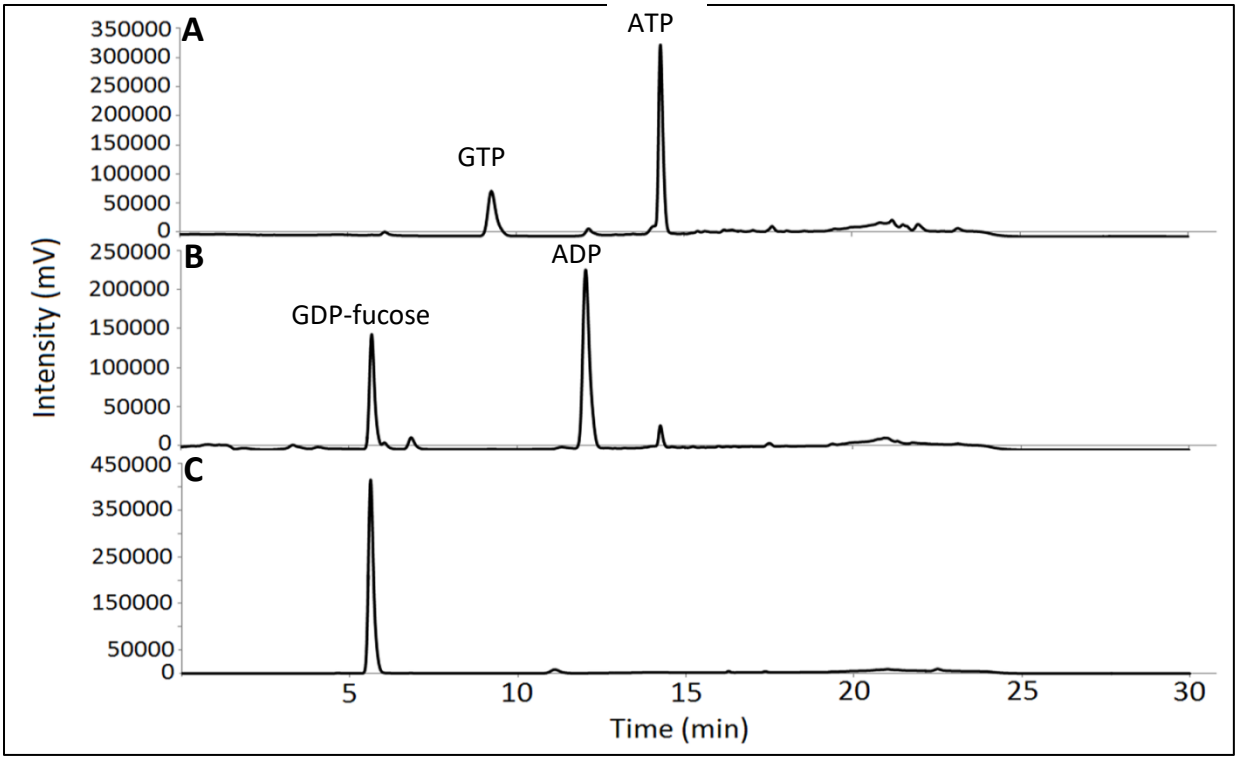

Figure AA5. Ion-pair reversed-phase HPLC for monitoring of the synthesis and purification of GDP-fucose through FKP mediated chemoenzymatic synthesis (Zhao et al. 2010). Hypersil™ ODS C18 column (120 A°, 5 µm, 4.6 mm X 250 mm, ThermoScientific) was used in this analysis. Buffer A was 100 mM potassium phosphate buffer at pH 6.4 containing 8 mM tetrabutylammonium hydrogen sulfate (Sigma-Aldrich). Buffer B was composed of 70% buffer A plus 30% acetonitrile. The elution gradient was as following: 100% buffer A for 8 min, 0-77% buffer B for 8 min, 77-100% buffer B for 1 min, 100% buffer B for 4 min, 100%-0% buffer B for 1 min, and finally 100% buffer A for 8 min to re-equilibrate the column. The flow rate was 1.3 ml/min, the UV detector was set at 254 nm, and the column temperature was 40 °C. The above chromatograms are: **A**) FKP reaction mixture at the beginning of the reaction **B**) Same reaction mixture by the end of the reaction at which all GTP is converted into GDP-fucose **C**) GDP-fucose after Bio-Gel P-2 purification and concentration.

Production of free $GlcNAcMan_5GlcNAc_2$ (hybrid) glycan for FUT8 assays

The $GlcNAcMan_5GlcNAc_2$ hybrid N-glycan was produced from the $GlcNAcMan_5GlcNAc_2$ (hybrid) IgG2 Fc glycoform prepared as described elsewhere in this manuscript. The hybrid N-glycan was released from the Fc using PNGase F. Since, the Fc dimer has two N-glycans conjugated to it, the resulting concentration of the free glycan is twice the starting concentration of the Fc. The complete release of the glycan from the Fc was confirmed by mass spectrometry and SDS-PAGE gel (Figure AA6 below)

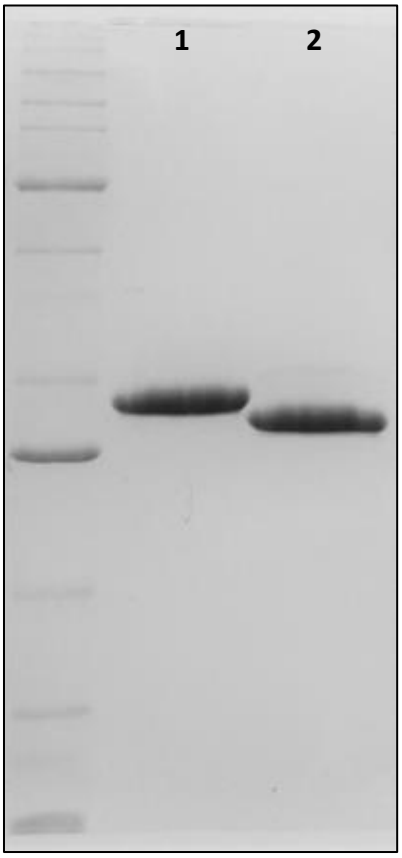

Figure AA6. SDS-PAGE analysis using 12% gel showing the complete conversion of glycosylated IgG2 Fc (lane 1) into deglycosylated IgG2 Fc (lane 2) and release of Asn297 N-glycan after digestion with PNGase F enzyme.

SDS-PAGE and western blotting

SDS-PAGE was performed as previously described [9] using 12% gels and a 3X reducing sample loading buffer (240 mM Tris HCl pH 6.8, 6% SDS, 30% glycerol, 2.3 M 2-Mercaptoethanol, and 0.04% bromophenol blue). For western blotting, the samples were also run on 12% SDS-PAGE then the resolved proteins on the gel were transferred into a PVDF membrane (BioRad Immun-Blot membrane for protein blotting) using BIO-RAD Trans-Blot Turbo Transfer System. The membrane was then blocked with 5% fat free milk in TTSB (20 mM Tris HCl, 500 mM NaCl, 0.05% Tween 20, pH 7.5 buffer). After washing with TTSB, the membrane was incubated with mouse anti-histidine$_6$-tag antibody as the primary antibody then with goat anti-mouse alkaline phosphatase secondary antibody. The histidine tagged proteins were then visualized on the membrane using 1-Step™ NBT/BCIP color development substrate from ThemoFisher Scientific.

Intact protein mass spectrometry

Intact protein mass was determined by injecting 15 µl of protein samples at concentrations of approximately 0.3 mg/ml under reducing conditions (10 mM dithiothreitol) into a reverse phase C4 column, 50 mm, 4.6 mm I.D. (Vydac 214 MS, 300 A pore size, 5µm particle size) using an Agilent 6520 Accurate-Mass Q-TOF LC/MS equipped with an ESI source. Solvent A was composed of 99.9% water, 0.08% formic acid, and 0.02% trifluoroacetic acid, while solvent B was composed of 99.9% acetonitrile, 0.08% formic acid, and 0.02% trifluoroacetic acid. A gradient elution was developed ranging from 5% B to 90% B within 7 min using a flow rate of 0.5 mL/min. Data acquisition was performed using Agilent Mass Hunter Acquisition software (Version B.02.00) while data analysis was performed using Agilent Mass Hunter Qualitative Analysis software (Version B.03.01).

References

(1) Temple, G. F. (2009) The completion of the Mammalian Gene Collection (MGC). *Genome Res. 19*, 2324–2333.

(2) Vidarsson, G., Dekkers, G., and Rispens, T. (2014) IgG subclasses and allotypes: From structure to effector functions. *Front. Immunol. 5*, 1–17.

(3) Edelman, G. M., Cunningham, B. A., Gall, W. E., Gottlieb, P. D., Rutishauser, U., and Waxdal, M. J. (1969) The covalent structure of an entire gammaG immunoglobulin molecule. *Proc. Natl. Acad. Sci. U. S. A. 63*, 78–85.

(4) Abhinandan, K. R., and Martin, A. C. R. (2008) Analysis and improvements to Kabat and structurally correct numbering of antibody variable domains. *Mol. Immunol. 45*, 3832–3839.

(5) Xiao, J., Chen, R., Pawlicki, M. A., and Tolbert, T. J. (2009) Targeting a homogeneously glycosylated antibody Fc to bind cancer cells using a synthetic receptor ligand. *J. Am. Chem. Soc. 131*, 13616–13618.

(6) Okbazghi, S. Z., More, A. S., White, D. R., Duan, S., Shah, I. S., Joshi, S. B., Middaugh, C. R., Volkin, D. B., and Tolbert, T. J. (2016) Production, Characterization, and Biological Evaluation of Well-Defined IgG1 Fc Glycoforms as a Model System for Biosimilarity Analysis. *J. Pharm. Sci. 105*, 559–574.

(7) Zhao, G., Guan, W., Cai, L., and Wang, P. G. (2010) Enzymatic route to preparative-scale synthesis of UDP-GlcNAc/GalNAc, their analogues and GDP-fucose. *Nat. Protoc. 5*, 636–46.

(8) Nakajima, K., Kitazume, S., Angata, T., Fujinawa, R., Ohtsubo, K., Miyoshi, E., and Taniguchi, N. (2010) Simultaneous determination of nucleotide sugars with ion-pair reversed-phase HPLC. *Glycobiology 20*, 865–871.

(9) Laemmli, U. K. (1970) Cleavage of structural proteins during the assembly of the head of bacteriophage T4. *Nature 227*, 680–685.

Appendix B

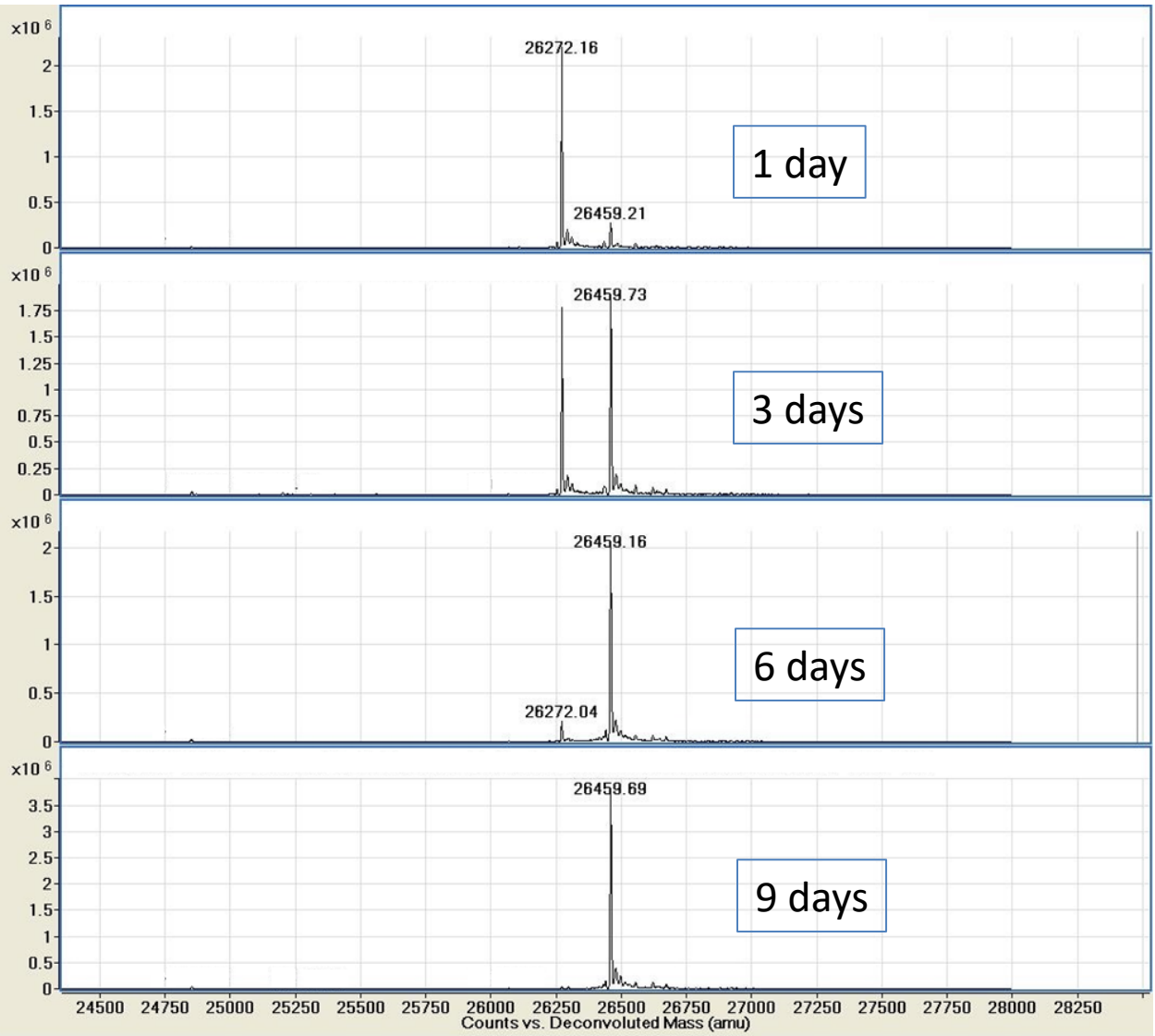

Figure B1. Representative time points of the one-pot (three steps) functionalization reaction of IgG2 Fc using FKP and FUT8.

Measuring the kinase activity of FKP

A continuous coupled spectrophotometric assay similar to one described previously (Gosselin et al. 1994)[1] was used to compare FKP kinase reaction rate for L-fucose or 6-azido-L-fucose. In this assay, the FKP reaction progress was followed by measuring ADP production with a pyruvate kinase/ lactate dehydrogenase (PK/LDH) coupled system to monitor NADH disappearance at 340 nm. This assay was performed in 50 mM HEPES buffer pH 7.5 containing ATP (1 mM), L-Fucose or 6-azido-L-fucose (1 mM), magnesium chloride (10 mM), potassium chloride (50 mM), phosphoenolpyruvate (0.75 mM), NADH (0.15 mM), 3 U pyruvate kinase (PK), and 4.2 U lactate dehydrogenase (LDH). The final volume was 150 µl and the reaction was started by the addition of FKP (9 µg) after letting the other components equilibrate for 5 min inside the cuvette at 37 °C. The decrease in NADH absorbance at 340 nm with time was followed using Evolution 260 Bio UV-visible spectrophotometer (ThermoScientific). The linear part of this decrease in NADH absorbance with time (slope) was used to compare FKP reaction initial velocity of the natural sugar (L-Fucose) with the analogue (6-azido-L-fucose) as shown in Figure B2.

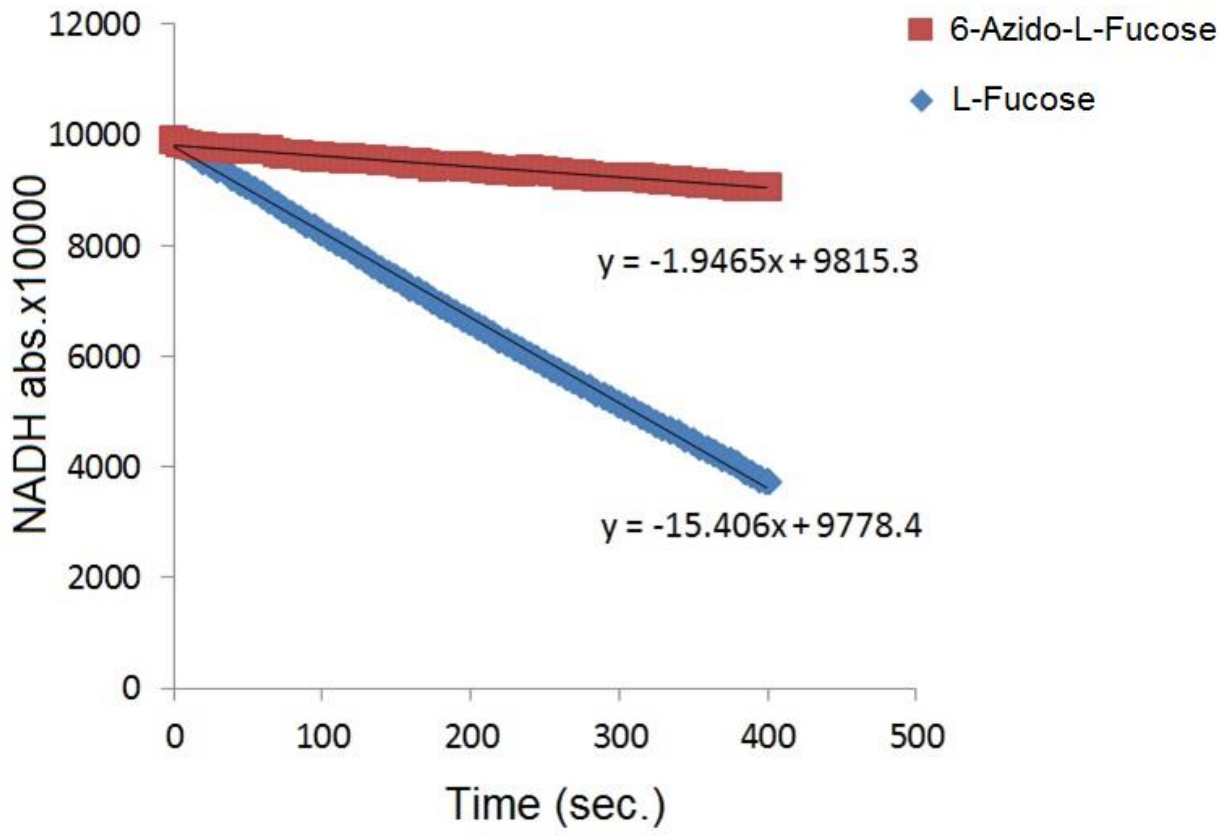

Figure B2. FKP kinase activity rate measurement using L-Fucose in comparison to using 6-azido-L-fucose.

General procedure for chemoenzymatic synthesis and purification of GDP-azidofucose

GDP-azidofucose was synthetized chemoenzymatically from 6-azido-L-fucose using the bifunctional enzyme L-fucokinase/guanosine 5'-diphosphate-L-fucose pyrophosphorylase (FKP). The synthesis and purification was followed up using ion pair chromatography method described in the next section (See also Figures BB1, BB2, and BB3). A 4-ml volume reaction was carried out in 100 mM HEPES buffer at pH 7.5. The reaction mixture contained 13 mg (5.9 mM) ATP, 11 mg (5.2 mM) GTP, 5.2 mg (6.3 mM) 6-azido-L-fucose, and 10 mM $MgCl_2$. The reaction was started by adding 1.5 mg FKP and incubated at 28 °C. After six hours, 3 units (15 µl) of yeast inorganic pyrophosphatase (Sigma-Aldrich) were added to the reaction mixture and the mixture was incubated at the same temperature for three days. Finally, 10 units of alkaline phosphatase (CIP, New England BioLabs) were added to the reaction mixture to dephosphorylate any free nucleotides and simplify subsequent size exclusion chromatography-based purification. After 16 hours of adding CIP, the reaction mixture was boiled for 5 minutes and chilled immediately on ice for 15 minutes to precipitate the enzymes used in this reaction and simplify subsequent purification. After chilling on ice, the reaction mixture was centrifuged at full speed for 15 minutes to get rid of the precipitated enzymes. The supernatant was then collected and concentrated to 1 ml by the mean of rotary evaporator. To separate the product (GDP-azidofucose) from the reaction mixture, the supernatant was loaded on a 2.5 cm diameter column containing 120 ml Bio-Gel P-2 resin (BioRad) pre-equilibrated with deionized water. The elution was carried out at a flow rate of 0.7 ml/min using deionized water as a mobile phase. The UV detector was set at 254 nm and several fractions were collected across the eluted peaks and checked for content using ion pair chromatography. The fractions containing pure GDP-

azidofucose were pooled together and concentrated by rotary evaporator and finally stored at -80 °C.

Ion-pair reversed-phase HPLC

An ion-pair reversed-phase HPLC method was developed based on a previous method reported by Nakajima et al. (2010)[2] to control the synthesis and purification of GDP-azidofucose. Hypersil™ ODS C18 column (120 A°, 5 μm, 4.6 mm X 250 mm, ThermoScientific) was used in this analysis. Buffer A was 100 mM potassium phosphate buffer at pH 6.4 containing 8 mM tetrabutylammonium hydrogen sulfate (Sigma-Aldrich). Buffer B was composed of 70% buffer A plus 30% acetonitrile. A 30 minutes elution gradient was developed as following: 100% buffer A for 8 min, 0-77% buffer B for 8 min, 77-100% buffer B for 1 min, 100% buffer B for 4 min, 100%-0% buffer B for 1 min, and finally 100% buffer A for 8 min to re-equilibrate the column for subsequent sample injection. The flow rate was 1.3 ml/min, the UV detector was set at 254 nm, and the column temperature was 40 °C.

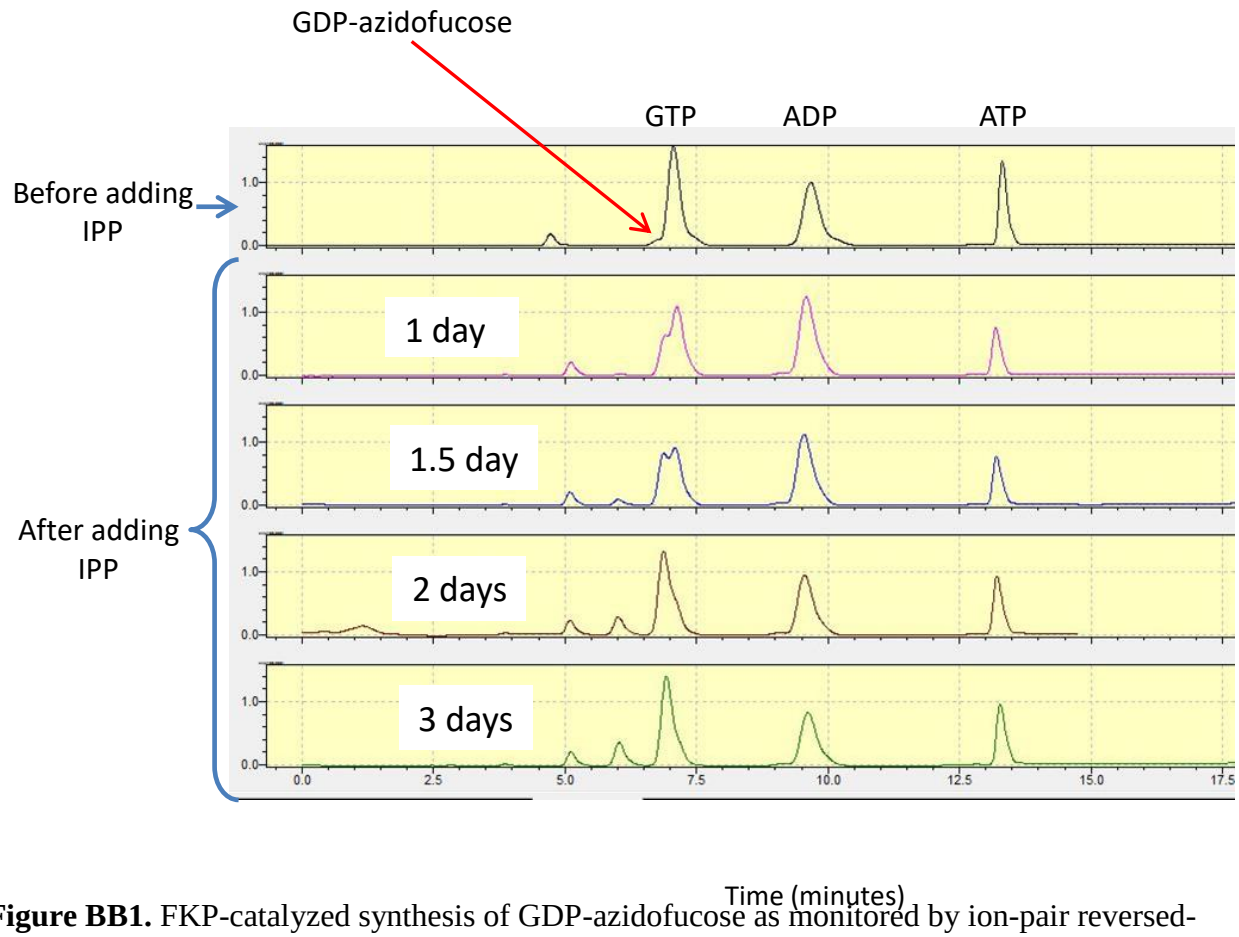

Figure BB1. FKP-catalyzed synthesis of GDP-azidofucose as monitored by ion-pair reversed-phase HPLC before and after adding inorganic pyrophosphatase (IPP).

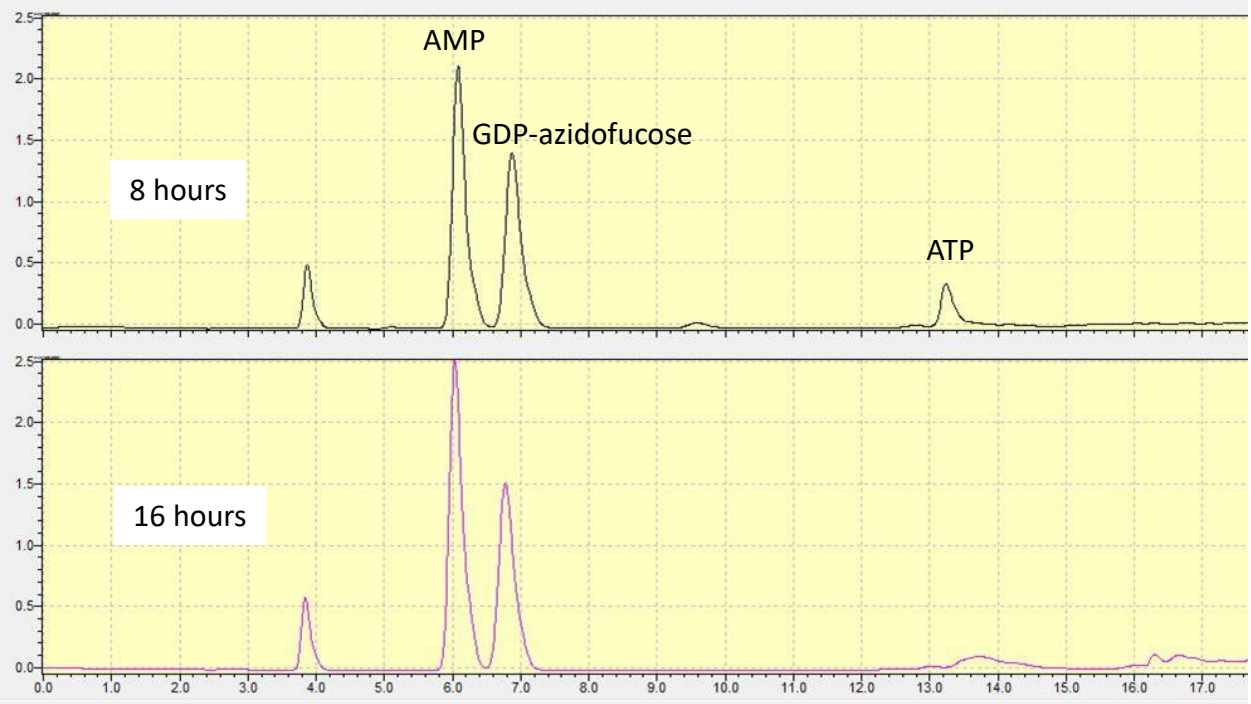

Figure BB2. Ion-pair reversed-phase HPLC monitoring of FKP-catalyzed chemoenzymatic synhesis of GDP-azidofucose after 8 and 16 hours of adding calf intestional phosphatass (CIP) to simplify subsequent (Bio-Gel P-2)-based purification of GDP-azidofucose.

Figure BB3. Eluted Bio-Gel P-2 fractions containg GDP-azidofucose checked by ion-pair reversed-phase HPLC.

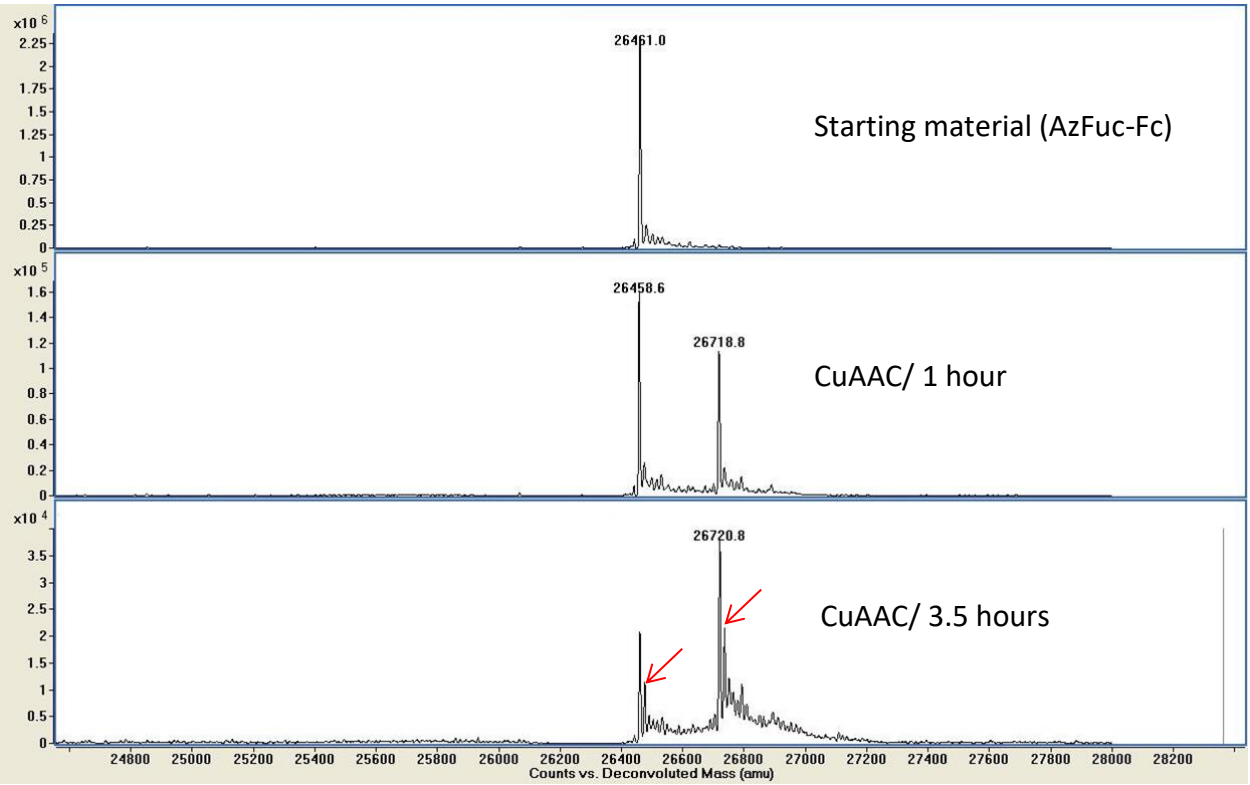

Figure B3. Reaction progress of Propargyl-Fc formation via CuAAC followed up by intact protein mass spectra showing a clear protein oxidation with time.

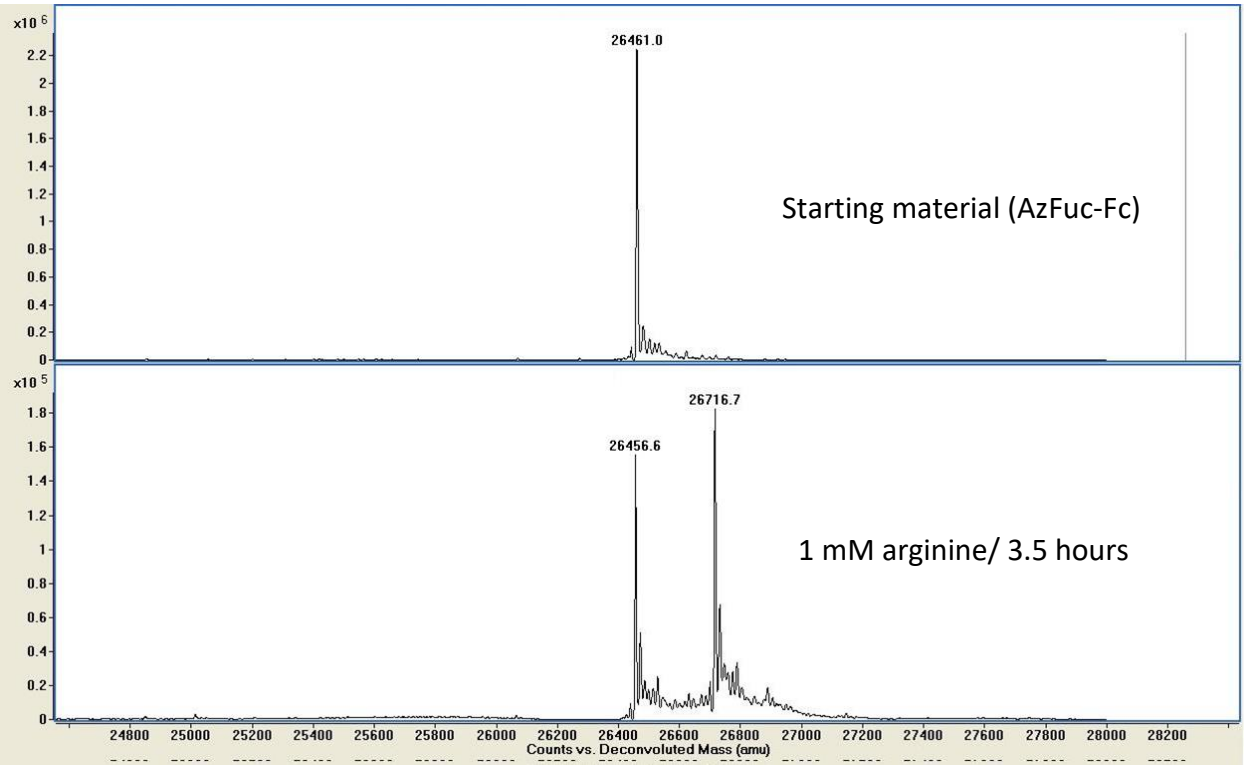

Figure B4. Effect of adding1 mM arginine on the CuAAC reaction.

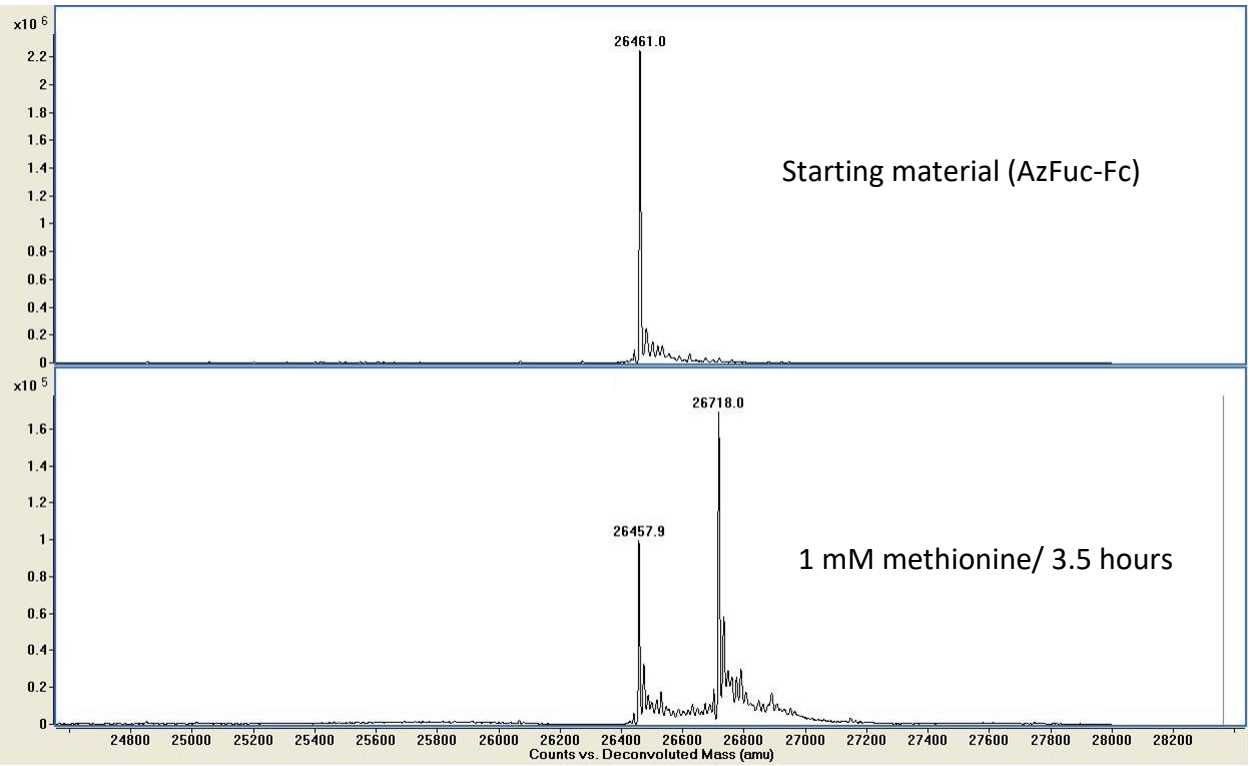

Figure B5. Effect of adding1 mM methionine on the CuAAC reaction.

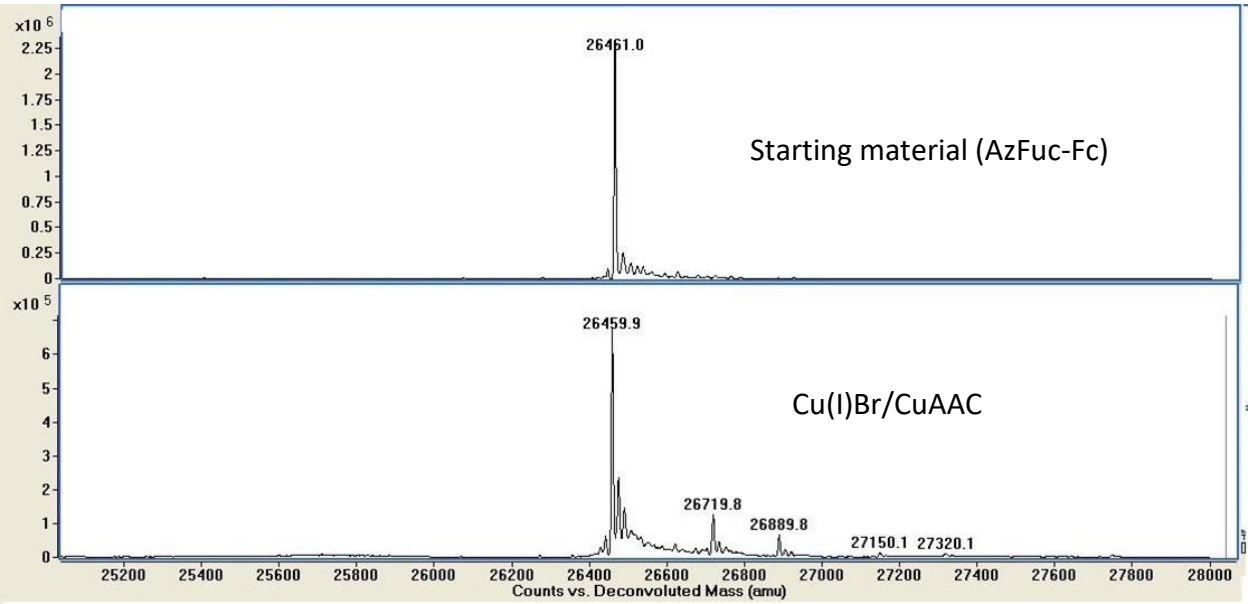

Figure B6. Using Cu(I)Br instead of $CuSO_4$/Sodium ascorbate in CuAAC reaction.

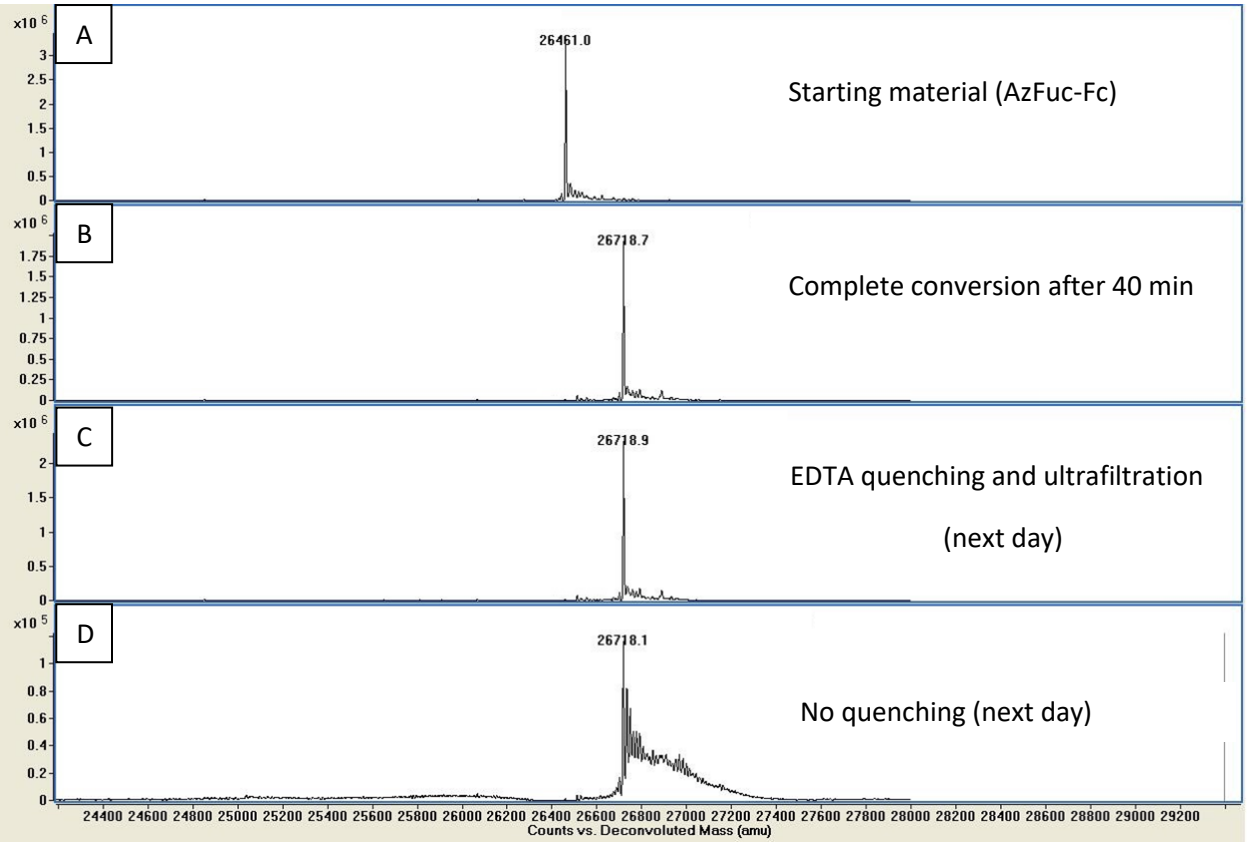

Figure B7. Combination of EDTA quenching and ultrafiltration to prevent protein oxidation during CuAAC reaction.

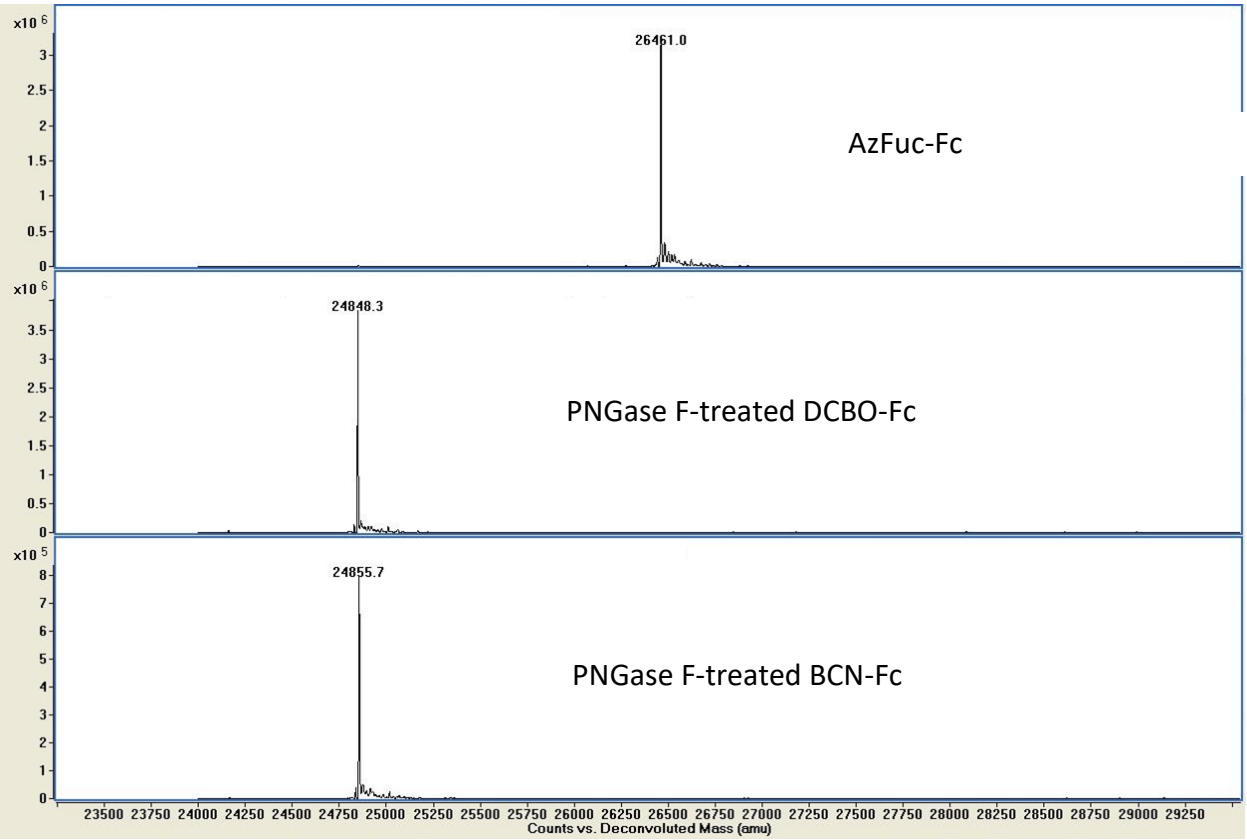

Figure B8. Deglycosylation of DBCO-Fc and BCN-Fc conjugates using PNGase F to conform the site of conjugation.

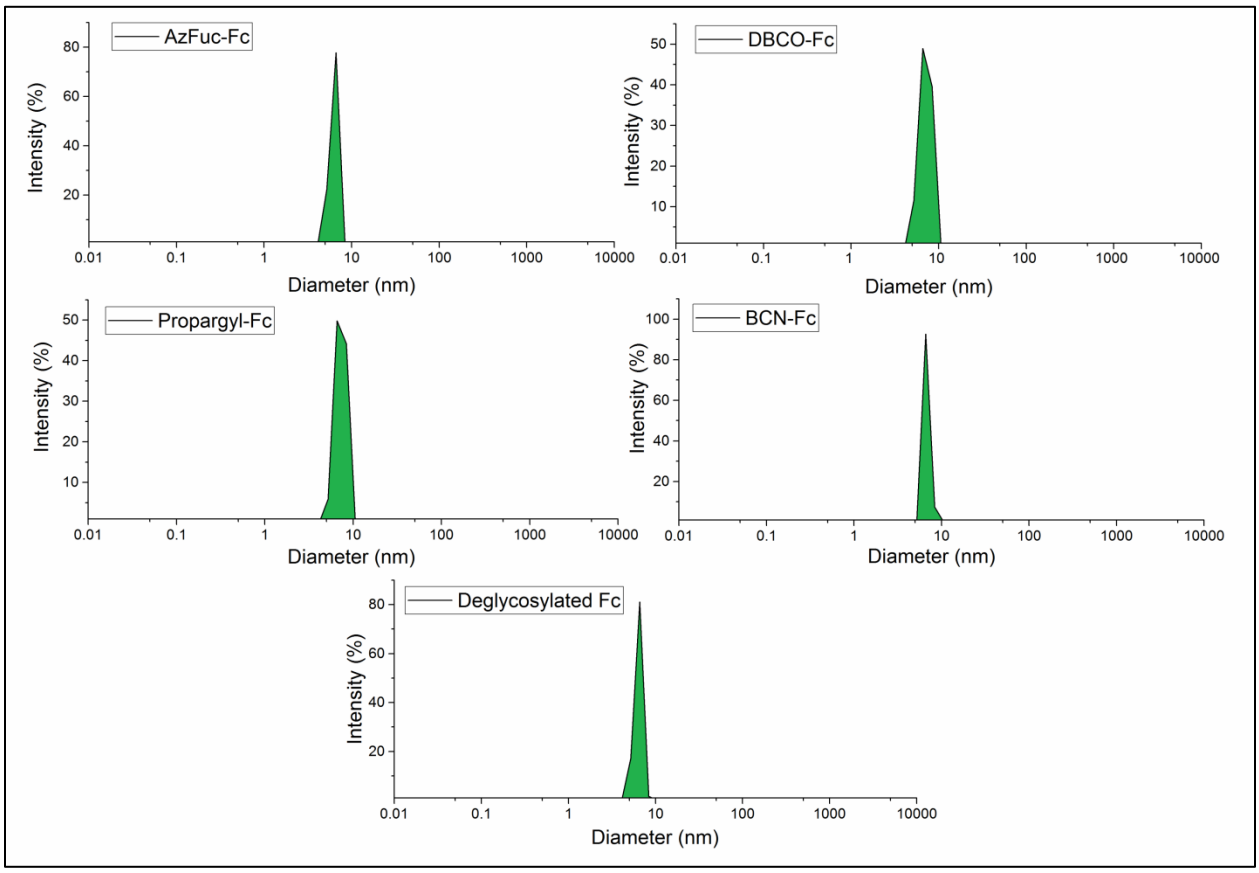

Figure B9. Dynamic light scattering (DLS) intensity-derived size distribution plot of IgG2 Fc variants in 20 mM phosphate buffer (pH 6.0) at 25 ^{o}C.

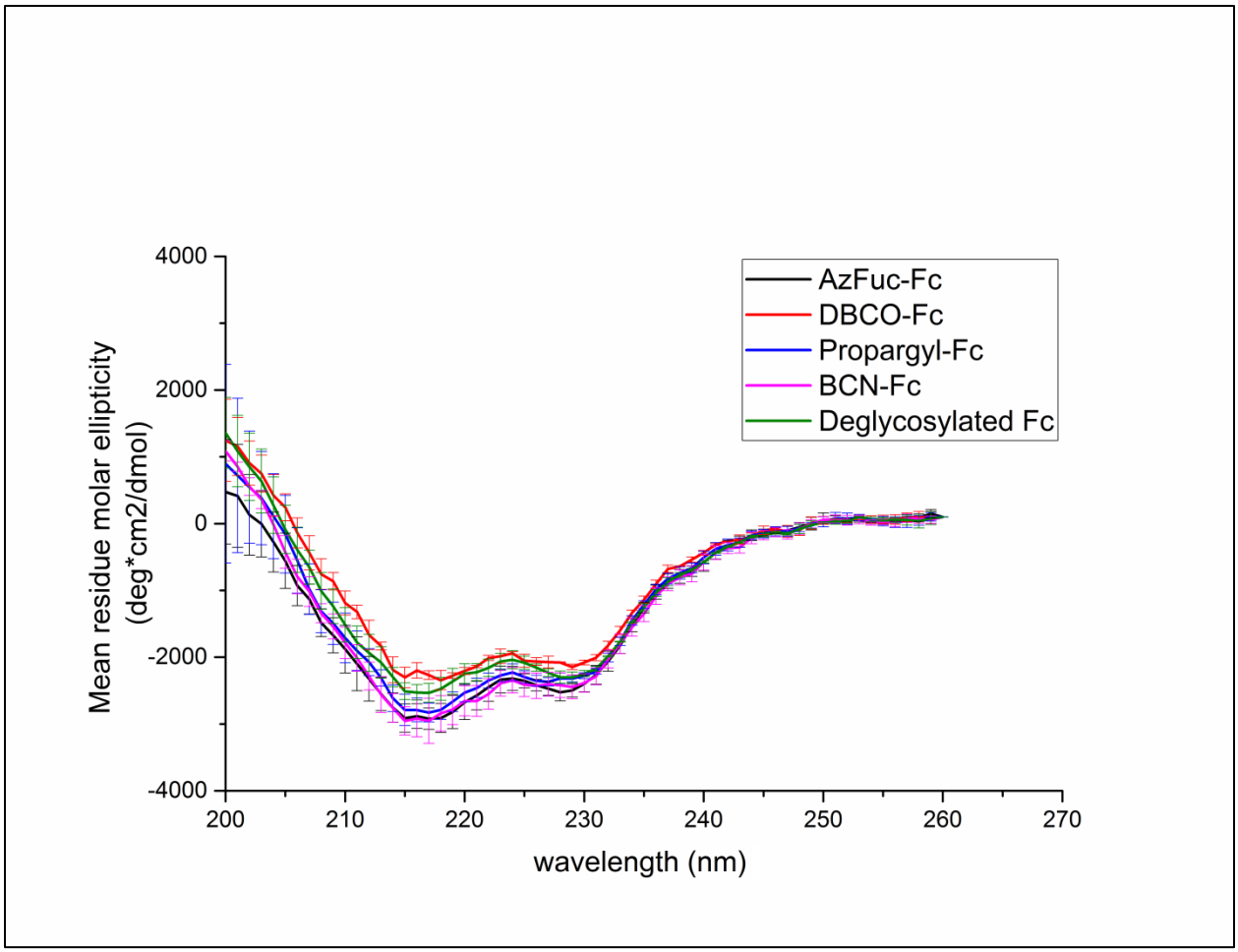

Figure B10. Far-UV circular dichroism spectra of Fc variants in 20 mM phosphate buffer (pH 6.0) at 10 °C. Error bar indicates standard deviation (N =3).

Table B1. Summary of thermal transition temperatures of Fc variants studied by different biophysical techniques

Techniques			AzFuc-Fc	DBCO-Fc	Propargyl-Fc	BCN-Fc	Deglyco. Fc
CD			70.0 ± 1.5	69.5 ± 1.5	70.0 ± 1.1	68.8 ± 0.4	63.5 ± 0.8
Intrinsic Trp fluorescence	Moment		64.6 ± 0.2	63.9 ± 0.5	64.3 ± 0.8	64.3 ± 0.9	62.2 ± 0.1
	Intensity	1	69.0 ± 0.01	67.7 ± 0.26	69.0 ± 0.04	68.4 ± 0.23	67.9 ± 0.23
		2	74.5 ± 0.15	74.4 ± 0.01	74.4 ± 0.01	74.3 ± 0.09	75.5 ± 1.76
Sypro orange			67.0 ± 0.02	66.0 ± 0.02	67.0 ± 0.01	67.0 ± 0.02	64.0 ± 0.06
DSC	1		68.7 ± 0.09	68.1 ± 0.06	68.9 ± 0.05	69.2 ± 0.12	65.2 ± 0.13
	2		76.4 ± 0.09	76.6 ± 0.06	76.6 ± 0.06	76.2 ± 0.14	75.2 ± 0.07

References

(1) Gosselin, S., Alhussaini, M., Streiff, M. B., Takabayashi, K., and Palcic, M. M. (1994) A continuous spectrophotometric assay for glycosyltransferases. *Anal. Biochem.*

(2) Nakajima, K., Kitazume, S., Angata, T., Fujinawa, R., Ohtsubo, K., Miyoshi, E., and Taniguchi, N. (2010) Simultaneous determination of nucleotide sugars with ion-pair reversed-phase HPLC. *Glycobiology 20*, 865–871.